NANNOPLANKTON AS INDICATORS OF CLIMATIC VARIABILITY IN THE UPPER PLIOCENE

A. J. Chepstow-Lusty

A dissertation submitted for the degree of Doctor of Philosophy at the University of Cambridge

Darwin College
Cambridge
June, 1990

DECLARATION

I hereby declare that this dissertation describes my original work except where acknowledgement is made in the text. It does not exceed the word limit and is not substantially the same as any work that has been, or is being, submitted to any other University for any degree, diploma or other qualification.

Alexander. J. Chepstow-Lusty

Alex. J. C-Lusty.

It is advisable to look from the tidepool to the stars and then back to the tidepool again.

John Steinbeck "The Log from the Sea of Cortez".

ACKNOWLEDGEMENTS

There are many people I would like to thank during this four year period. In total random order of gratitude, I owe a great deal to Jenny, Ruth and Rachel.

In the laboratory itself thanks go out to: Jamie, Liping and J. P. providing company during the late hours; both Simons helping me with computers; ; Mike for his continual friendliness and helpfulness; and not least of all the easy going-ness of Loraine, Roy, Margarat, Andrew, Rainer, Jackie and Dave.

Outside of the laboratory, I have not forgotten Clive, Neil, Roslyn; my parents who still don't know what I've been doing all these years; Rachel no. 2, Julie, Carolyn, Donna, Sheila, Daryl and the Howards.

I must not forget where the funds came from to keep me going: NERC, Brooks Fund and BP.

Lastly, I am grateful to the patience of Nick and Jan and their unhassling support. Jan's Discoaster data for DSDP Sites 552 and 607, Cores V32-127 and V28-127 allowed this to be a truly global study and Nick provided the most up to date timescale for the Pliocene. I was very fortunate to be able to work on the best material available and we accomplished a great deal together.

NANNOPLANKTON AS INDICATORS OF CLIMATIC VARIABILITY IN THE UPPER PLIOCENE

ALEXANDER. J CHEPSTOW-LUSTY

Discoasters are the remains of an enigmatic group of nannoplankton, whose last representatives disappeared globally at 1.89 Ma. The one million years prior to their extinction has been analysed in high time resolution and a global database has been developed from ten sites in the Atlantic, Indian and Pacific Oceans.

It has been shown that the variability in Discoaster abundance at low latitudes cannot be attributed solely to changes in sea-surface temperature; discoasters were demonstrated to be suppressed at upwelling sites. In combination with global satellite images of phytoplankton blooms (Lewis, 1989) and maps of modern sea-surface temperatures (CLIMAP, 1981), Discoaster abundance variations were interpreted in terms of the interplay between productivity pressure and sea-surface temperature.

Discoasters thrived in the Indian Ocean at Site 709 (4°S) in warm waters with little productivity pressure, whereas Discoaster abundance was suppressed at Sites 677 (1°N) and 662 (1°S) in the Pacific and Atlantic, which although located in warm waters, were affected by upwelling. In addition to the reduced Discoaster abundances associated with upwelling, sea-surface temperature gradients are a significant factor when comparing high and low latitude sites. A marked drop in Discoaster abundance is apparent between 41°N and 56°N (i.e., between Sites 607 and 552).

Relative abundances of species in the Discoaster assemblage revealed clearly their contrasting environmental preferences; D. brouweri was produced under a wide range of conditions, favouring warm, low productivity waters; D. asymmetricus and D. tamalis were produced in higher abundances relative to D. brouweri during cooler, low productivity episodes; D. pentaradiatus showed highest absolute abundance in warm, low productivity waters, although increasing in relative abundance at higher latitudes; D. surculus increased in relative abundance in high productivity regions and in cooler waters. At all sites, though most markedly at higher latitudes, Discoaster abundances declined after 2.4 Ma, when glaciation began in the North Atlantic.

CONTENTS

CHAPTER 1: GENERAL INTRODUCTION AND METHODS

1:1 Discoasters and their utility in palaeoceanographic studies

Discoasters are known in the oceanic record from the upper Paleocene to the upper Pliocene, when the last two representatives of the genus disappeared synchronously just below the base of the Olduvai subchron, 1.89 Ma (Takayama, 1970; Rio, 1982; Backman and Shackleton, 1983; Driever, 1988). Numerous studies have shown that discoasters are particularly common in low latitude sediments and therefore probably favoured warm water masses (e.g. Haq and Lohmann, 1976; Bukry, 1978). The organism from which discoasters evolved is not known, but was presumably related to the coccolithophorids. Discoasters are favourable for quantitative study as they resist dissolution better than planktonic foraminifera or most placoliths (Lohmann and Carlson, 1981). A number of factors probably affected their distribution, but this genus has in the past been thought to be especially sensitive to temperature (Haq and Lohmann, 1976).

One feature that makes the discoasters, especially in the Pliocene, such a useful group is that they appear to produce well defined synchronous Last Appearance Datums (LAD's). This has been shown especially by Backman and Shackleton (1983) from interpolation with magnetostratigraphy from e.g. Cores V28-179 and V32-127 in the Pacific Ocean. It cannot be overstated how useful this makes the discoasters for constructing age models. Most biostratigraphic groups show diachroneity to a large extent as shown in the Pliocene by

TABLE 1:2 List of Sites Studied

ATLANTIC SITES

HOLE	LOCATION	WATER DEPTH(M)	REFERENCE
662A	1°S 11°W	3,824	Ruddiman, Sarnthein et al., 1988.
659A	18°N 21°W	3,067	" "
658A	20°N 18°W	2,263	" "
607	41°N 33°W	3,427	Ruddiman, Kidd, Thomas et al., 1987.
552A	56°N 23°W	2,304	Roberts, Schnitker et al., 1984.

INDIAN SITES

709C	4°S 61°E	3,038	Backman, Duncan et al., 1988.
716B	5°N 73°E	533	" "

PACIFIC SITES

677A	1°N 84°W	3,461	Becker, Sakai, Merrill et al., 1987.
V28-179	5°N 140°W	4,509	Shackleton and Opdyke, 1977.
V32-127	35°N 178°E	3,927	Backman and Shackleton, 1983.

Dowsett (1989). However, here we have a group sensitive to palaeoclimatic changes that provides fixed datums, which is very important in the absence of magnetostratigraphy. This means we have the basis for comparing Discoaster abundances between sites and developing a detailed global palaeoceanographic history of the conditions causing these fluctuations. The time interval investigated is approximately the million years preceding the extinction of the discoasters (i.e. 1.89-2.90 Ma) using closely spaced samples (around 3 ka). At the two Indian Ocean sites, Sites 709 and 716, the time interval is extended back to 3.5 Ma.

1:2 Selection of sites

To develop a global perspective of Discoaster abundance changes in the upper Pliocene, the sites in this study had to be carefully selected (Table 1:2, Fig 1:2). The sites had to contain undisturbed sequences in the relevant time interval with reasonably high sedimentation rates (>3cm/ka). The only exceptions to this are Site 552 at 56°N in the North Atlantic with a sedimentation rate of approximately 1cm/ka and the Pacific Cores V28-179 and V32-127 with sedimentation rates of 0.4cm/ka and 0.3cm/ka respectively. We were interested in how Discoaster abundances varied within an ocean as a function of increasing latitude, as well as upwelling versus non-upwelling conditions. The Discoaster data for DSDP Sites 552 and 607, and Cores V32-127 and V28-179 was collected by Jan Backman.

A latitudinal transect of five sites in the North Atlantic were selected to demonstrate this (Chapter 2): ODP Site 662 (1°S), ODP Site 659 (18°N), ODP Site 658 (20°N), DSDP 607 (41°N) and DSDP 552 (56°N).

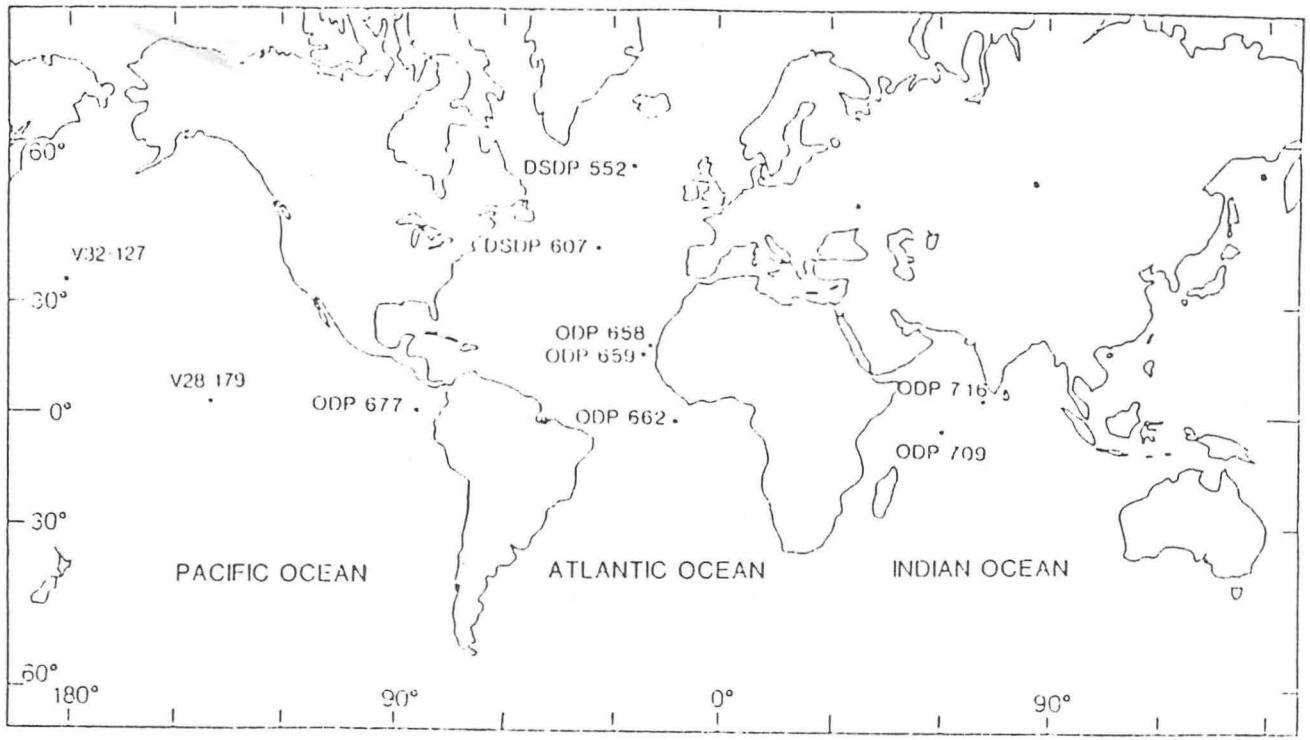

Figure 1:2 Location of all sites in study

ODP Sites 659 and 658 are in relatively close proximity. The former is our open ocean reference site contrasted with the latter upwelling site. Chapter 2 forms the basis for our biochronology of the discoasters, backed up with Discoaster datums obtained from Cores V32-127 and V28-179. These were especially useful because magnetostratigraphy was available (Backman and Shackleton, 1983).

In Chapter 3, a comparison is made between Discoaster abundances at three sites at the equator in three different oceans. The three sites selected were ODP Site 662 (Atlantic), ODP Site 677 (Pacific) and ODP Site 709 (Indian). Sites 662 and 677 are affected by upwelling, whereas Site 709 is situated in a stable warm water mass of modest productivity.

In Chapter 4, we compare Discoaster abundance variations at two Indian ocean sites, Sites 709 and 716 with similar sea-surface temperature today. They differ in that Site 716 is affected by upwelling induced by southwesterly monsoon winds. In Chapter 5, we examine the taxonomic and ecological relationships between the different Discoaster species.

Chapter 6 looks at Discoaster abundance variation at Sites 607 and 677 using orbitally tuned timescales (Raymo et al., 1989; Shackleton, Berger and Peltier, in press). In the final chapter, Chapter 7, a global synthesis of all the sites is attempted, including the two Pacific sites, Cores V32-127 and V28-179. These are from the central and north Pacific respectively and are compared with Site 677 from the east Pacific.

In this thesis, we are particularly concerned with two environmental parameters affecting Discoaster abundance: sea-surface temperature and produc-

tivity pressure. Two major sources of information have been used to try and assess if these parameters can be separated or if they were exerting a combined influence. Maps of modern sea-surface temperatures for February and August may give us some idea of the range of temperatures at the site localities to which discoasters may have been exposed (CLIMAP, 1981). Secondly, this can be combined and contrasted with global satellite images from NASA (Lewis, 1989) of phytoplankton concentrations. The overall geography and climate control productivity and these patterns today are thought to have been similar in the Pliocene. Modern phytoplankton concentrations may therefore act as a proxy indicator of productivity pressure on Discoaster abundances in Pliocene times. For the first time, oceanographers have the ability to view the global distribution of photosynthetic organisms in the world's oceans from space. This has major implications for palaeoceanography, because although the picture may not be exactly the same in upper Pliocene times, it gives us a global overview of what is possible with which to compare our data.

1:3 Species of Discoasters

Seven species of Discoaster were analysed in this work, but D. variabilis occurs only at the beginning of the time interval investigated at most sites, 1.89-2.90 Ma. All the species, except D. variabilis are shown in Plate 1.

PLATE 1. SPECIES OF DISCOASTER

1. D. brouweri Tan Sin Hok
2. D. triradiatus Tan Sin Hok
3. D. pentaradiatus Tan Sin Hok
4. D. surculus Martini and Bramlette
5. D. asymmetricus Gartner
6. D. tamalis Kamptner

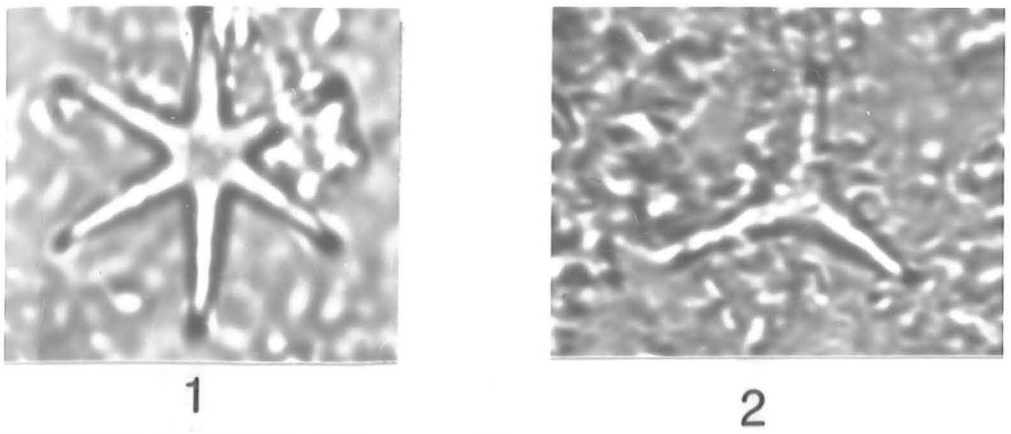

PLATE 1.

1:3:1 Brief Taxonomy

Discoaster brouweri Tan Sin Hok, 1927

Remarks: This species is confined to six rayed specimens, of which the rays are bent downwards and taper.

Discoaster triradiatus Tan Sin Hok, 1927

Remarks: This species is confined to three rayed specimens, of which the rays are bent downwards and taper. D. triradiatus and D. brouweri are the only pair of Pliocene discoasters having a simultaneous extinction. D. triradiatus is probably not a different species, but the triradiate form of the D. brouweri group.

Discoaster pentaradiatus Tan Sin Hok, 1927

Remarks: This species includes all slender five rayed discoasters with bifurcated ray tips. Frequently, the slender bifurcated ray tips are not preserved, but even in their absence D. pentaradiatus can be distinguished from Discoaster asymmetricus by its overall symmetry.

Discoaster surculus Martini and Bramlette, 1963

Remarks: This six rayed species is stockier than D. brouweri, and is characterized by trifurcated ray tips and parallel sided arms.

Discoaster asymmetricus Gartner, 1969

Remarks: This five rayed species is distinguished by its asymmetry. In addition unlike D. pentaradiatus, D. asymmetricus is optically homogeneous and lacking in bifurcations at the ray tips.

Discoaster tamalis Kamptner, 1967

Remarks: This species is distinguished by its four rays and cannot be confused

with other forms.

Discoaster variabilis Martini and Bramlette, 1963

Remarks: This species includes all six rayed discoasters with a more or less pronounced bifurcation on the ray tips.

1:3:2 Assumptions

During this study, we have made a number of assumptions about a group of marine microfossils which died out globally at 1.89 Ma. We presume that their nearest relatives were the coccolithophorids, and hence that discoasters are the remains of photo-autotrophic algae. During the time interval investigated, 1.89-3.00 Ma, we also make the assumption that the different Discoaster species have not changed their ecological requirements.

Another major assumption is that the distribution and abundance of discoasters in the sediment is an accurate reflection of what was happening in the surface waters. Faecal pellet transfer of coccoliths has been found today to be the major method of both rapidly transporting and preserving them to the ocean floor (Schrader, 1971; Honjo, 1977). Probably, zooplankton feeding on the " discoasterophorid" have sent them to the ocean floor contained in faecal pellets.

In the construction of the age models, we furthermore make a number of assumptions. We assume that if there is a change in the sedimentation rate at the control point used (frequently a Discoaster datum), this point marks where the rate has changed in time. Obviously, this is not gen erally true. Ideally, one needs more control points. Likewise, we assume that there is a constant sedimentation rate between the control points. This is similarly unrealistic, but this would be

highly desirable. Lastly, much of what we have attempted here hinges on the global synchroneity of Discoaster datums and whether these are as reliable as we think they are.

1:4 Semi-quantitative counting technique

The semi-quantitative counting technique used here follows that of Backman and Shackleton (1983). Although this method should be described as semi-quantitative, Backman and Shackleton (1983) demonstrated a very high correlation with absolute concentration data at Core V28-239; in this case they obtained counts of absolute abundances following a procedure developed by A. McIntyre. A known quantity of sediment is diluted in a known volume of aqueous solution from which a defined volume is filtered through a 0.8 micron filter. The microfossils are evenly distributed on the filter, of which a part is placed on an SEM stub. Under SEM, selected taxa are counted at a given magnification for a defined number of view fields. Hence, the total number of counted microfossils can be related to the number of microfossils per gram sediment. However this is a much slower process than the semi-quantitative technique described below, and is not suitable for the type of study undertaken in this thesis.

1:4:1 Preparation of smear slides and selection of view fields

All the smear slides from Sites 659, 658, 662, 709, 677 and 716 were prepared from raw sediment. The material from DSDP Sites 552 and 607 represent fine fractions, where the sediments have been sieved (63μm) to remove foraminifera.

A small piece of the sediment is placed on a microscope slide to which a drop of distilled water is added. Using the flat end of a tooth-pick this is spread out into a thin layer composed of stripes of sediment. The slide is placed on a hot-plate and a piece of the mounting medium Crystalbond was melted on top and a cover-slip attached. Bubbles were removed by gentle pressure with a small spatula. After cooling, washing away excess sediment and labelling, the slide is ready for viewing under the microscope. This whole procedure only takes a few minutes.

When counting, although we are aware of the other components of the assemblage (see section 1:6) and possible non-biogenic inputs e.g. aeolian dust, we are quantifying selected taxa. The important feature about this method is counting a defined number of view fields (normally related to the overall abundance of the taxon throughout the site) at a medium constant density background at a certain magnification. This means that if counts have been made at different magnifications or using different microscopes, they can be directly compared since the abundance data is expressed relative to unit area of slide scanned (i.e. number of specimens per square millimeter). According to Backman and Shackleton (1983), a convenient grain density distribution on the slide is approximately 250 nannofossil specimens/particles per 0.3 mm view field diameter. Basically, a medium constant density means that the nannofossils/particles are not stacked into clumps, nor are they widely spaced. It is essential that this consistency in density is maintained between samples. However, it soon becomes apparent to the biostratigrapher what the correct density should be because high

density backgrounds make counting too difficult and low density backgrounds are too rapid.

1:4:2 Repeatability of accuracy at Pacific Site V28-240

An example of the reliability of these abundance counts is shown at V28-240 (Fig 1:4:2a). A set of thirty six smear-slides was analysed for total Discoaster abundance/mm2 through a selected depth interval. Twenty fields of view were selected at a magnification of 10 x 100, which is equivalent to a view field diameter of 0.18mm. This set was counted a second time.

The two abundance patterns are basically the same and every important abundance feature is present, though a few minor differences occur in the size of the abundance peaks. A high positive correlation can similarly be shown if the abundance counts are plotted against each other (Fig. 1:4:2b).

1:4:3 Correlation between A and B-Holes at Site 659

This semi-quantitative counting technique can furthermore be shown to be an accurate method for correlating between holes at the same site. Two intervals of similar depth were selected at Holes 659A and 659B, after the offset between the holes had been taken into account. This interval was known to be within the Discoaster triradiatus acme, and was carefully selected away from any core breaks where there would be any possibility of disturbance or reworking. The D. triradiatus acme is a limited interval between 1.89-2.07 Ma (Backman and Shackleton, 1983). Smear slides were prepared for both intervals with a sampling interval of 10cm, counting twenty fields of view using a magnification of 15 x 40, which is equivalent to 0.3mm D. triradiatus and D. brouweri are the diameter.

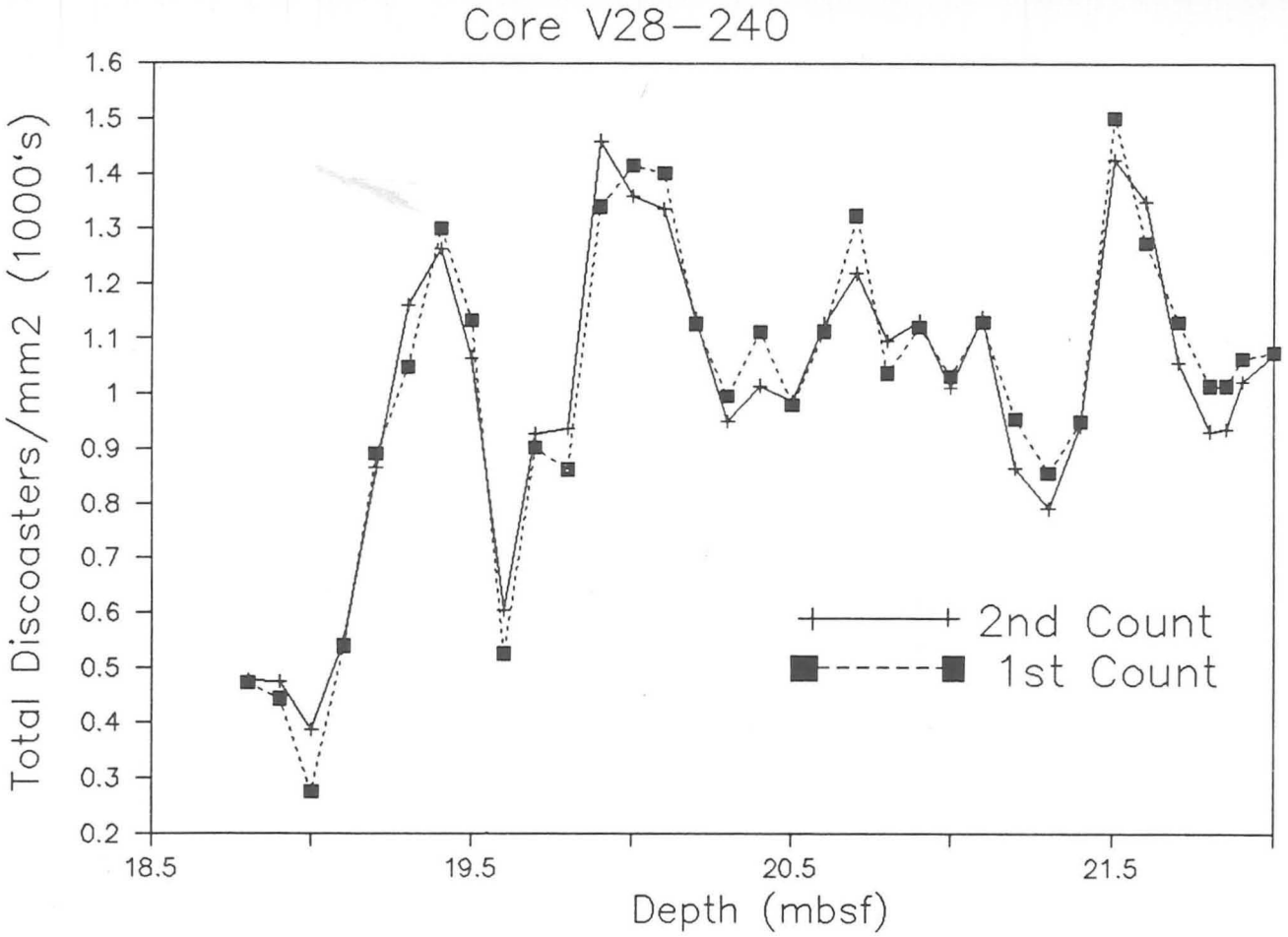

Figure 1:4:2a
Comparison of counting consistency at Core V28-240

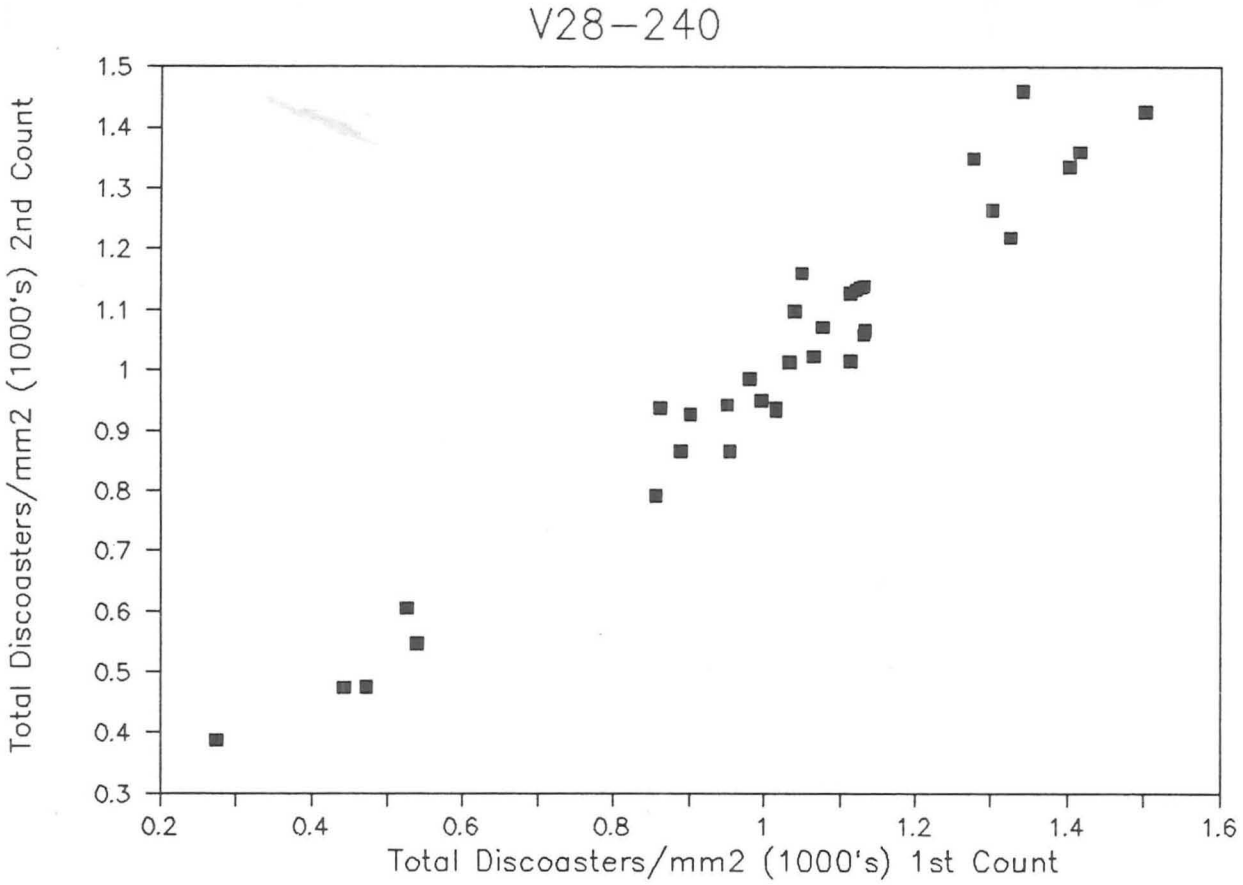

Figure 1:4:2b
Correlation between two sets of counts at V28-240

only Discoaster species present through this interval at both holes. The abundance patterns for both species shows a high correlation between Holes 659A and 659B (Fig. 1:4:3). By using two species, the correlation between the holes is further reinforced. The reliability of this technique means that it is possible to switch between holes at disturbed intervals, such as at core breaks to obtain the best sequence available at a site.

1:4:4 Benefits of counting technique

There are many benefits associated with this technique. As has been shown, this method is an extremely simple, rapid way of gathering data that correlates well with more laborious techniques for quantifying absolute abundances of nannoplankton (Backman and Shackleton, 1983). Only tooth-pick size samples of sediment are required and this can be very significant in obtaining sample requests and sharing material in interdisciplinary studies. The technique as demonstrated above, apart from being accurate, is repeatable. Different biostratigraphers can take the original material and produce very similar results. It can also serve as a technique for correlating between holes at the same site as seen at Site 659. In summary, this methodology results in two major products: firstly, large data sets can be rapidly obtained for the abundances of a few taxa; secondly, this can be combined with assesssing if extinctions are synchronous over large geographic areas by comparing a few widely spaced sites. Of course, this must be performed at a close sampling interval (circa 3 ka). Additional information about background reworking of selected taxa will be revealed from high

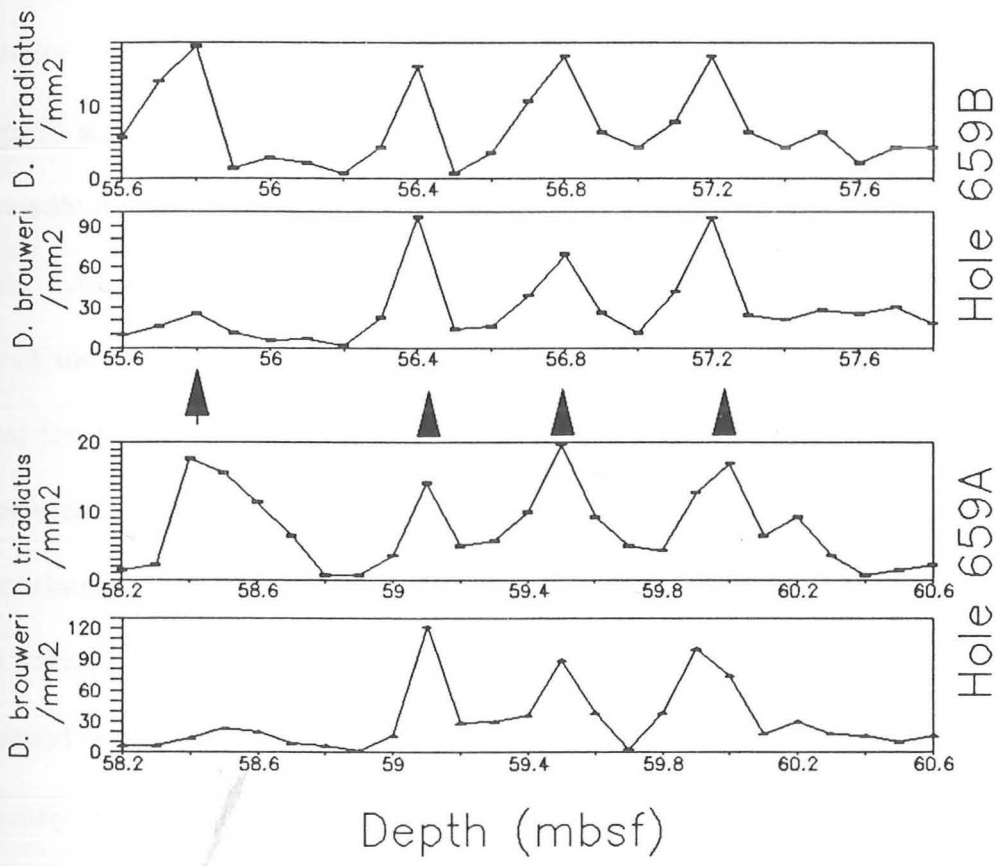

Figure 1:4:3
Correlation between Holes 659A and 659B using semi-quantitative counting technique.

resolution quantitative studies such as these.

1:5 Orbital Forcing and Climatic Variation

1:5:1 Introduction

Climate is now recognised as being continually variable, on all scales of time. In consideration of the complexity of the behaviour of the climatic system, it is not surprising that numerous theories have been advanced to account for climatic variability. No one process can account for all the variability that is observed on any given scale of variation (Mitchel, 1976). The origin of climatic variability may be broadly divided into two categories. The first are processes internal to the climatic system, that involve interactions (i.e. feedbacks) between the different parts of the system. The second are processes external to the climate system, that involve forcing of the system by events or changes whose occurences are independent of the state of the system. External forcing mechanisms can include those related to solar variability, earth-orbital changes, volcanic eruptions, and today various human influences on the environment. We are particularly concerned with earth-orbital changes, whose effects on the climate system is frequently referred to as orbital forcing.

1:5:2 Astronomical Elements

The long term variations in the geometry of the earth's orbit and rotation are thought to have been the fundamental causes of climatic change for the past two or three million years. Although, this astronomical theory has evolved since the early work of J. Adhemar and J. Croll in the 19th century, and even since the

first detailed calculations made by M. Milankovitch (1941), the principles have remained the same. Orbital perturbations influence significantly climate and hence glaciation by changing the seasonal and latitudinal distribution of incoming solar radiation. These orbital perturbations are due to the gravitational effects of the different planets on the earth's orbit and the various components can be expressed as a quasi-periodic function of time. A clear account of how this hypothesis developed into a major theory in palaeoclimatology is given by Imbrie and Imbrie (1979).

If the solar output is assumed to be constant, the amount of solar radiation striking the top of the atmosphere at any given latitude and season is fixed by three elements of the earth's orbit:-

1. Eccentricity: the earth moves in a slightly elliptical path during its annual revolution around the sun. The elliptical path today causes the earth to be closest to the sun (perihelion) around January 3rd (Fig. 1:5:2a), and around July 5th it is furthest away from the sun (aphelion). This results in the earth today receiving approximately 3.5% more solar radiation than the annual mean (outside the atmosphere) at perihelion and approximately 3.5% less at aphelion. Eccentricity is therefore not constant; its present value is 0.017, but it has ranged from 0 (circular) to 0.06 (maximum eccentricity). The most important term in its series expansion has a period of 413 ka, with the immediate following ones having peaks ranging between 95 ka and 136 ka, contributing to a peak which is often loosely referred to as the 100 ka eccentricity cycle (Berger, 1978).

2. Obliquity: the tilt of the earth's axis (measured from the normal to the plane

of the orbit) varies about one and a half degrees either side of its average angle of 23½°, producing a mean period of 41 ka (Fig. 1:5:2b). When the tilt is decreased from its present value of 23½°, the polar regions receive less sunlight than they do today. When the tilt is increased, polar regions receive more sunlight.

3. Precession: changes in the seasonal timing of perihelion and aphelion result from a wobble in the earth's axis of rotation as it moves around the sun (Figs 1:5:2b and 1:5:2c). The effect of the wobble (which is independent of variations in axial tilt) is to change the timing of the solstices and the equinoxes relative to the extreme positions the earth occupies on its elliptical path around the sun. Therefore, 11,000 years ago , perihelion occurred when the Northern Hemisphere's midwinter was tilted towards the sun (mid-June) rather than in the Northern Hemisphere's midwinter, as is the case today. Naturally, precessional effects are opposite in the Northern and Southern Hemispheres. In low resolution geological spectra, a single peak with a mean period of 21 ka can be seen, but higher resolution spectra reveals two peaks of 23 and 19 ka (e.g. Hays et al., 1976).

Clearly, the effects of precession of the equinoxes on radiation receipts will be modulated by variations in eccentricity. When the orbit is near circular the seasonal timing of perihelion is insignificant. However, at maximum eccentricity, seasonal timing is crucial when differences in solar radiation can be very large.

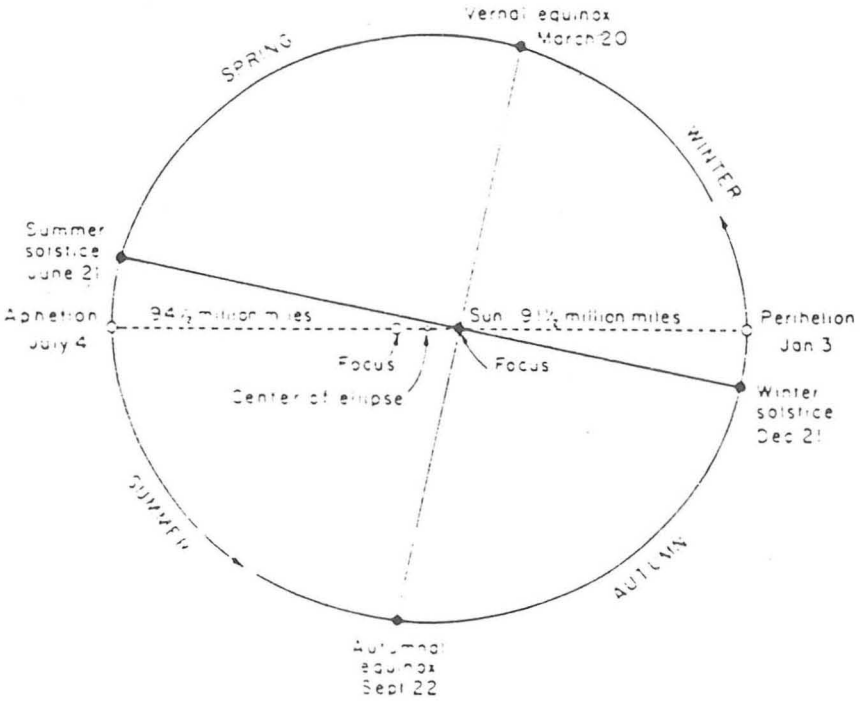

Figure 1:5:2a. Equinox and Solstice. At the eqinoxes, the earth's axis is pointed at right angles to the sun, and the day and night are of equal length all over the globe. At the summer solstice, the North Pole is tipped in the direction of the sun and the northern hemisphere has the longest day of the year. At the winter solstice, the North Pole is tipped away from the sun, and the northern hemisphere has the shortest day of the year .

Figure 1:5:2b Precession and Obliquity. The gravitational pull of the sun and moon on the equatorial bulge of the earth results in its axis of rotation moving slowly around a circular path once every 26,000 years. Independently of this cycle of axial precession, the tilt of the earth's axis (measured from the vertical) varies about 1½° on either side of its average angle of 23½°.
(Imbrie and Imbrie, 1979).

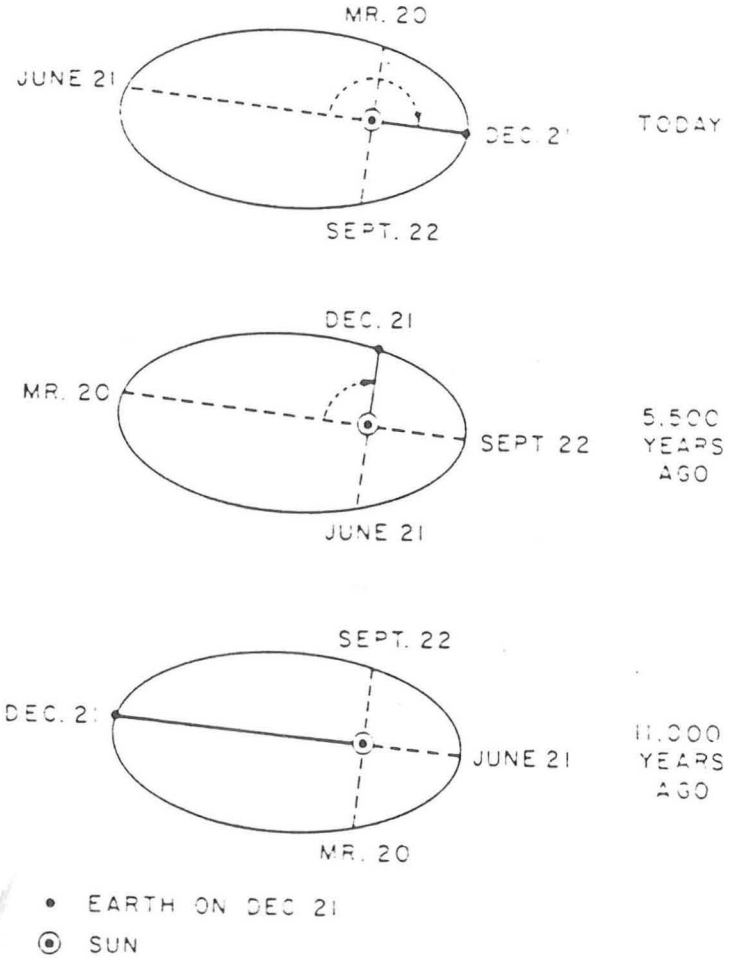

Figure 1:5:2c Precession of the equinoxes. Owing to axial precession and eccentricity, the positions of equinox (March 20 and September 22) and solstice (June 21 and December 21) shift slowly around the earth's elliptical orbit, and complete one full cycle about every 22,000 years. Eleven thousand years ago, the winter solstice occurred near one end of the orbit. Today, the winter solstice occurs near the opposite end of the orbit. As a result, the earth-sun distance measured on December 21 changes. (Imbrie and Imbrie, 1979).

The solar radiation receipts of low latitudes are mainly affected by variations in eccentricity and precession of the equinoxes, whereas higher latitudes are mainly affected by variations in obliquity.

1:5:3 Spectral Analysis

One objective of this thesis was to discover to what extent in the million years prior to their extinction, the Discoaster record is modulated by orbital forcing. Hays et al. (1976) had demonstrated that geological spectra contain substantial variance components at many frequencies similar to those obtained by Berger (1977) from astronomical computations. On both oxygen isotopic (ice volume) and temperature-radiolarian spectra, Hays et al. (1976) revealed at a composite deep-sea core from the Indian Ocean (RC11-120 and E49-18), peaks for cycles roughly 100, 42, 23 and 19 ka long (Fig. 1:5:3). The time interval examined was the past 468,000 years. The time interval we have examined is approximately 1.89-2.90 Ma, except at the two Indian Ocean sites, where our record extends back to 3.5 Ma.

Spectra of palaeoclimatic indicators have been found to change in space and time. For example, Ruddiman and McIntyre (1981) have demonstrated that the sea-surface response of the North Atlantic at 41°N is dominated by variance in the 23 ka band, whereas at 44°S in the Indian Ocean it is dominated by variance in the 100 ka band. About the stability of the insolation spectra in time, Berger (1977) has compared the time intervals 1.6-2.4 Ma and 2.4-3.2 Ma and revealed much weaker 41 and 19 ka signals in the former time interval, with moderate to strong 41 and 19 ka signals in the latter time interval.

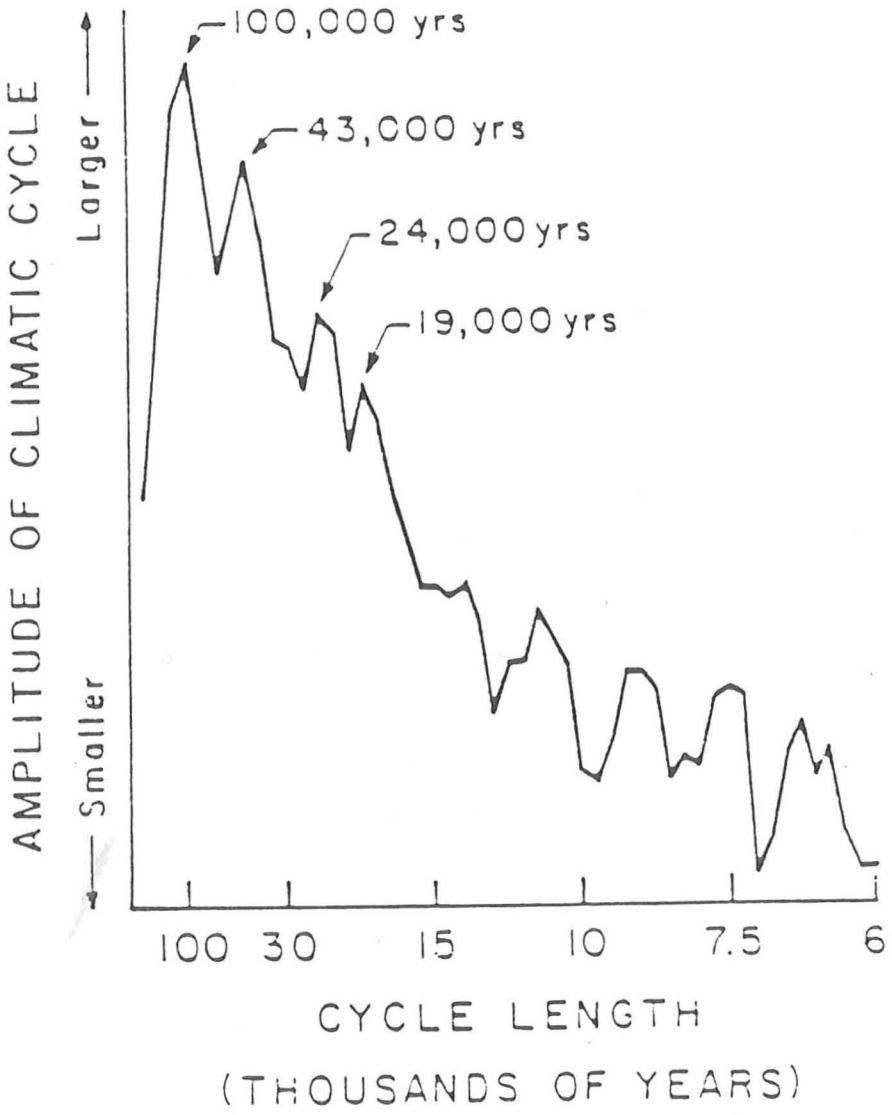

Figure 1:5:3 Spectrum of climatic variation over the past half-million years. It shows the relative importance of different climatic cycles in the isotopic record of two Indian Ocean cores from Hays et al., 1976. (Imbrie and Imbrie, 1979).

Therefore, in our Pliocene Discoaster record, we did not know what to expect by carrying out spectral analysis. We obtained continuous data sets for the time interval analysed from sites with high sedimentation rates (>3cm/ka) to resolve climatic fluctuations with periods below 20 ka. Age-models were constructed as discussed in Chapters 2, 3 and 4 using biostratigraphic and magnetostratigraphic control points. This produced a continuous record of Discoaster abundance versus time. However, geological time series are not studied as continuous signals, but as a set of equally spaced observations. These estimates are made by linear interpolation and extrapolation e.g. 3 ka was selected as our uniform time interval.

The time series is considered to be made up of a number of periodic curves of different frequencies. The spectrum specifies how much of the total observed variance (i.e. the deviation from the mean squared) is represented by individual frequency components. Thus, the variation originally examined in the time domain (e.g. Total Discoaster Abundance versus time) are now examined in the frequency domain (e.g. variance of Total Discoaster Abundance versus frequency). To convert the frequency values to periodicity values, the uniform time interval of e.g. , 3 ka, is divided by the frequency. In Chapter 6, astronomically tuned timescales have been constructed for Sites DSDP 607 and ODP 677 back into the Upper Pliocene. Spectral analysis is performed on the total Discoaster data sets with these new timescales and compared with the old timescales based on magneto- and biostratigraphy.

1:6 Other components of Assemblage

It is realized that the discoasters only represent a small part of the assemblage examined. Important palaeoclimatic information can also be obtained from the other components of the complete assemblage. We counted the abundances of Coccolithus pelagicus and centric diatoms at Sites 709, 677 and 716, and Calcidiscus macintyrei at Site 709. The abundances of these are shown versus sub-bottom depth and age (same age-models as in Chapters 3 and 4) in Appendix C. C. pelagicus and C. macintyrei are furthermore shown relative to the complete Discoaster assemblage (Wei et al., 1988). We hope this may form the basis of much future work, but its evaluation was beyond the scale of this present study (see Chapter 7, section 7:5 Future Work).

CHAPTER 2: COMPARISON OF DISCOASTER ABUNDANCE VARIATIONS FROM THE NORTH ATLANTIC: SITES 552, 607, 659, 658 AND 662 ; EVIDENCE FOR PLANKTON RESPONDING TO ORBITAL FORCING

2:1 INTRODUCTION

In this study, the abundances of the Discoaster species are compared in five sites covering a wide latitudinal range of the North Atlantic. The approach adopted will form the basis for comparison with other oceans leading finally towards a synthesis which may give us a record of global ocean temperature changes and/or nutrient levels. This chapter provides the biostratigraphic framework for using Discoaster datums. The ages of Discoaster datums from Pacific sites V28-179 and V32-127, estimated on the basis of reliable magnetostratigraphy, provide an essential basis for this framework (Backman and Shackleton, 1983).

This study analyzes Discoaster abundance variations as a function of latitude in the North Atlantic with high time resolution. If the Discoaster events displayed diachroneity over a latitudinal range of 57°, this would undermine the construction of age-models. In the absence of reliable magnetostratigraphy, diachroneity could present major problems for comparing

sites. This is shown not to be a problem and in terms of geological time Discoaster events are virtually synchronous which makes them a particularly useful group.

Individual species of discoasters are further compared between sites as a percentage of the complete Discoaster assemblage. Sea-surface temperatures in the present day and upper Pliocene ocean are thought to have been similar (Shackleton, Berger and Peltier, in press). The abundances of the Discoaster species have therefore been compared with modern sea-surface temperatures from the CLIMAP maps (CLIMAP, 1981). In Table 2:2, the sea-surface temperatures for February and August are shown at the five sites.

These type of continuous quantitative estimates of Discoaster abundances encourage the use of spectral analysis in order to determine to what extent orbital forcing is imprinted on the Discoaster record at these sites.

2:2 Background on site localities

The five sites chosen (Fig. 2:2, Table 2:2) were chosen to contrast with each other either in terms of latitude, upwelling versus non-upwelling systems, or the effects of cool/warm currents. The sites possess good sequences of upper Pliocene sediment, and except for Hole 552A fairly high sedimentation rates (>3cm/ka). Sample spacing was at 10 cm intervals except for Sites 607 and 658 which were at 15 cm and 30 cm intervals respectively. (Site 659, 10cm≈3ka; Site 662, 10cm ≈ 2ka; Site 552, 10cm ≈ 8ka; Site 607, 15cm ≈ 3ka; Site 658, 30cm ≈ 3ka)

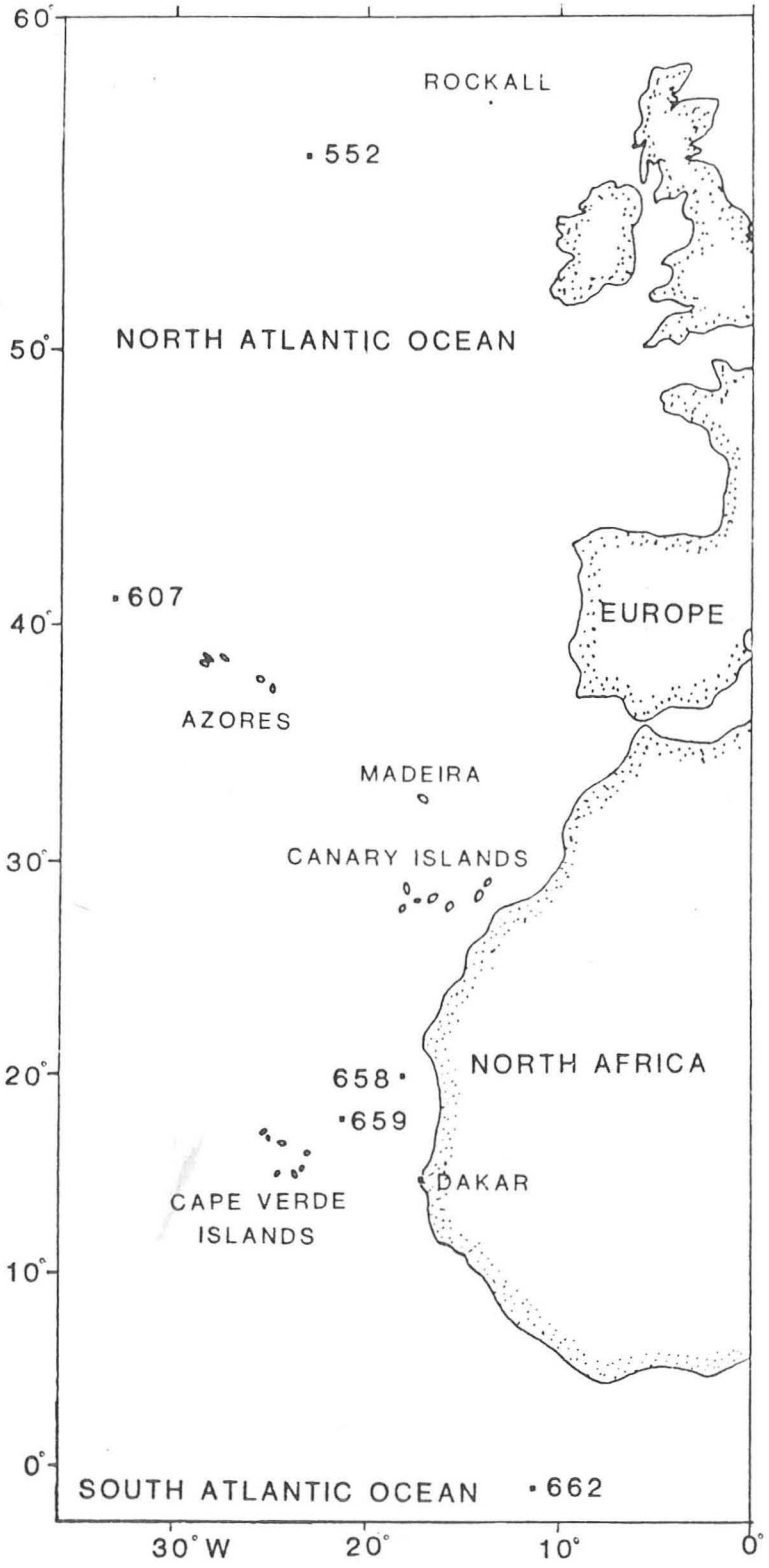

Figure 2:2 Location of sites studied in North Atlantic.

TABLE 2:1

Modern sea-surface temperatures at Sites 662, 659, 658, 607 and 552 (CLIMAP, 1981).

	February	August
Site 662	27°C	23°C
Site 659	20°C	25°C
Site 658	18°C	22°C
Site 607	13°C	23°C
Site 552	9°C	14°C

TABLE 2:2

North Atlantic sites selected, their geographic positions and water depth.

Hole	Location	WATER Depth(m)	Reference
662A	1°S 11°W	3,824	Ruddiman, Sarnthein et al., 1988.
659A	18°N 21°W	3,067	" "
658A	20°N 18°W	2,263	" "
607	41°N 33°W	3,427	Ruddiman, Kidd, Thomas et al., 1987.
552A	56°N 23°W	2,304	Roberts, Schnitker et al., 1984.

2:2:1 Site 659

This site was selected as an open ocean, low latitude reference site. It is located on top of the Cape Verde Plateau. The oceanographic setting is not complicated by the cool Canaries Current, or large input of terrigenous matter from northwest Africa. The lithology is mostly nannofossil-foraminiferal ooze with good preservation and no noticeable dissolution in the interval studied.

2:2:2 Site 658

This site was the contrasting upwelling, high productivity site chosen, in relatively close proximity to Site 659. It is located on the continental slope 160 km west off Cape Blanc, and lies beneath a major productive cell of permanent oceanic upwelling. The sediments are hemipelagic due to the combined effect of oceanic production and continental influence.

2:2:3 Site 662

This site is located close to the equator on the upper eastern flank of the mid-Atlantic Ridge. The relevant stratigraphic interval is a nannofossil and foraminifer-nannofossil ooze. Site 662 is influenced by the South Equatorial Current, which is the continuation of the Benguela Current. Situated within the equatorial divergence, Site 662 is affected by upwelling and hence high productivity conditions.

2:2:4 Site 607

This site is presently located along the northernmost part of the subtropical gyre. In the late Pliocene this area was exposed to major circulation changes and lower temperatures (Ruddiman and kidd et al., 1988). The lithology is interbedded foraminiferal nannofossil oozes and marls representing the North Atlantic glacial-interglacial cycles. The Discoaster data for this site was obtained by Jan Backman.

2:2:5 Site 552

This site is at the northernmost latitude of the transect. The Discoaster data for this site was obtained by Backman et al., (1986). Site 552 was drilled on the southwest margin of the Rockall Plateau. The lithology is similar to that of Site 607, consisting of cycles of alternating beds of foraminiferal-nannofossil ooze and calcareous marls and mud. These lithological cycles began abruptly about 2.4 Ma. Prior to this age, the lithology is a uniform foraminiferal-nannofossil and nannofossil ooze.

2:3 AGE-MODELS AND SEDIMENTATION RATES

2:3:1 Biostratigraphic and/or magnetostratigraphic control points ?

In the absence of magnetostratigraphic data from Sites 659 and 662, and

imprecise data from Site 658, all age-models are based on biostratigraphic datums. Reliable magnetostratigraphies were obtained at Sites 607 and 552 (Clement and Robinson, 1987; Zimmerman et al., 1984). Only three stratigraphic datums have been selected as control points for the age models at each site. Discoaster events were especially selected in the absence of magnetostratigraphic datums (Table 2:3:1). The rationale was to produce internally consistent age models between the five sites.

2:3:2 Site 659

Magnetostratigraphic data were available for most of Hole 659B, but magnetic reversals were unambiguous only in the upper section of Hole 659A, above the Olduvai subchron (Tauxe et al., 1989). Using distinct D. brouweri abundance peaks for correlation, it was possible to switch from Hole 659A to Hole 659B to obtain the extinction event, which was not recovered in 659A. Most of the species events fit a single line of the age- depth plot (Fig. 2:3:2). To develop the age model, the datums of the extinctions of D. brouweri and D. triradiatus at 1.89 Ma, the base of the D. triradiatus acme at 2.07 Ma and the extinction of D. tamalis at 2.65 Ma were used (Table 2:3:2a). Site 659 may provide new information concerning the extinction of D. surculus. Backman and Shackleton (1983) originally determined the extinction of D. surculus from several piston cores having magnetostratigraphy. Core V32-127 (North Pacific) provided an unambiguous final sharp decline in abundance of D. surculus and the age of this event was estimated to range from

Table 2:3:1 Summary of *Discoaster* events between 1.89 to 3.00 Ma from previous work (e.g., Backman and Shackleton, 1983; Backman *et al.*, 1986) * Estimate for extinction from this study.

Species	Age(Ma)	Event
D. brouweri	1.89	Extinctiom
D. triradiatus	1.89	Extinction
D. triradiatus	2.07	Peak Abundance began
D. pentaradiatus	2.33-2.43	Extinction
D. surculus	2.42-2.46	Extinction
D. surculus	2.39	Extinction *
D. asymmetricus	2.65	Abundance decline
D. tamalis	2.65	Extinction
D. variabilis	2.87-2.93	Extinction

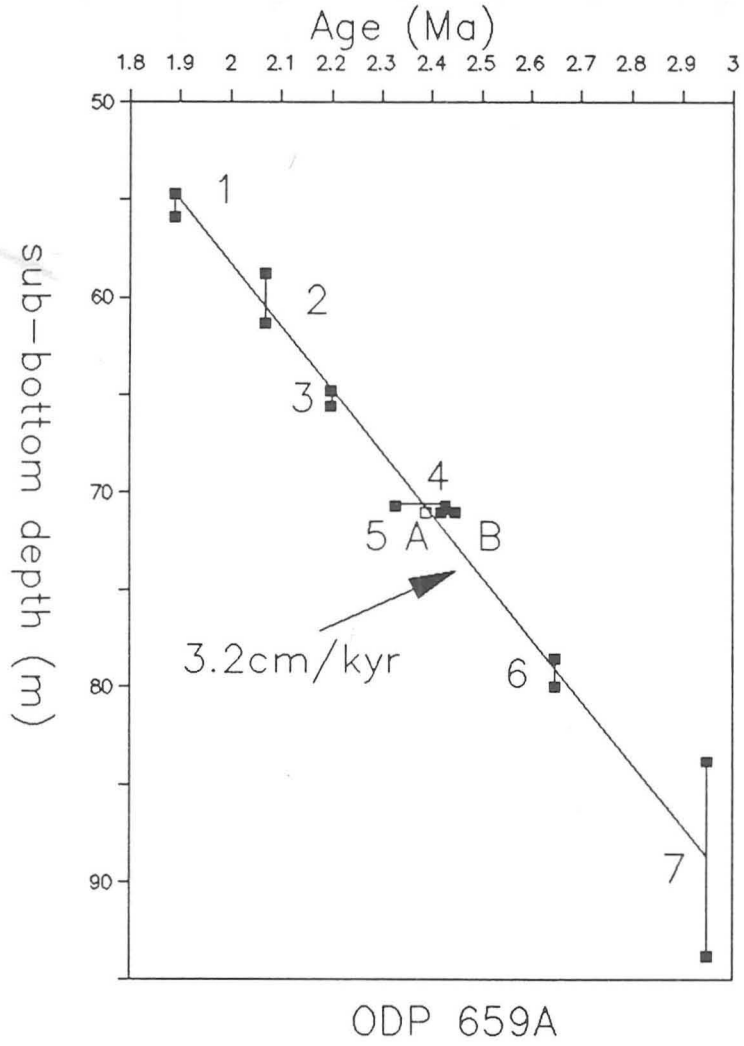

Figure 2:3:2 Age/depth relationships of biochronologic control points in Hole 659A.
Refer to Table 2:3:2b for control points used.

35

Table 2:3:2a Summary of control points used in age-models

Datum	Age(Ma)	Depth(mbsf)	Event	Sedimentation Rate
HOLE 659A				
D. brouweri	1.89	54.8	Extinction	
D. triradiatus	2.07	60.6	Peak Abundance began	3.2cm/ka
D. tamalis	2.65	79.4	Extinction	3.2cm/ka
HOLE 658A				
D. brouweri	1.89	126.4	Extinction	
D. surculus	2.39	166.0	Extinction	7.9cm/ka
G. altispira	2.95	220.0*	Extinction	9.6cm/ka
HOLE 662A				
D. brouweri	1.89	123.2	Extinction	
D. surculus	2.39	151.4	Extinction	5.6cm/ka
G. altispira	2.95	168.5*	Extinction	3.1cm/ka
HOLE 607				
D. brouweri	1.89	82.86	Extinction	
D. surculus	2.39	106.78	Extinction	4.8cm/ka
Kaena	2.99	130.73	Onset	4.0cm/ka
HOLE 552A				
D. brouweri	1.89	35.2	Extinction	
D. surculus	2.39	42.5	Extinction	1.4cm/ka
Kaena	2.99	48.6	Onset	1.0cm/ka

* (Weaver et al., 1989)

TABLE 2:3:2b Datum levels used to construct Fig. 2:3:2

HOLE 659A

Number	Datum level	Depth(mbsf)	Age(Ma)
1	LAD *D. brouweri*	54.7-55.9	1.89
2	Base of *D. triradiatus* acme	59.8-61.3	2.07
3	LAD *G. miocenica*	64.8-65.6	2.20
4	LAD *D. pentaradiatus*	70.7	2.33-2.43
5	LAD *D. surculus*	71.0	**A** 2.39(**B**2.42-2.45)
6	LAD *D. tamalis*	78.5-80.0	2.65
7	LAD *G. altispira*	83.8-93.8	2.95

A estimated from Fig. 2:3:2
B Backman and Shackleton, 1983

TABLE 2:3:3 Datum levels used to construct Fig.2:3:3

HOLE 658A

Number	Datum level	Depth(mbsf)	Age(Ma)
1	LAD *D. brouweri*	124.7-126.9	1.89
2	Base of *D. triradiatus* acme	135.0-145.0	2.07
3	LAD *G. miocenica*	154.3-157.7	2.20
4	LAD *D. pentaradiatus*	165.5	2.33-2.43
*5	LAD *D. surculus*	166.0	2.39
6	LAD *D. tamalis*	197.7-201.3	2.65
7	LAD *G. altispira*	214.9-224.4	2.95
D	Diagenetic event	157.8-158.4	2.30+

*LAD for *D. surculus* taken as 2.39 Ma from Site 659 (Table 2:3:2 b)

+ inferred from Fig. 2:3:3

2.38 to 2.44 Ma in this core. Subsequently Backman and Pestiaux (1987) derived an age ranging from 2.42 to 2.46 Ma for the D. surculus extinction event, based on a less clear final abundance pattern obtained from DSDP Hole 606 (North Atlantic). The question of whether or not this species experienced a synchronous extinction in different ocean basins (or latitudes) thus will remain open until additional independent evidence, like highly resolved stable isotope stratigraphy can be used for precise calibration. Currently the uncertainty is about 80 ka , between 2.38 and 2.46 Ma.

The three Leg 108 sites, Sites 658, 659 and 662 analyzed in this study reveal rather similar patterns of abundance variation of D. surculus, particularly towards the end of its range, finishing with a final sharp abundance peak which is likely to be synchronous. The Plio-/Pleistocene sedimentation rate at Site 659 appears extremely constant (Ruddiman, Sarnthein et al., 1988), fitting all available biostratigraphic datum events from the LAD of D. brouweri at 1.89 Ma to the LAD of G. altispira at 2.95 Ma (Fig. 2:3:2 and Table 2:3:2b). Only the LAD of D. surculus falls slightly off the line if the age estimate from DSDP Site 606 is used. As a working hypothesis the age of the extinction of D. surculus is re-estimated on the basis of the apparently linear sedimentation rate at Site 659. This gives a value of 2.39 Ma for the final abundance peak which is within the range of the estimates derived from Core V32- 127 (Backman and Shackleton, 1983). This value of 2.39 Ma has been used for all other investigated sites in order to produce consistent age models.

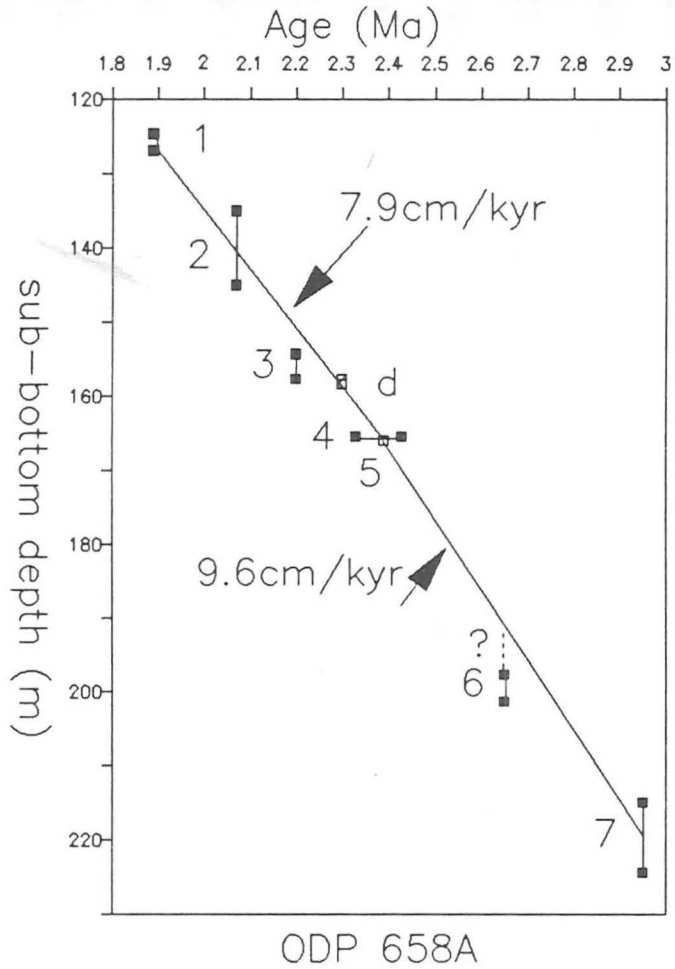

Figure 2:3:3 Age/depth relationship of biochronologic and magnetostratigraphic control points in Hole 658A. Refer to Table 2:3:3 for control points used.

2:3:3 Site 658

Magnetostratigraphic data is available for the interval representing the base of the Olduvai, but the Matuyama/Gauss boundary transition was scattered over a long depth interval and is considered unreliable. Only biostratigraphic datums have been used in order to be internally consistent in the construction of the age-depth plot at Site 658 (Fig. 2:3:3 and Table 2:3:3). Discoaster brouweri provided a clear extinction, but the base of the D. triradiatus acme has a fairly wide depth range which probably is due to the low numbers of these two species. A line was drawn through the extinction of D. brouweri to the extinction of D. surculus passing through the range of estimates for the base of the D. triradiatus acme and the extinction of D. pentaradiatus.

For the rest of the age-depth plot for Site 658, a line was drawn from the extinction of D. surculus through the extinction of G. altispira at 2.95 Ma (Ruddiman, Sarnthein et al., 1988). Discoaster tamalis was not useful in the age-depth plot as it occurred in too low numbers to give a reliable datum. In the age- model the extinction datums of D. brouweri, D. surculus and G. altispira were used (Table 2:3:2a).

An interesting diagenetic event, the formation of a possible "hardground" occurs at between 157.8 and 158.4 mbsf, is associated with some reworking of D. pentaradiatus and D. surculus. This diagenetic event necessitated a change of drilling from Hydraulic Piston Corer (HPC) to Extended Core Barrel (XCB). The age-model suggests an age of approximately

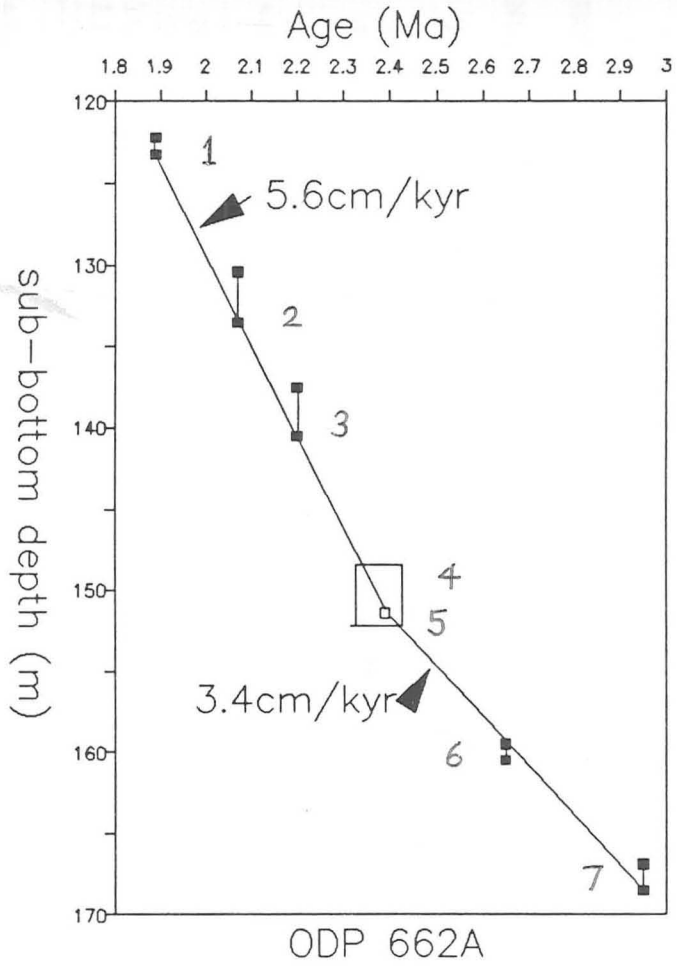

Figure 2:3:4 Age/depth relationships of biochronologic control points in Hole 662A. Refer to Table 2:3:4 for control points used.

TABLE 2:3:4 Datum levels used to construct Fig. 2:3:4

HOLE 662A

Number	Datum level	Depth(mbsf)	Age(Ma)
1	LAD *D. brouweri*	122.2-123.2	1.89
2	Base of *D. triradiatus* acme	130.4-133.5	2.07
3	LAD *G. miocenica*	137.5-140.5	2.20
4	LAD *D. pentaradiatus*	148.3-152.1	2.33-2.43
* 5	LAD *D. surculus*	151.4	2.39
6	LAD *D. tamalis*	159.5-160.5	2.65
7	LAD *G. altispira*	166.9-168.5	2.95

TABLE 2:3:5 Datum levels used to construct Fig.2:3:5

HOLE 607

Number	Datum level	Depth(mbsf)	Age(Ma)
1	Olduvai (Termination)	72.08-74.18	1.66
2	(Onset)	81.68-82.46	1.88
3	LAD *D. brouweri*	81.80-83.10	1.89
4	Base of *D. triradiatus* acme	90.60-91.48	2.07
5	LAD *D. pentaradiatus*	106.35-107.38	2.33-2.43
*6	LAD *D. surculus*	106.78-108.52	2.39
7	Matuyama/Gauss boundary	108.98-110.57	2.47
8	LAD *D. tamalis*	111.90-116.68	2.65
9	Kaena (Termination)	126.68-128.18	2.92
10	(Onset)	129.68-131.78	2.99
11	Mammoth(Top)	133.28-135.05	3.08
12	(Bottom)	137.78-139.28	3.18

*LAD for *D. surculus* taken as 2.39 Ma from Site 659 (Table 2:3:2b)

2.3 Ma for the diagenetic event.

2:3:4 Site 662

There was no magnetic stratigraphy available at Site 662 (Fig. 2:3:4 and Table 2:3:4), and reworking was noticeably greater than at Sites 659 and 658. This site was affected by slumping, but this was only above the interval studied. Due to the reworking, some events such as the base of the D. triradiatus acme were difficult to identify precisely. Discoaster pentaradiatus was heavily reworked through the interval, and it is important to have some concept of the background reworking level when defining extinction events. Discoaster surculus again displays a distinct peak immediately prior to its extinction. The extinction of D. tamalis (2.65 Ma) is clearly defined. From the age-depth plot, the extinction of D. brouweri, D. surculus and G. altispira were selected as datums to be used in the age- model (Table 2:3:2a).

2:3:5 Site 607

Reliable magnetic stratigraphy was obtained at Site 607 (Fig. 2:3:5 and Table 2:3:5) (Clement and Robinson, 1987). A straight line connects the top of the Olduvai with the extinction of D. surculus at 2.39 Ma, passing through the base of the Olduvai, the extinction of D. brouweri, the base of the acme of D. triradiatus and the extinction of D. pentaradiatus. Prior to 2.39 Ma, there is a slightly lower sedimentation rate, but a constant rate is evident between the extinction of D. surculus and the onset of the Mammoth (3.18 Ma), passing

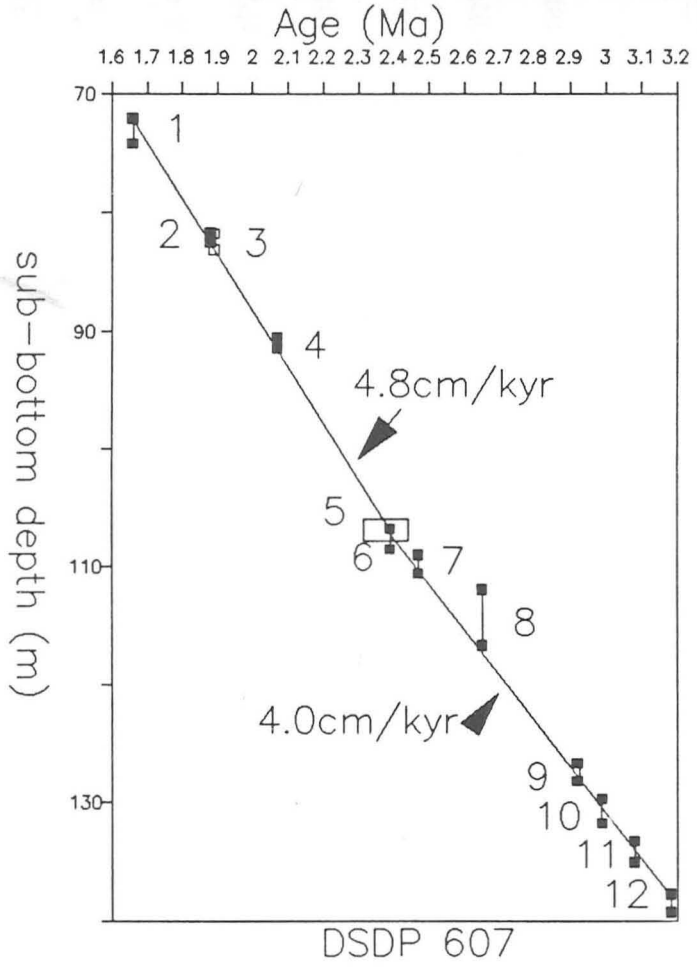

Figure 2:3:5 Age/depth relationships of biochronologic and magnetostratigraphic control points in Hole 607. Refer to Table 2:3:5 for control points used.

through the Matuyama/Gauss boundary, the termination and onset of the Kaena and the termination of the Mammoth at 3.08 Ma. Discoaster tamalis was not useful because the extinction was disguised by reworking, clearly indicated by the presence of R. pseudoumbilica (LAD 3.56 Ma). From the age-depth plot, the LAD of D. brouweri and D. surculus and the midpoint in terms of subbottom depth of the onset of the Kaena (2.99 Ma) were selected as control points for the age-model (Table 2:3:2a).

2:3:6 Site 552

Reliable magnetic stratigraphy was available at Site 552 and helped verify that in spite of the extremely low abundances of discoasters at such high latitudes, the events recognized were genuine and not an artifact of reworking (Fig. 2:3:6 and Table 2:3:6)(Backman et al., 1986). An apparently linear sedimentation rate connects the termination of the Olduvai and the extinction of D. surculus (2.39 Ma), passing through the extinction of D. brouweri, (and close to the onset of the Olduvai), the base of the D. triradiatus acme and the extinction of D. pentaradiatus. Prior to 2.39 Ma, there is a slight reduction in the sedimentation rate, but a straight line can be drawn through the Matuyama/Gauss boundary, the extinction of D. tamalis and the onset of the Kaena, passing close to the termination of the Kaena. From the age-depth plot, the LAD of D. brouweri, D. surculus and the onset of the Kaena were selected as control points for the age-model (Table 2:3:2a). Sedimentation rates at this site were much lower than any of the other sites.

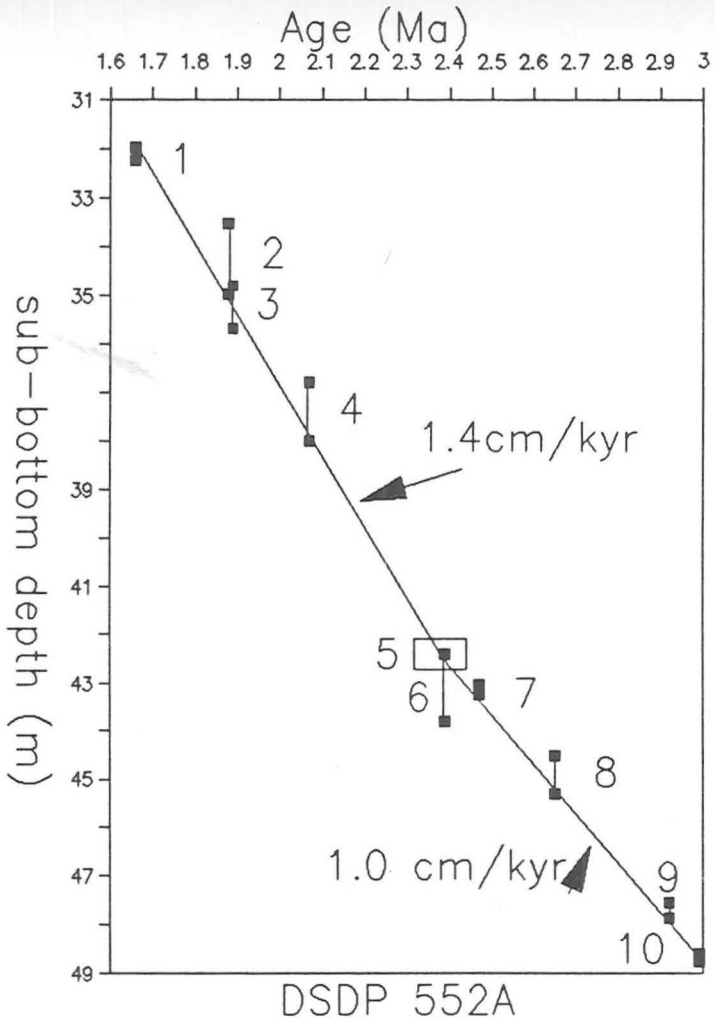

Figure 2:3:6 Age/depth relationship of biochronologic and magnetostratigraphic control points in Hole 552A. Refer to Table 2:3:6 for control points used.

TABLE 2:3:6 Datum levels used to construct Fig.2:3:6

HOLE 552A

Number	Datum level	Depth(mbsf)	Age(Ma)
1	Olduvai (Termination)	31.96-32.24	1.66
2	(Onset)	33.53-34.96	1.88
3	LAD *D. brouweri*	34.80-35.69	1.89
4	Base of *D. triradiatus* acme	36.79-38.00	2.07
5	LAD *D. pentaradiatus*	42.20-42.60	2.33-2.43
*6	LAD *D. surculus*	42.40-43.80	2.39
7	Matuyama/Gauss boundary	43.04-43.24	2.47
8	LAD *D. tamalis*	44.50-45.30	2.65
9	Kaena (Termination)	47.53-47.86	2.92
10	(Onset)	48.58-48.75	2.99

*LAD for *D. surculus* taken as 2.39 Ma from Site 659 (Table 2:3:2b).

2:4 Discoaster species abundance patterns

Smear slides were prepared and counted as described by Backman and Shackleton (1983). The number of viewfields selected is related to the overall abundance of discoasters at each site. Normally a constant number of viewfields are used for a single site, except possibly during intervals of extremely low abundances. The abundances between sites are made directly comparable by multiplying by a conversion factor which gives the abundances per mm^2 of slide. In Site 659, only 20 viewfields were counted in view of the high Discoaster abundances. This is at a viewfield diameter of 0.3 mm which contains roughly 250 nannofossils or other particles in each viewfield. In Site 658, where the abundances observed were found to be much lower, 40 viewfields were used. Similarly, at Site 662, 40 viewfields were counted. At Site 552, where low abundances were observed due to its high latitiude, 100 viewfields were used. Lastly, at Site 607, the second highest latitude site, 30 viewfields were counted at a viewfield diameter of 0.28mm, as a different microscope was used for this site (J. Backman, Pers. Comm.) Because all counts were converted to number per unit area, this method was found to be a convenient tool for rapidly gathering reproducible data and for comparing different sites.

2:4:1 Discoaster brouweri and Discoaster triradiatus

The extinction of these two species appears synchronous at 1.89 Ma. An interesting phenomenon occurs globally at 2.07 Ma, when D. triradiatus

increases in the proportion (>20%) relative to D. brouweri, whereas prior to 2.07 Ma it is relatively insignificant (Backman and Shackleton, 1983). This relationship between D. brouweri and D. triradiatus is clearly shown at all five sites (Figs. 2:4:1a-e). Backman and Shackleton (1983), Backman et al. (1986) and Backman and Pestiaux (1987), only illustrated the abundance of D. triradiatus relative to D. brouweri and not the absolute abundances of D. triradiatus. The D. triradiatus acme is compared between the five sites in Figure 2:4:1f. At all sites this acme is observed including DSDP 552, where the time resolution and abundances are low. It should be mentioned prior to 2.07 Ma that anomalously high percentages of D. triradiatus in relation to the sum of itself and D. brouweri are the result of a few specimens of D. triradiatus occurring during times of low abundance of D. brouweri. An example of this occurs at Site 607 (Fig. 2:4:1a) at 2.3 Ma when the triradiate form composes 50%, representing only one specimen of D. triradiatus and one specimen of D. brouweri.

In Figure 2:4:1g, the mean abundance of D.triradiatus/mm^2 is shown versus modern sea surface temperature at the five sites. This shows the drastic reduction in abundance above 41°N and with upwelling conditions. Figure 2:4:1h displays the mean of the percentage relationship between D. brouweri and D. triradiatus versus modern sea-surface temperature. This clearly demonstrates that the D. triradiatus acme is independent of latitude or upwelling conditions in spite of the variation in absolute abundances.

Discoaster brouweri is the only species covering the complete time interval

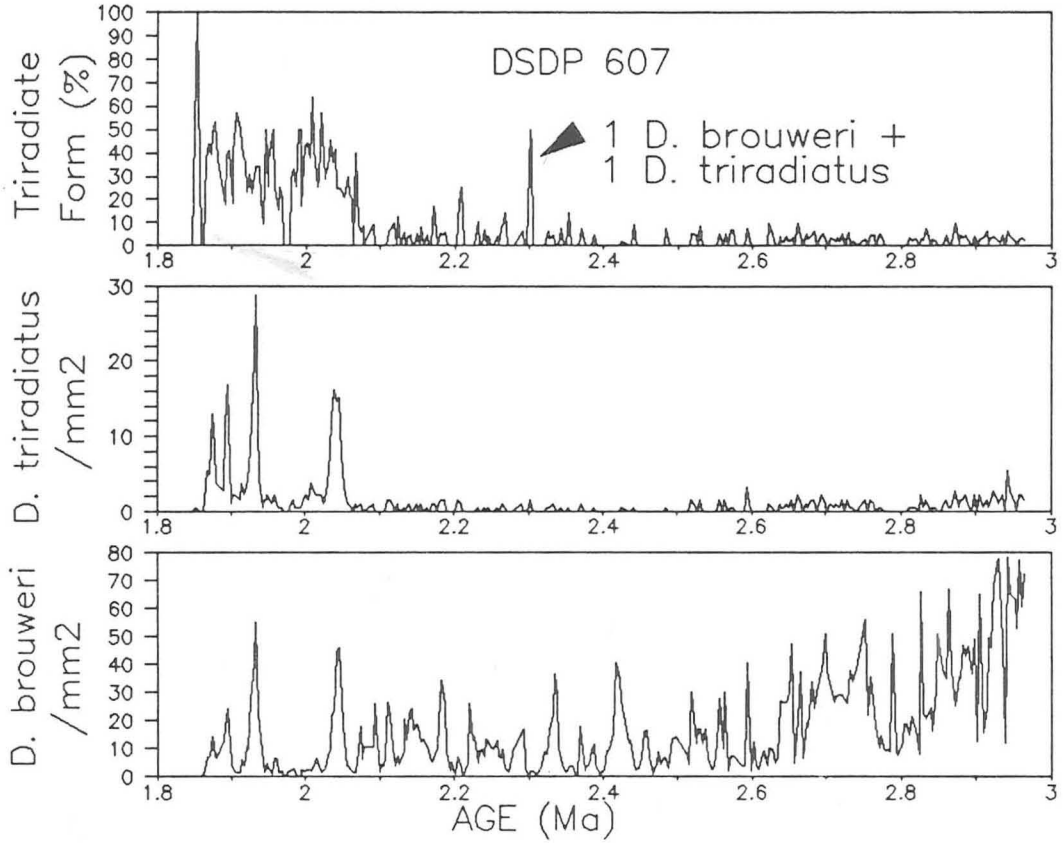

Figure 2:4:1a Abundance plots of D. brouweri and D. triradiatus at Site 607. The percentage of the triradiate form is the relative abundance of D. triradiatus to the sum of this species with D. brouweri

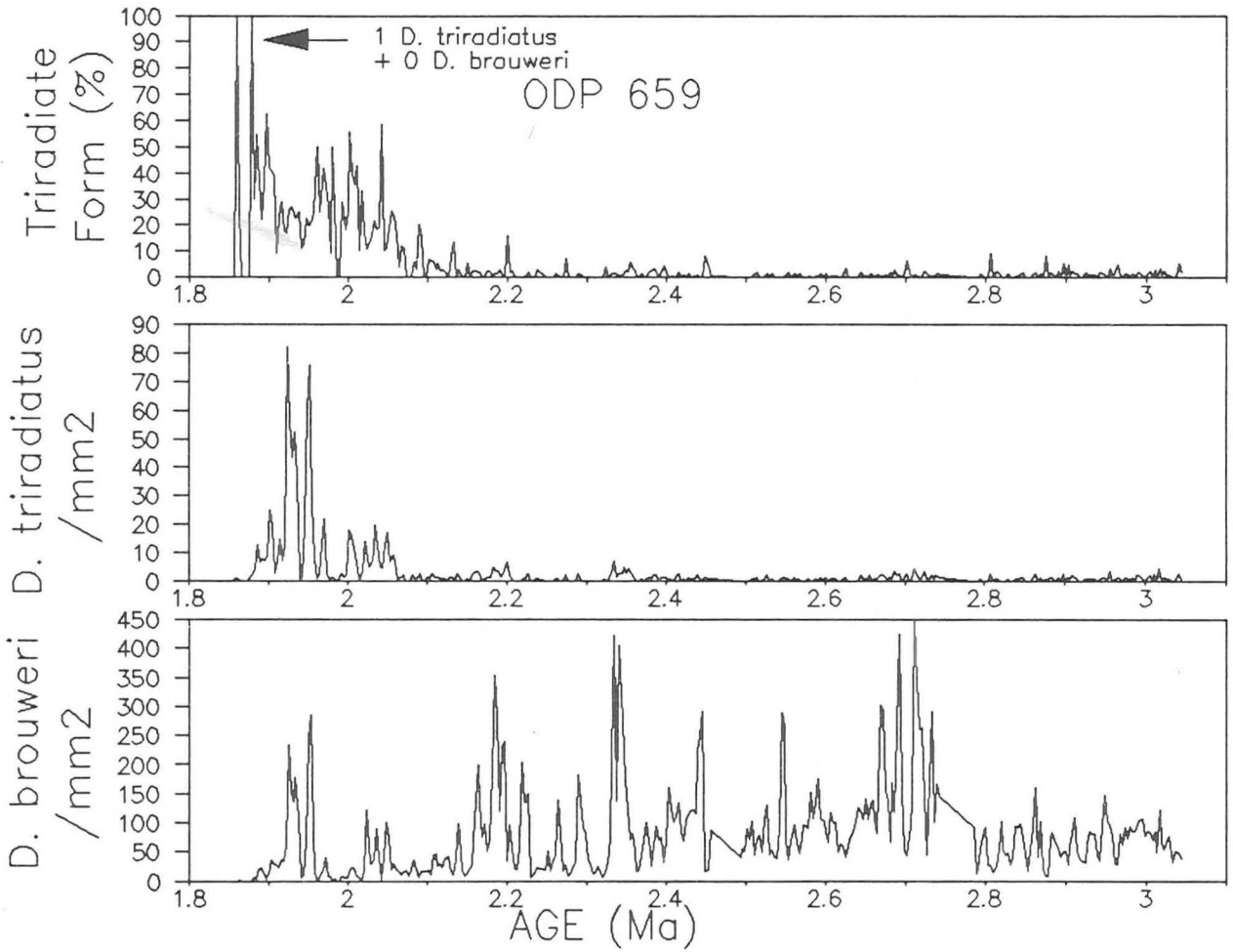

Figure 2:4:1b Abundance plots of D. brouweri and D. triradiatus at Site 659.

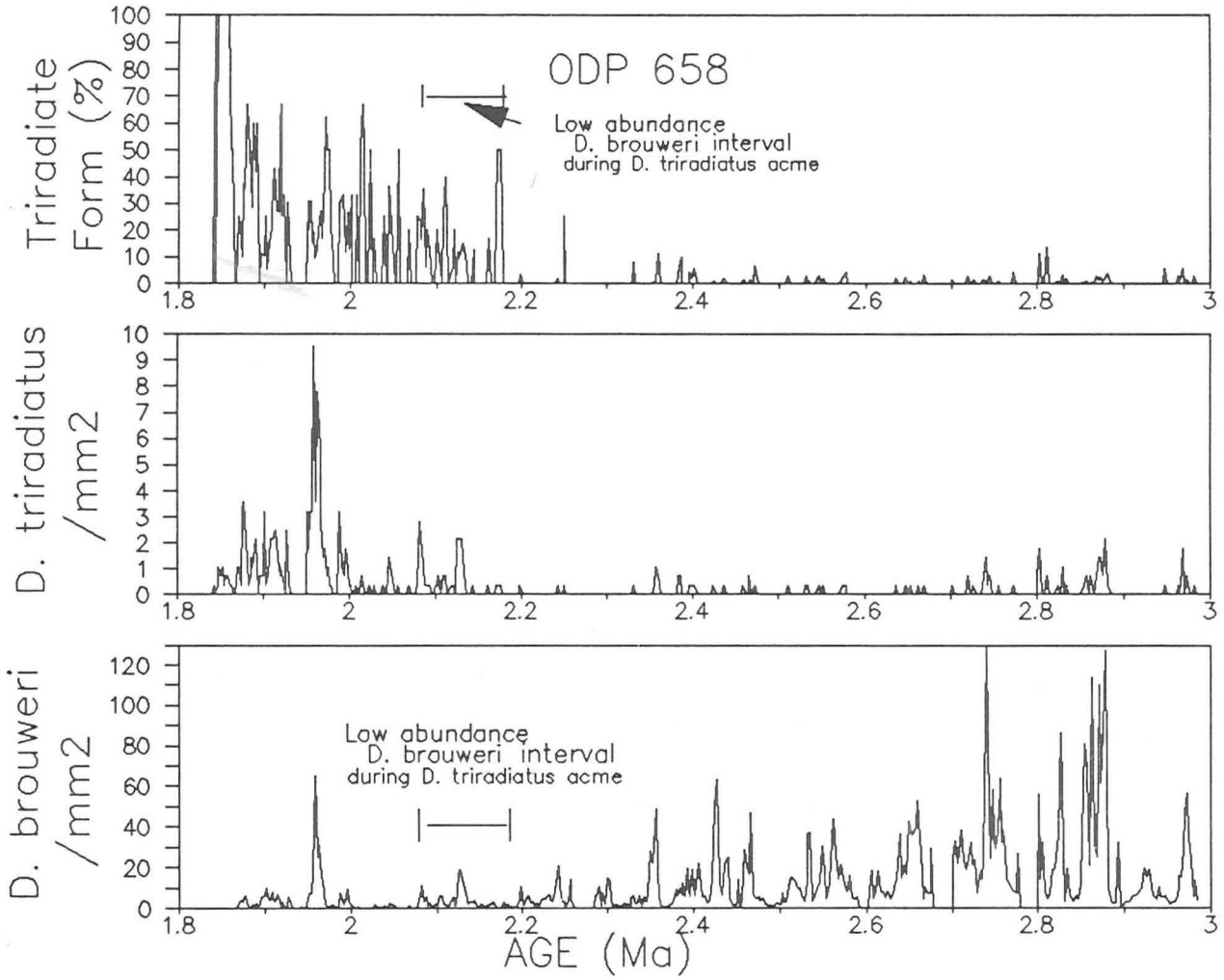

Figure 2:4:1c Abundance plots of D. brouweri and D. triradiatus at Site 658.

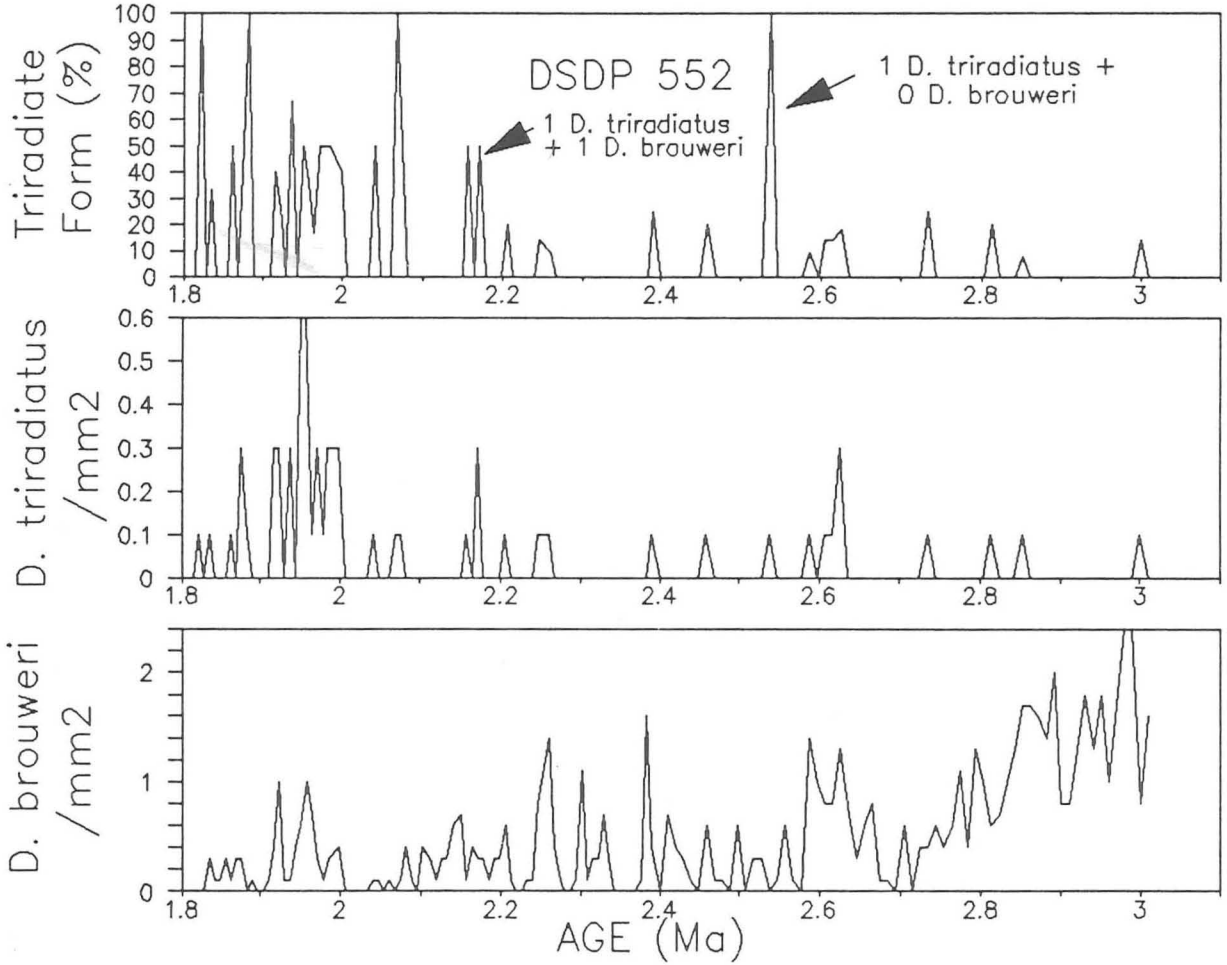

Figure 2:4:1d Abundance plots of D. brouweri and D. triradiatus at Site 552.

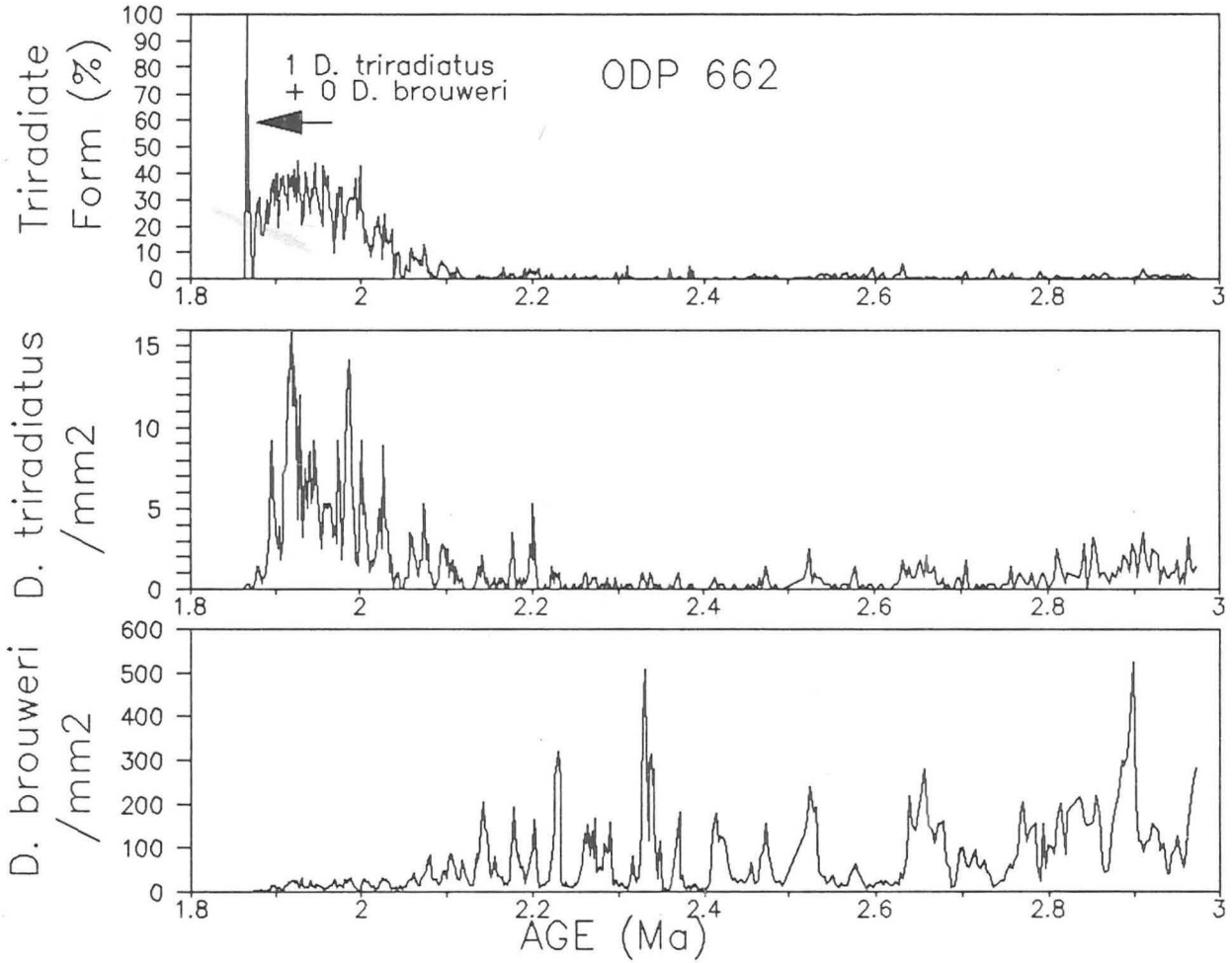

Figure 2:4:1e Abundance plots of D. brouweri and D. triradiatus at Site 662

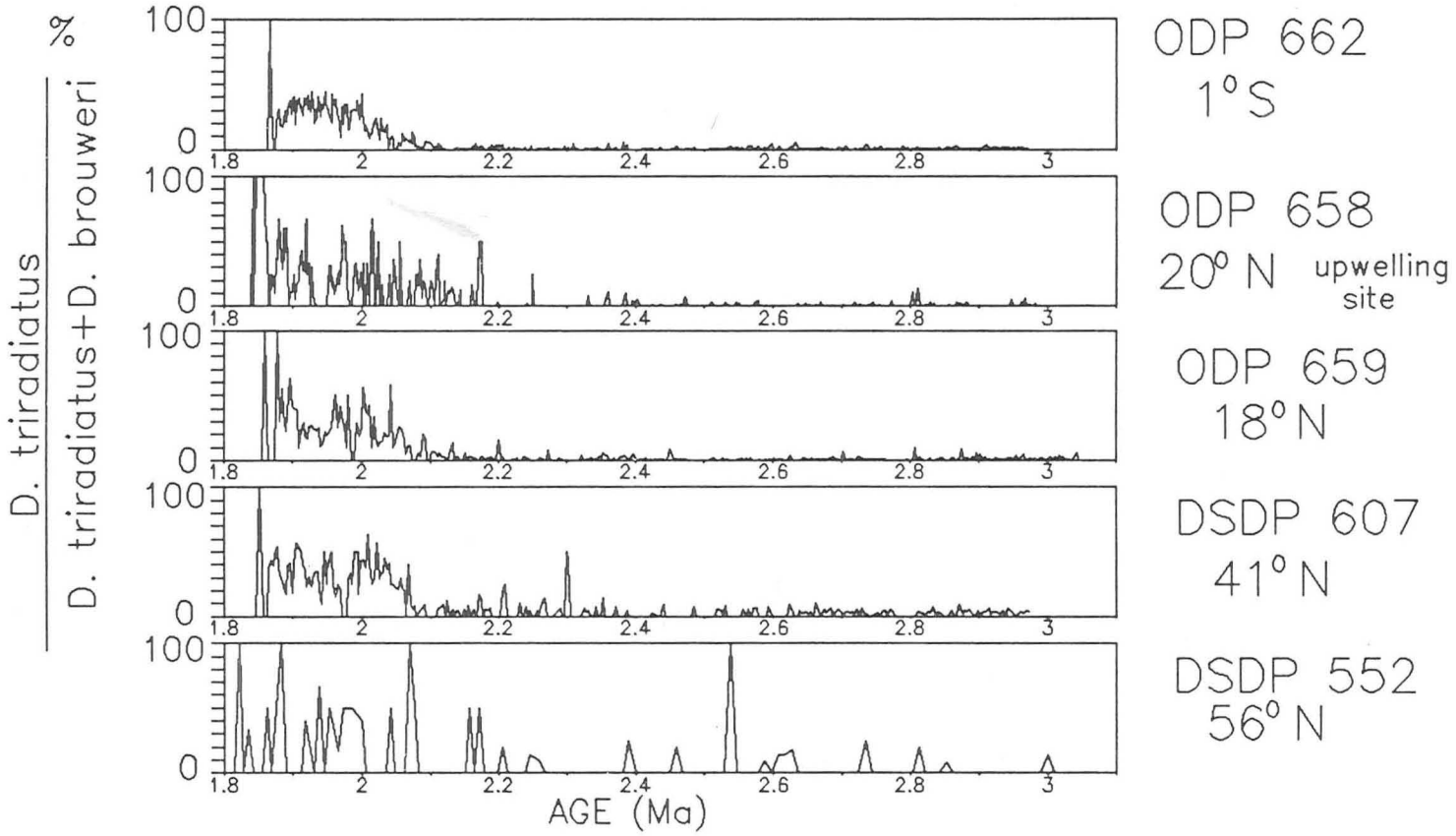

Figure 2:4:1f Percentage abundance plots of D. triradiatus as a percentage of the sum of D. triradiatus and D. brouweri at Sites 552, 607, 659, 658 and 662.

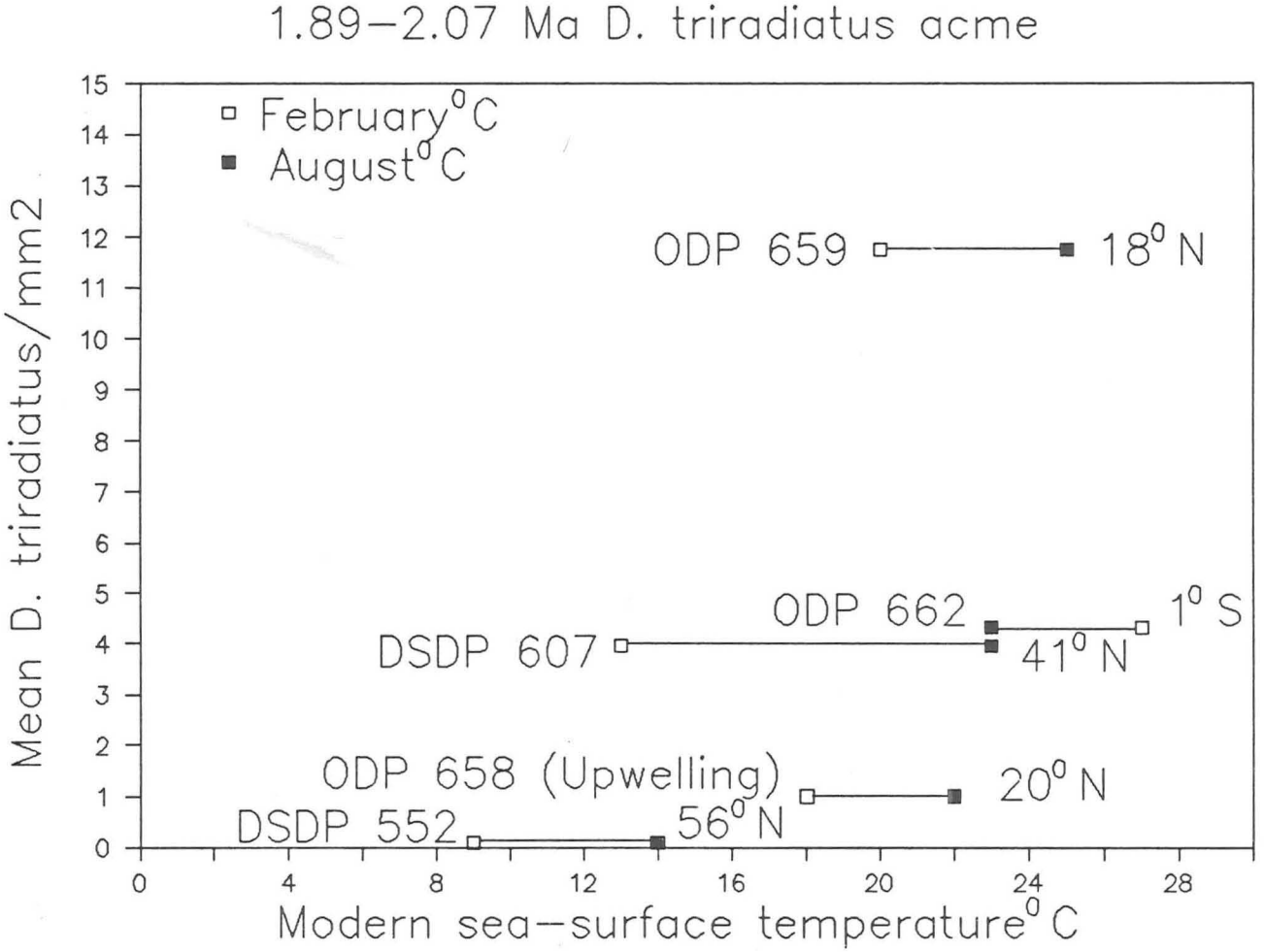

Figure 2:4:1g Mean D. triradiatus/mm2 versus modern sea–surface temperature at Sites 552, 607, 659, 658 and 662.

studied i.e., 1.89-3.00 Ma. Besides the brief acme of D. triradiatus, D. brouweri is the sole surviving species between approximately 1.89-2.35 Ma (Fig. 2:4:1i). The gradual abundance reduction of D. brouweri through time is very apparent. A marked abundance reduction in D. brouweri at approximately 2.4 Ma is clearly seen, especially at the high latitude and upwelling sites. In Figure 2:4:1j, the mean of D. brouweri/mm^2 is shown versus modern sea-surface temperature for the five sites. This shows a distinct abundance reduction for D. brouweri above 18°N and with upwelling conditions.

Figure 2:4:1k shows the relative abundance of D. brouweri as a percentage of the complete Discoaster assemblage. The interesting phenomenon is to be noted prior to 2.35 Ma, when moving into the range of the other Discoaster species. This shows that the other species form a greater component of the Discoaster assemblage with increasing latitude and upwelling conditions. If the mean relative abundance of D. brouweri is plotted against modern sea-surface temperature, this trend is clearly demonstrated (Fig. 2:4:1l).

2:4:2 Discoaster pentaradiatus and Discoaster surculus

The abundance of these two species has been compared in different cores and ocean basins by Backman and Shackleton (1983), Backman et al. (1986) and Backman and Pestiaux (1987) and the extinctions are estimated to occur at 2.35-2.45 Ma. It is widely agreed that D. surculus disappeared slightly earlier than D. pentaradiatus (e.g., Martini, 1971; Bukry, 1973a, 1975), which is confirmed at the five Atlantic sites discussed here.

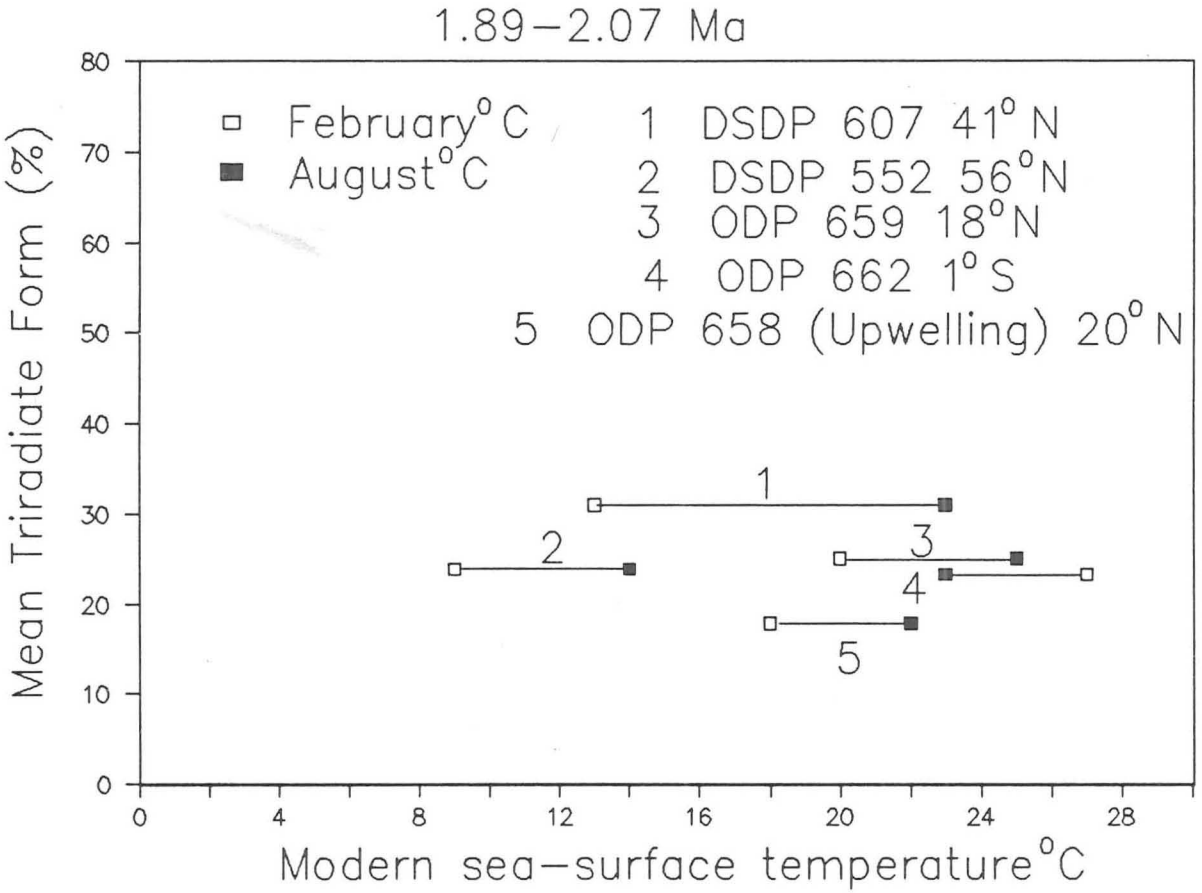

Figure 2:4:1h Mean Triradiate Form (%) versus modern sea–surface temperature at Sites 552, 607, 659, 658 and 662.

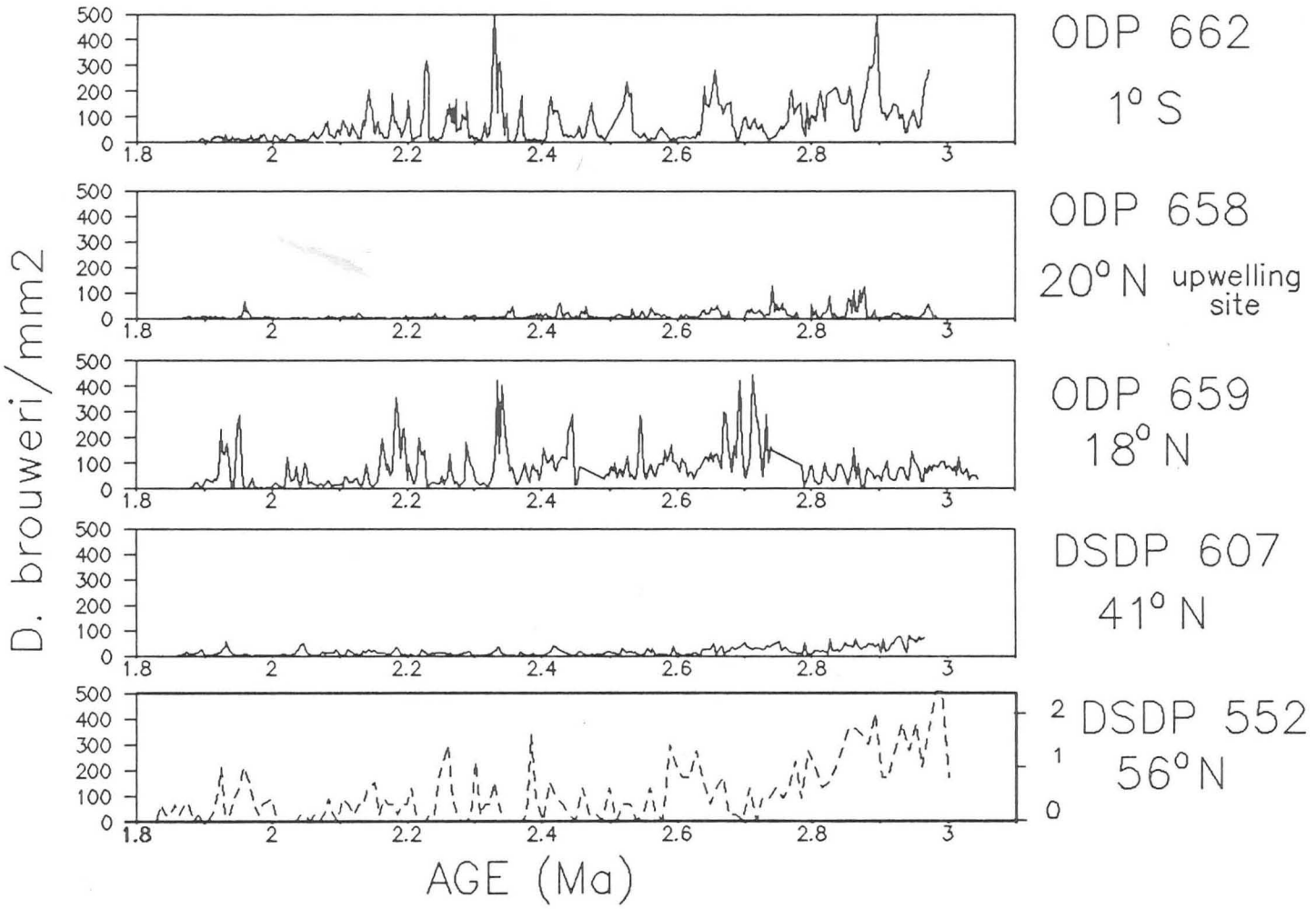

Figure 2:4:1i Abundance plots of D. brouweri at Sites 552, 607, 659, 658 and 662.

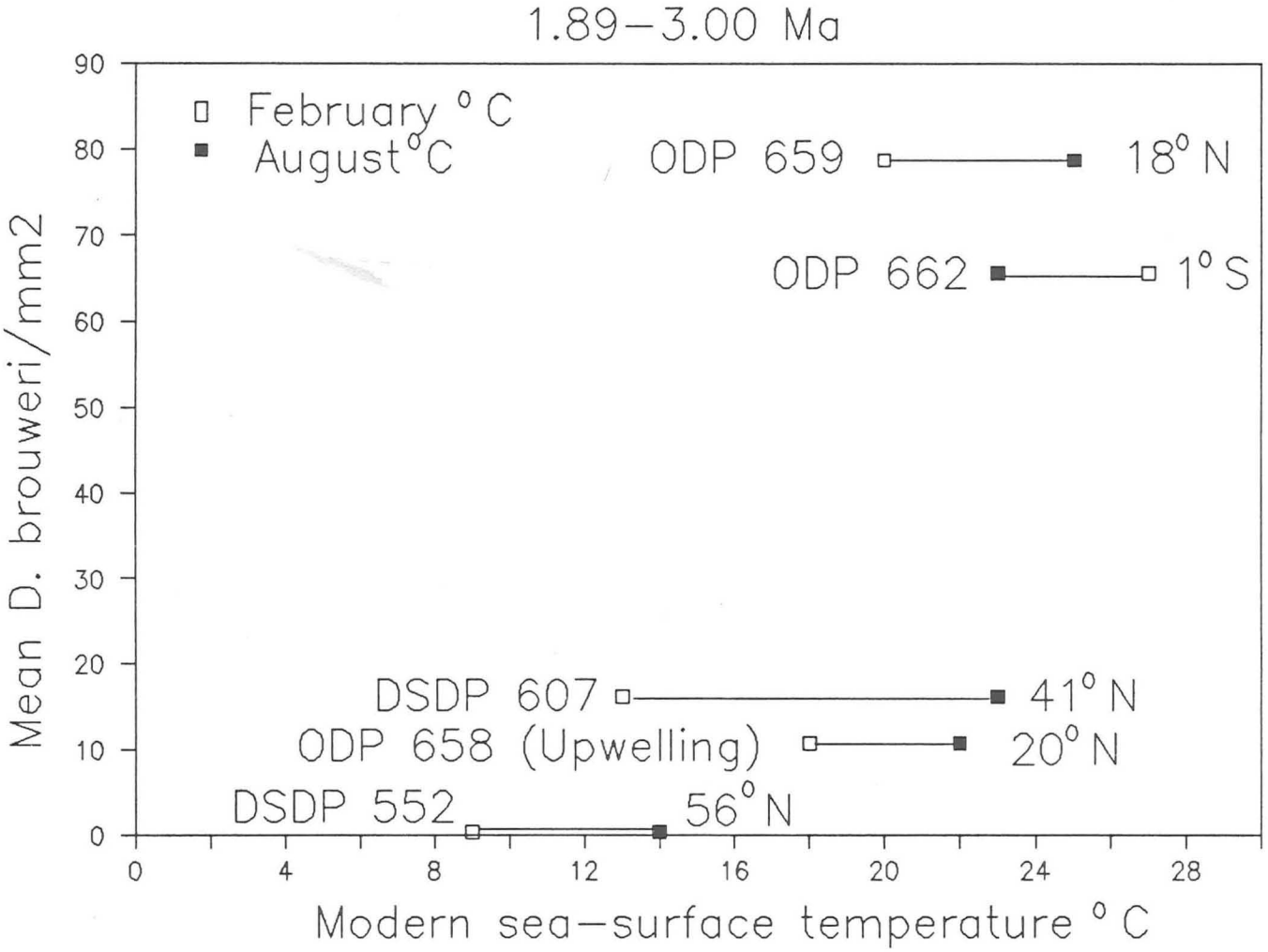

Figure 2:4:1j Mean D. brouweri/mm2 versus modern sea–surface temperature at Sites 552, 607, 659, 658 and 662.

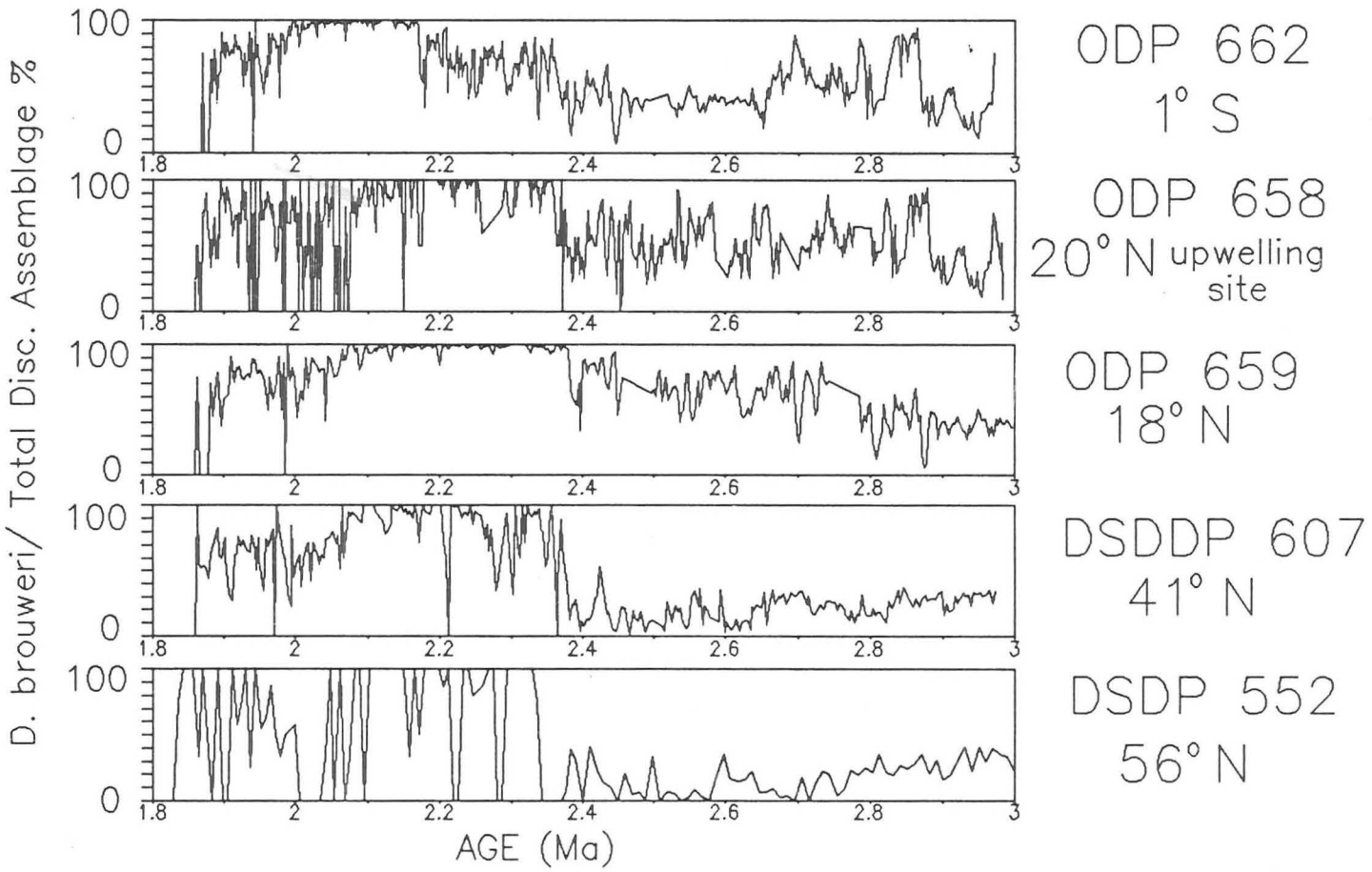

Figure 2:4:1k Percentage abundance plots of D. brouweri at Sites 552, 607, 659, 658 and 662.

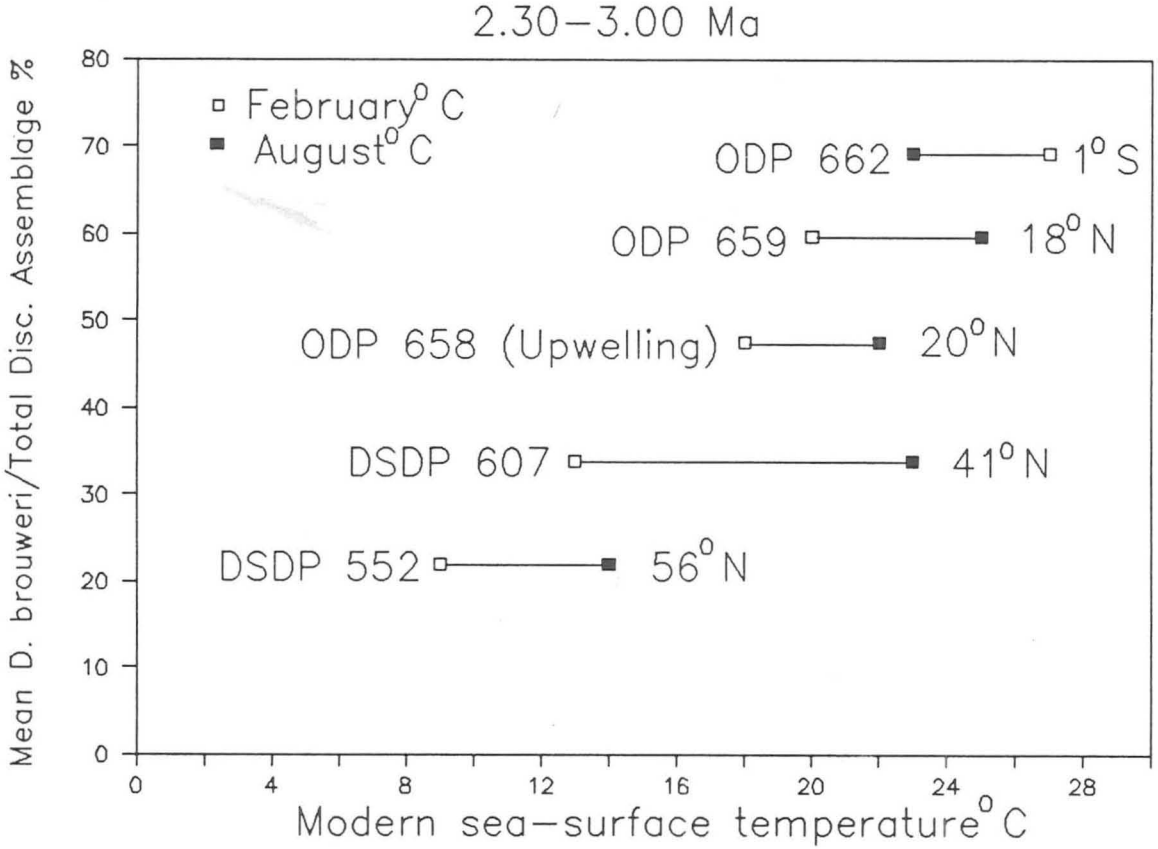

Figure 2:4:11 Mean percentage D. brouweri /Total Discoaster Assemblage versus modern sea–surface temperature at Sites 552, 607, 659, 658 and 662.

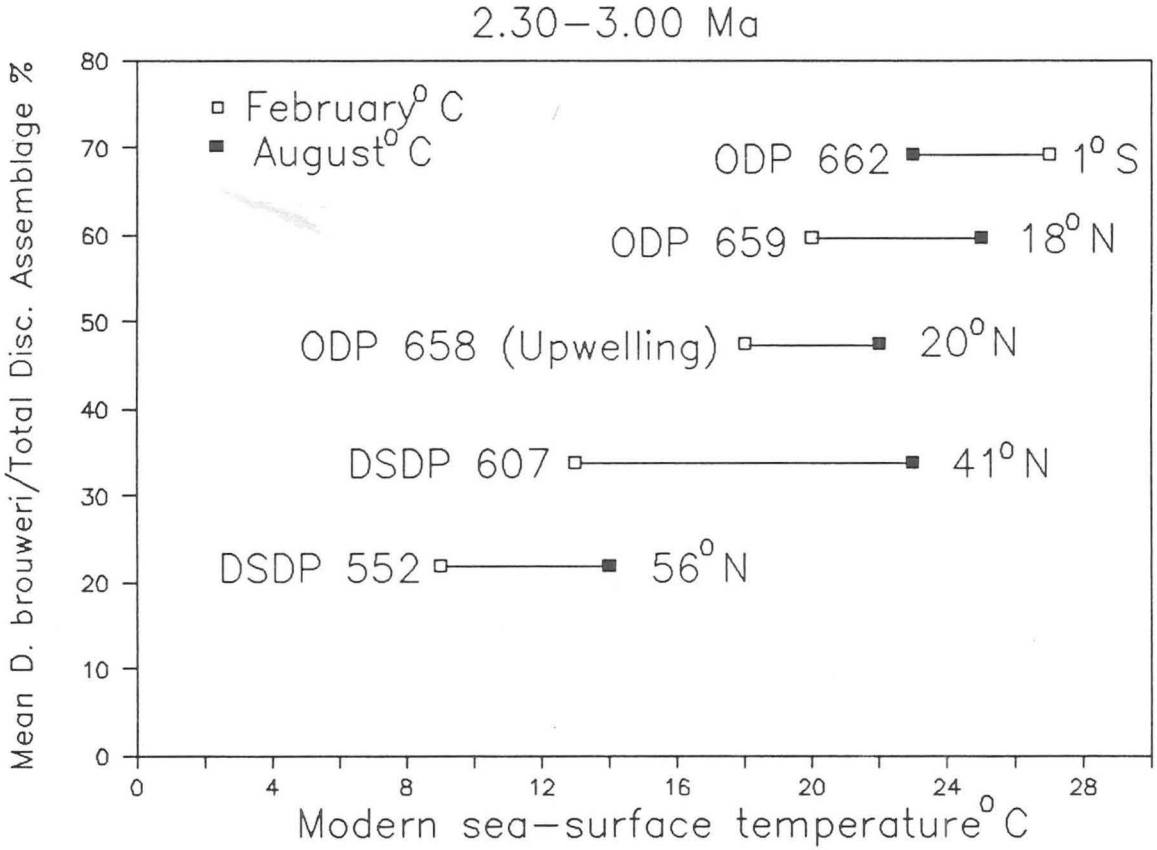

Figure 2:4:11 Mean percentage D. brouweri /Total Discoaster Assemblage versus modern sea–surface temperature at Sites 552, 607, 659, 658 and 662.

Figure 2:4:2a shows the abundance of D. pentaradiatus at the five sites. The patterns in this are simplified by showing the mean abundance of D. pentaradiatus versus modern sea surface temperature (Fig. 2:4:2b). One would conclude that there is a drastic reduction in absolute abundance above 41°N and with upwelling conditions. If D. pentaradiatus is displayed as a percentage of the complete Discoaster assemblage, it becomes apparent that D. pentaradiatus forms a constant high proportion of the assemblage at all five sites (Fig. 2:4:2c). This is demonstrated even clearer by plotting the mean relative abundance of D. pentaradiatus versus modern sea-surface temperature (Fig. 2:4:2d). There appears to be a minor increase of D. pentaradiatus within the complete Discoaster assemblage with increasing latitude.

Discoaster surculus (Fig. 2:4:2e) was found to finish with a final sharp peak at the end of its range in the three Leg 108 sites (Sites 658, 659 and 662) which is assumed to be synchronous. Bukry (1978) observed that amongst the "warm water" genus Discoaster, D. surculus favoured the cooler end of the warm water spectrum. There is a definite increase with higher latitude and upwelling conditions. Between 41°N and 56°N, a drastic reduction in absolute abundance of D. surculus occurs. These patterns can further be represented by plotting the mean abundance of D. surculus/mm² versus modern sea-surface temperature (Fig. 2:4:2f).

By representing D. surculus as a percentage of the complete Discoaster assemblage reveals even clearer trends (Fig. 2:4:2g). Discoaster surculus is shown to increase within the Discoaster assemblage as a function of increasing latitude

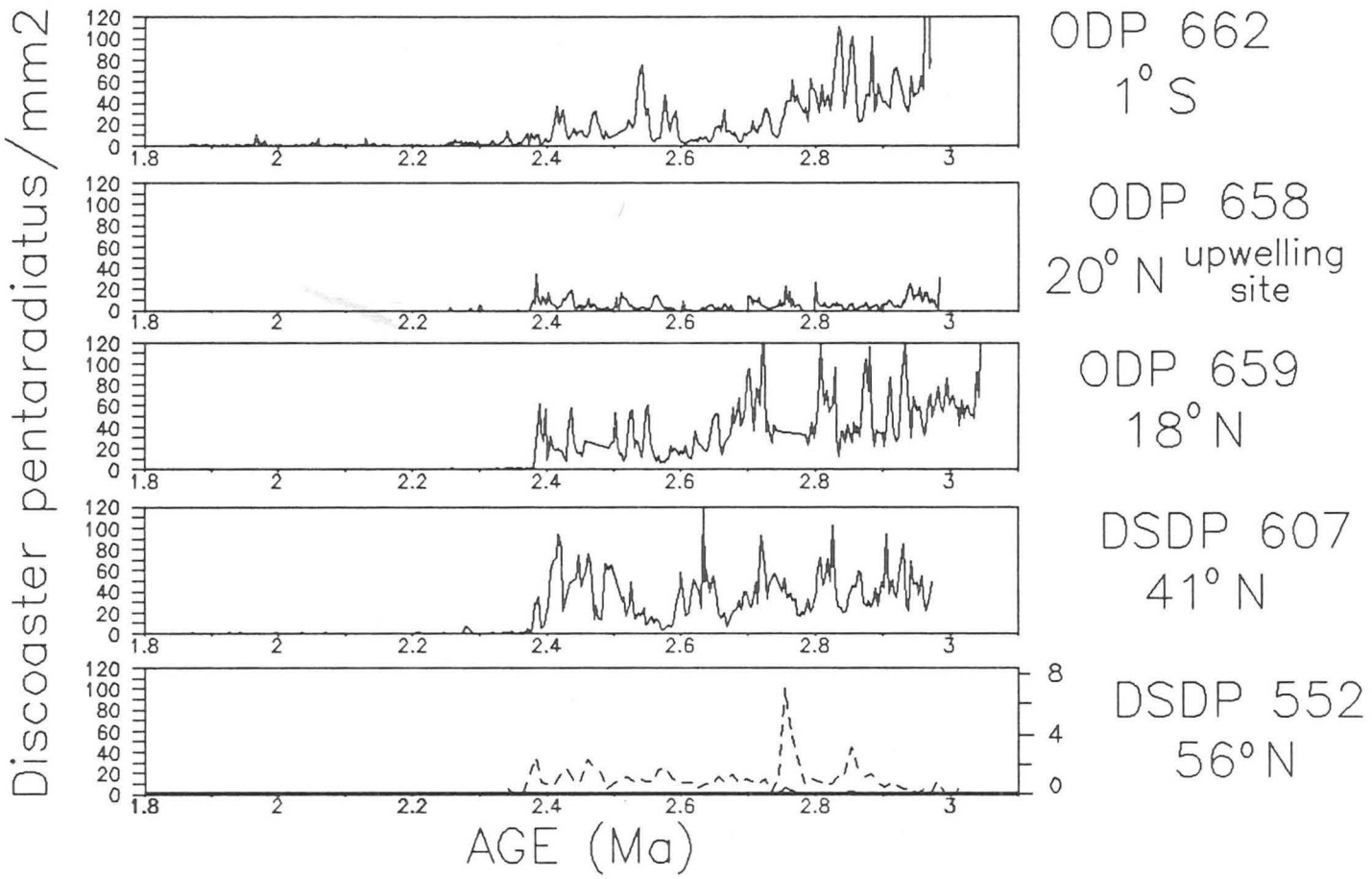

Figure 2:4:2a Abundance plots of D. pentaradiatus at Sites 552, 607, 659, 658 and 662. The abundance scale has been reduced five times in comparison with the abundance plots of D. brouweri.

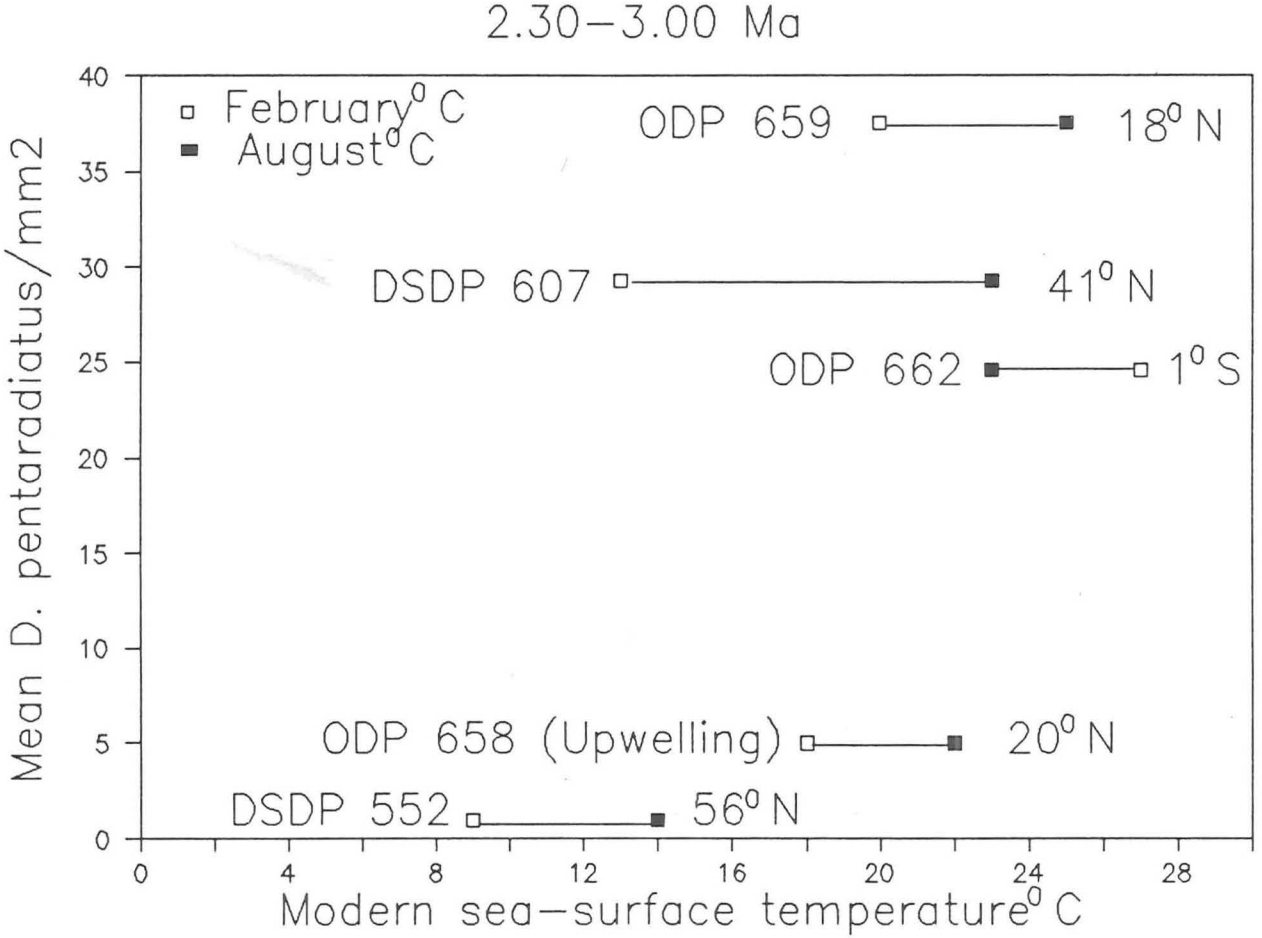

Figure 2:4:2b Mean D. pentaradiatus/mm2 versus modern sea–surface temperature at Sites 552, 607, 659, 658 and 662.

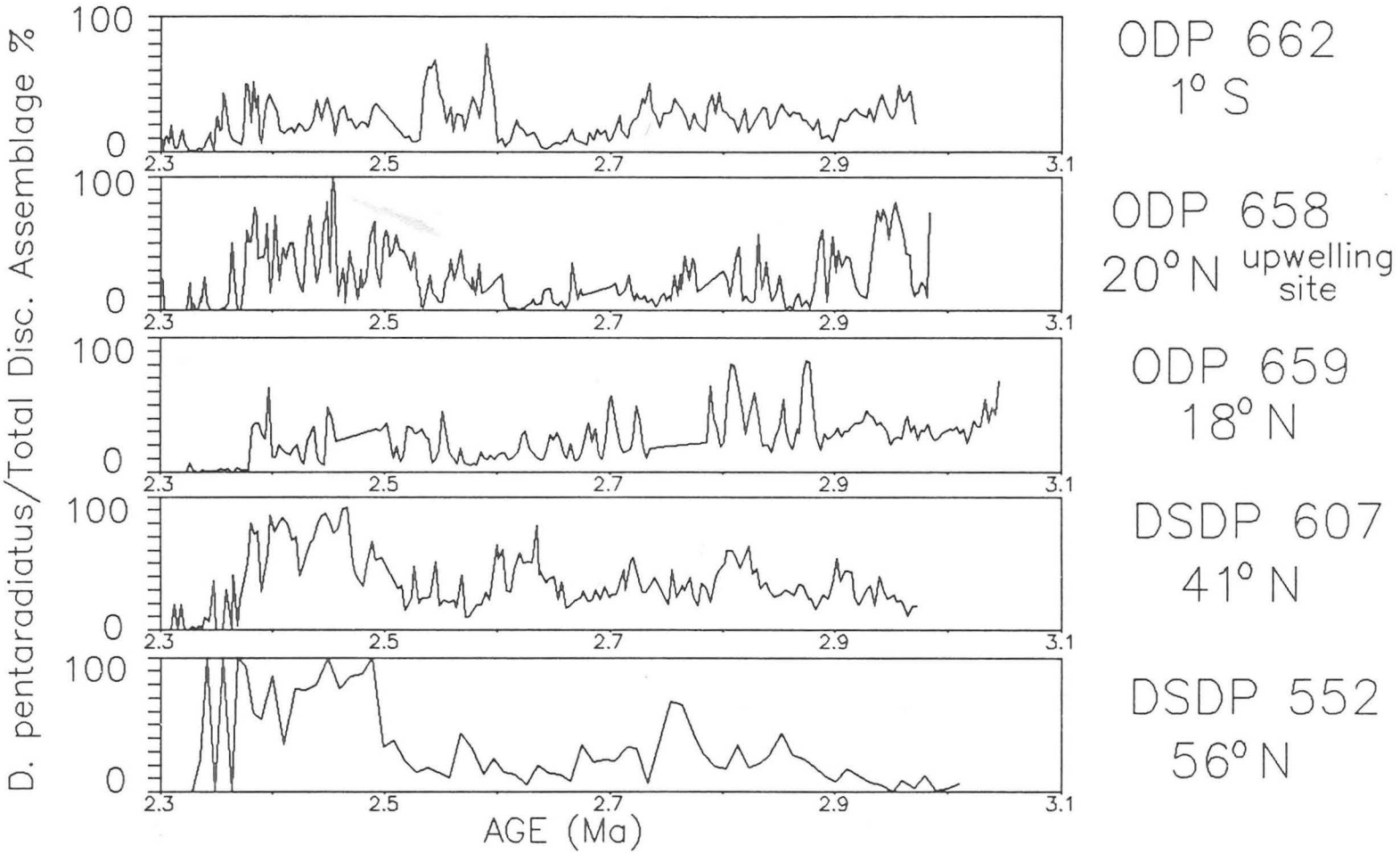

Figure 2:4:2c Percentage abundance plots of D. pentaradiatus at Sites 552, 607, 659, 658 and 662.

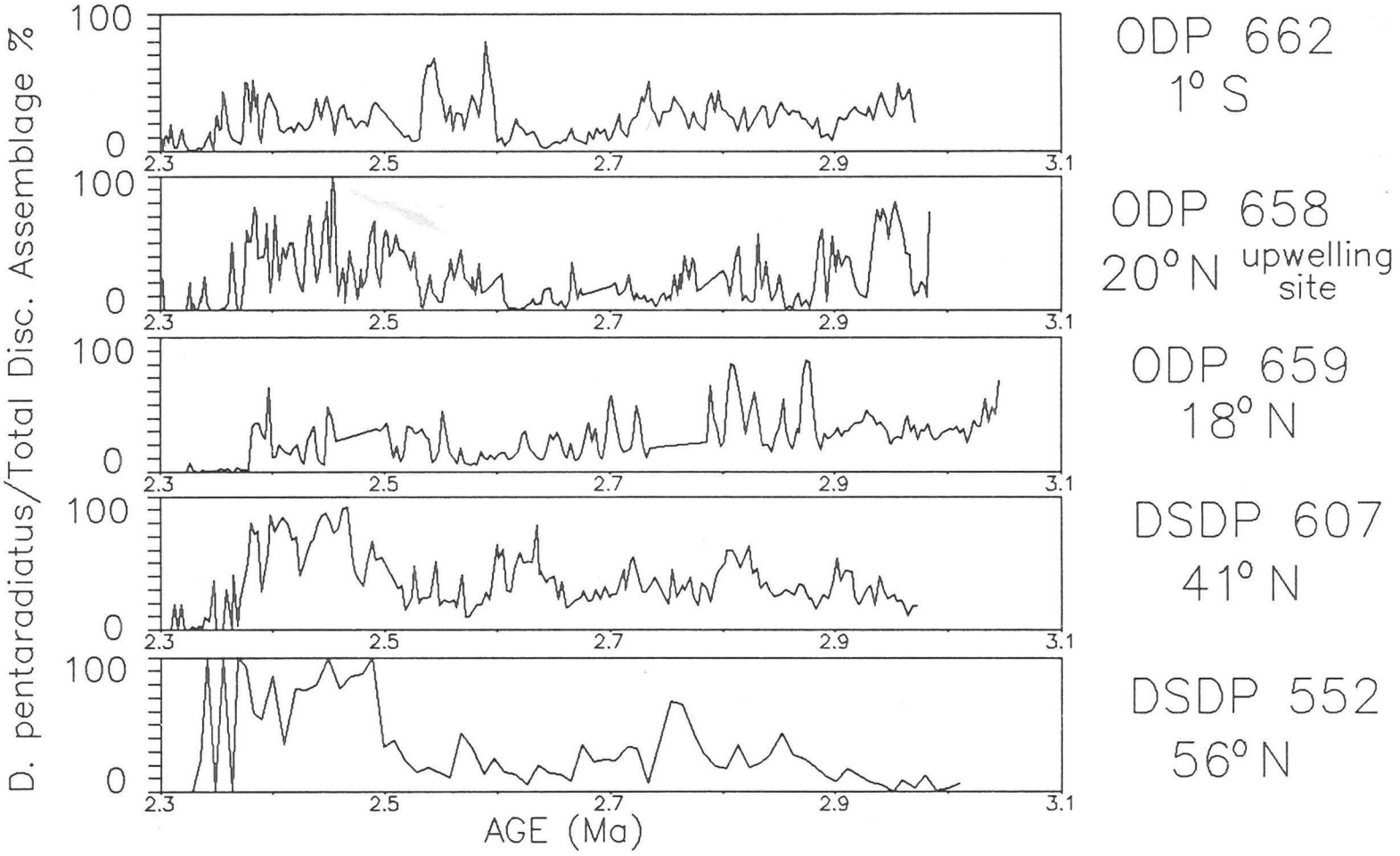

Figure 2:4:2c Percentage abundance plots of D. pentaradiatus at Sites 552, 607, 659, 658 and 662.

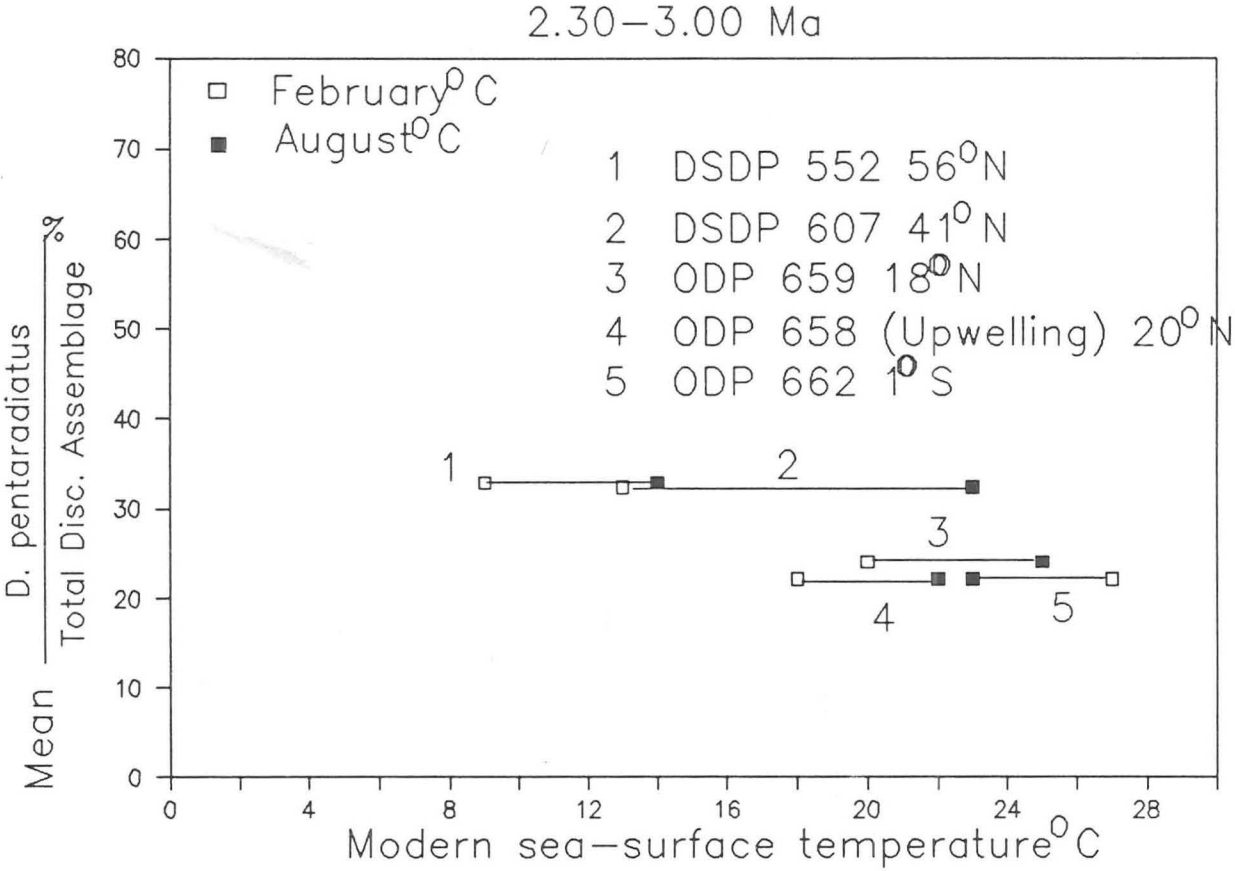

Figure 2:4:2d Mean percentage D. pentaradiatus /Total Discoaster Assemblage versus modern sea–surface temperature at Sites 552, 607, 659, 658 and 662.

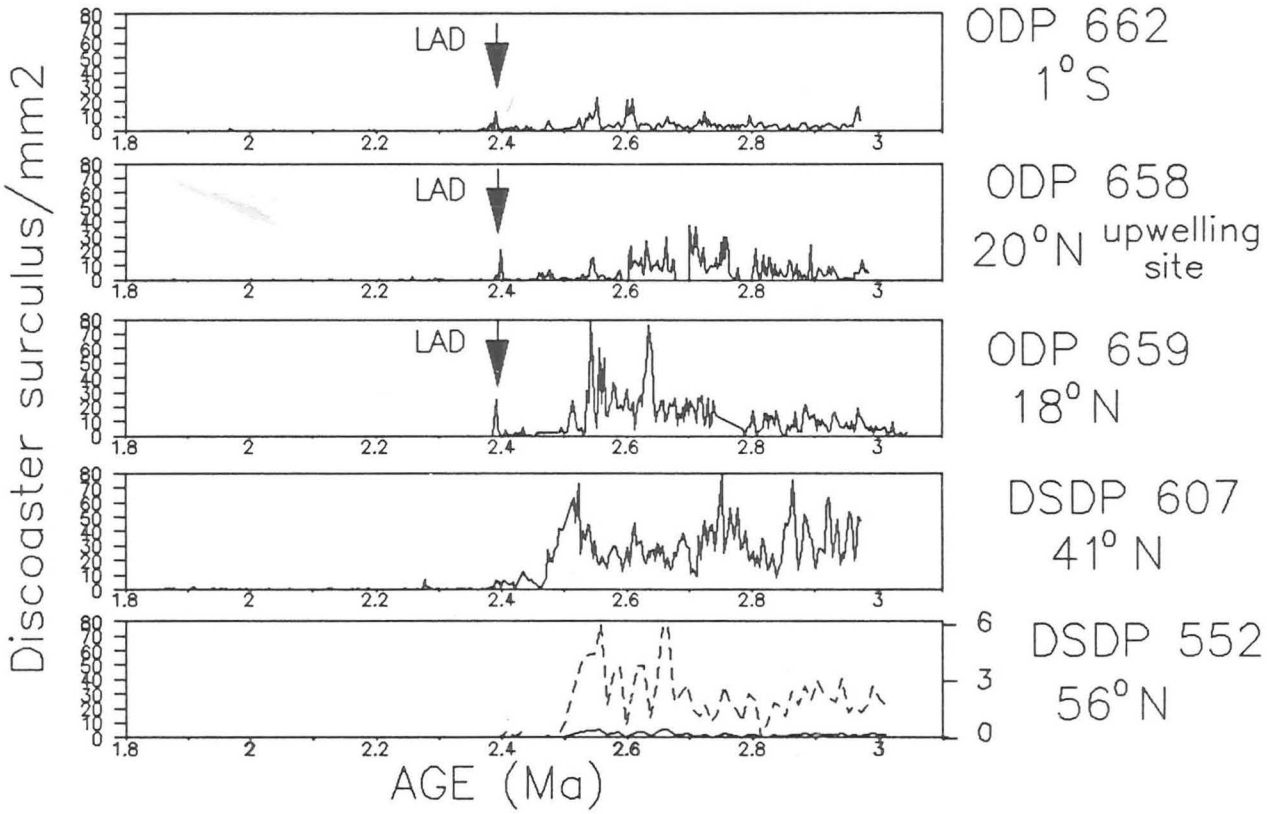

Figure 2:4:2e Abundance plots of D. surculus at Sites 552, 607, 659, 658 and 662. The abundance scale has been reduced twice in comparison with the abundance plots of D. pentaradiatus

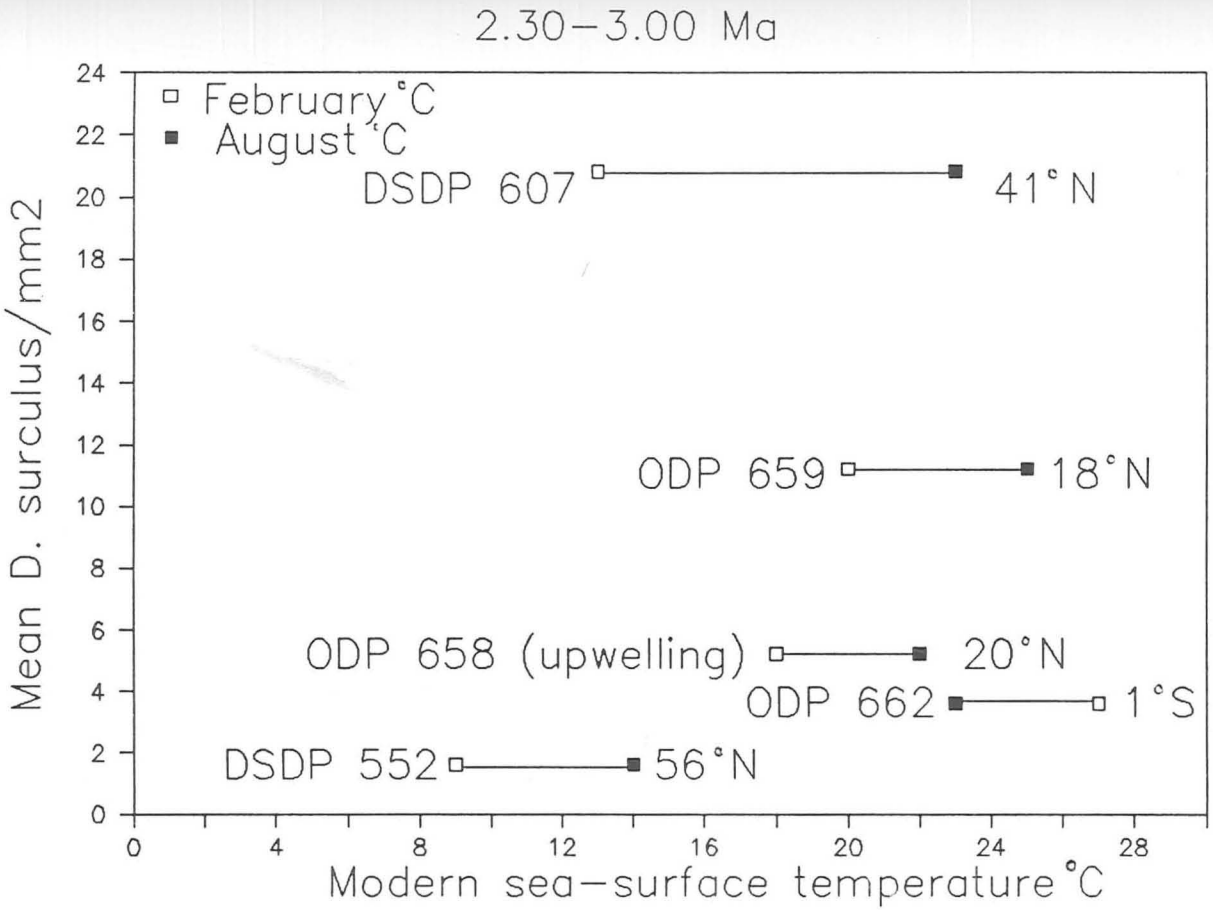

Figure 2:4:2f Mean D. surculus/mm2 versus modern sea–surface temperature at Sites 552, 607, 659, 658 and 662.

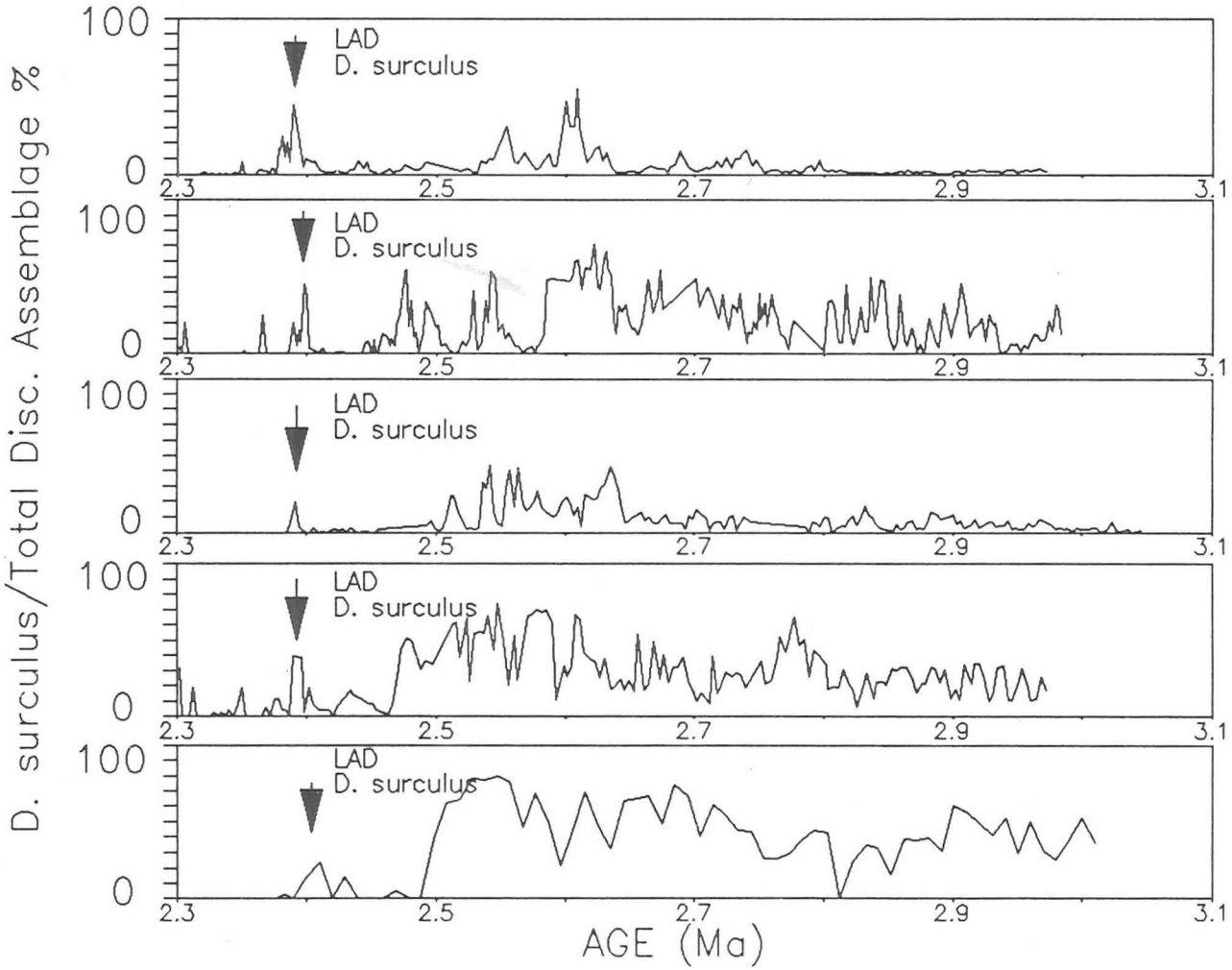

Figure 2:4:2g Percentage abundance plots of D. surculus at Sites 552, 607, 659, 658 and 662.

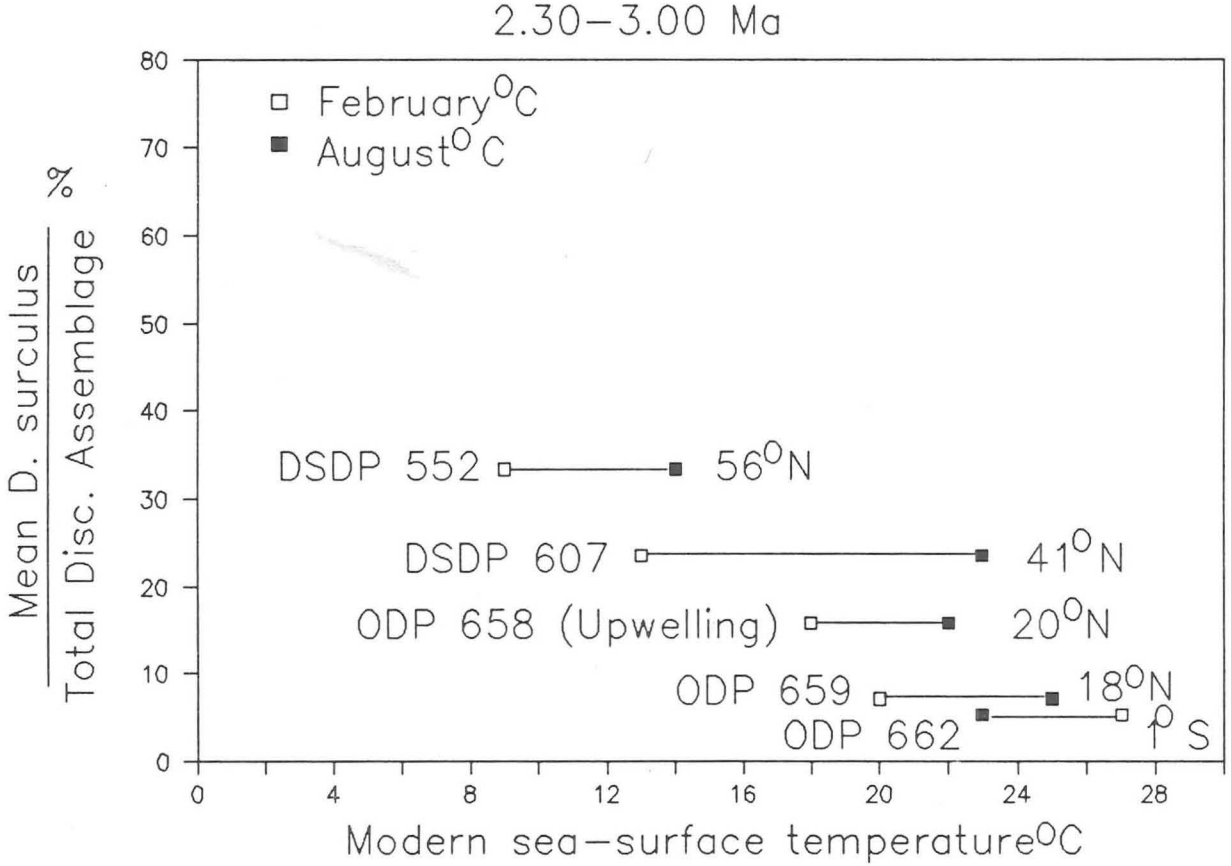

Figure 2:4:2h Mean percentage D. surculus /Total Discoaster Assemblage versus modern sea–surface temperature at Sites 552, 607, 659, 658 and 662.

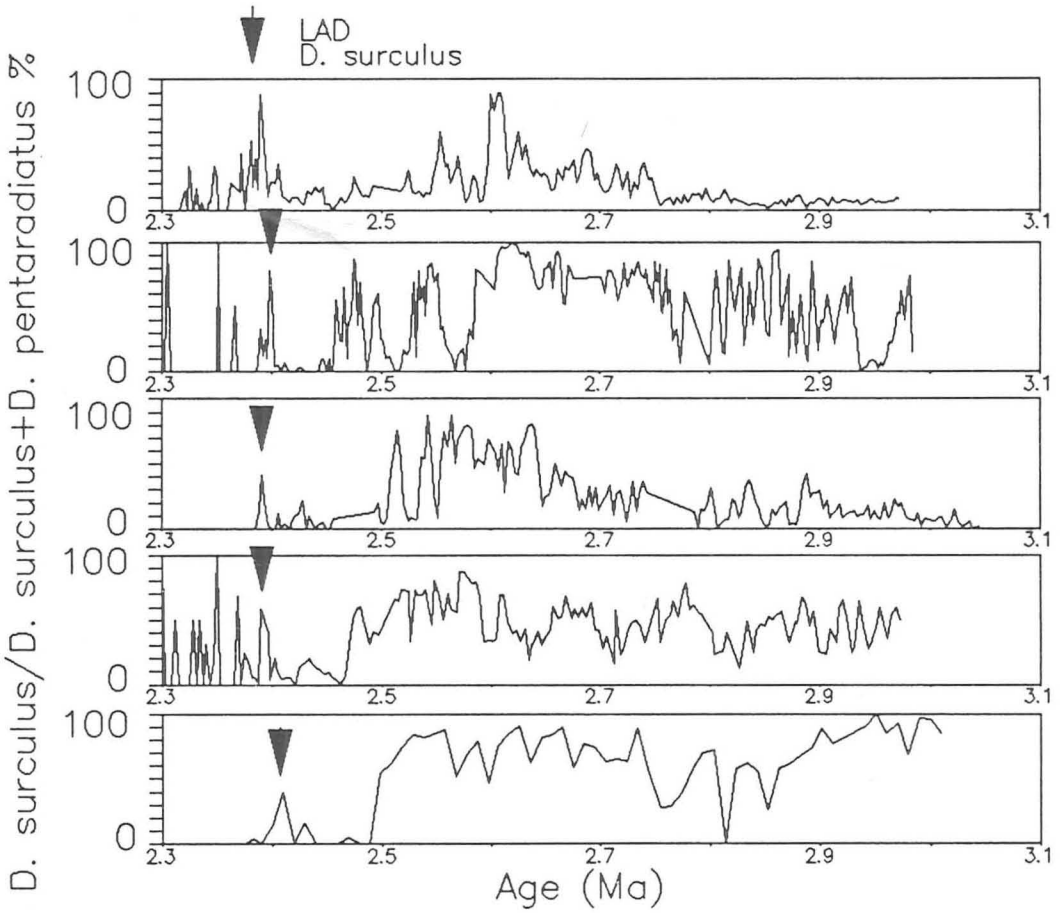

Figure 2:4:2i Abundance plots of D. surculus as a percentage of the sum of D. surculus and D. pentaradiatus at Sites 552, 607, 659, 658 and 662.

and upwelling conditions. This trend is further displayed by plotting the mean relative abundance of D. surculus versus modern sea-surface temperature (Fig. 2:4:2h). Relative abundances of D. surculus reveals final abundance peaks at the high latitude sites not seen in the absolute abundances.

In all five sites , D. pentaradiatus and D. surculus frequently exhibit an inverse abundance relationship (Backman and Shackleton, 1983). This relationship is examined in closer detail in Chapter 5. Discoaster surculus is further represented here as a percentage of the sum of D. surculus and D. pentaradiatus. This re-emphasizes how D. surculus increases with latitude and upwelling conditions (Fig. 2:4:2i). Similarly, the high latitude sites can be seen to display a distinct final abundance peak. The relationship between D. pentaradiatus and D. surculus may provide a potential tool for determining subtle temperature or productivity changes, if we assume that these two species had different ranges of ecological tolerance.

2:4:3 Discoaster asymmetricus and Discoaster tamalis

The abundance of these two species co-varies as shown in the almost identical abundance patterns at each site (Figs. 2:4:3a and 2:4:3b). This phenomenon has been demonstrated by Backman and Shackleton (1983); Backman et al. (1986); Backman and Pestiaux (1987) and seems to suggest strong taxonomic affinity. Sites 659, 662 and 607 indicate a clear reduction in abundance through the time interval for both these species up until the extinction of D. tamalis at 2.65 Ma. Discoaster asymmetricus continues to exist in low

abundances. This low abundance phenomenon after 2.65 Ma is seen at all five sites, and this is not simply reworking (Backman, 1986).

There is a drastic drop in abundance of D. asymmetricus and D. tamalis between 41°N and 56°N, and at the upwelling site, Site 658. These trends are shown clearer by plotting the mean abundance of D. asymmetricus and D. tamalis versus modern sea-surface temperature (Figs. 2:4:3c & 2:4:3d). If D. asymmetricus and D. tamalis are plotted as a percentage of the complete Discoaster assemblage, this demonstrates further an increase within the assemblage with increasing latitude, but not upwelling conditions (Fig. 2:4:3e & 2:4:3f).

Another interesting feature is that D. tamalis and D. asymmetricus frequently mimic the abundance of D. brouweri at the five sites, especially at higher latitudes. This may indicate taxonomic affinity between these three species and is discussed in greater detail in chapter 5. If D. tamalis is represented as a percentage of the sum of D. tamalis, D. asymmetricus and D. brouweri, the increase of D. tamalis with latitude, but not upwelling conditions is accentuated (Fig. 2:4:3g). This trend can be enhanced further still by representing the sum of D. tamalis and D. asymmetricus as a percentage of the sum of these two species and D. brouweri (Fig. 2:4:3h). If this is plotted versus modern sea-surface temperature, there is a clear relationship showing the relative increase in production of D. asymmetricus and D. tamalis with higher latitude (Fig. 2:4:3i). Upwelling is not only limited to Site 658. Site 662, which is located within the equatorial divergence, is also affected by upwelling to some extent, causing a

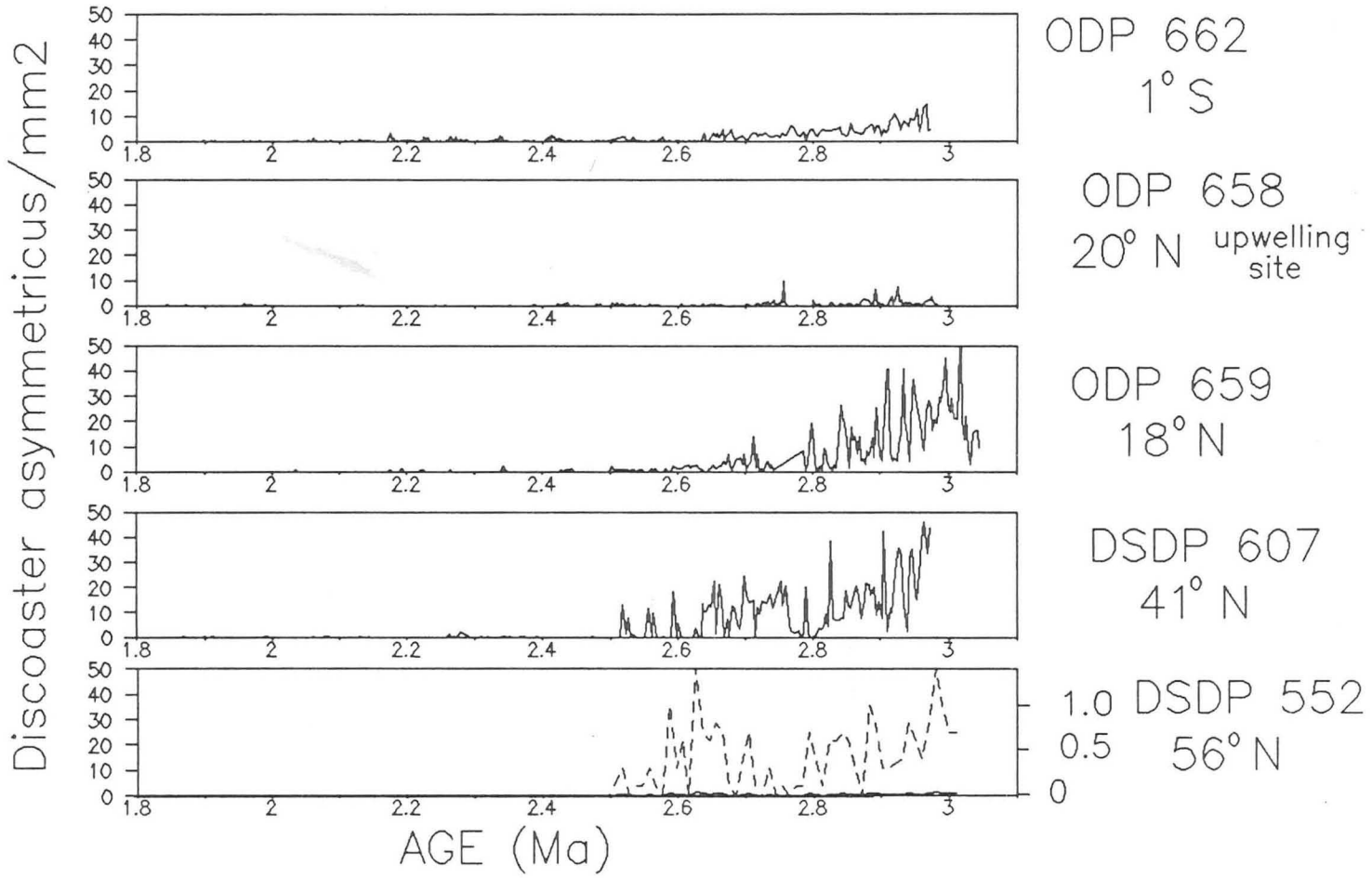

Figure 2:4:3a Abundance plots of D. asymmetricus at Sites 552, 607, 659, 658 and 662. The abundance scale is the same as D. surculus and D. tamalis

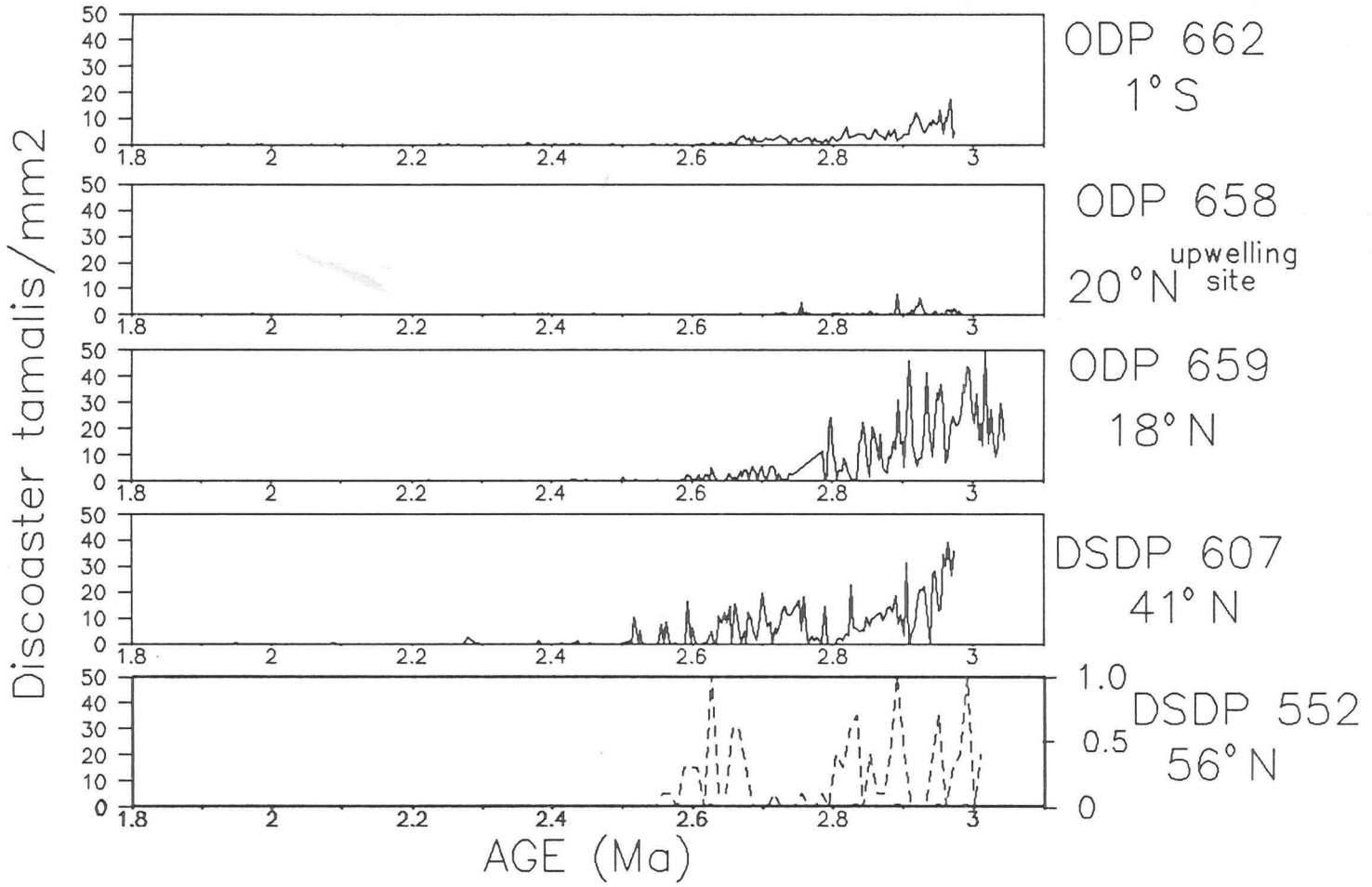

Figure 2:4:3b Abundance plots of D. tamalis at Sites 552, 607, 659, 658 and 662. The abundance scale is the same as D. surculus and D. asymmetricus

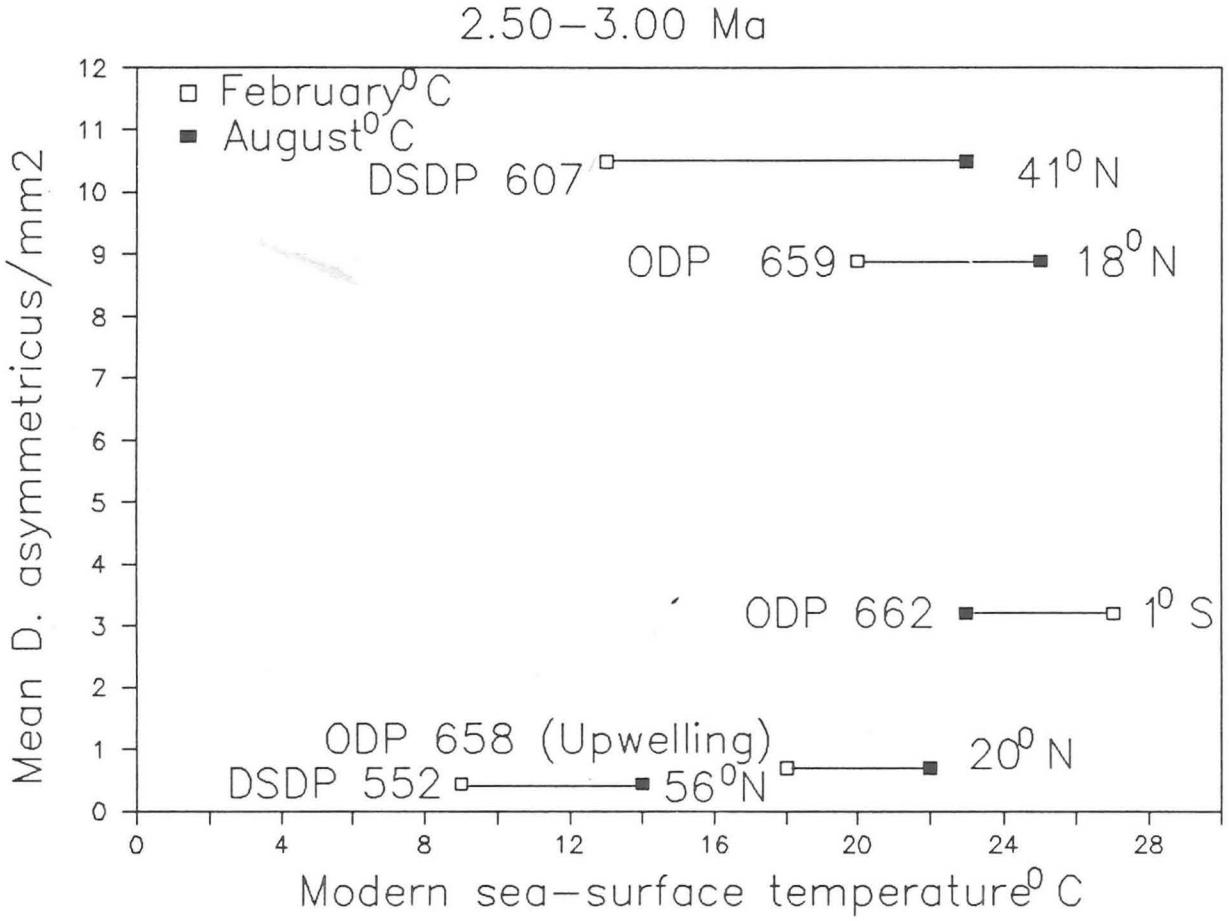

Figure 2:4:3c Mean D. asymmetricus/mm2 versus modern sea–surface temperature at Sites 552, 607, 659, 658 and 662.

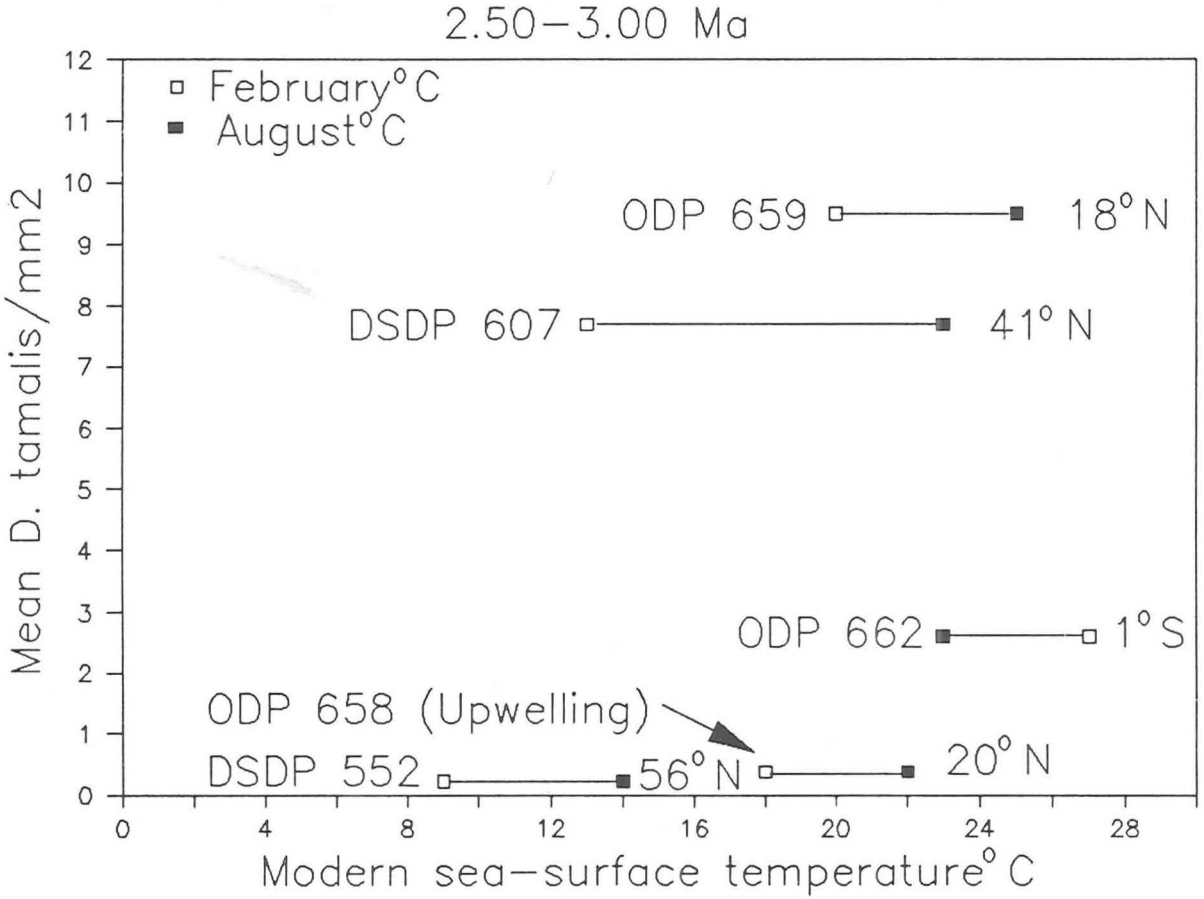

Figure 2:4:3d Mean D. tamalis/mm2 versus modern sea–surface temperature at Sites 552, 607, 659, 658 and 662.

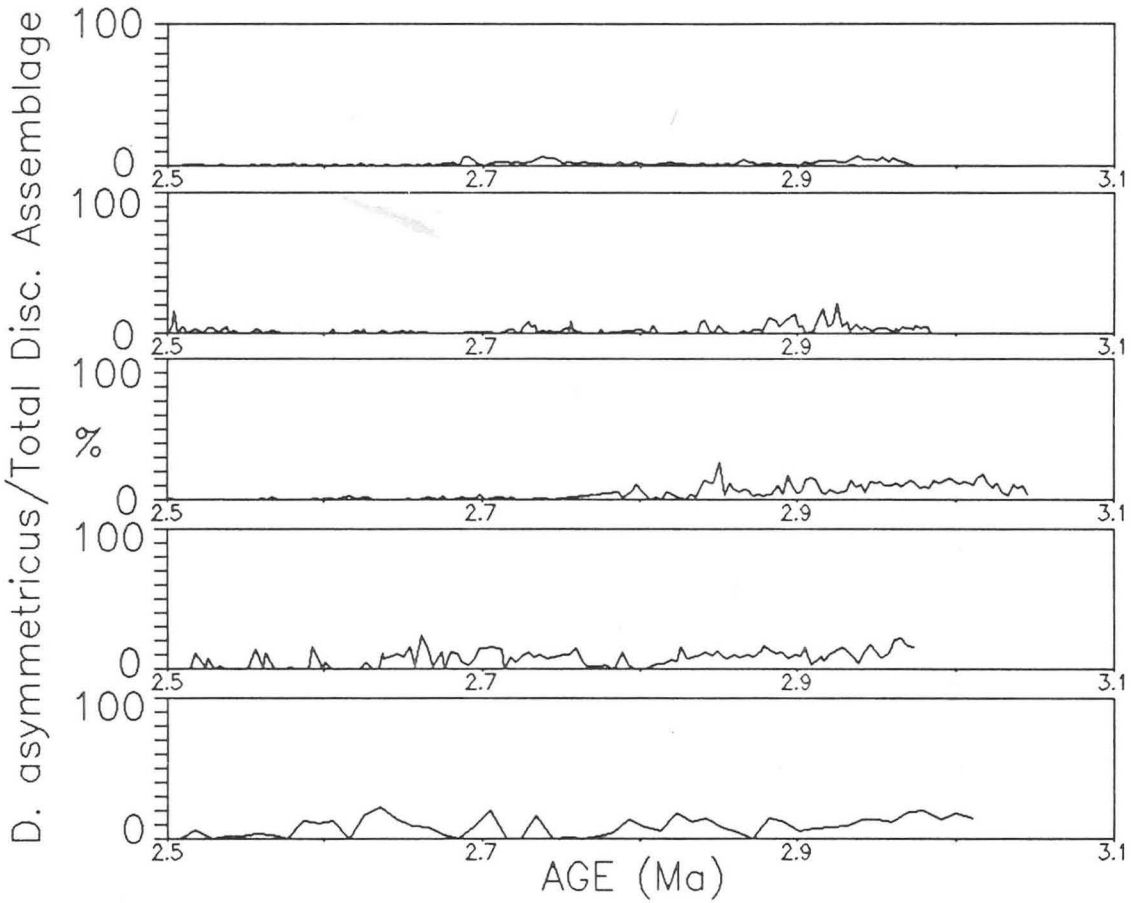

Figure 2:4:3e Percentage abundance plots of D. asymmetricus at Sites 552, 607, 659, 658 and 662.

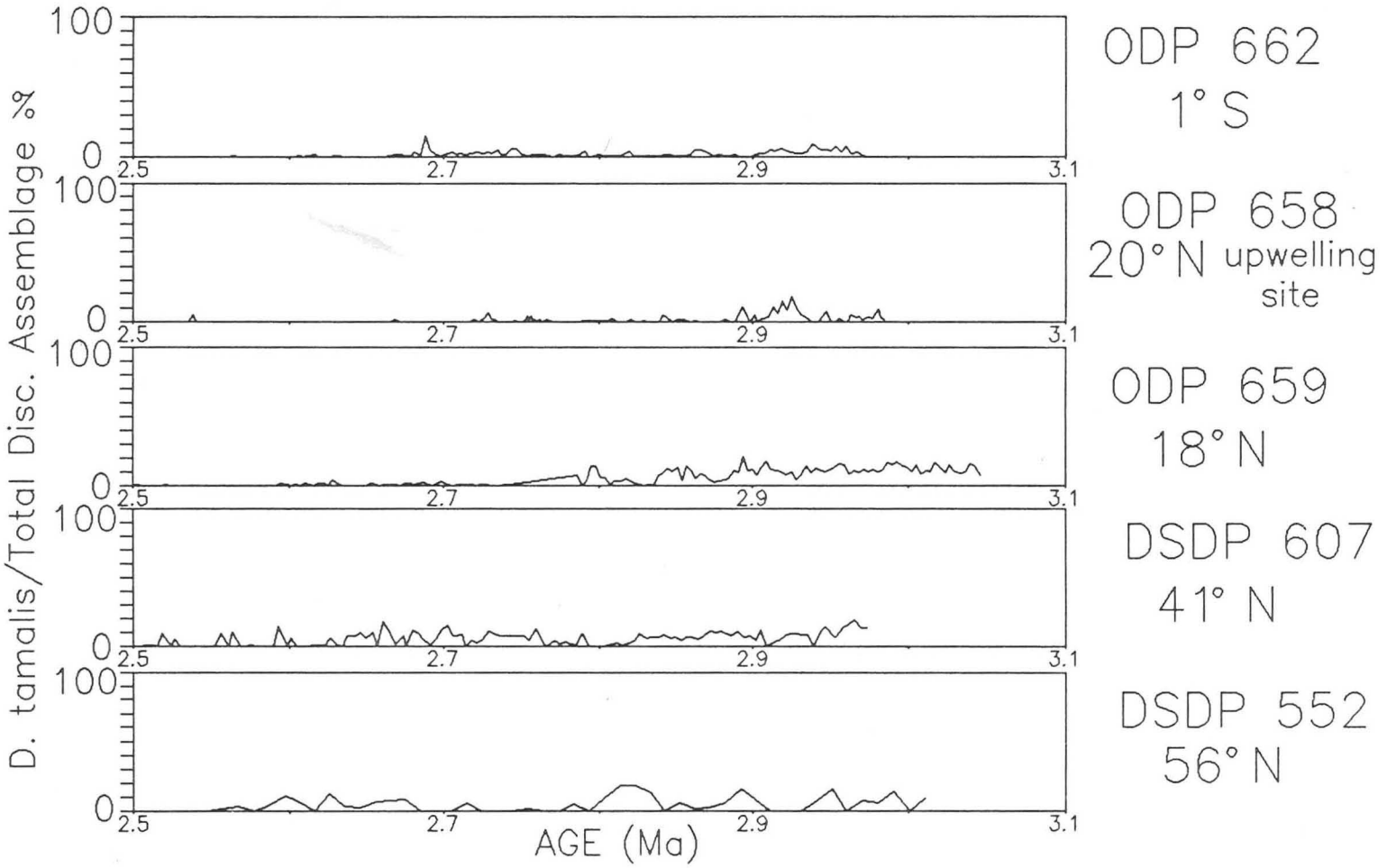

Figure 2:4:3f Percentage abundance plots of D. tamalis at Sites 552, 607, 659, 658 and 662.

similar suppression.

2:4:4 Discoaster variabilis

This species occurs only at the start of the time-interval investigated (Fig. 2:4:4). Using the age-models as discussed, we were interested to what extent the extinction of D. variabilis was synchronous in the North Atlantic. Could the LAD of D. variabilis, at sites lacking magnetostratigraphy, offer a better datum than the planktonic foraminifer G. altispira (LAD 2.95) ? This would make it especially useful since G. altispira occurs in very low abundances away from the tropics and is prone to dissolution.

Sites 658, 662 and 552 appear to produce an extinction for D. variabilis at approximately 2.9 Ma, but Site 659 has a well defined extinction at approximately 2.8 Ma. At Site 607, this event is poorly defined and could occur from 2.8-2.9 Ma. Since Site 659 lacks magnetic data for this time interval, whereas Site 552 has good magnetostratigraphy, we will define the LAD of D. variabilis as occurring at approximately 2.9 Ma. This is only a working hypothesis for age-models at future sites lacking in magnetostratigraphy or a good datum for G. altispira in this time interval.

2:5 Total Discoaster Abundance

Excluding D. variabilis, which begins to appear in small numbers at the base of our time interval, it is only at 2.65 Ma that all the Discoaster species

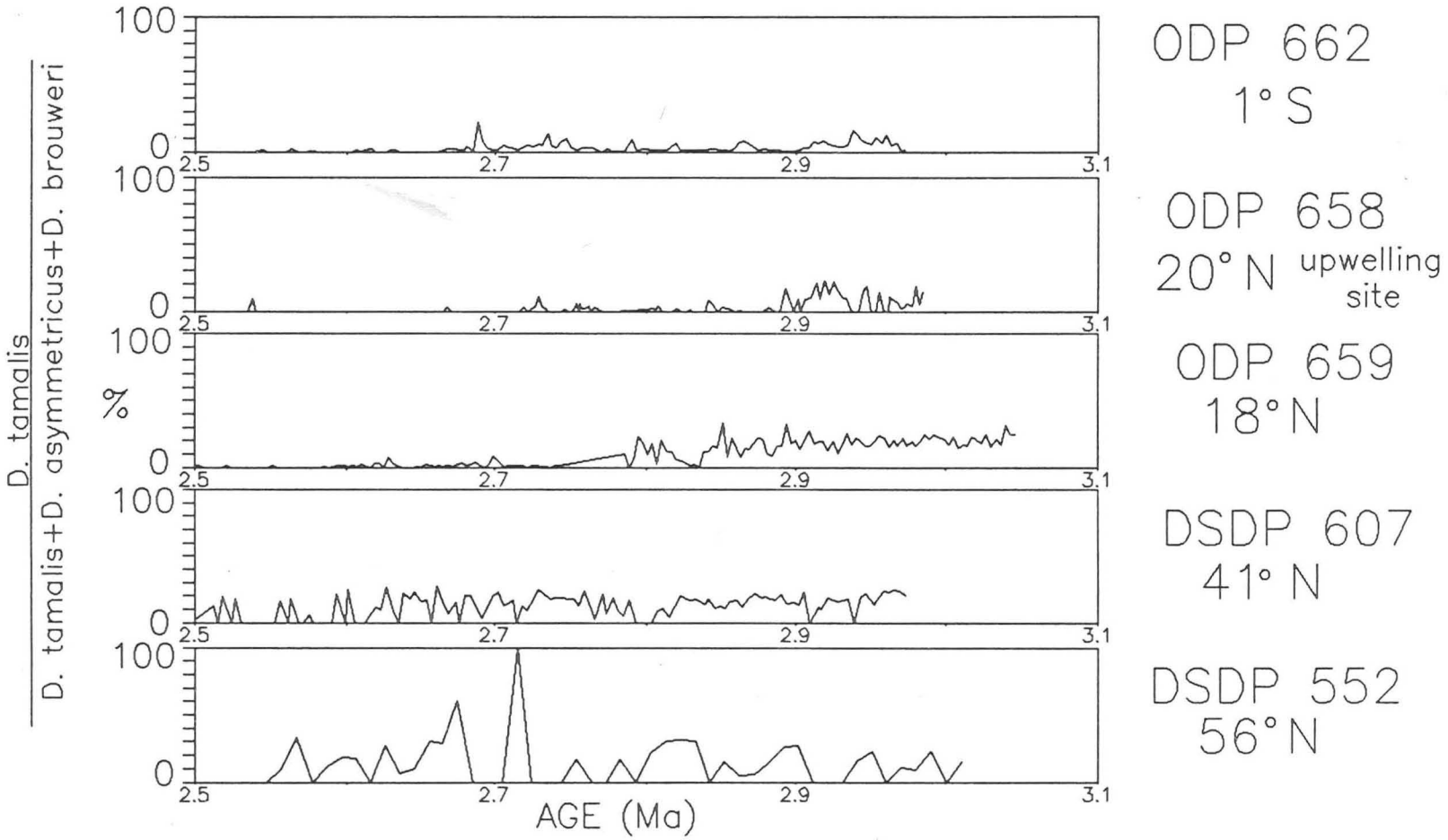

Figure 2:4:3g Abundance plots of D. tamalis as a percentage of the sum of D. tamalis , D. asymmetricus and D. brouweri at Sites 552, 607, 659, 658 and 662.

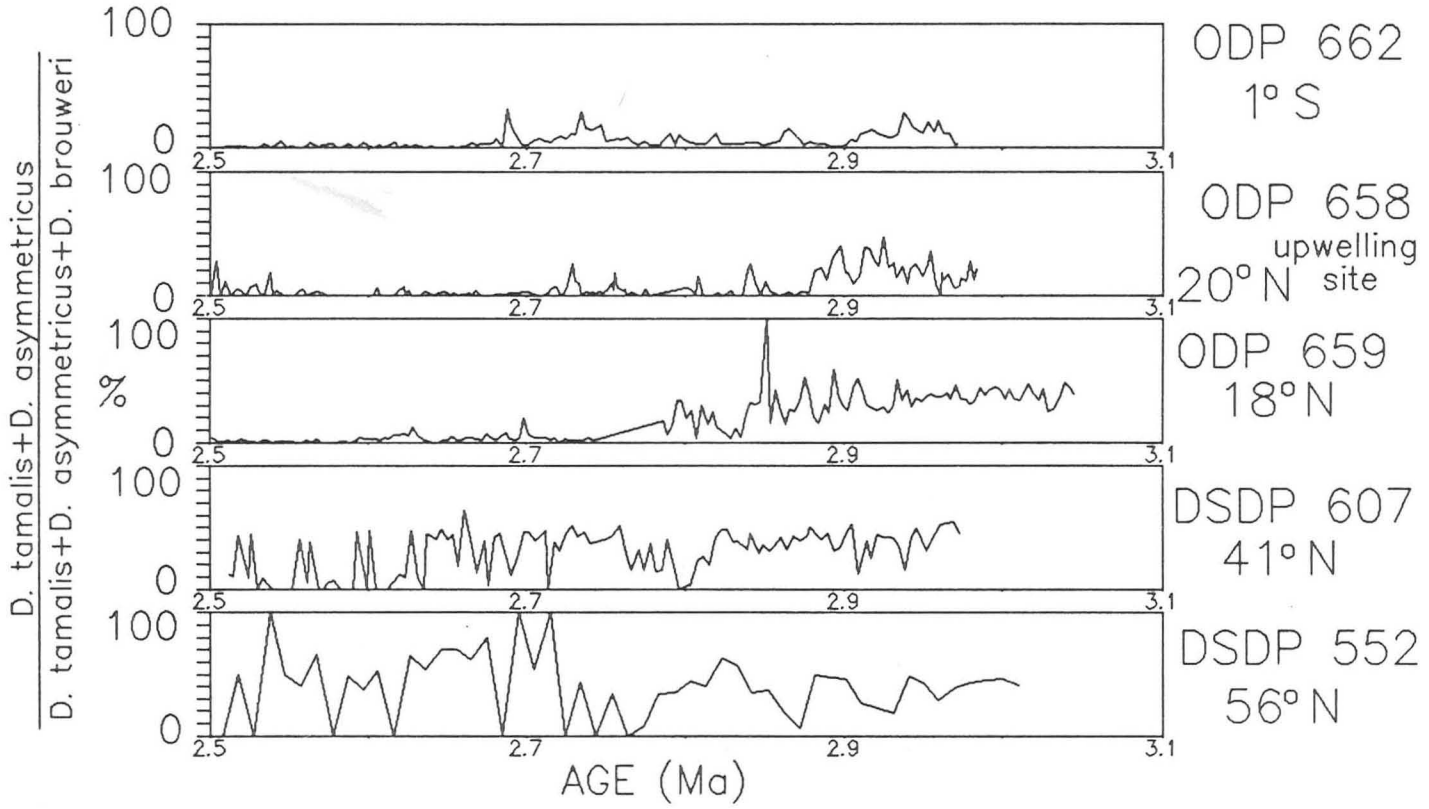

Figure 2:4:3h Abundance plots of D. tamalis and D. asymmetricus as a percentage of the sum of these two species and D. brouweri at Sites 552, 607, 659, 658 and 662.

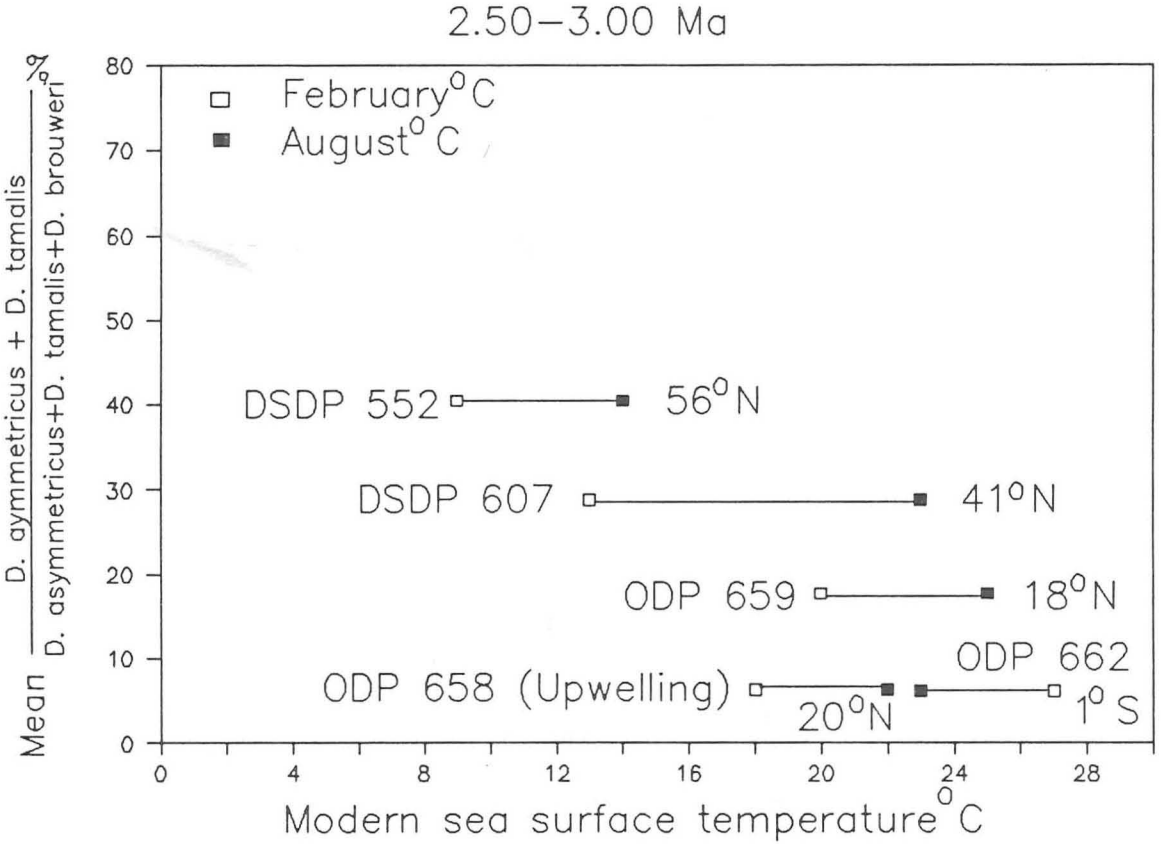

Figure 2:4:3i Mean percentage D. asymmetricus + D. tamalis /D. as + D. ta + D. brouweri versus modern sea–surface temperature at Sites 552, 607, 659, 658 and 662.

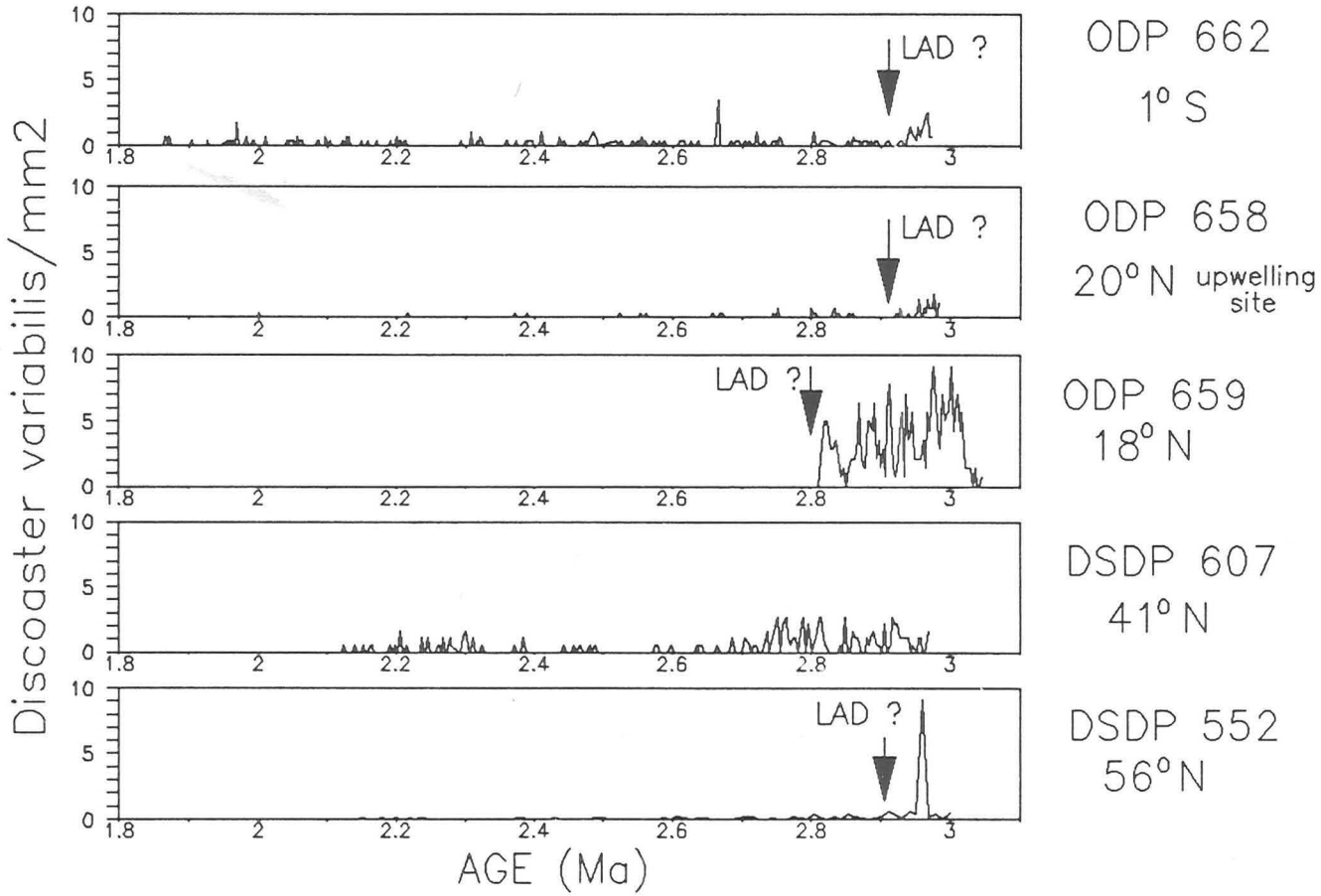

Figure 2:4:4 Abundance plots of D. variabilis at Sites 552, 607, 659, 658 and 662.

are present. Discoaster brouweri is the only species covering the complete time interval. After 2.39 Ma, D. brouweri is the only species apart from the brief acme of D. triradiatus. Of the other species D. pentaradiatus and D. surculus are numerically most significant. Figure 2:5a displays the total Discoaster abundances at the five sites. Here again is seen the familiar drastic reduction in abundance between 41°N and 56°N, and with upwelling conditions. This pattern is similarly shown by plotting the mean total Discoaster abundance versus modern sea-surface temperature (Fig 2:5b).

Shackleton et al. (1984) have shown that the onset of Northern Hemisphere glaciation was a well defined event at about 2.4 Ma, and it may correlate with the sudden abundance reduction of discoasters at 2.4 Ma at Sites 607 and 552 and the following 50 ka at Site 658. At the latter site this may even indicate an intensification of upwelling, which may have been less intense before.

At Site 662, discoasters are still reasonably abundant, but the effects of upwelling associated with equatorial divergence and the South Equatorial Current appear to reduce their overall numbers. It is very clear at Site 662 that short term variations are imprinted on a long term trend of Discoaster abundance reduction. Similarly, considering that Site 659 was selected as the reference site and is located in the tropics where the sea-surface temperatures would be thought to be relatively constant, it was not expected that Discoaster variations would be so marked.

To account for the dilution effect by high sedimentation rates, the

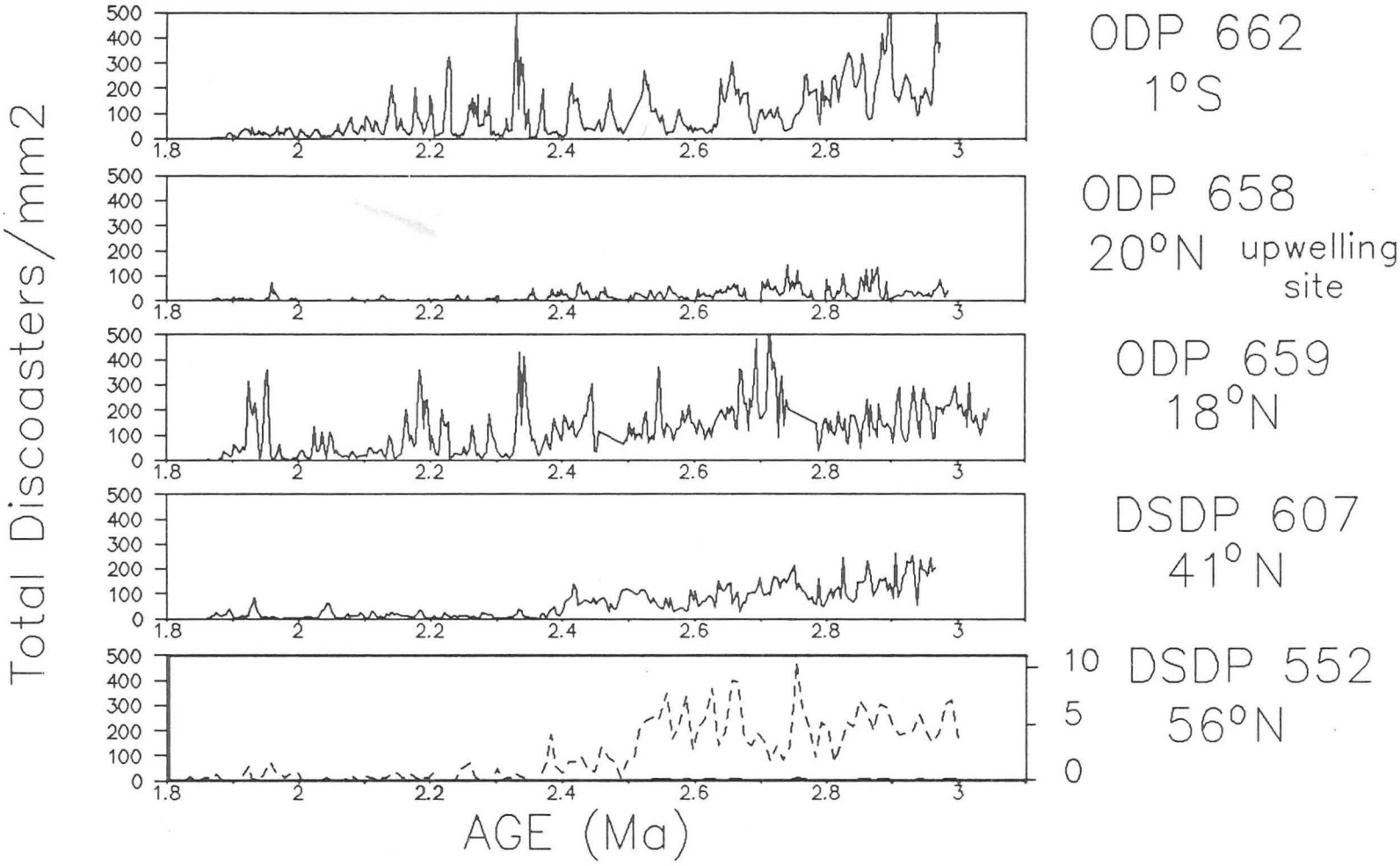

Figure 2:5a Plots of total Discoaster abundance at Sites 552, 607, 659, 658 and 662.

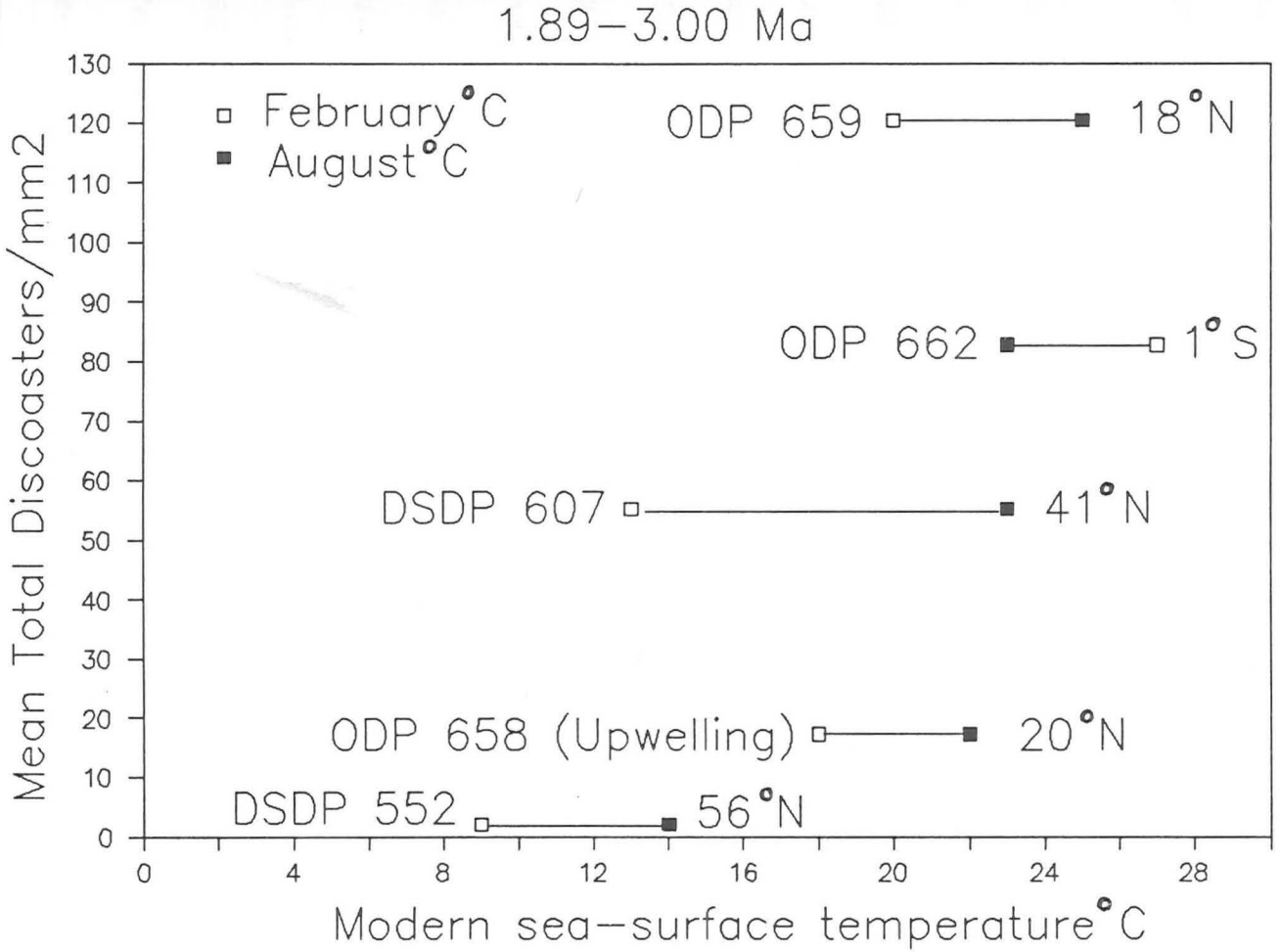

Figure 2:5b Mean Total Discoasters/mm2 versus modern sea–surface temperature at Sites 552, 607, 659, 658 and 662.

observed abundances should be multiplied by the sedimentation rates to give a figure more closely proportional to accumulation rates for each species. Sites 607, 659 and 662 would still be roughly comparable as shown, but Site 658 would be increased by a factor of 2-3 compared to these sites though still showing much lower abundances. Site 552, however, would be reduced further by roughly a factor of 3 to show even lower abundances.

2:6 Spectral Analysis

Numerous studies have shown that the late Plio-Pleistocene paleoclimate was responding to orbital forcing (e.g. Hays et al., 1976; Pisias and Leinen, 1984; Pestiaux and Berger, 1984). Since many groups of nannoplankton are restricted to specific temperature ranges (e.g., McIntyre, 1967; Okada and Honjo, 1973; Okada and McIntyre, 1979), it would be expected that their abundances would respond to changes in sea-surface temperature resulting from orbital forcing. Backman et al. (1986) and Backman and Pestiaux (1987) have demonstrated this at Sites 606 and 552. At Site 606, variance at the frequency of all three orbital elements were obtained, dominated by the 400 ka periodicity. At Site 552, only the eccentricity and obliquity periodicities were present. Obliquity was dominant at this site. Precessional periodicities may have been undetectable due to the low sedimentation rate, resulting in a temporally coarse sampling interval.

In this chapter, spectral analysis is performed on data sets obtained by linear interpolation between the biostratigraphic and

magnetostratigraphic control points selected for the age models (Table 2:3:2a). The data sets have been divided into two time intervals 1.88-2.39 Ma and 2.39-3.00 Ma (Figure 2:6). The reason is that at approximately 2.39 Ma several important events occur, including sudden cooling in the North Atlantic, changes in the sedimentation rate, total Discoaster abundance reduction, the extinction of D. surculus and the near extinction of D. pentaradiatus.

For the purposes of this analysis the sum of all the Discoaster species were investigated in order to reduce the effect of the idiosyncracies of particular species. There is frequently an order of magnitude change in Discoaster abundances associated with apparently regularly spaced abundance peaks which indicates that there is a large signal available for spectral analysis.

During the time interval 1.88-2.39 Ma, D. brouweri is effectively the only species present except between 1.89 and 2.07 when D. triradiatus had its acme. At Sites 662, 552 (precession very weak) and 607, concentrations of variance around the frequencies of the orbital elements of eccentricity (100kα), obliquity (41kα) and precession (21kα) are distinguished. At Site 658, only a possible eccentricity signal is noticeable in this time interval which is due to the presence of relatively few abundance peaks. At Site 659, the obliquity periodicity occurs but is less well defined than the eccentricity and precessional periodicities.

Between 2.39-3.00 Ma, when a greater Discoaster diversity is present, the

Figure 2:6 Spectral power density estimated on 2 time intervals of the total Discoaster data set at Sites 552, 607, 659, 658 and 662. B. W. indicates band width.

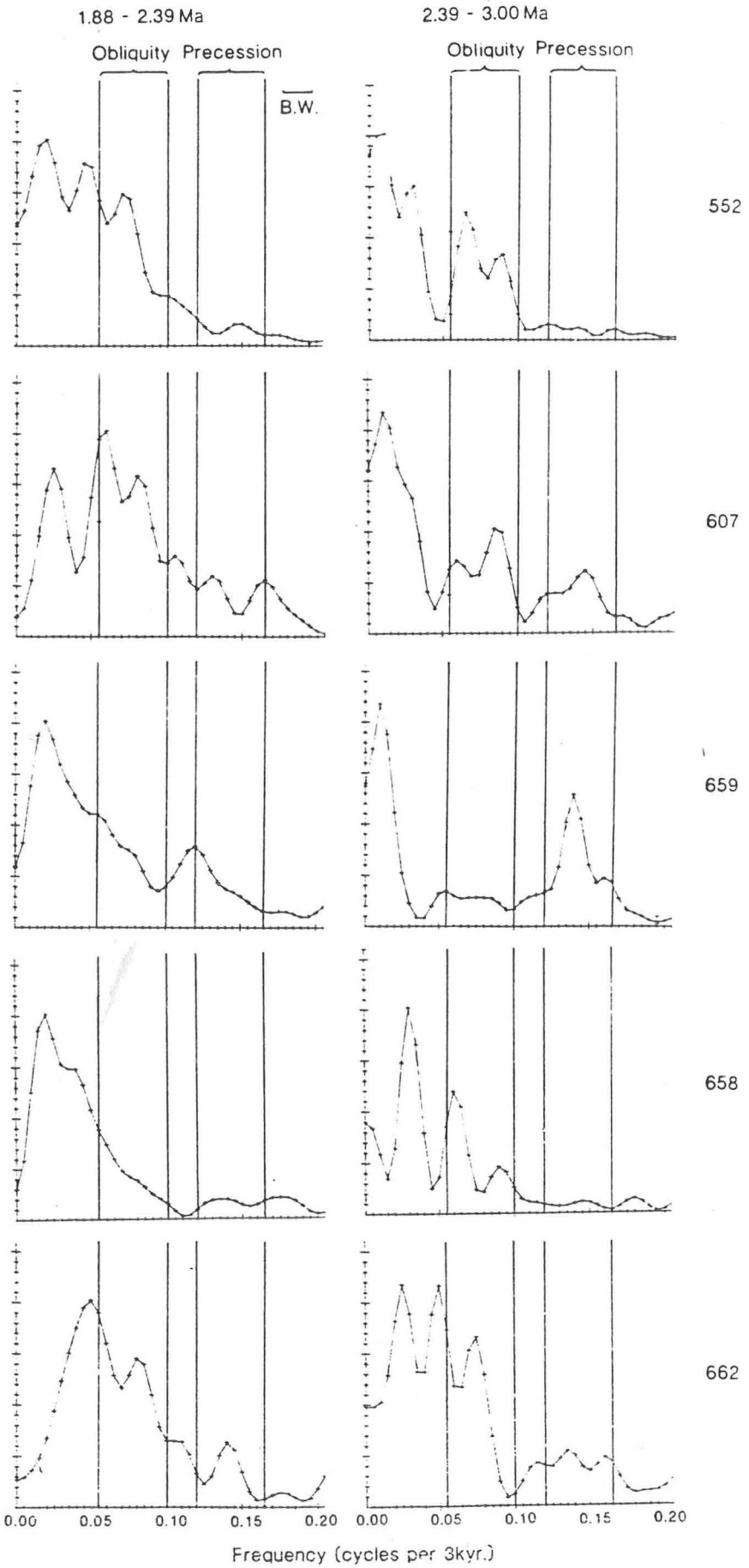

obliquity periodicity is distinct at all the sites except Site 659, which is dominated by the precessional periodicities. There is some indication of the influence of eccentricity at all sites, but precession is only clearly indicated at Sites 662, 659 and 607.

In chapter 6, oxygen isotope data has been used in the generation of an orbitally tuned timescale for Site 607 in order to gain a better estimate of the characteristics of the forced components of Discoaster variability. Our strategy here was to investigate whether in the presence of both marked aperiodic fluctuations in the abundance of individual species, and a long- term decline towards extinction in the Discoaster group, it would still be possible to detect the periodicities characteristic of orbital forcing. Our data suggests that this is indeed possible.

2:8 Discussion

Orbital forcing has been shown to be strongly imprinted on the Discoaster abundances at these sites, partly acting through sea surface temperature variability. Total Discoaster abundances are reduced with increasing latitude and as a function of decreasing age towards their extinction. Is this solely due to a reduction in temperature with latitude and through time?

Previous studies have suggested that Discoaster abundances are responding only to temperature changes (e. g., Haq and Lohmann, 1976). However, the results from this work especially from the tropical sites showing large

abundance variations clearly suggest that other factors must be important. The valleys in the Site 662 record are, in terms of abundance, on the same order as the abundances observed at the high latitude site, Site 552. It is considered unlikely that the equatorial surface water temperatures ever approached those existing at 56°N in the North Atlantic at any given Pliocene time. Thus, one possible factor is thought to be productivity pressure. In view of the suppressed abundances at the upwelling site, (Site 658) it seems tenable to conclude that regions of high productivity are associated with reduced Discoaster abundance. The Discoaster assemblage appears to tolerate a wide temperature range up to 41°N, but between this latitude and 56°N, a threshold is reached beyond which the abundances are suddenly reduced. In Plates 2 and 3, the five sites are shown superimposed on satellite images from NASA of phytoplankton abundance in the North Atlantic for February and October respectively. This is believed to reflect productivity and may be used as a proxy indicator of the possible productivity pressure on discoasters in Pliocene times. Site 658 is located in a constant upwelling area throughout the year, and this reflects how productivity pressure would have suppressed the Discoaster abundance. For certain months, this upwelling area expands to include the area in which Site 659 is located , but this is a seasonal fluctuation and not a constant feature. Site 662 likewise reflects strong seasonal upwelling and the equatorial divergence is clearly shown in October. Site 552 with extremely subdued Discoaster abundances may have experienced seasonal major productivity pressure as indicated by the high

PLATE 2.

Sites located on satellite image of phytoplankton growth in February, 1979 in North Atlantic basin (after Lewis, 1989)

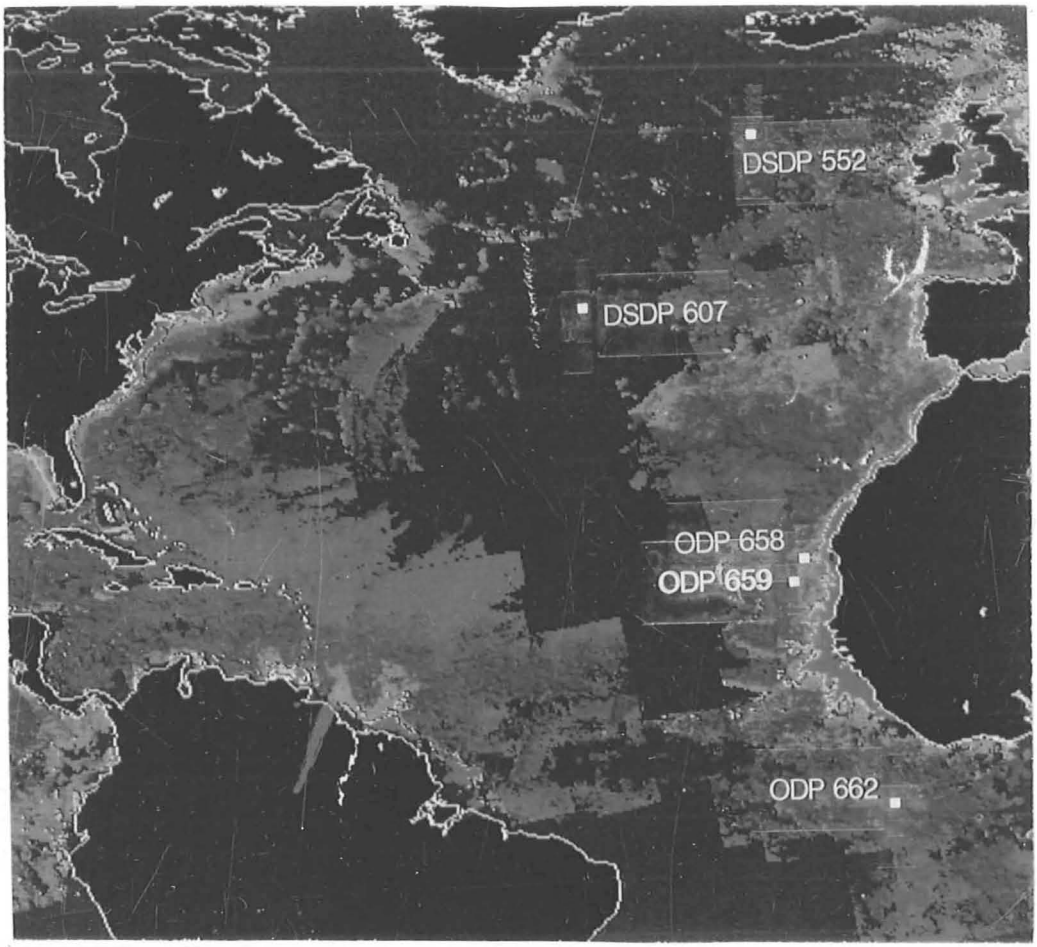

Purple –minimum phytoplankton concentration

red– maximum phytoplankton concentration

PLATE 3.

Sites located on satellite image of phytoplankton growth in October, 1979 in North Atlantic basin (after Lewis, 1989)

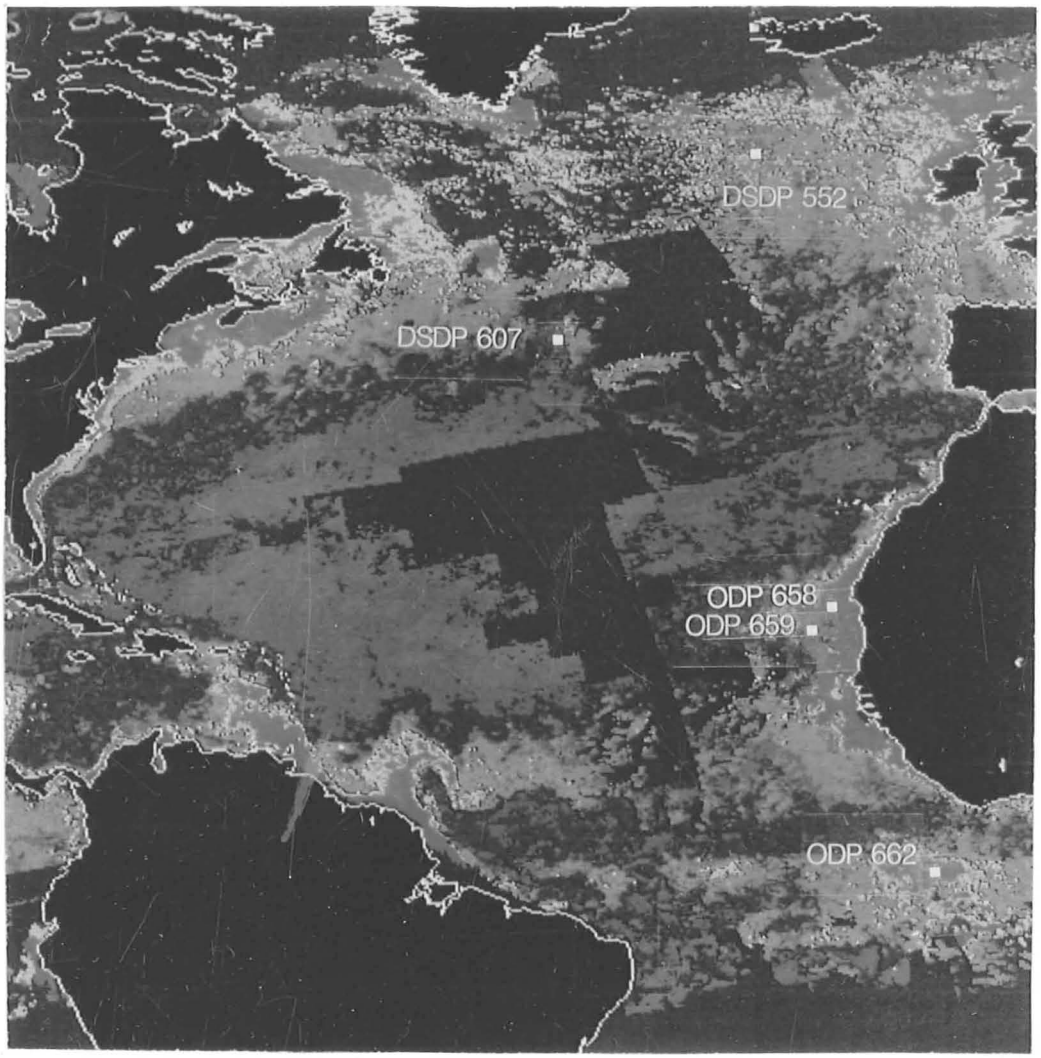

concentration of phytoplankton blooms today in October (Plate 3).

Discoaster brouweri was certainly reduced in abundance with latitude. Prior to 2.38 Ma, D. surculus and D. pentaradiatus comprise an important component of the Discoaster assemblage. Rapid cooling in the North Atlantic at 2.4 Ma (Shackleton et al., 1984) seems to correlate coincidentally with the extinction of these two species at 2.39 and 2.38 Ma respectively. Discoaster surculus increased significantly relative to D. brouweri as a function of increasing latitude and upwelling conditions. The distribution of D. surculus through time, however, shows no clear trend of abundance reduction and seems to signal less than any of the other species a reduction of sea surface temperatures. It seems probable that the distribution of D. surculus through time and space was in response to a productivity signal. Nevertheless, latitude does limit the distribution of D. surculus and its abundance is reduced above 41°N, though D. surculus becomes an even greater component of the Discoaster assemblage, especially relative to D. brouweri and D. pentaradiatus.

As far north as 18°N , D. pentaradiatus shows a clear trend of reduction through time, but north of this latitude no such trend is apparent. This species maintained a fairly constant abundance up to 41°N, excluding the upwelling site, Site 658; D. pentaradiatus was less abundant at higher latitudes though relative to D. brouweri, D. pentaradiatus was still increasing in abundance. This was not the case relative to D. surculus, which was dominant to D. pentaradiatus at the upwelling site, Site 658 and northernmost sites.

These two species clearly demonstrate an inverse abundance relationship, so what could have been their differences in ecological requirements? Discoaster surculus may have favoured cooler, more nutrient rich waters, and D. pentaradiatus may have preferred slightly warmer, less nutrient rich waters. Assuming ecological tolerances did not shift greatly through time, D. brouweri may have favoured even warmer, less nutrient rich waters.

The co-variaton of D. brouweri with D. triradiatus, and D. brouweri with D. asymmetricus and D. tamalis seems to suggest taxonomic affinity. Discoaster tamalis and D. asymmetricus were also produced in virtually identical abundances, but only one of these species disappeared globally at 2.65 Ma. Discoaster asymmetricus continued to occur in low abundance as late as 2.2 Ma, though the true extinction is indistinct. Discoaster asymmetricus and D. tamalis show a distinct trend of reduction in abundance through time up until 2.65 Ma, but actually increase in abundance relative to D. brouweri with increasing latitude. A possible solution is that a calcareous nannoplankton species produced D. asymmetricus and D. tamalis in equal amounts in its structure, but more commonly with higher latitude and lower temperature.

Some species of coccolithophorids today are known to produce different types of coccoliths in the same organism at the same time or under different ecological conditions (Parke and Adams, 1960; Okada and McIntyre, 1979).

2:9 Summary

1. Total Discoaster abundance is reduced by increasing latitude. Prior to 2.38 Ma the abundance of D. brouweri declines more rapidly with increasing latitude than the abundance of other species such as D. pentaradiatus and D. surculus.

2. D. surculus forms a greater component of the Discoaster assemblage with increasing latitude and in upwelling conditions

3. D. asymmetricus and D. tamalis increase with latitude relative to D. brouweri, with which they appear taxonomically related.

4. Marked fluctuations in the abundance of discoasters are in the frequency range of earth orbital variations. However, the high variability observed in the tropics cannot solely be related to temperature changes resulting from orbital forcing, but may imply that varying productivity pressure was the primary control.

5. The extinctions of D. surculus and D. pentaradiatus, and drastic total abundance reduction north of 18°N and at the upwelling site, Site 658 seems to correlate with an abrupt drop in sea-surface temperature in the North Atlantic at 2.4 Ma. At sites south of 20°N the extinction of D. surculus is characteristically preceded by a distinctive brief peak in abundance.

CHAPTER 3: UPPER PLIOCENE DISCOASTER ABUNDANCE VARIATIONS IN THREE EQUATORIAL SITES FROM THE ATLANTIC, PACIFIC AND INDIAN OCEANS; THE SIGNIFICANCE OF PRODUCTIVITY PRESSURE AT LOW LATITUDES.

3:1 Introduction

In this chapter, the abundances of the Discoaster species are compared between three sites close to the equator in different oceans. This includes Site 662, which was the southernmost site in the North Atlantic transect discussed in Chapter 2. The data are used furthermore to compare individual species as a percentage of the total Discoaster assemblage. The mean absolute and relative abundances of Discoaster species are compared with modern sea-surface temperatures (CLIMAP, 1981). The sea-surface temperatures for February and August are shown in Table 3:1. The time interval investigated is approximately the million years preceding the extinction of the discoasters i.e. between 1.9-3.0 Ma (1.9-3.5 Ma for Site 709) using closely spaced samples.

3:2 BACKGROUND ON SITE LOCALITIES

The three sections selected (Fig. 3:2, Table 3:2) represent sites with the

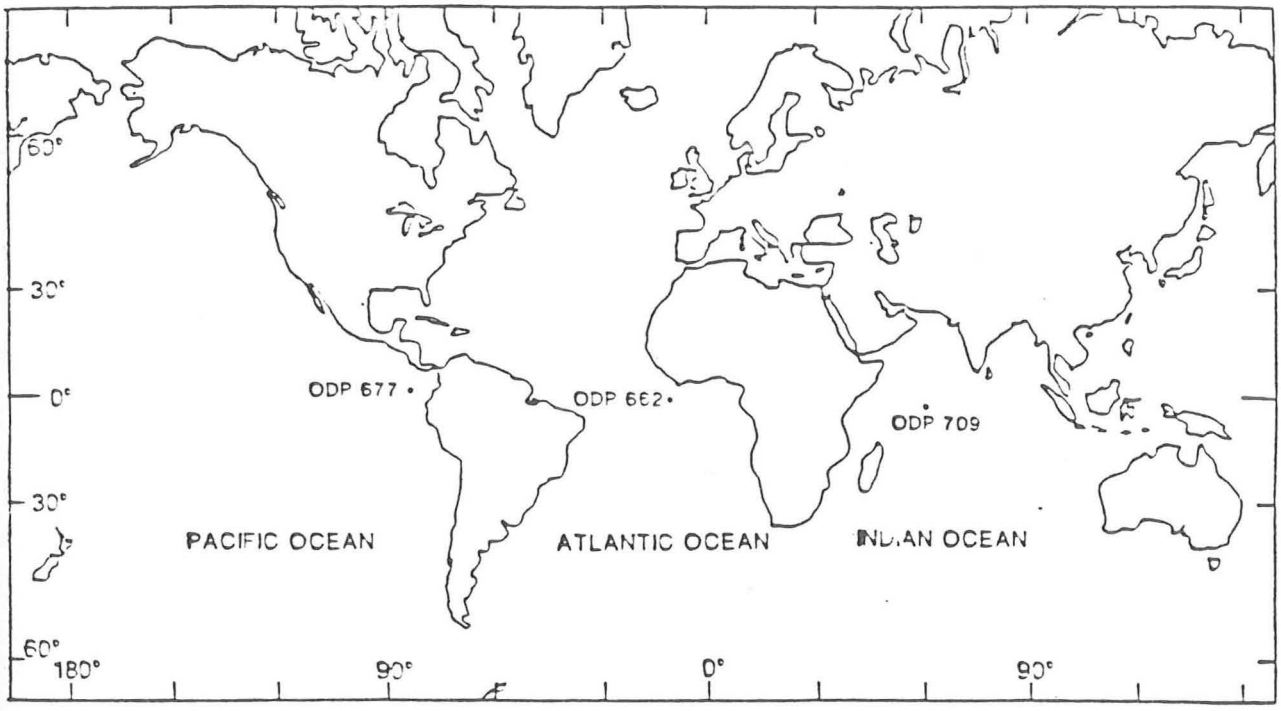

Figure 3:2 Location of sites in study

TABLE 3:1

Modern sea-surface temperatures at equatorial sites 662, 677 and 709 (CLIMAP, 1981).

	February	August
Site 662	27°C	23°C
Site 677	26°C	24.5°C
Site 709	28°C	27.5°C

TABLE 3:2

Equatorial sites selected, their geographic positions and water depth.

HOLE	LOCATION	WATER DEPTH(M)	REFERENCE
		ATLANTIC SITE	
662A	1°S 11°W	3,824	Ruddiman, Sarnthein et al., 1988.
		INDIAN SITE	
709C	4°S 61°E	3,038	Backman, Duncan et al., 1988.
		PACIFIC SITE	
677A	1°N 84°W	3,461	Becker, Sakai, Merrill et al., 1987

best Pliocene sequences available today close to the equator. Sites 662 and 677 were sampled at 10 cm intervals and Site 709 at 5 cm intervals. (Site 662, 10cm ≈ 2ka; Site 677, 10cm ≈ 0·2 ka; Site 709, 5cm ≈ 0·5 ka)

3:2:1 Site 662

This is located close to the equator on the upper eastern flank of the mid-Atlantic Ridge (Ruddiman, Sarnthein, et al., 1988). The interval analysed has a lithology of nannofossil and foraminifer ooze. This site is influenced by the South Equatorial Current and is within the equatorial divergence, and hence is affected by upwelling conditions and high productivity.

3:2:2 Site 709

This site is located in the western equatorial Indian Ocean and is situated in a small basin perched near the summit of the Madingley Rise, a regional topographic high between the Carlsberg Ridge and the northern Mascarene Plateau (Backman, Duncan, et al., 1988). The irregular basement topography is draped with sediments, varying in thickness from less than 50 m to over 400 m. The sediments alternate from clay bearing nannofossil oozes to nannofossil oozes. This site is thought to be located under a stable warm water mass of modest productivity.

3:2:3 Site 677

This site is located about 3 km south of Site 504 in the eastern

equatorial Pacific between the Ecuador and Panama Fracture Zones in a major upwelling area (Becker, Sakai, Merrill et al., 1987). The sediments are composed of siliceous calcareous nannofossil ooze of pelagic origin (Houghton, 1990). Site 677 is located in an area representing a latitudinal band of high biological activity for at least several hundred thousand years, associated with the Peru Current and equatorial divergence (Moore et al., 1973).

Shackleton and Hall (1983) obtained a high resolution (2.5 ka sampling interval) oxygen isotopic record of climatic variation for the eastern equatorial Pacific Ocean from Hole 504B. They demonstrated that the Pliocene sediments in this region may preserve an unusually good isotopic record from a high sedimentation rate environment. Site 677 would therefore be expected to contain a record of Discoaster abundance variability which is unusually rich in detail.

3:3 AGE-MODELS AND SEDIMENTATION RATES

3:3:1 Biostratigraphic and/or magnetostratigraphic control points?

Magnetostratigraphic data were poor or were lacking at all sites. The age-models are based therefore on biostratigraphic datums, especially those related to Discoaster events for internal consistency. The age-model for Site 662 is discussed in Chapter 2. From the age-model of Site 662, the LAD (Last Appearance Datum) of Discoaster variabilis occurred approximately at 2.90 Ma

(Fig. 2:4:4). Discoaster variabilis was used in constructing the age-depth plots for the other two sites in conjunction with the LAD of G. altispira at 2.95 Ma. Globoquadrina altispira may be prone to dissolution and low abundances.

3:3:2 Site 709

A longer time interval of between approximately 1.88-3.50 Ma was analysed (Fig. 3:3:2, Table 3:3a). Calcidiscus macintyrei (LAD 1.45 Ma) and Reticulofenestra pseudoumbilica (LAD 3.56 Ma), both coccolith datums, are included in the age-model (Table 3:3c). Clearly defined datums were provided by the LAD's of D. brouweri, D. triradiatus, D. tamalis and the base of the acme of D. triradiatus. The LAD of D. pentaradiatus at 2.38 Ma by extrapolation from Site 659 fits the age-depth plot well. However, no distinctive final peak is ascertained for the LAD of D. surculus at 2.39 Ma in relation to the D. pentaradiatus extinction at 2.38 Ma as seen at Sites 662, 658 and 659. The LAD's of these two species are thought to be very close as shown in Chapter 2 with D. surculus disappearing of the order 10-20 ka prior to D. pentaradiatus. By interpolation between the LAD of D. pentaradiatus, the minor peak of D. surculus at 23.05 mbsf (metres below sea-floor) is assumed to represent its LAD at 2.39 Ma. Specimens recorded after this event were mostly worn, and are considered reworked. For the age-model, D. variabilis (LAD 2.90 Ma) was used instead of the LAD of G. altispira at 2.95 (Nick Shackleton, Pers. Comm.) because the former is determined with better

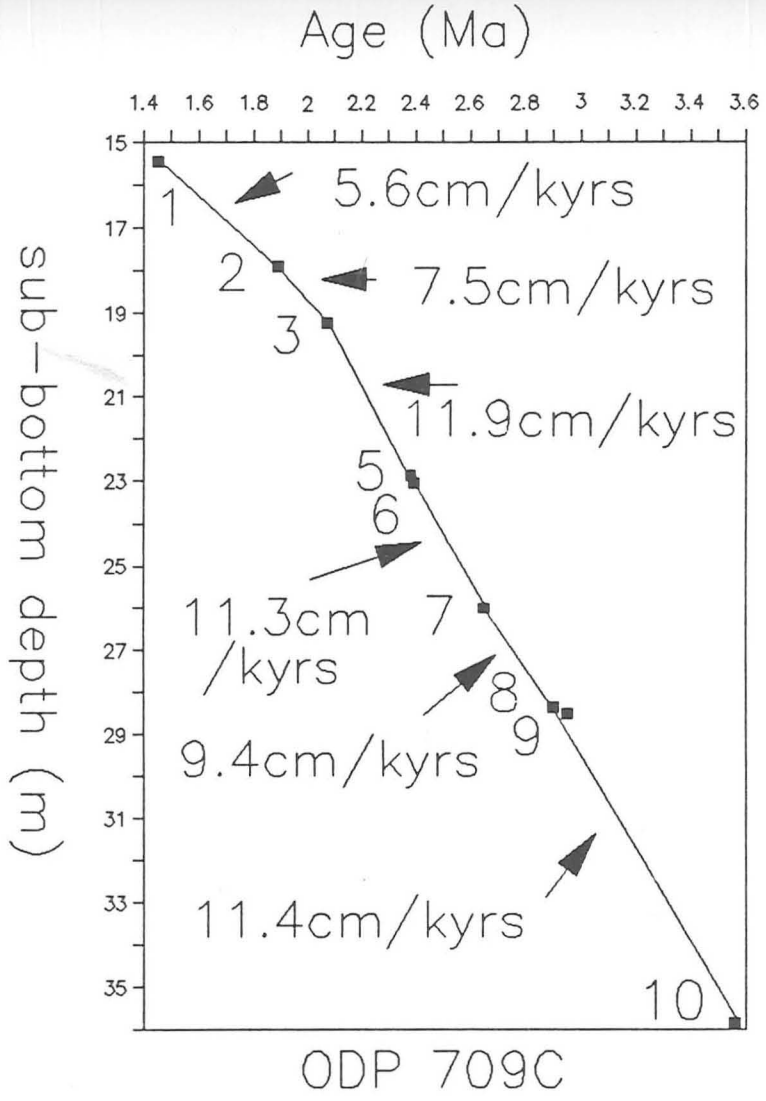

Figure 3:3:2 Age/depth relationships of biochronologic control points in ODP 709C. Refer to Table 3:3a for control points used.

TABLE 3:3

Table 3:3a. Datum levels used to construct Fig. 3:3:2

HOLE 709C

		DEPTH (mbsf)	AGE (ma)
1	LAD *C. macintyrei*	15.45	1.45
2	LAD *D. brouweri* & *D. triradiatus*	17.90	1.89
3	Base of *D. triradiatus* acme	19.25	2.07
*5	LAD *D. pentaradiatus*	22.85	2.38
*6	LAD *D. surculus*	23.05	2.39
7	LAD *D. tamalis*	26.00	2.65
+8	LAD *D. variabilis*	28.35	2.90
9	LAD *G. altispira*	28.50	2.95
10	LAD *R. pseudoumbilica*	35.85	3.56

Table 3:3b. Datum levels used to construct Fig. 3:3:3

HOLE 677A

2	LAD *D. brouweri* & *D. triradiatus*	73.68	1.89
3	Base of *D. triradiatus* acme	90.50	2.07
*6	LAD *D. surculus*	96.50	2.39
D	Abrupt decline in diatoms	104.20	2.50#
7	LAD *D. tamalis*	113.80	2.65
+8	LAD *D. variabilis*	128.00	2.90
9	LAD *G. altispira*	130.20	2.95

* LADs for *D. surculus* and *D. pentaradiatus* taken as 2.39 Ma and 2.38 Ma respectively from Site 659.
+ LAD for *D. variabilis* as approximately 2.90 Ma estimated from Site 662.
# inferred from age-depth plot

Table 3:3c. Summary of control points used in age-models

Hole 662A (Sampling interval=10cm)

Datum	Age (Ma)	Depth (mbsf)	Event	Sedimentation Rate
D. brouweri	1.89	123.2	Extinction	
				5.6cm/ka
D. surculus	2.39	151.4	Extinction	
				3.1cm/ka
G. altispira	2.95	168.5	Extinction	

Hole 709C (Sampling interval=5cm)

C. macintyrei	1.45	15.45	Extinction	
				5.6cm/ka
D. brouweri	1.89	17.90	Extinction	
				7.5cm/ka
D. triradiatus	2.07	19.25	Peak Abundance began	
				11.9cm/ka
D. surculus	2.39	23.05	Extinction	
				11.3cm/ka
D. tamalis	2.65	26.00	Extinction	
				9.4cm/ka
D. variabilis	2.90	28.35	Extinction	
				11.4cm/ka
R. pseudoumbilica	3.56	35.85	Extinction	

Hole 677A (Sampling interval=10cm)

D. brouweri	1.89	73.68	Extinction	
				93.4cm/ka
D. triradiatus	2.07	90.50	Peak Abundance began	
				18.8cm/ka
D. surculus	2.39	96.50	Extinction	
				66.5cm/ka
D. tamalis	2.65	113.80	Extinction	
				54.7cm/ka
G. altispira	2.95	130.20	Extinction	

precision and the use of the latter introduced a minor change in sedimentation rate.

3:3:3 Site 677

High sedimentation rates characterize this upwelling site. The mutual extinction of D. brouweri and D. triradiatus is clearly defined (Fig. 3:3:3, Table 3:3b). Prior to their extinctions, the abundances of these taxa are low prior to this event. The event is unlikely to be the result of reworking, since D. triradiatus occurs in such low abundances further down the core. These events are almost invisible when plotted on the same scale as Site 709. At DSDP 504, a "hiatus" was thought to occur at the D. triradiatus acme (Backman and Shackleton, 1983). At Site 677, when D. triradiatus is plotted as a percentage of D. brouweri plus D. triradiatus, the extinction event and the base of the acme at 2.07 Ma can both be clearly seen.

Between the LAD of D. brouweri (1.89 Ma) and the base of the D. triradiatus acme (2.07 Ma), there is an unusually high sedimentation rate of 93.4 cm/ka (Table 3:3c). This is reduced to 18.8 cm/ka between the latter datum and the LAD of D. surculus at 2.39 Ma, identified by a distinctive abundance peak. This reduced rate is still much higher than observed at any of the other sites. Strangely, D. pentaradiatus appears virtually absent or very suppressed in sediments younger than approximately 2.9 Ma.

The sedimentation rate is at least three times higher between 2.39 and

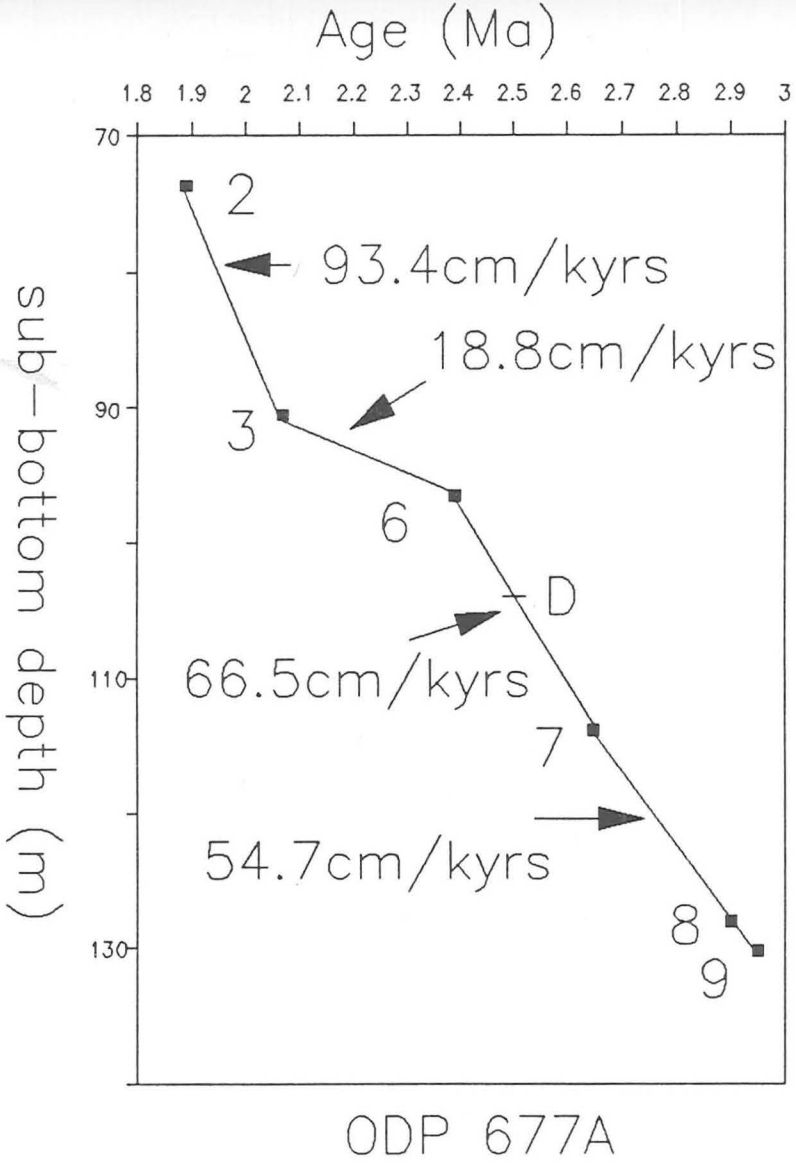

Figure 3:3:2 Age/depth relationships of biochronologic control points in ODP 677A. Refer to Table 3:3b for control points used.

2.95 Ma at Site 677 than in the corresponding intervals at Sites 709 and 662. Clearly defined LAD's for D. surculus, D. tamalis, D. variabilis and G. altispira (Nick Shackleton, Pers. Comm.) fall almost on a straight line. A sudden reduction in diatom abundance at 104.20 mbsf is inferred from the age-depth plot as occurring approximately at 2.50 Ma.

3:4 DISCOASTER SPECIES ABUNDANCE PATTERNS AND RELATIVE ABUNDANCES WITHIN THE ASSEMBLAGE

The number of fields of view counted is related to overall abundance patterns at each site but was constant for all samples at each site. A relatively constant background density is maintained at a view field diameter of 0.3 mm. At Sites 677, 662 and 709, the number of fields of view counted were 30, 40 and 20, respectively. The absolute and not the relative abundances for Discoaster variabilis are only shown since it occurs at the end of the time interval analysed for Sites 677 and 662.

3:4:1 Discoaster brouweri and Discoaster triradiatus

These two species have a synchronous extinction at 1.89 Ma (e.g., Backman and Shackleton, 1983), and are the last two species of the genus Discoaster to disappear. Discoaster brouweri (Fig. 3:4:1a) is the only species covering the complete time interval investigated as seen in Chapter 2. Besides the brief acme with Discoaster triradiatus between 1.89 and 2.07 Ma, D.

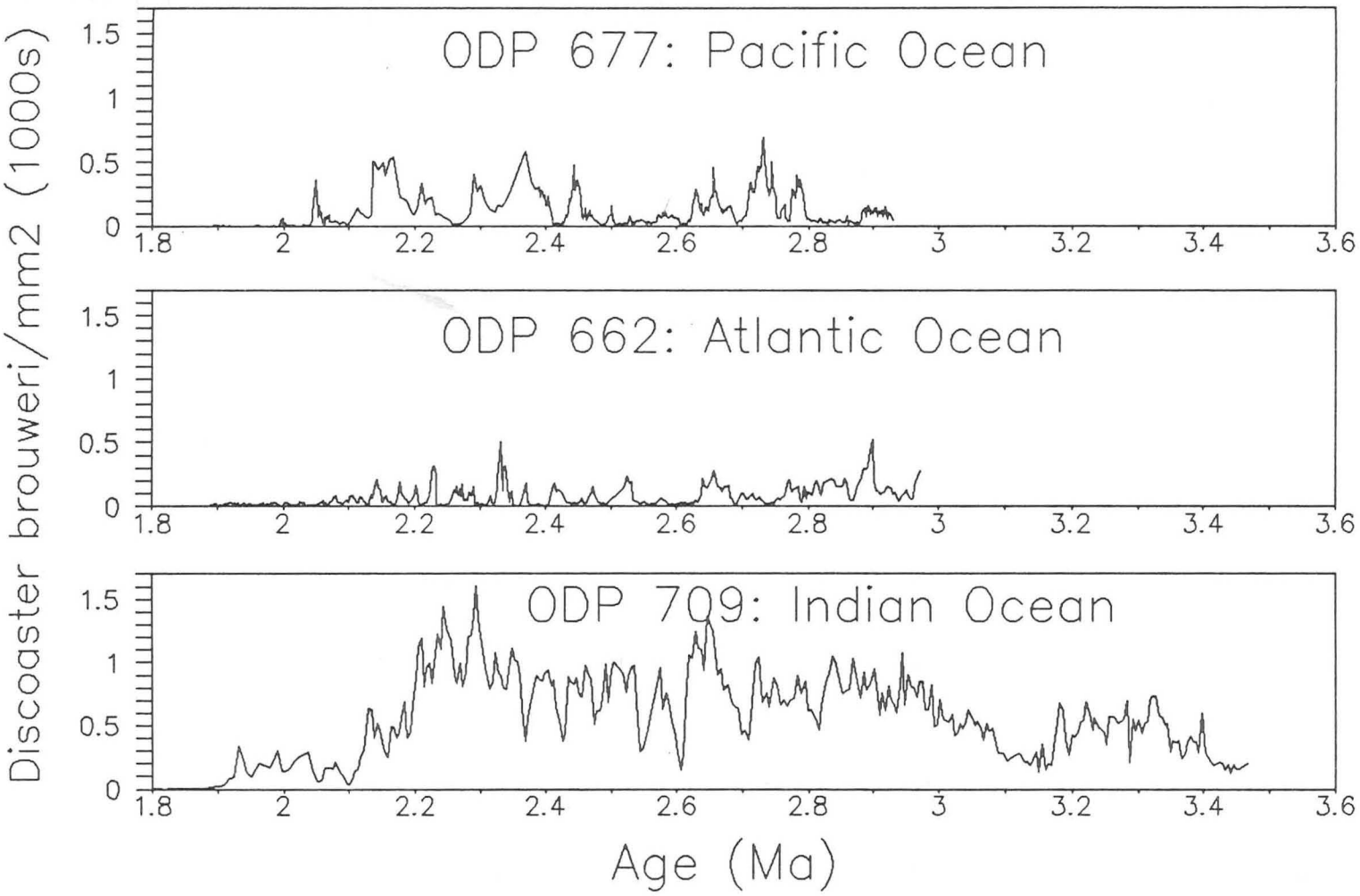

Figure 3:4:1a Abundance plots of D. brouweri at Sites 709, 662 and 677.

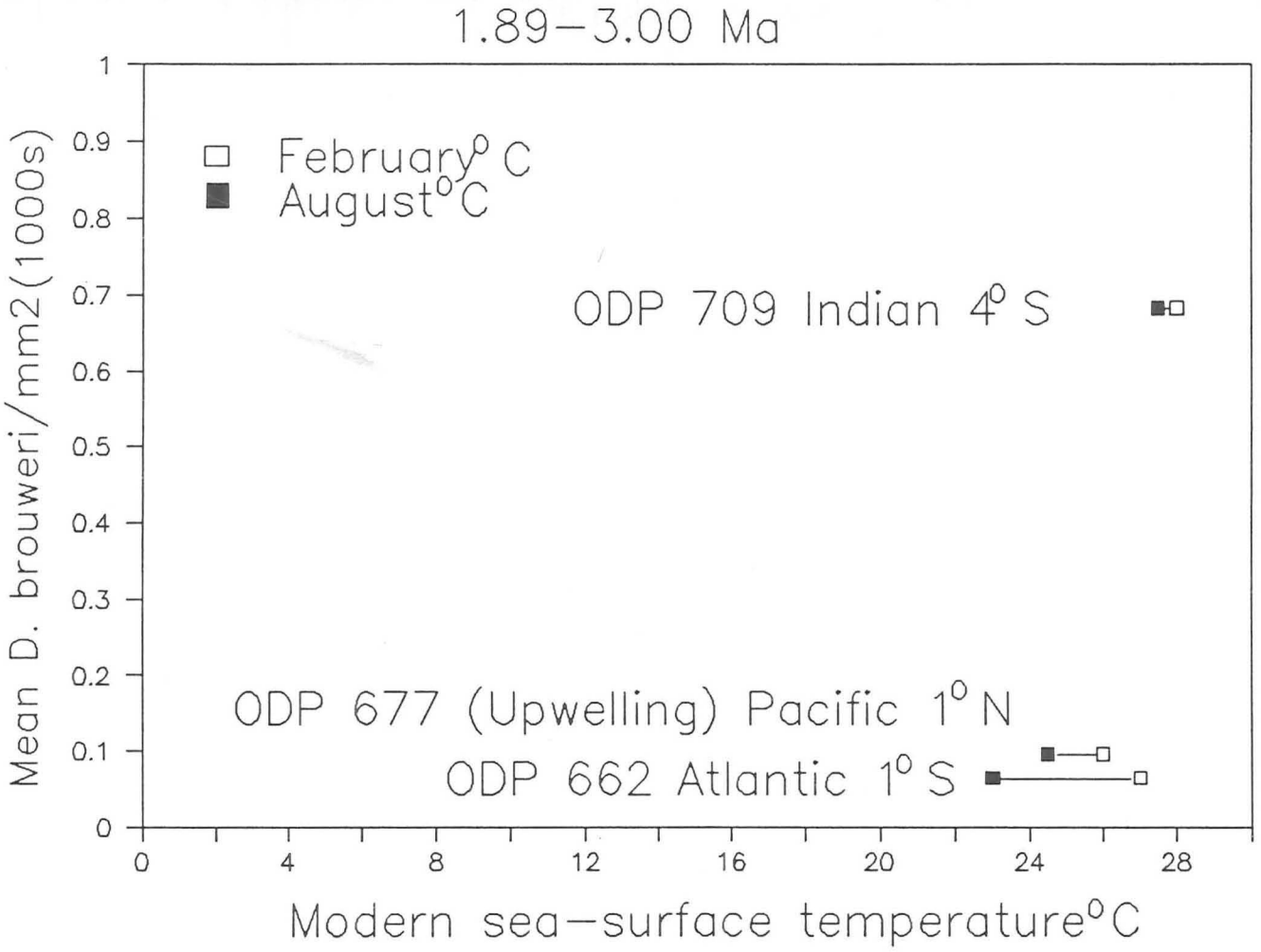

Figure 3:4:1b Mean D. brouweri/mm2 versus modern sea–surface temperature at Sites 709, 662 and 677.

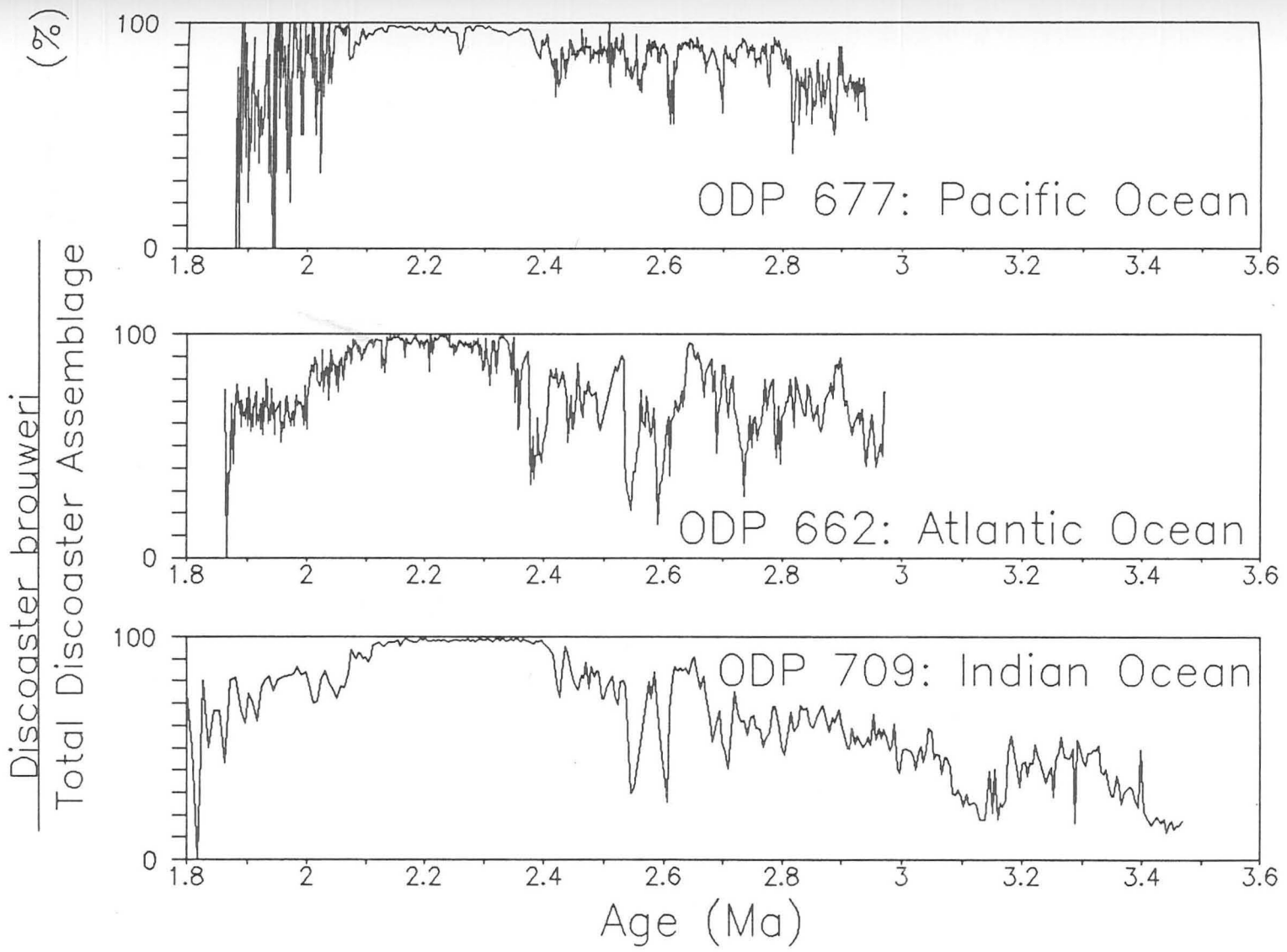

Figure 3:4:1c Percentage abundance plots of D. brouweri at Sites 709, 662 and 677.

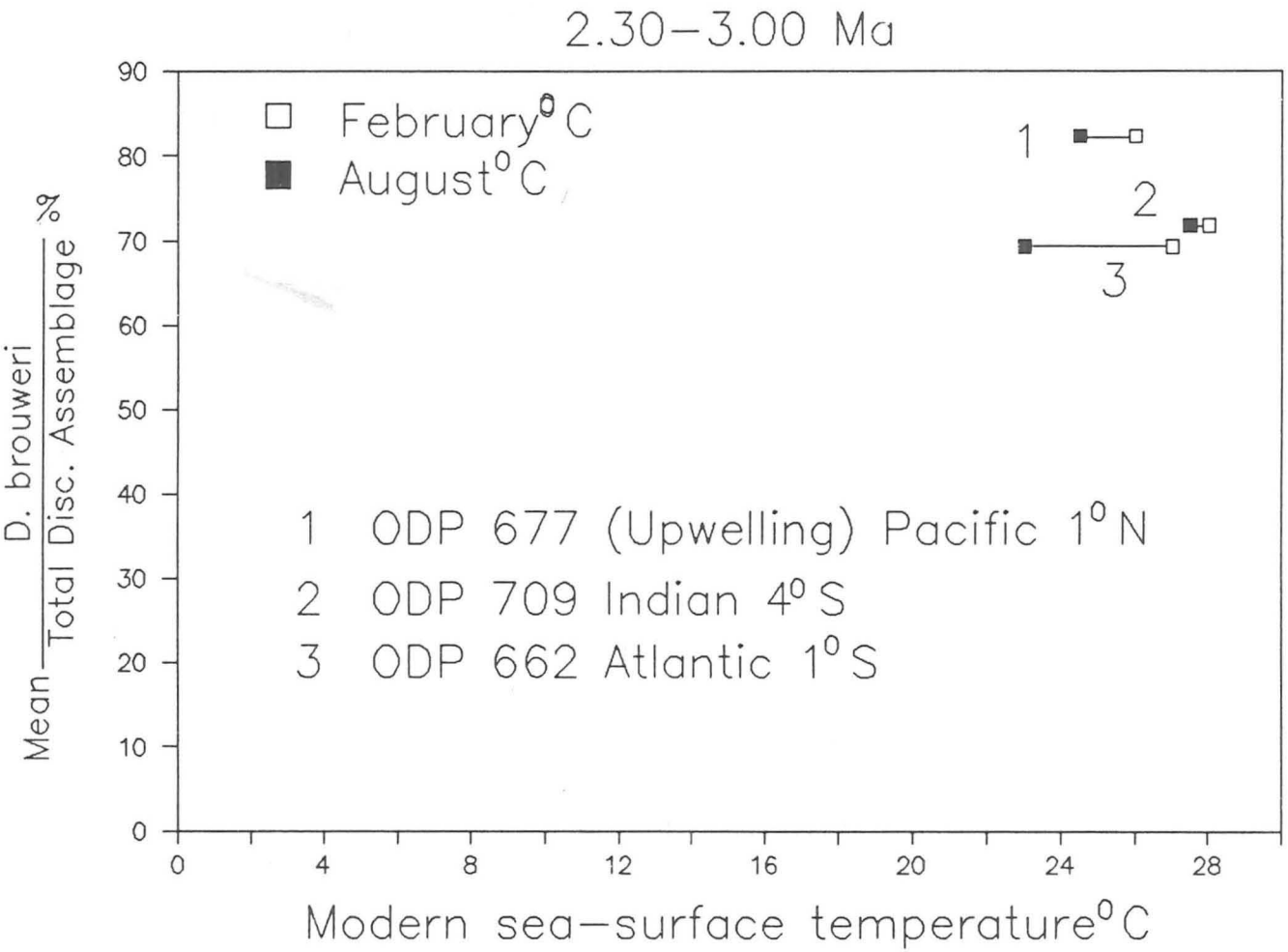

Figure 3:4:1d Mean D. brouweri percentage versus modern sea–surface temperature at Sites 709, 662 and 677.

brouweri is the sole survivor after approximately 2.38 Ma. The mean abundance of D. brouweri is shown between 1.89-3.00 Ma versus modern sea-surface temperature (Fig. 3:4:1b). This clearly emphasises the higher absolute abundances of D. brouweri in the Indian Ocean site in comparison to the lower similar abundances in the Pacific and Atlantic sites despite the similar temperatures. Other factors must therefore be important. Prior to 2.38 Ma, D. brouweri is a major component of the complete Discoaster assemblage (Fig. 3:4:1c). If the mean abundance of D. brouweri relative to the complete Discoaster assemblage is displayed versus modern sea-surface temperature, this reveals a high proportion of D. brouweri at all three sites (Fig. 3:4:1d). At the upwelling site, Site 677, D. brouweri composes the highest proportion of the complete Discoaster assemblage. In Chapter 2, the relative abundance of D. brouweri was shown to decrease in the North Atlantic with increasing latitude.

All these sites demonstrate abundance reduction through time of D. brouweri, especially during the 200 ka prior to the extinction event.

Discoaster triradiatus has distinct acmes at all three sites (Fig. 3:4:1e). The mean abundance of D. triradiatus is shown between 1.89-2.07 Ma versus modern sea-surface temperature (Fig. 3:4:1f). This reveals the recurring trend of high abundances of D. triradiatus at the warmer Indian Ocean site, and suppressed abundances at the Pacific and Atlantic sites. Since the minor temperature differences cannot account for these abundance differences, other factors must be considered. The Discoaster triradiatus acme is emphasised clearer by the percentage relationship with D. brouweri (Fig. 3:4:1g). The mean relative

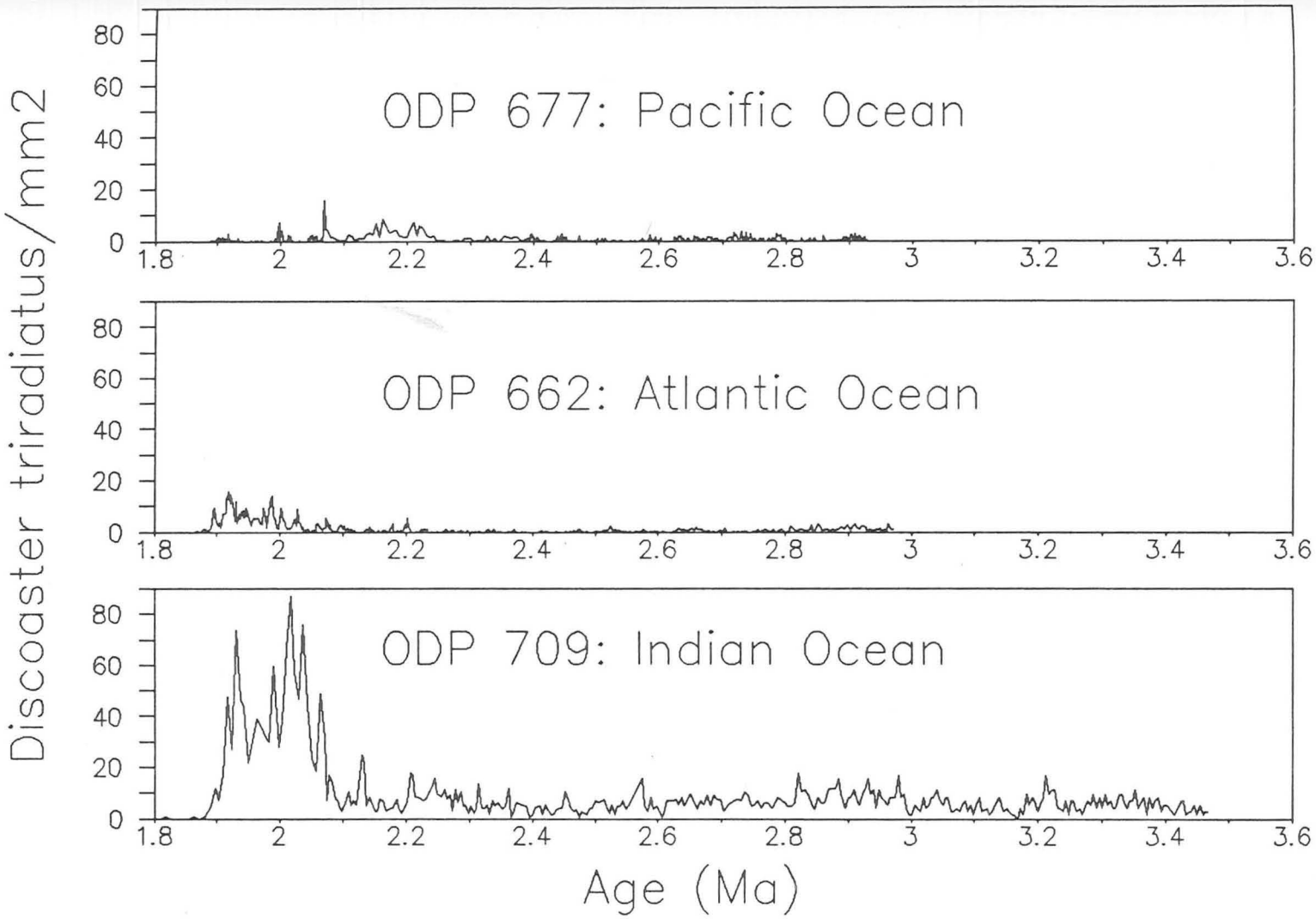

Figure 3:4:1e Abundance plots of D. triradiatus at Sites 709, 662 and 677.

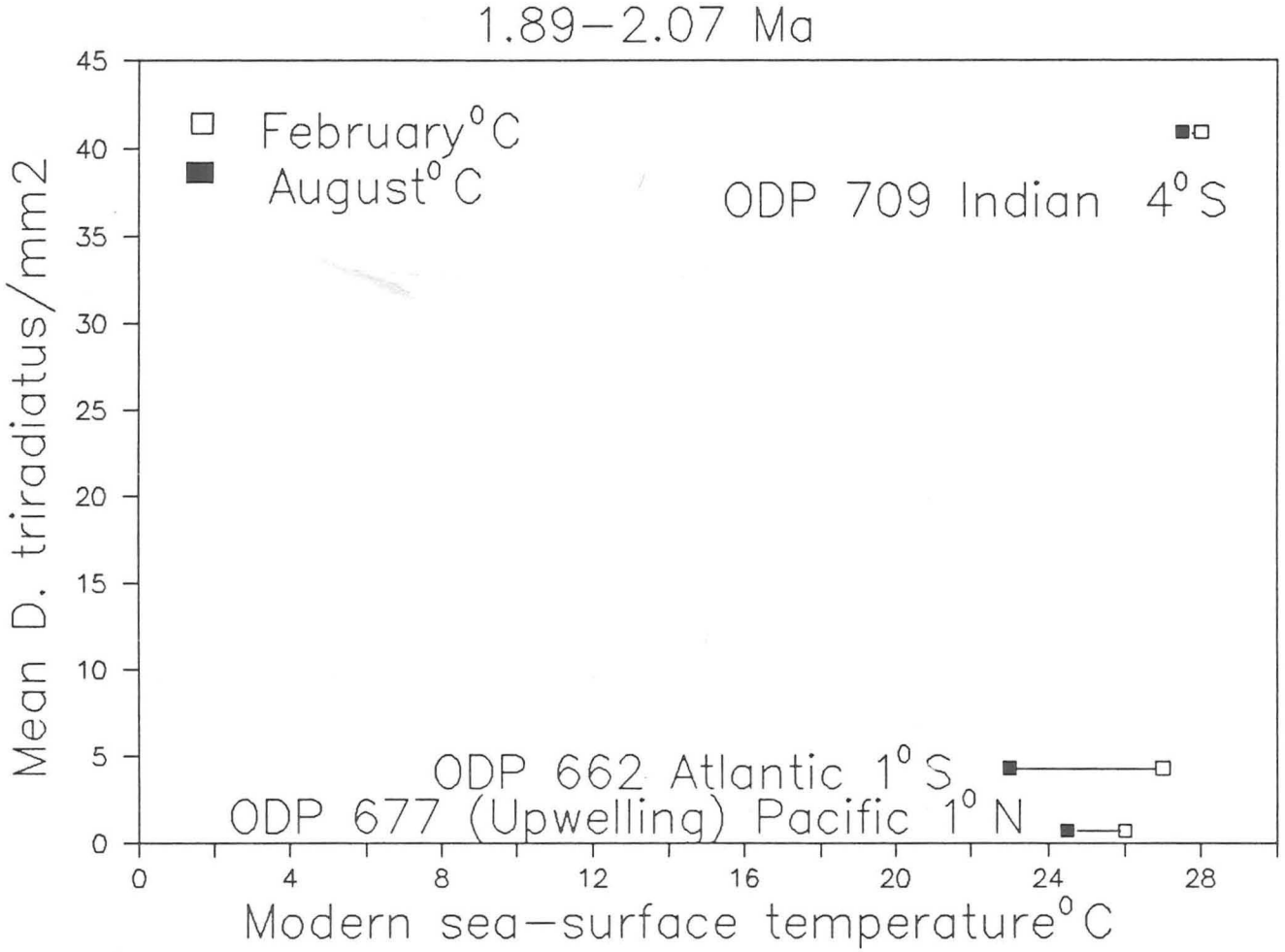

Figure 3:4:1f Mean D. triradiatus/mm2 versus modern sea–surface temperature at Sites 709, 662 and 677.

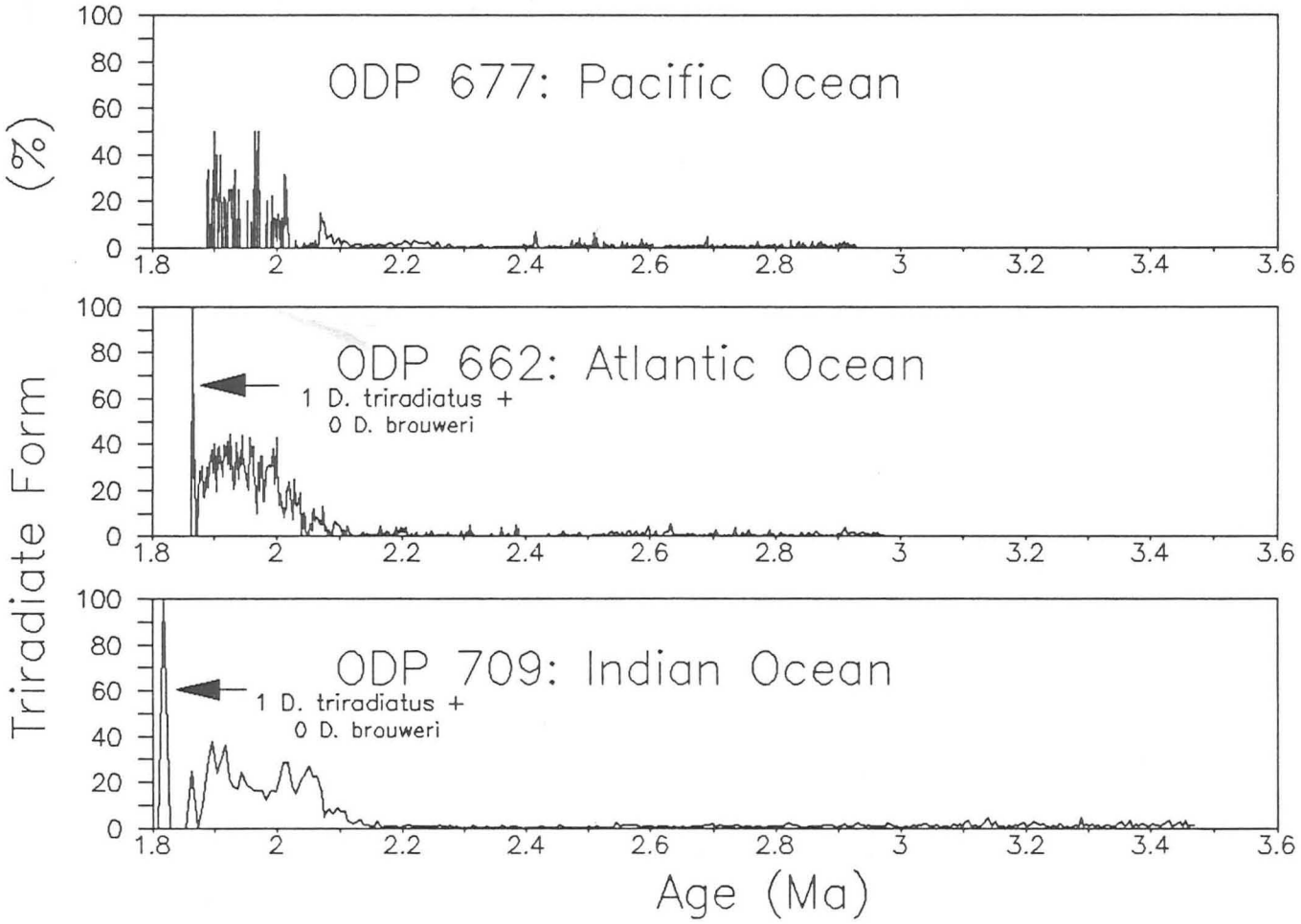

Figure 3:4:1g Percentage abundance plots of D. triradiatus as a percentage of the sum of D. triradiatus and D. brouweri at Sites 709, 662 and 677.

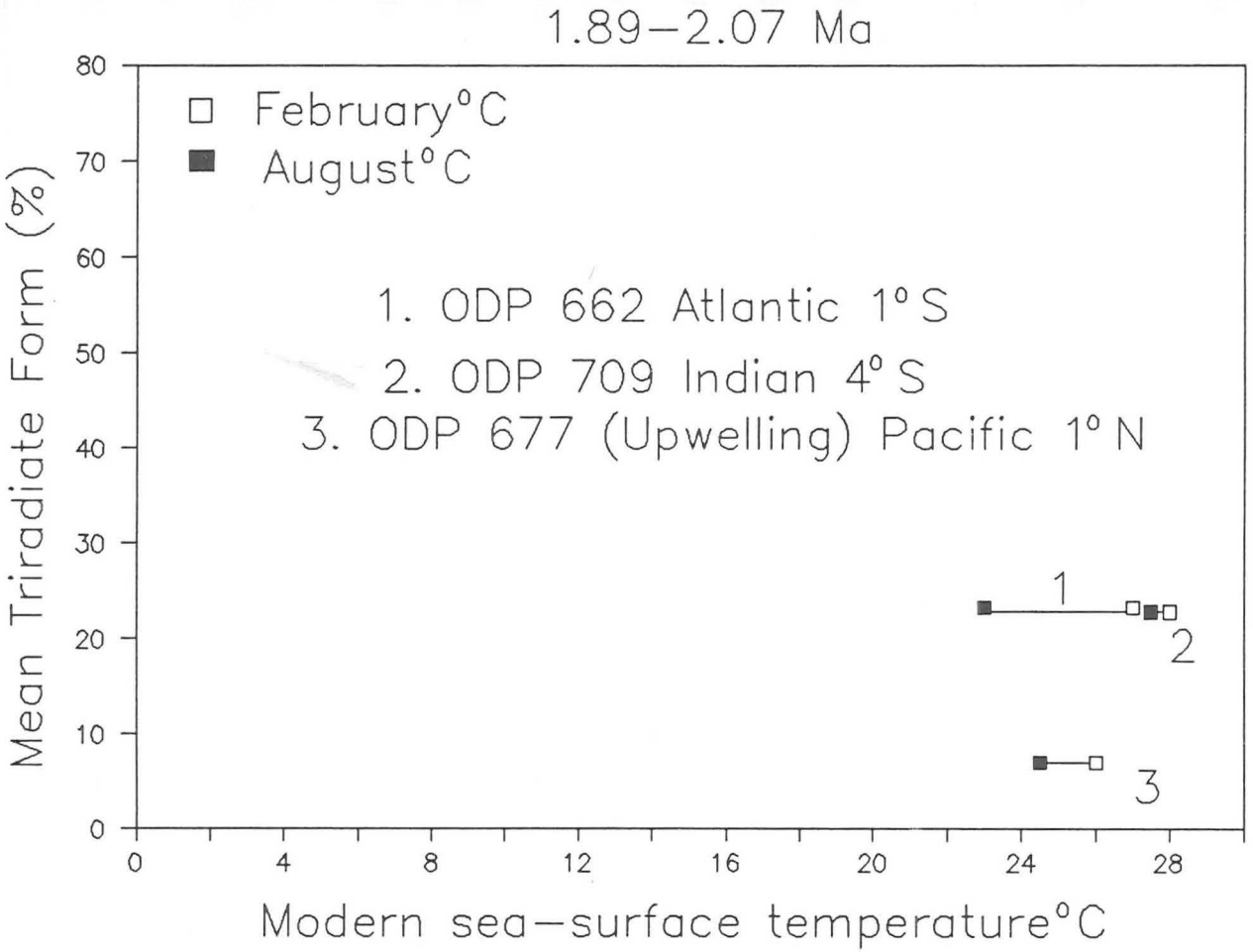

Figure 3:4:1h Mean percentage of D. triradiatus divided by the sum of itself and D. brouweri versus modern sea–surface temperature at Sites 709, 662 and 677

abundance of D. triradiatus in relation to its sum with D. brouweri is plotted versus sea-surface temperature (Fig. 3:4:1h). This reflects the consistent relationship between D. brouweri and D. triradiatus of 20% at the Indian and Atlantic sites. A lower value, however, is recorded at the Pacific upwelling site, Site 677, where abundances of both these species are suppressed during this interval.

3:4:2 Discoaster pentaradiatus and Discoaster surculus

These two species have been recorded from different oceans as having close extinctions between 2.35-2.45 Ma. Discoaster surculus is generally agreed to precede Discoaster pentaradiatus by a short time interval (Bukry, 1973; Backman and Shackleton, 1983; Backman et al., 1986; Backman and Pestiaux, 1987). In Chapter 2, dates of 2.38 and 2.39 Ma were assigned respectively, to D. pentaradiatus and D. surculus from Site 659. Core V32-127, from which a palaeomagnetic record is available displayed the same final abundance peak for D. surculus and this age was used in Site 659.

Discoaster pentaradiatus (Fig. 3:4:2a) was very rare in the upwelling site, Site 677, especially after 2.9 Ma. Site 709 may show much greater abundances than Site 662, but both reveal a clear trend in abundance reduction through time up to the extinction event. The mean abundance of D. pentaradiatus between 2.30-3.00 Ma is shown versus modern sea-surface temperature (Fig. 3:4:2b). This emphasises the high abundances of D. pentaradiatus at the Indian

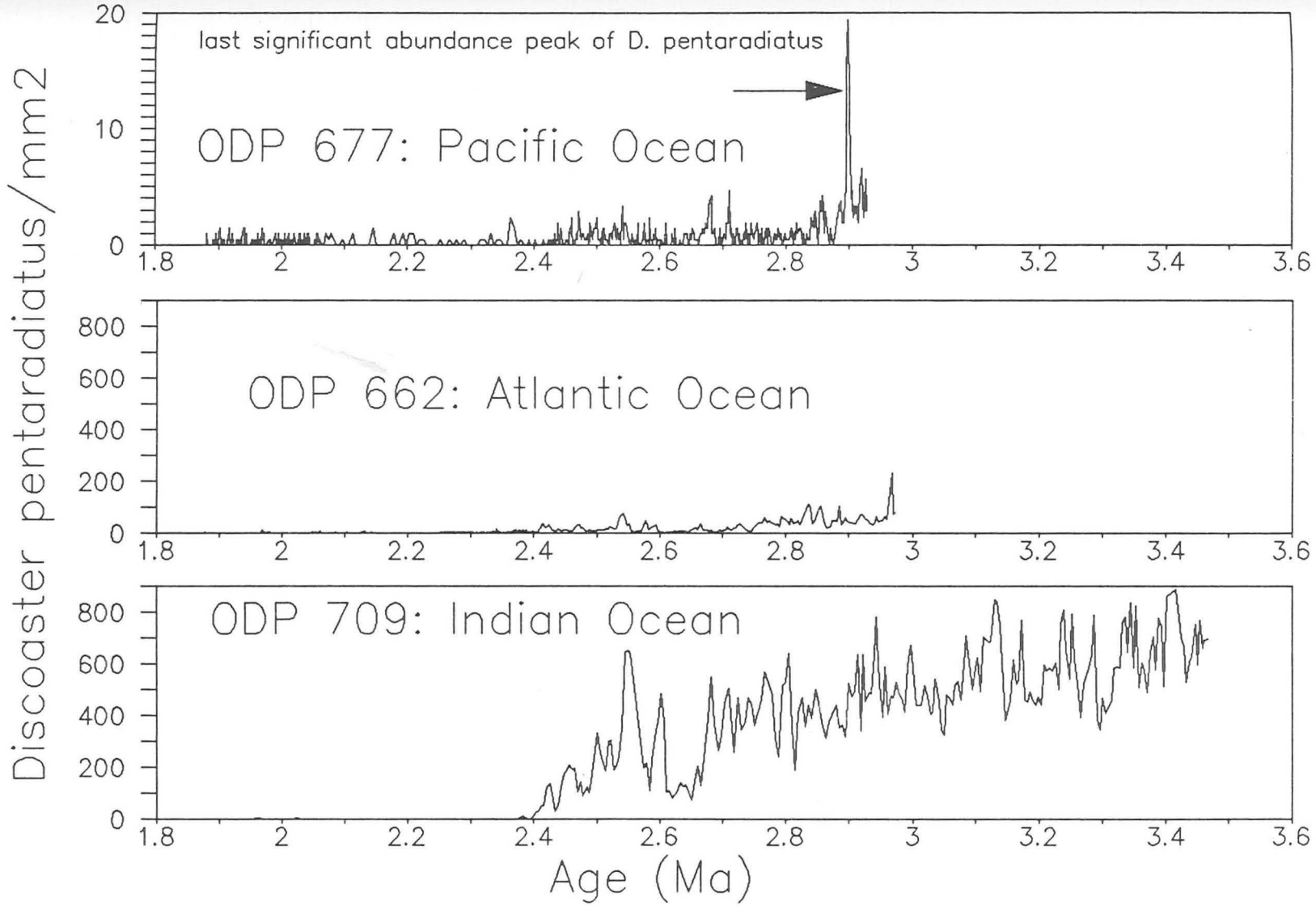

Figure 3:4:2a Abundance plots of
D. pentaradiatus at Sites 709, 662 and 677.

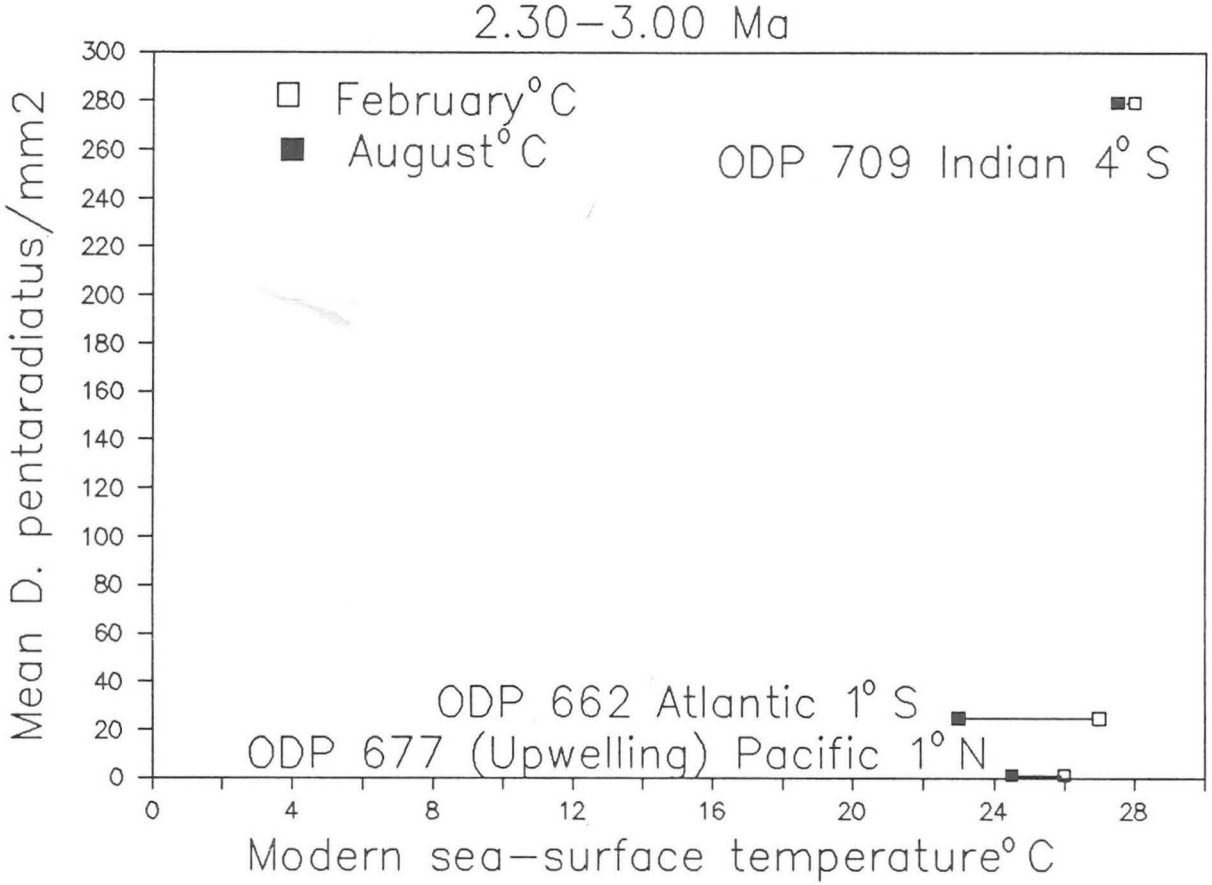

Figure 3:4:2b Mean D. pentaradiatus/mm2 versus modern sea–surface temperature at Sites 709, 662 and 677.

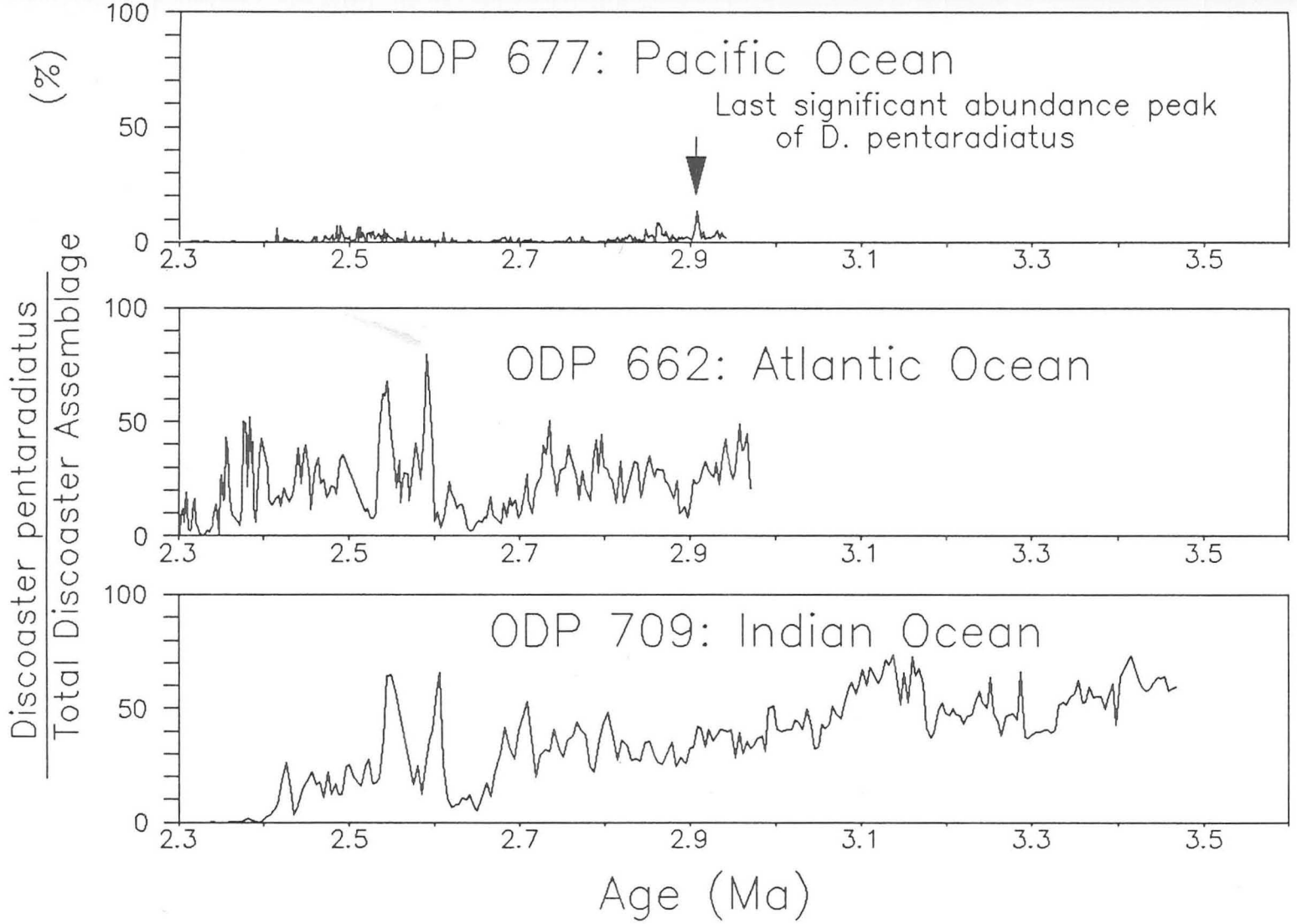

Figure 3:4:2c Percentage abundance plots of D. pentaradiatus at Sites 709, 662 and 677.

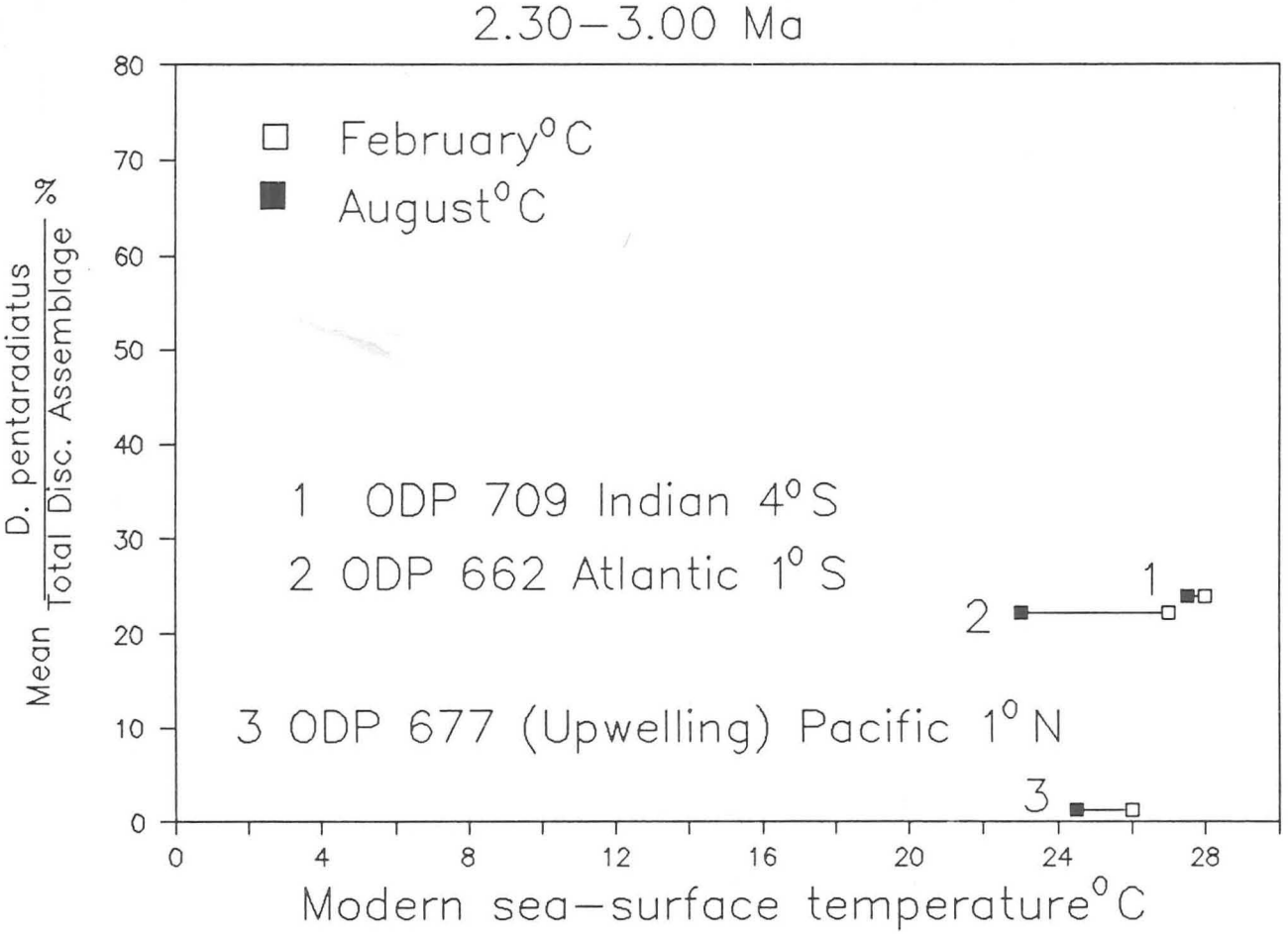

Figure 3:4:2d Mean D. pentaradiatus percentage versus modern sea–surface temperature at Sites 709, 662 and 677.

Ocean site. Factors other than temperature must suppress the abundances of D. pentaradiatus at Site 677. If D. pentaradiatus is shown as a percentage of the total Discoaster assemblage (Fig. 3:4:2c), similar relative abundances are revealed at the Indian and Atlantic sites, even if absolute abundances are different. This feature is further reflected if the mean relative abundance of D. pentaradiatus between 2.30-3.00 Ma is shown versus modern sea-surface temperature (Fig. 3:4:2d).

Discoaster surculus lacks the distinctive final abundance peak at the Indian Ocean site as found at the Atlantic and Pacific sites, though this species occurs in greater abundances at the former site (Fig. 3:4:2e). Compared to the other Discoaster species, D. surculus does not reveal a clear gradual abundance reduction through time up to its extinction event. In view of the overall suppressed abundances of discoasters at the upwelling site, Site 677, D. surculus shows high abundances. The mean abundance of D. surculus between 2.30-3.00 Ma is displayed versus modern sea-surface temperature (Fig 3:4:2f). This shows that D. surculus of all the Discoaster species is most comparable at the Indian and Pacific sites. As a component of the total Discoaster assemblage, D. surculus is unimportant at Site 709, but significant at the higher productivity sites, Sites 677 and 662 (Fig. 3:4:2g). This trend is further shown by displaying the mean relative abundance of D. surculus versus modern sea-surface temperature (Fig. 3:4:2h). Slightly cooler temperatures at Sites 677 and 662 may favour the production of D. surculus.

Sites 662 and 709 further display the frequent inverse abundance

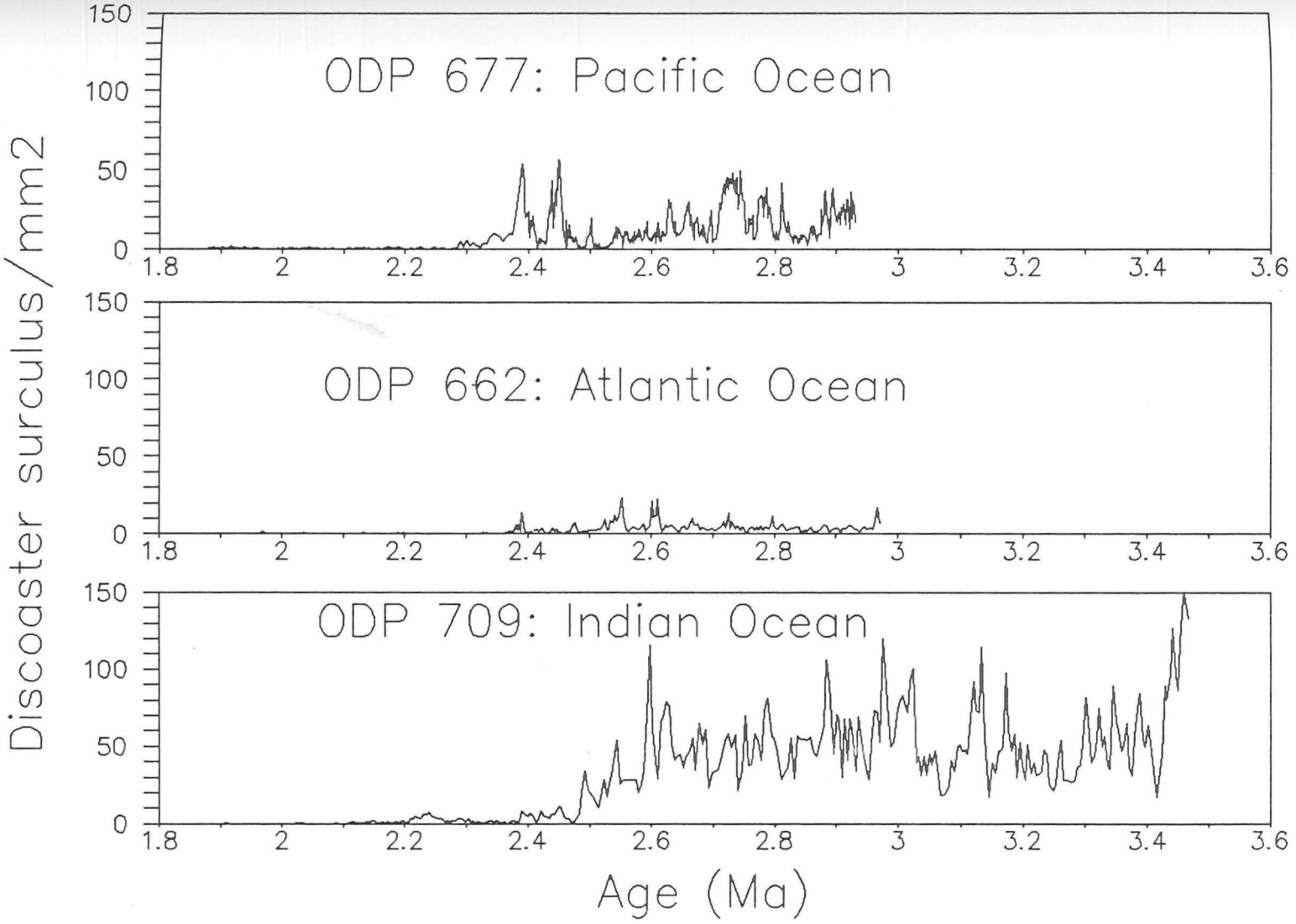

Figure 3:4:2e Abundance plots of D. surculus at Sites 709, 662 and 677.

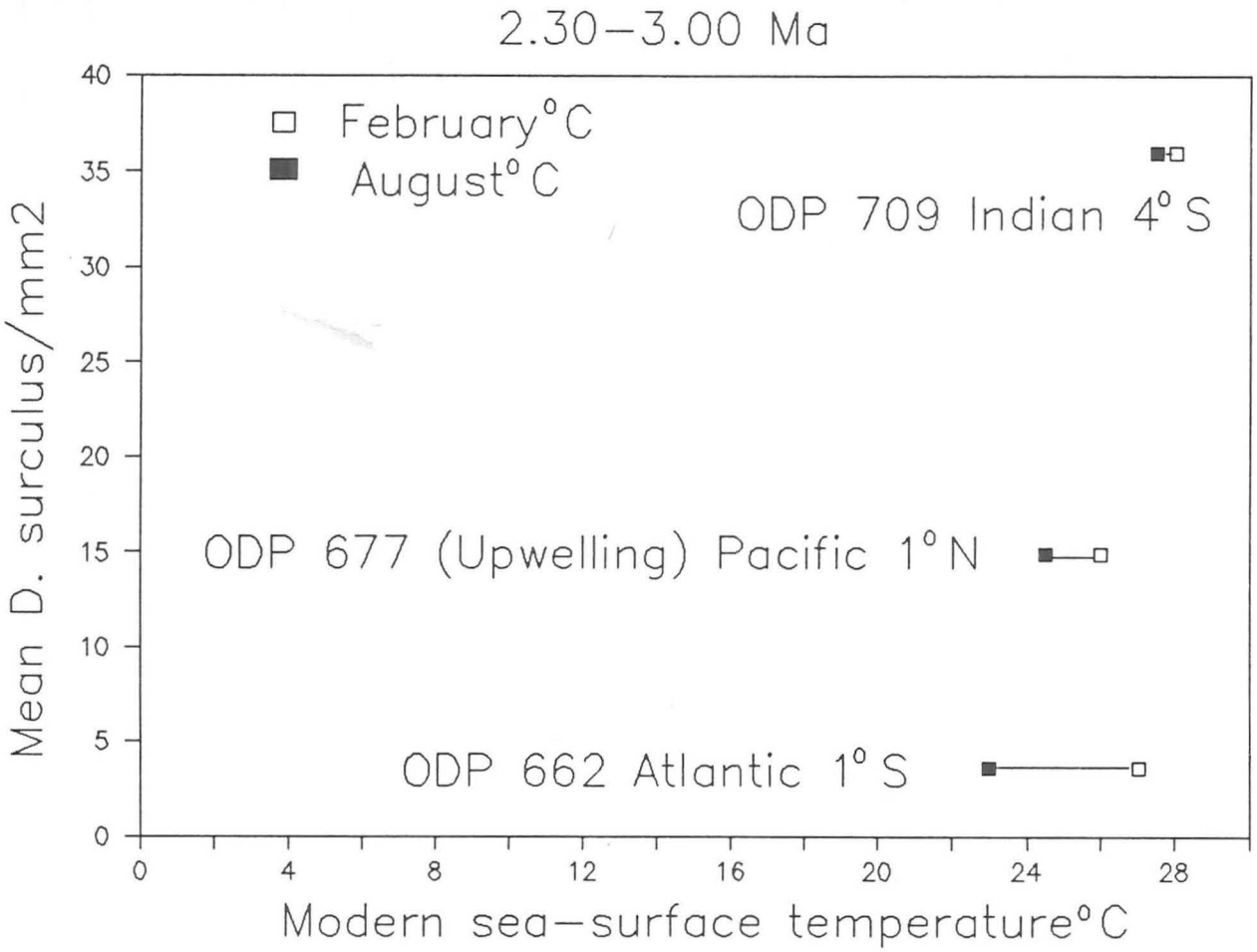

Figure 3:4:2f Mean D. surculus/mm2
versus modern sea–surface temperature
at Sites 709, 662 and 677.

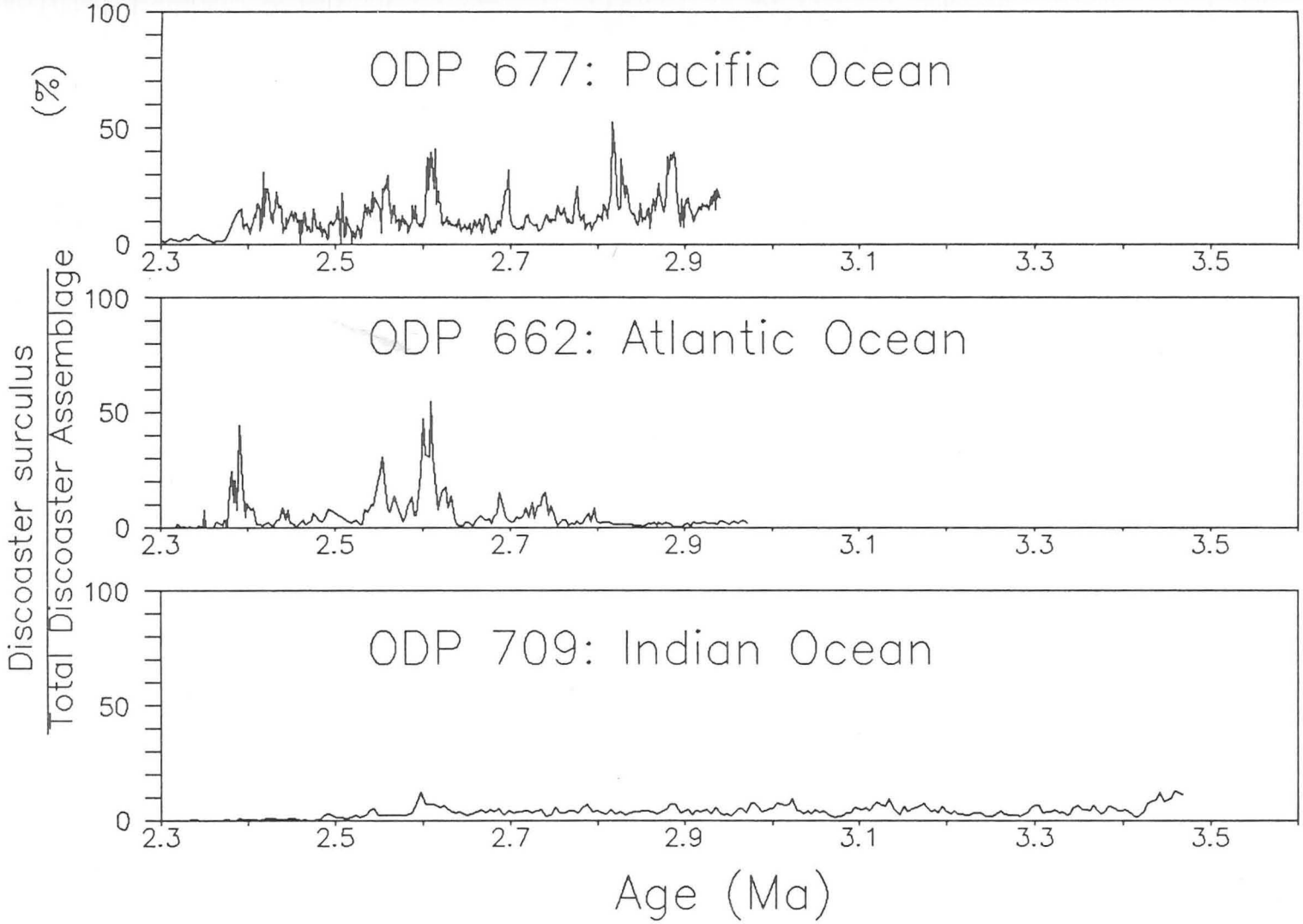

Figure 3:4:2g Percentage abundance plots of D. surculus at Sites 709, 662 and 677.

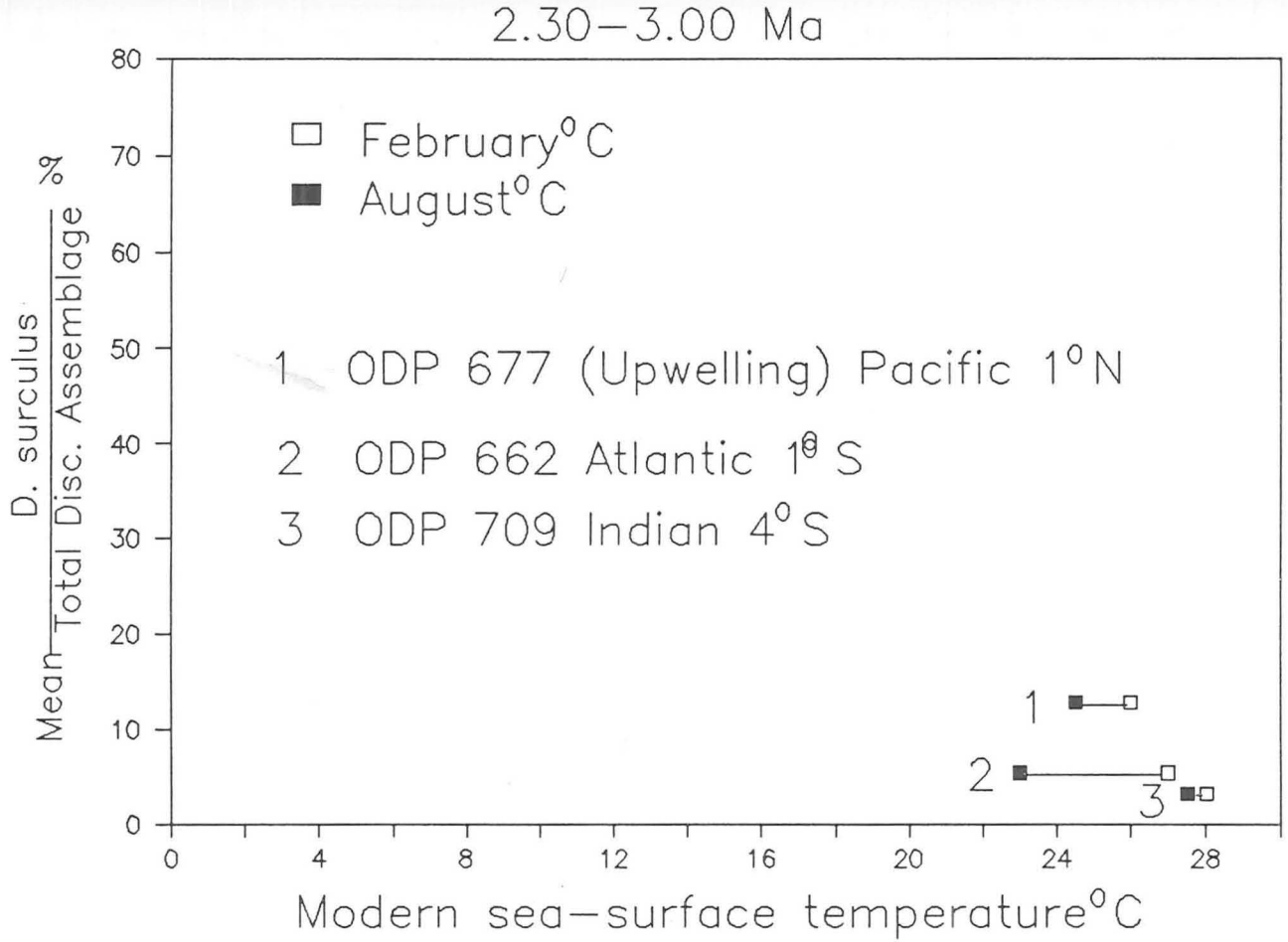

Figure 3:4:2h Mean D. surculus percentage versus modern sea–surface temperature at Sites 709, 662 and 677.

relationship of D. pentaradiatus and D. surculus, which appear to have had different ecological requirements. This is discussed further in Chapter 5.

3:4:3 Discoaster asymmetricus and Discoaster tamalis

These two species co-vary at all three sites and are thought to be taxonomically related (Backman and Shackleton, 1983). The main difference as seen in Chapter 2 is at 2.65 Ma, when D. tamalis becomes extinct, D. asymmetricus shows a major abundance decline but continues in reduced abundances (Backman, 1986). The reduction in abundance through time until 2.65 Ma for both species is clearly demonstrated (Figs. 3:4:3a & 3:4:3b). In terms of absolute abundances, the Indian Ocean site shows much higher abundances of D. asymmetricus and D. tamalis than the Atlantic or Pacific sites. This can be shown further by displaying the mean abundance of D. asymmetricus and D. tamalis versus modern sea-surface temperature (Figs. 3:4:3c & 3:4:3d). This cannot be explained by the minor temperature differences.

As a percentage of the total Discoaster assemblage, however, D. asymmetricus and D. tamalis are shown to be suppressed at all sites (Figs. 3:4:3e & 3:4:3f). Nevertheless, if the mean relative abundances of D. asymmetricus and D. tamalis are displayed versus modern sea-surface temperature, a slight increase in their proportion is revealed with cooler, lower productivity waters (than Site 677) as seen at the Atlantic site, Site 662 (Figs 3:4:3g & 3:4:3h). In Chapter 2, the co-variation between D. brouweri, D. asymmetricus and D. tamalis indicated that they may be taxonomically related. If the relative abundance of D. tamalis is

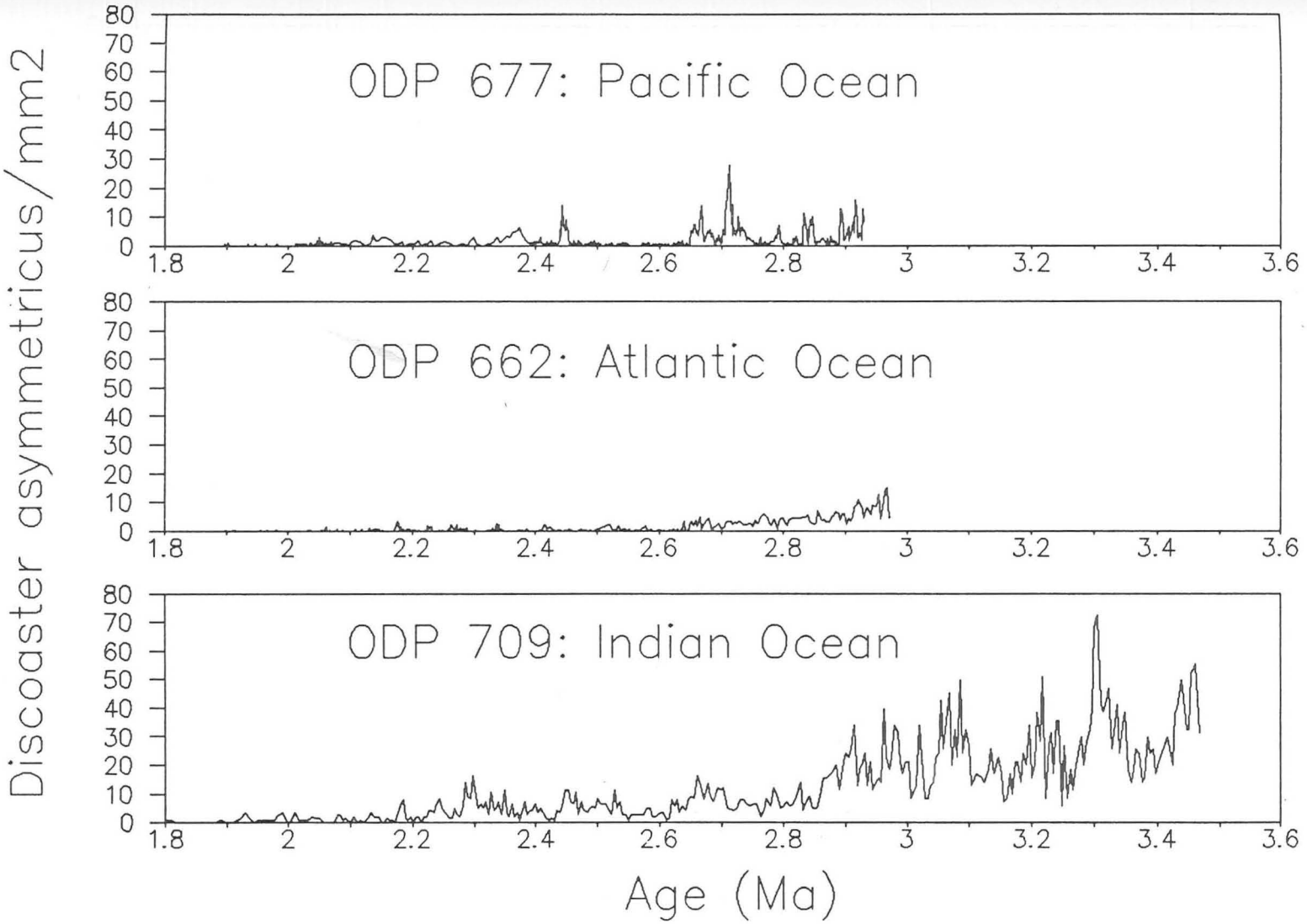

Figure 3:4:3a Abundance plots of D. asymmetricus at Sites 709, 662 and 677.

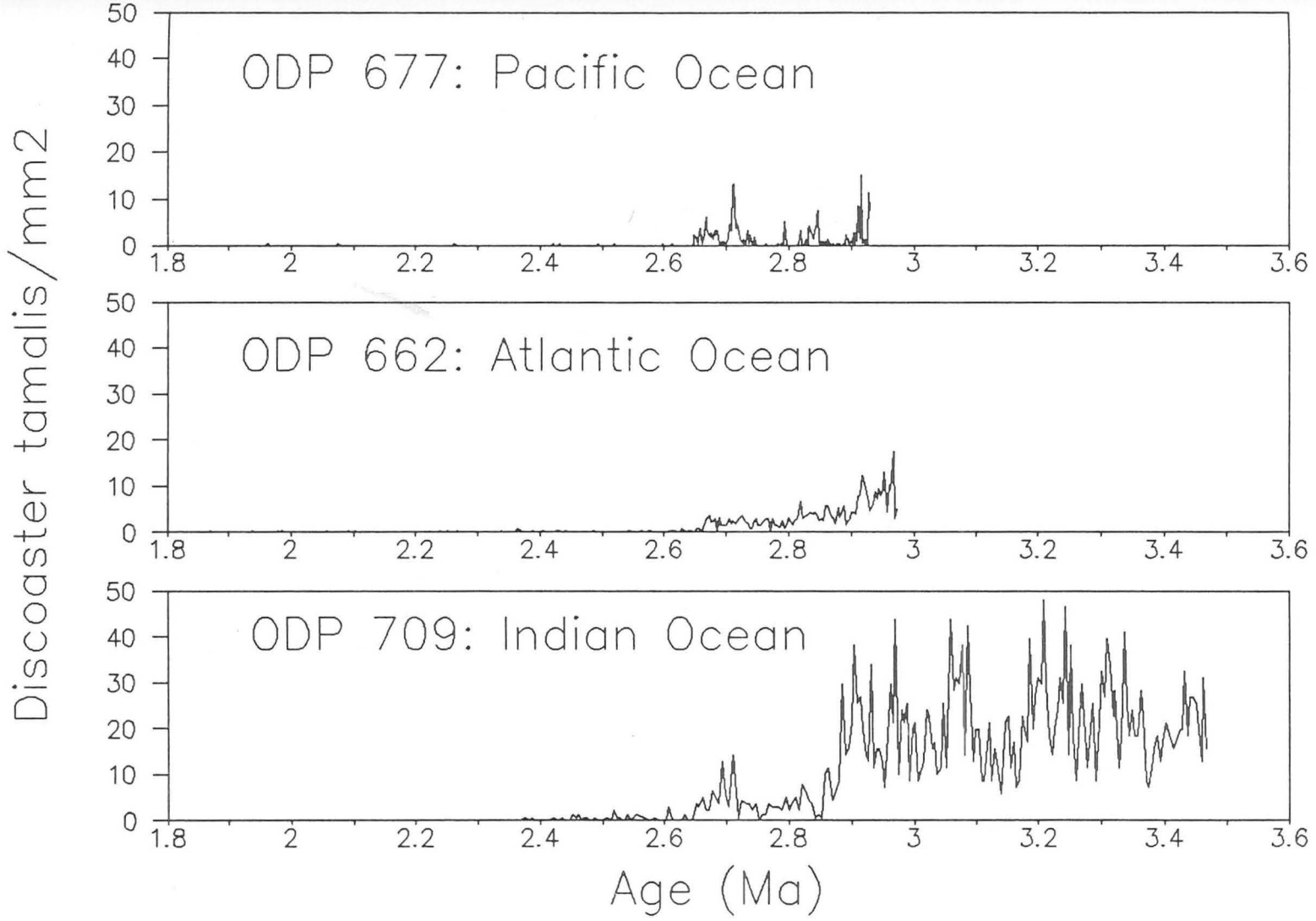

Figure 3:4:3b Abundance plots of D. tamalis at Sites 709, 662 and 677.

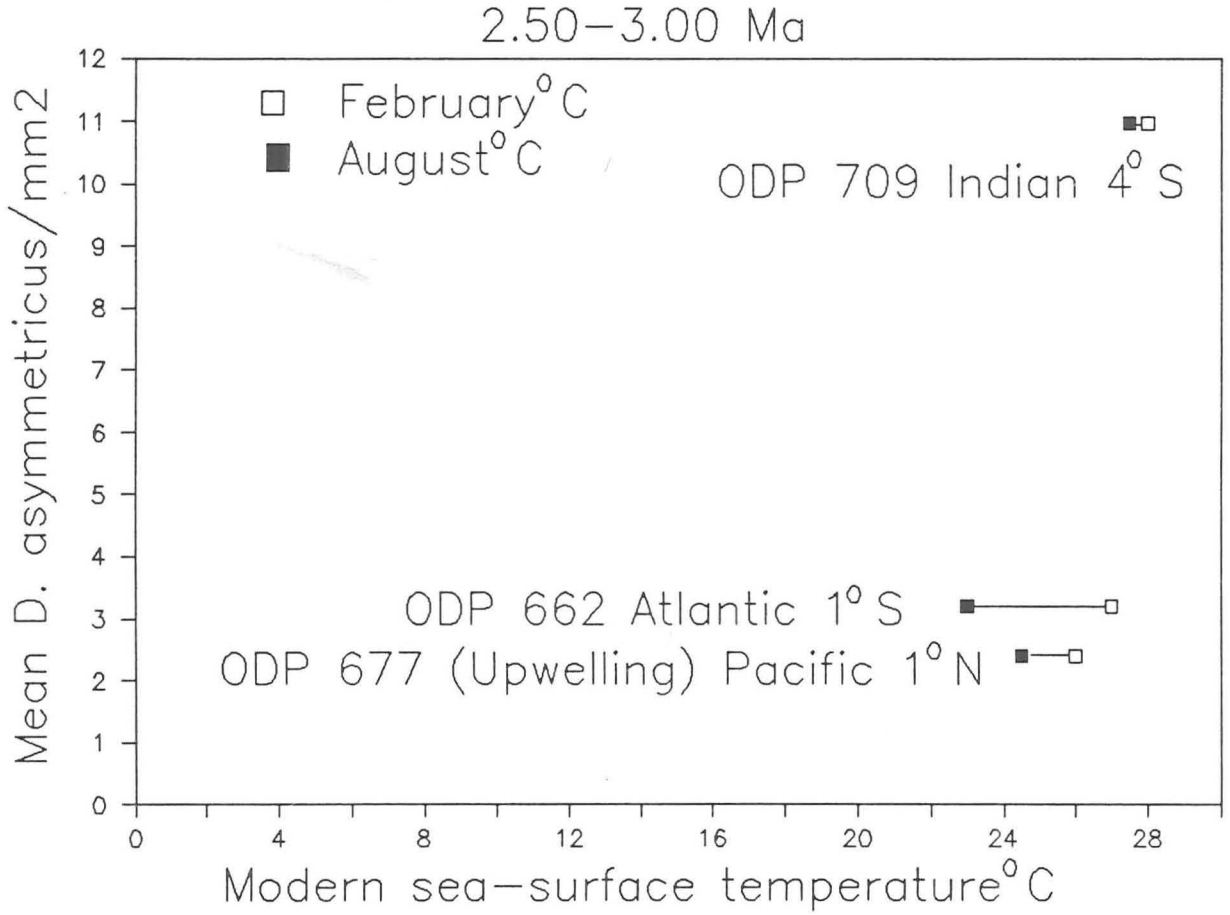

Figure 3:4:3c Mean D. asymmetricus/mm2 versus modern sea–surface temperature at Sites 709, 662 and 677.

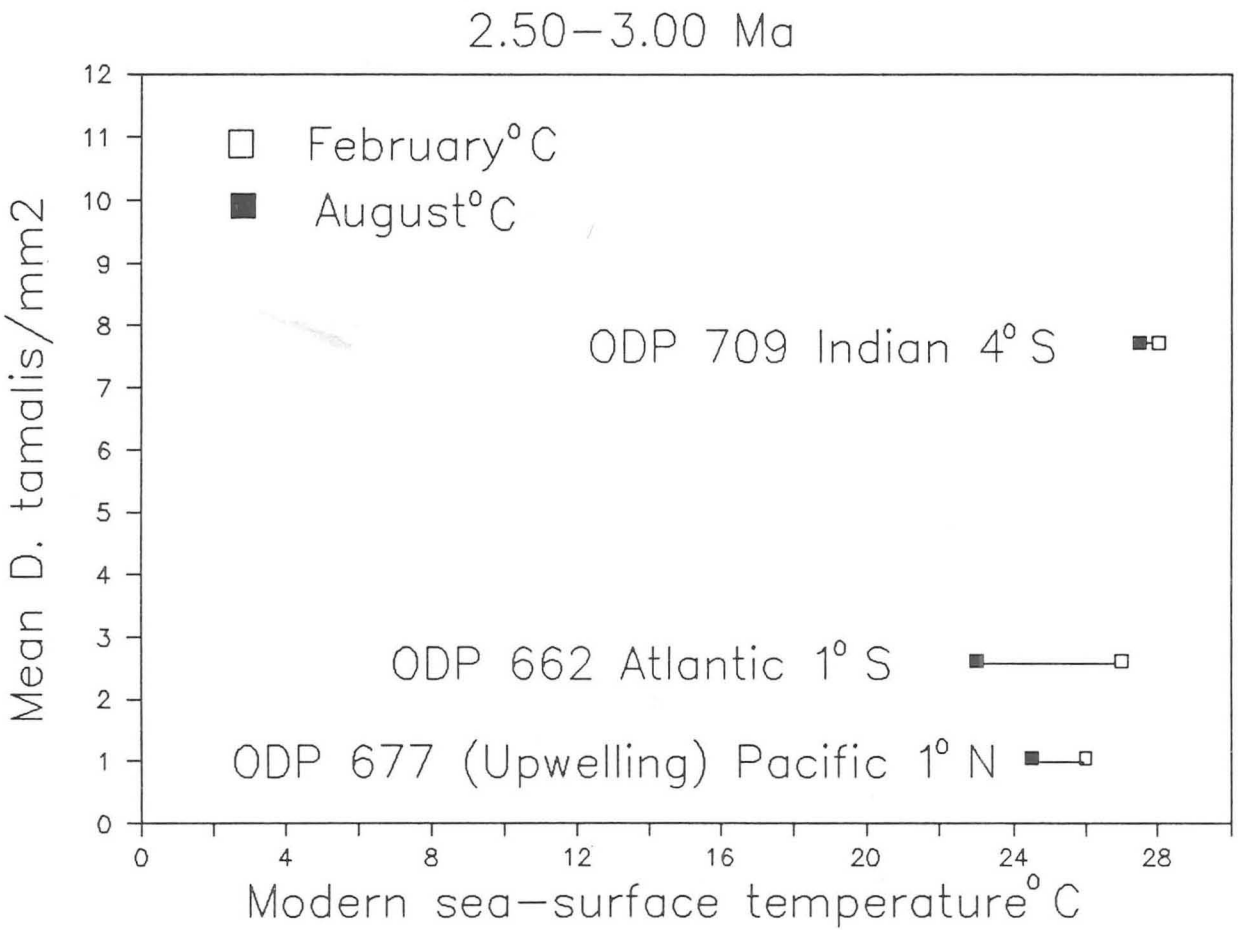

Figure 3:4:3d Mean D. tamalis/mm2
versus modern sea–surface temperature
at Sites 709, 662 and 677.

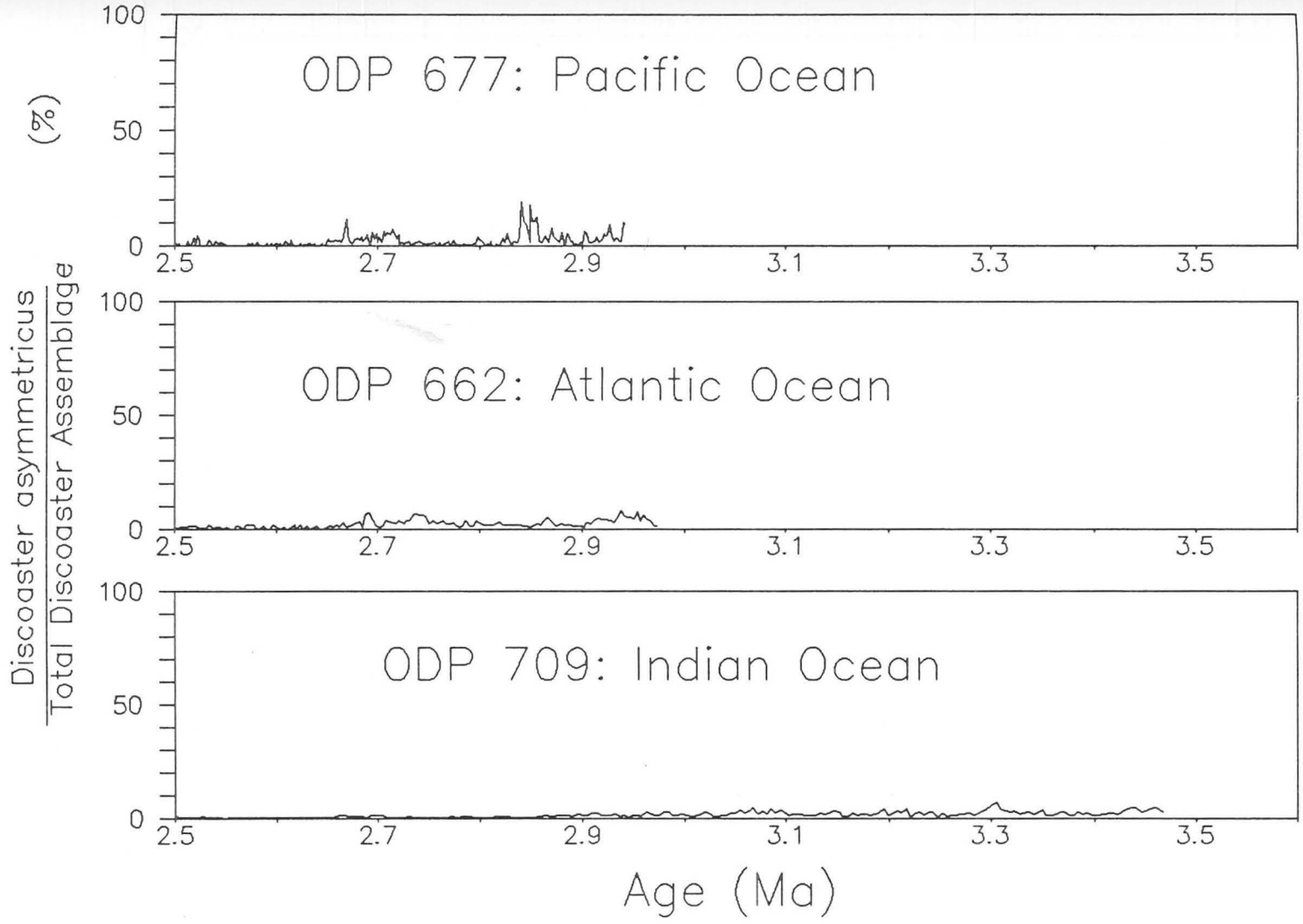

Figure 3:4:3e Percentage abundance plots of D. asymmetricus at Sites 709, 662 and 677.

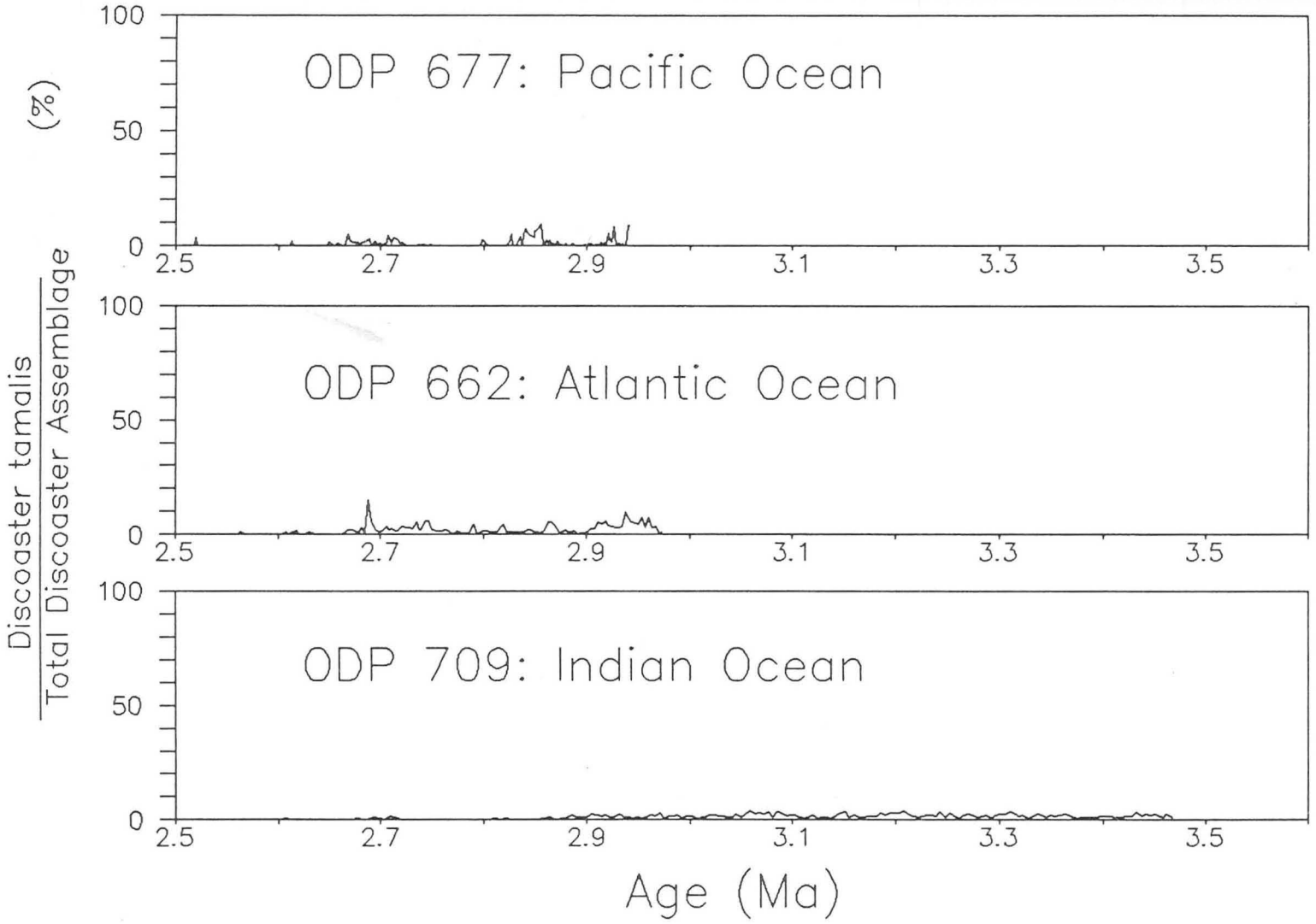

Figure 3:4:3f Percentage abundance plots of D. tamalis at Sites 709, 662 and 677.

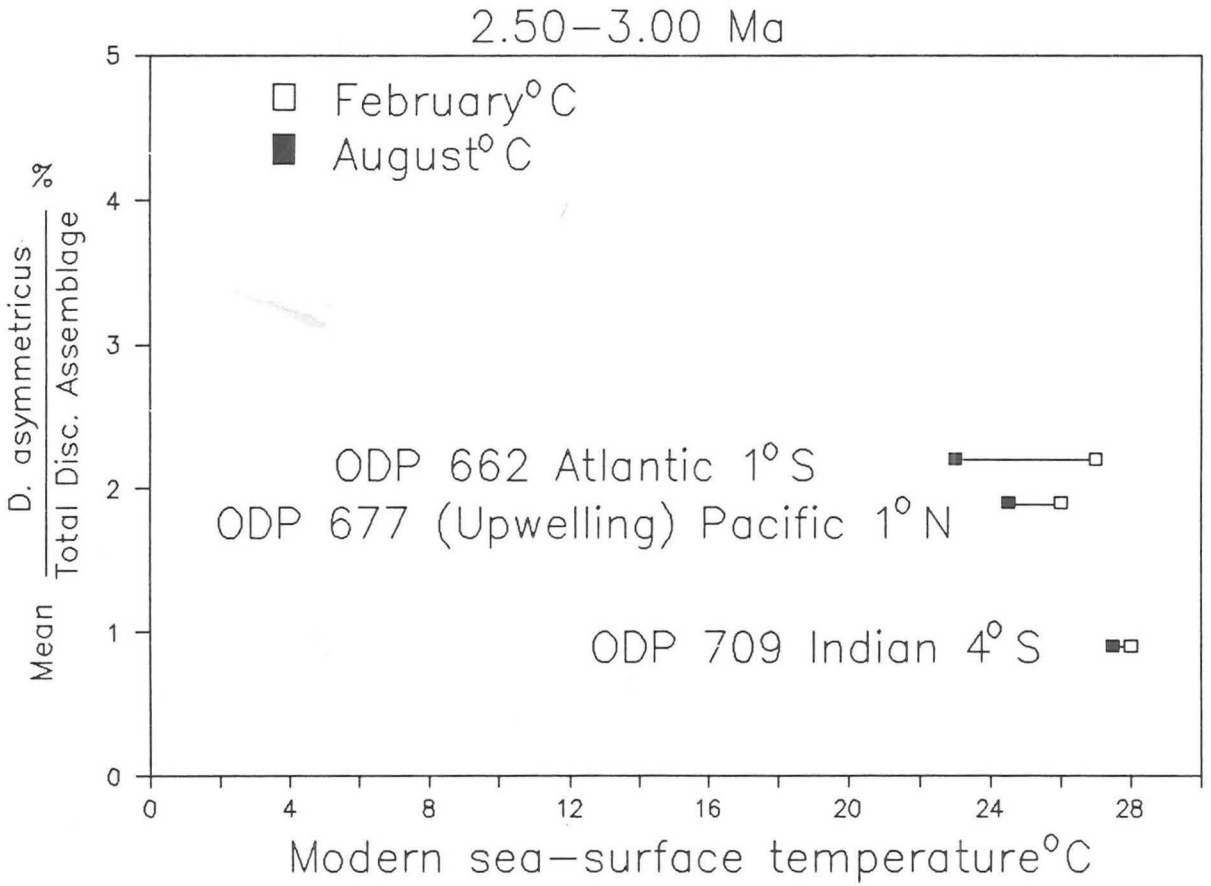

Figure 3:4:3g Mean D. asymmetricus/mm2 versus modern sea–surface temperature at Sites 709, 662 and 677.

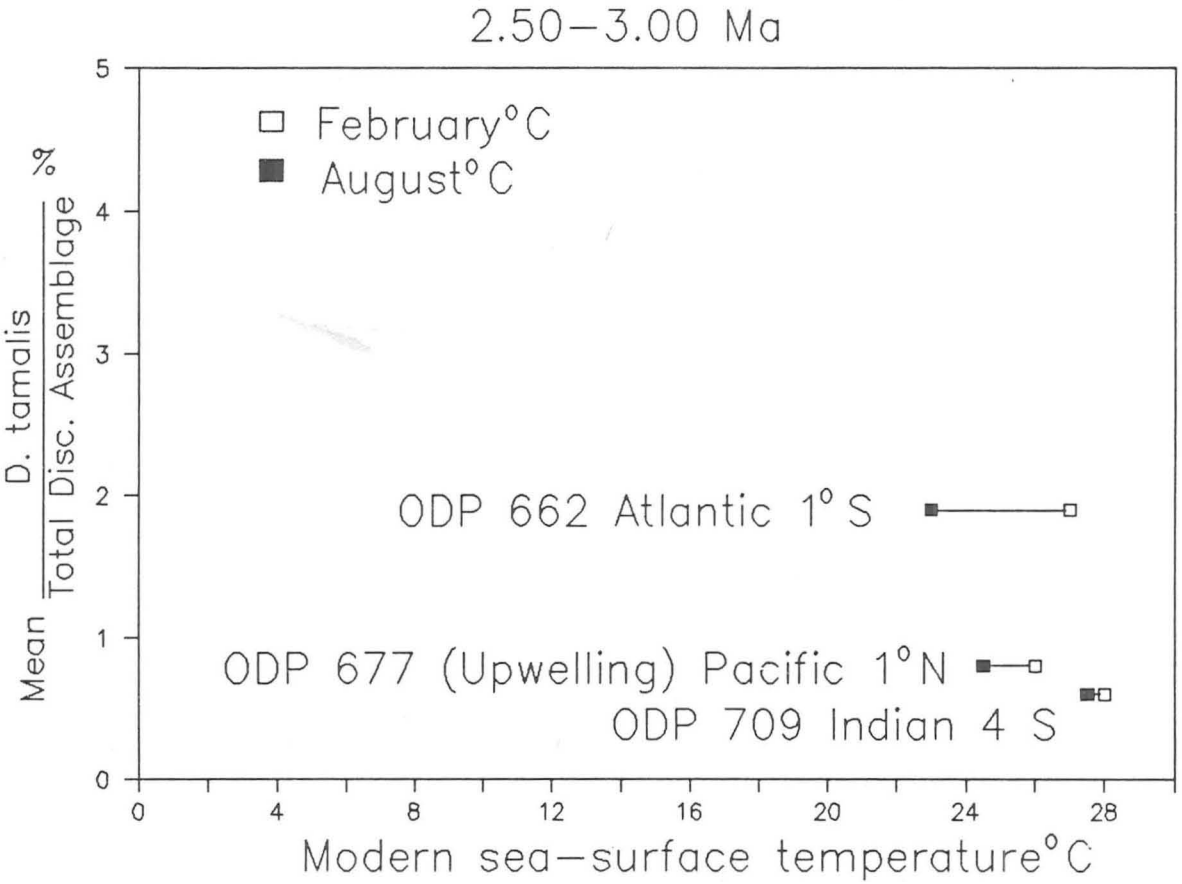

Figure 3:4:3h Mean D. tamalis percentage versus modern sea–surface temperature at Sites 709, 662 and 677.

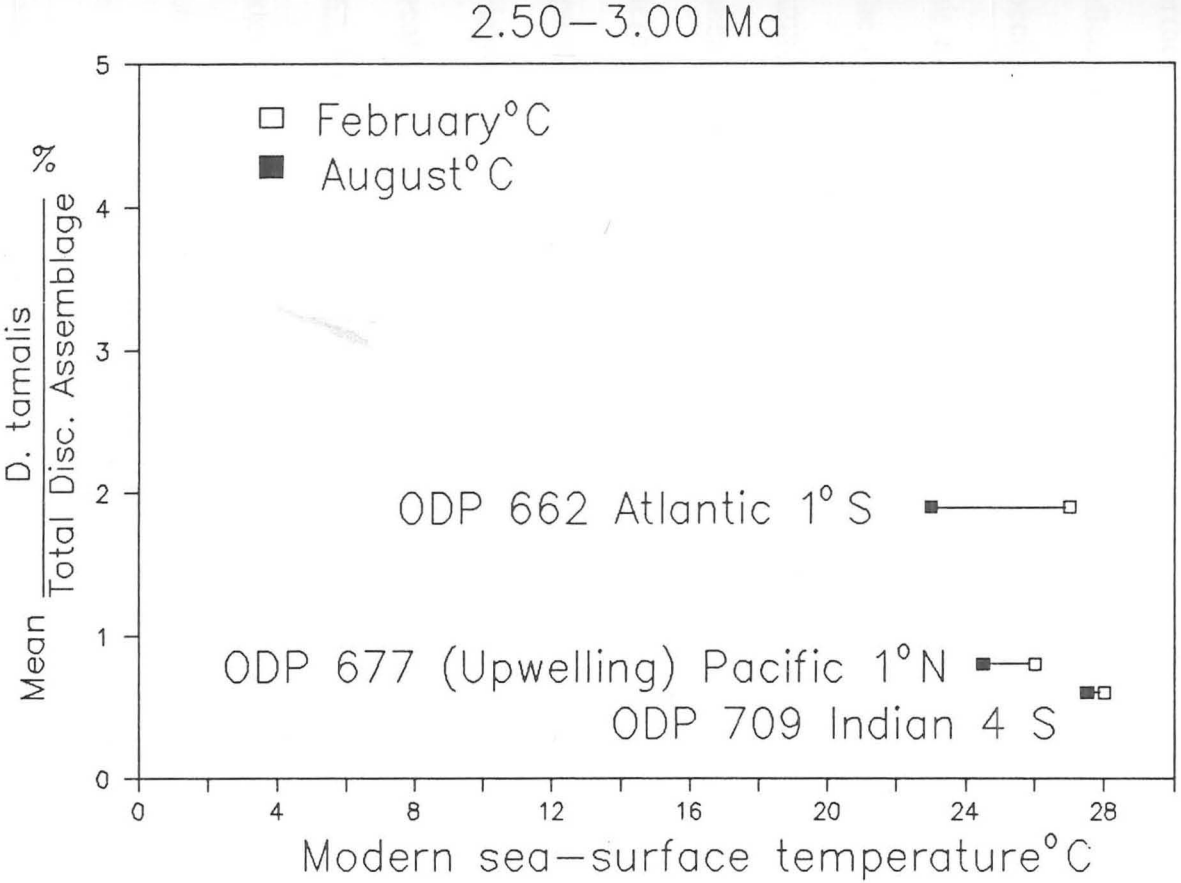

Figure 3:4:3h Mean D. tamalis percentage versus modern sea–surface temperature at Sites 709, 662 and 677.

shown as a percentage of the sum of this species and D. asymmetricus and D. brouweri, this reflects further an increase at the Atlantic site (Fig. 3:4:3i). This can be displayed clearly by plotting the mean relative abundance of D. tamalis versus modern sea-surface temperature (Fig 3:4:3j).

By displaying the sum of the relative abundance of D. tamalis and D. asymmetricus as a percentage of the sum of these two species and D. brouweri, a further increase is apparent at the Atlantic site (Fig 3:4:3k). This trend is likewise reflected by showing the mean relative abundance of the sum of these two species versus modern sea-surface temperature (Fig 3:4:3l). This indicates that this may be linked with the decrease in temperature at Site 662.

The patterns manifested here confirm the trends in Chapter 2. In Chapter 2, D. tamalis and D. asymmetricus were found to increase relative to D. brouweri as a function of increasing latitude, but not upwelling conditions in the North Atlantic. Here at the equator, the trends are subtle but apparent. Site 677 is a major upwelling site associated with cooler temperatures and high productivity. The relative abundances of D. asymmetricus and D. tamalis are hence suppressed, but greater than the warmer, lower productive waters of the Indian Ocean site. Site 662, located within the equatorial divergence, is affected by upwelling to a lesser extent than Site 677 and cooler extremes of temperature.

3:4:4 Discoaster variabilis

In Chapter 2, a datum of approximately 2.9 Ma for D. variabilis was put forward from Sites 552, 662 and 658. Only the first of these sites had an age-model based on magnetostratigraphy. This was only a working hypothesis to be used at future

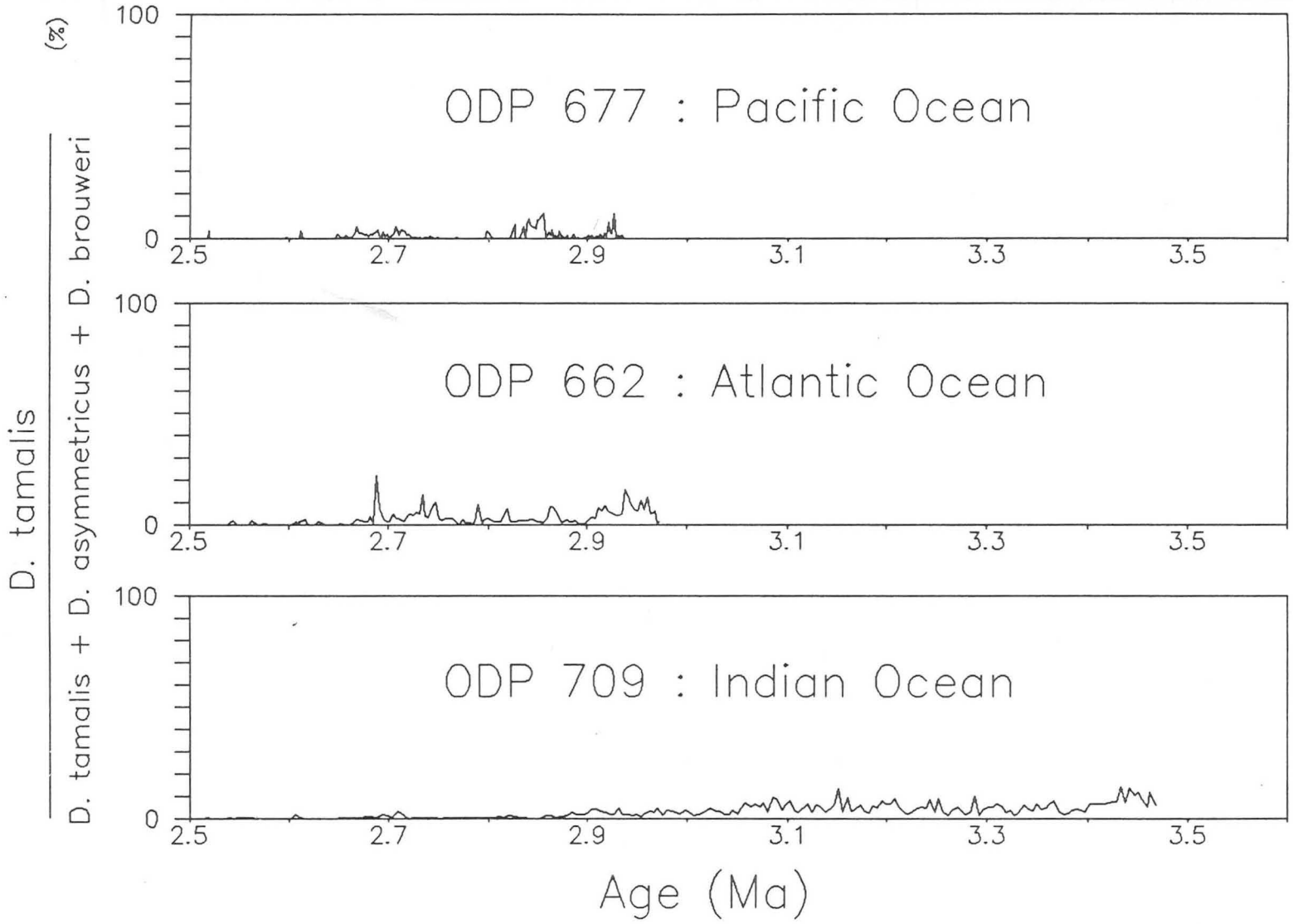

Figure 3:4:3i Percentage abundance plot of D. tamalis divided by the sum of itself, D. asymmetricus and D. brouweri.

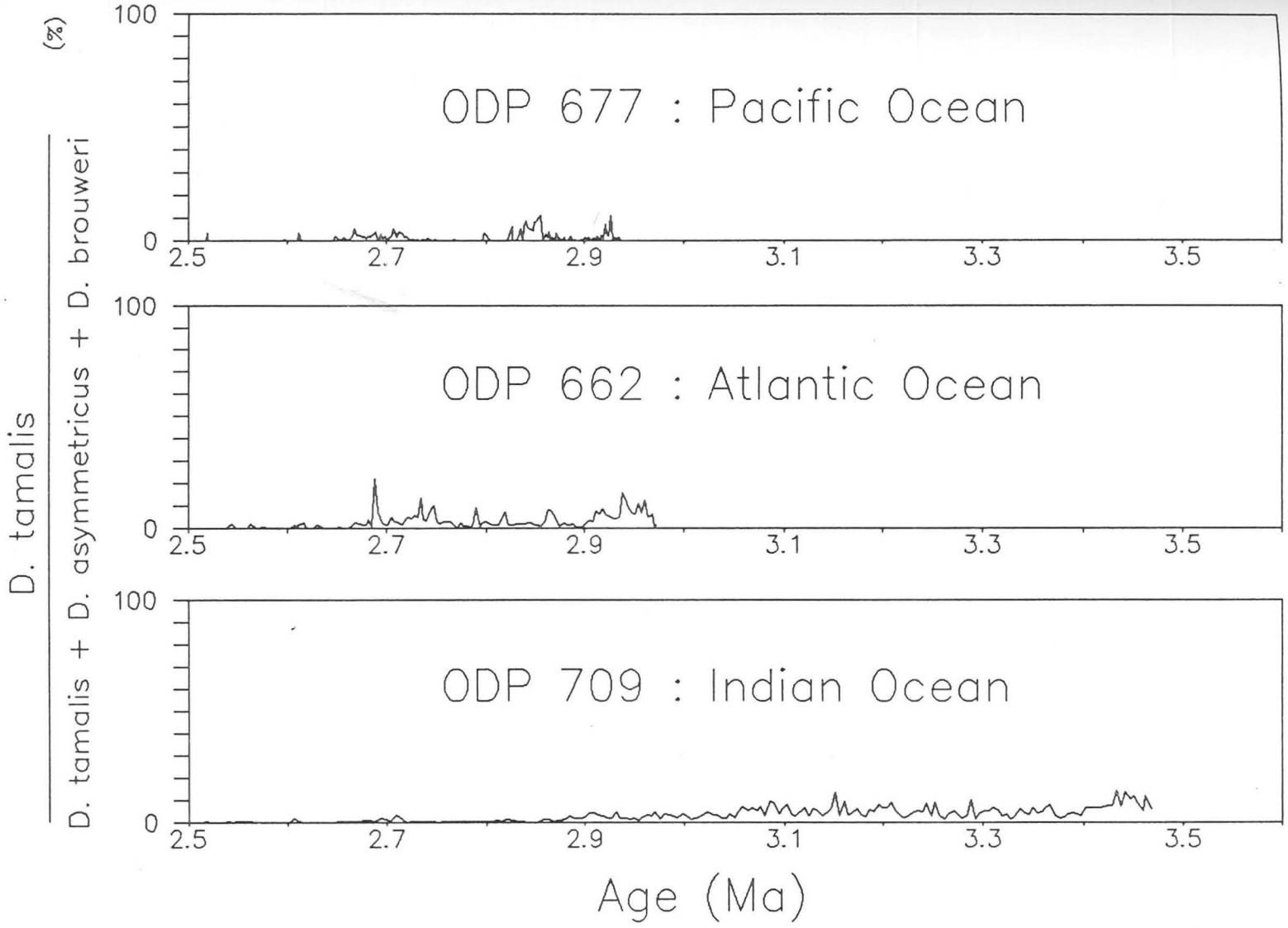

Figure 3:4:3i Percentage abundance plot of D. tamalis divided by the sum of itself, D. asymmetricus and D. brouweri.

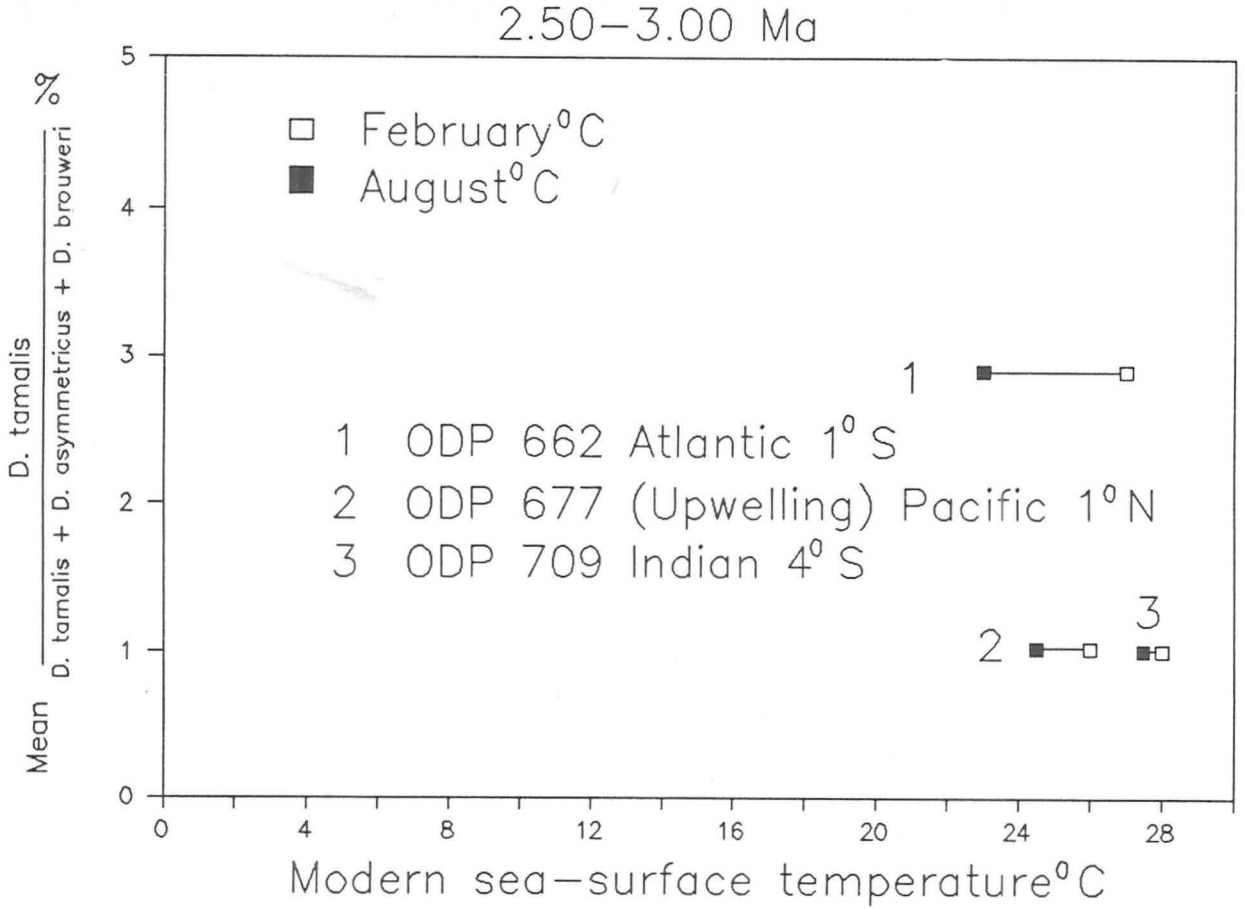

Figure 3:4:3j Mean percentage of D. tamalis divided by the sum of itself and D. asymmetricus and D. brouweri versus modern sea–surface tempareture at Sites 709, 662 and 677.

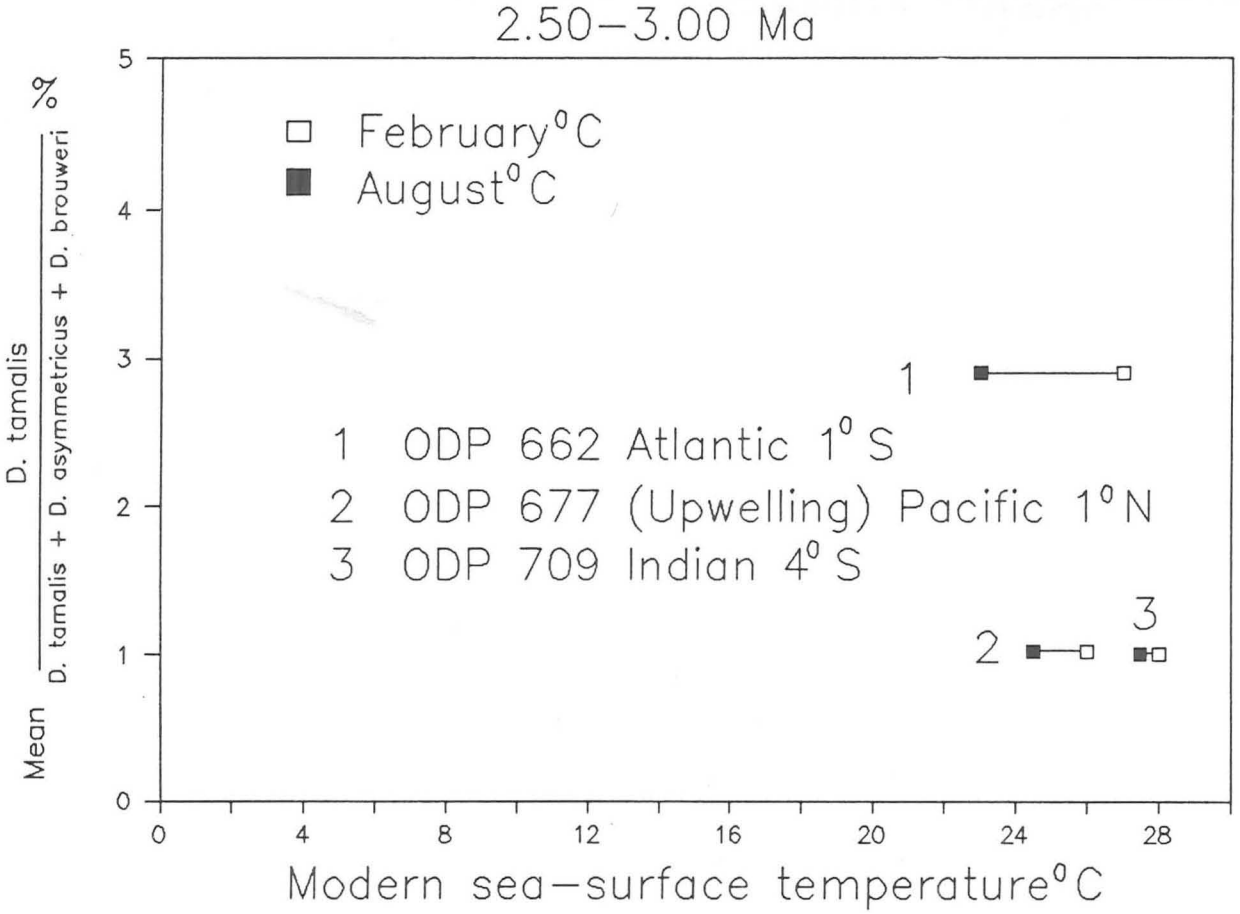

Figure 3:4:3j Mean percentage of D. tamalis divided by the sum of itself and D. asymmetricus and D. brouweri versus modern sea–surface tempareture at Sites 709, 662 and 677.

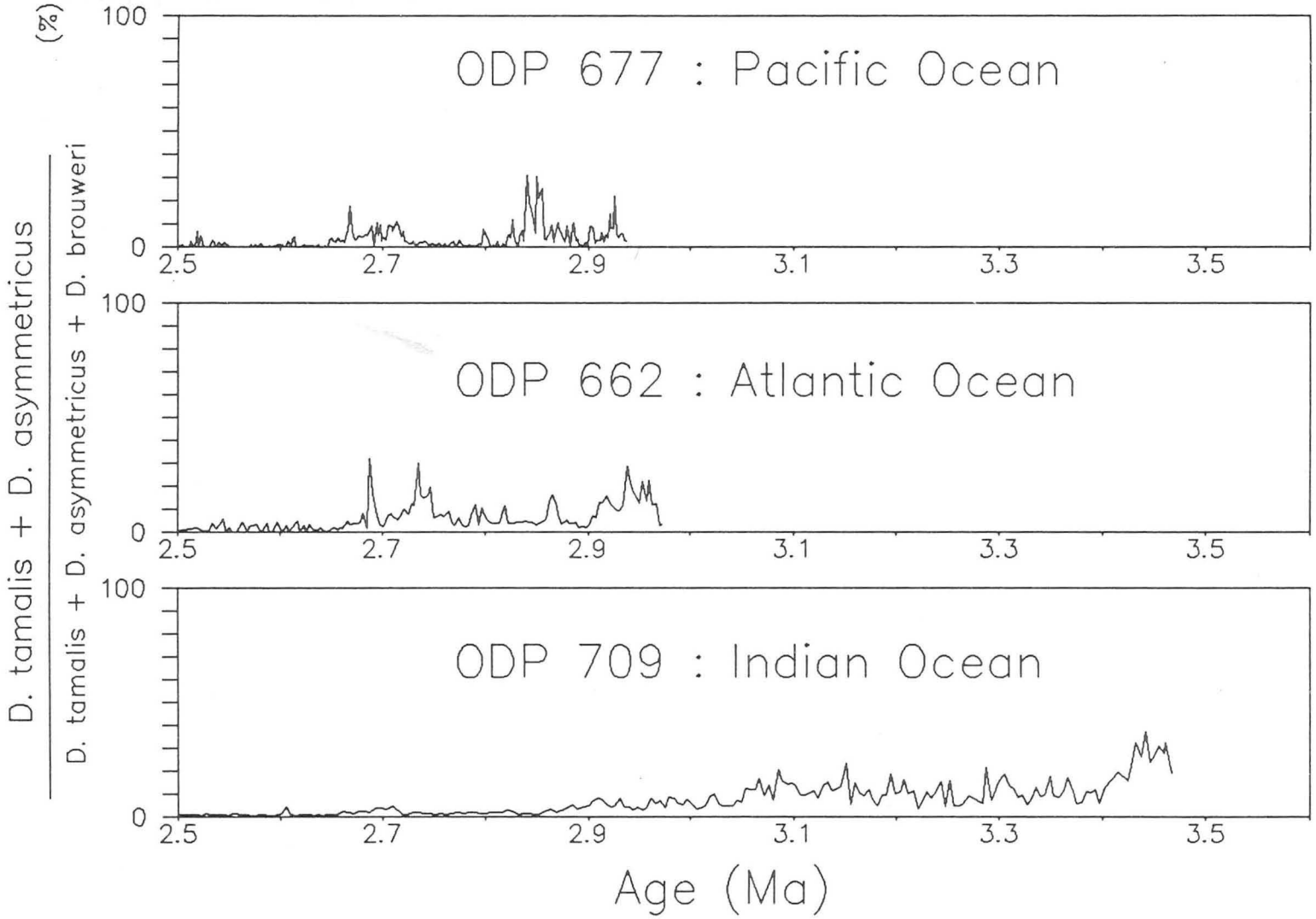

Figure 3:4:3k Percentage abundance plot of D. tamalis and D. asymmetricus divided by the sum of themselves and D. brouweri

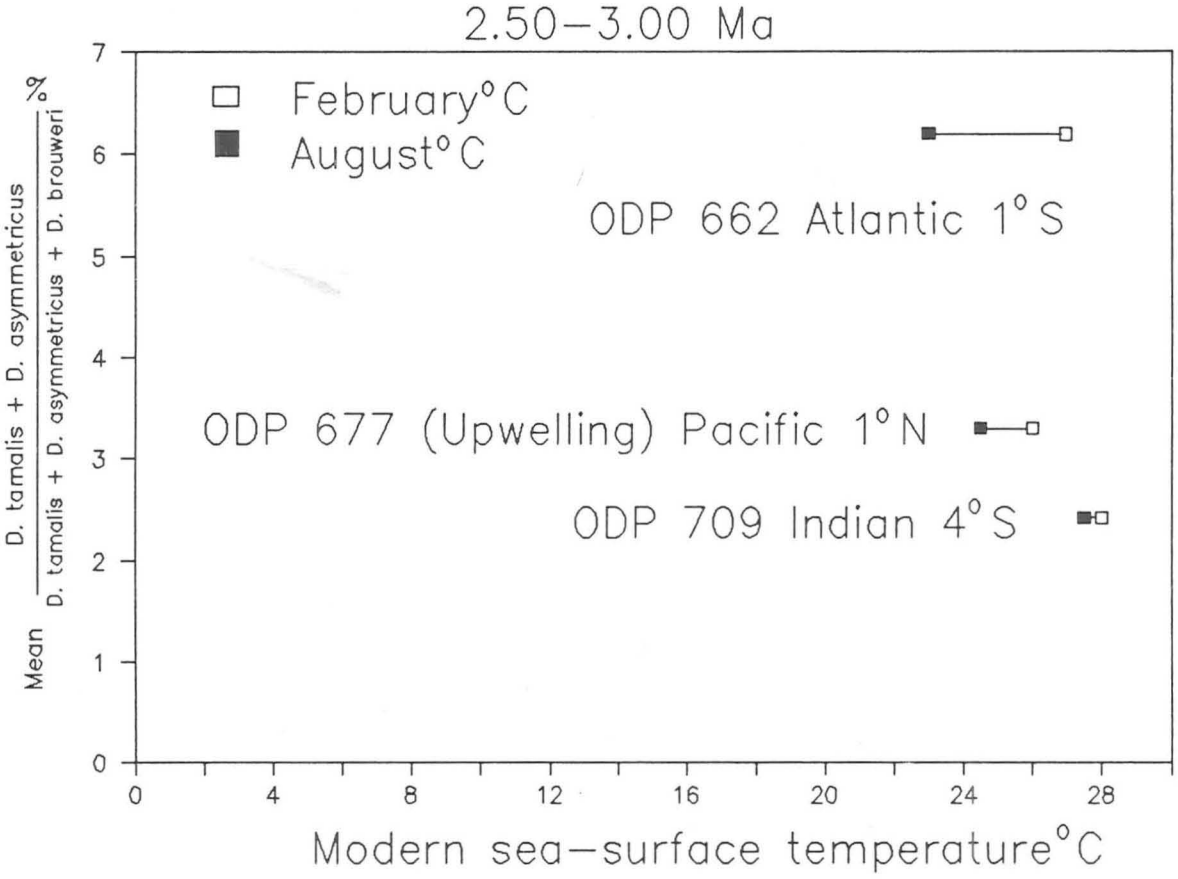

Figure 3:4:31 Mean percentage of D. tamalis and D. asymmetricus divided by the sum of themselves and D. brouweri versus modern sea–surface temperature at Sites 709, 662 and 677.

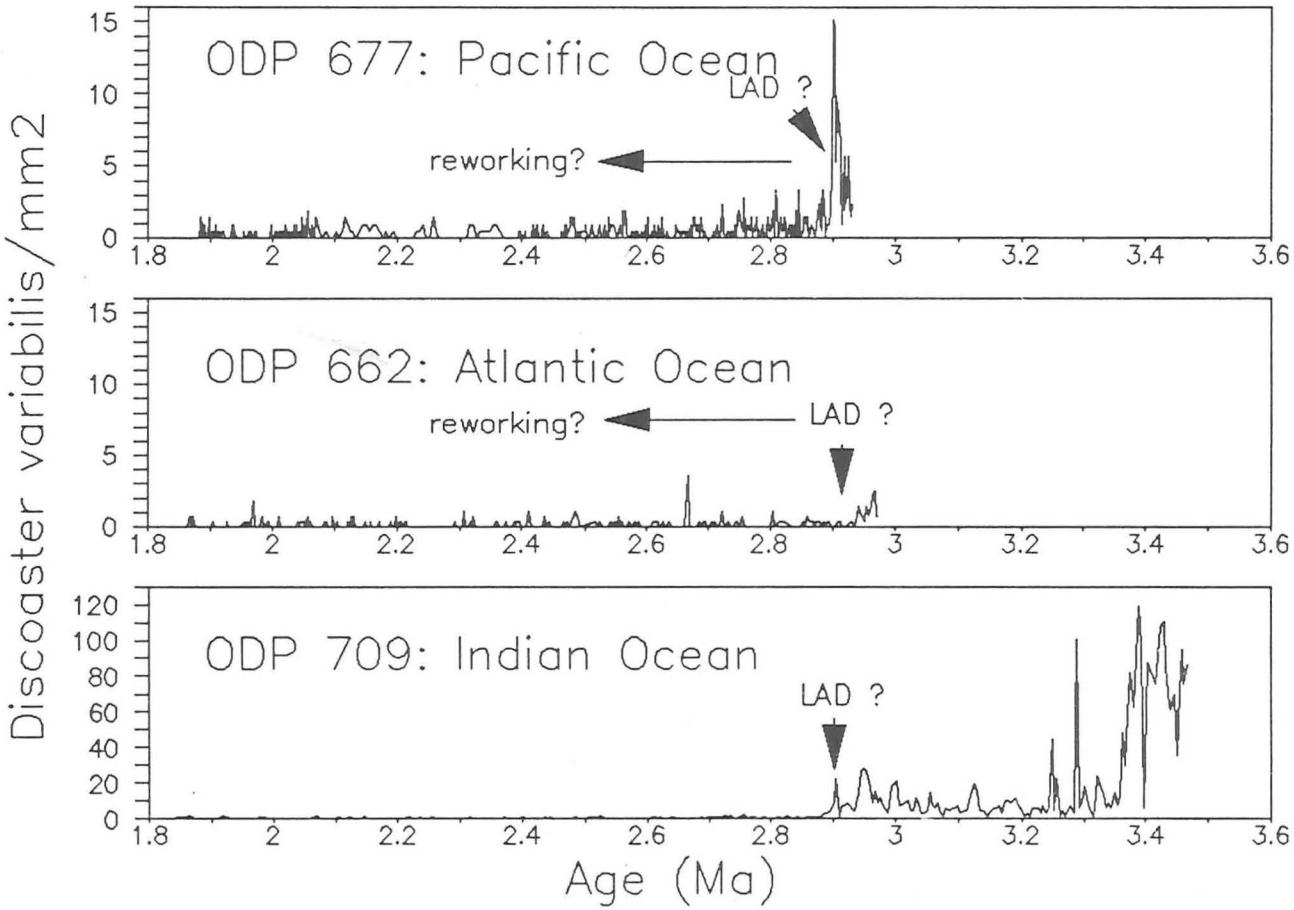

Figure 3:4:4 Abundance plots of D. variabilis at Sites 709, 662 and 677.

sites if there was any uncertainty concerning the reliability of the planktonic foraminifer datum G. altispira (2.95 Ma). In reality, the LAD for D. variabilis may be argued to be a little older at 2.92 Ma from Sites 552, 662 and 658. Only at the Indian Ocean site, with a record extending back to almost 3.5 Ma, was D. variabilis used in the age-model (Figure 3:4:4). At the Pacific site, Site 677, G. altispira was used in the age-model, which produced a distinct final abundance peak for D. variabilis at 2.9 Ma. The occurrence of D. variabilis after 2.9 Ma is considered to represent reworking.

3:5 Total Discoaster Abundance

Only prior to 2.65 Ma are six species of Discoaster present. D. variabilis, the seventh species of Discoaster is only present approximately prior to 2.9 Ma i.e. the end of the time interval studied at Sites 677 and 662. The records for the total of six species are similar to those of D. brouweri at Sites 677 and 662 (Fig. 3:5a). Prior to 2.35 Ma at Site 709, the other Discoaster species, especially D. pentaradiatus, make major changes to the record.
Much of the cyclicity so apparent in the D. brouweri record at all the sites is disguised at Site 709.

Site 709 overshadows the other two sites in total Discoaster abundance. This can be easily demonstrated by displaying the mean total abundance of discoasters versus modern sea-surface temperature (Fig. 3:5b). The subtle differences in temperature cannot solely explain this. Both Sites 709 and 662 show a gradual

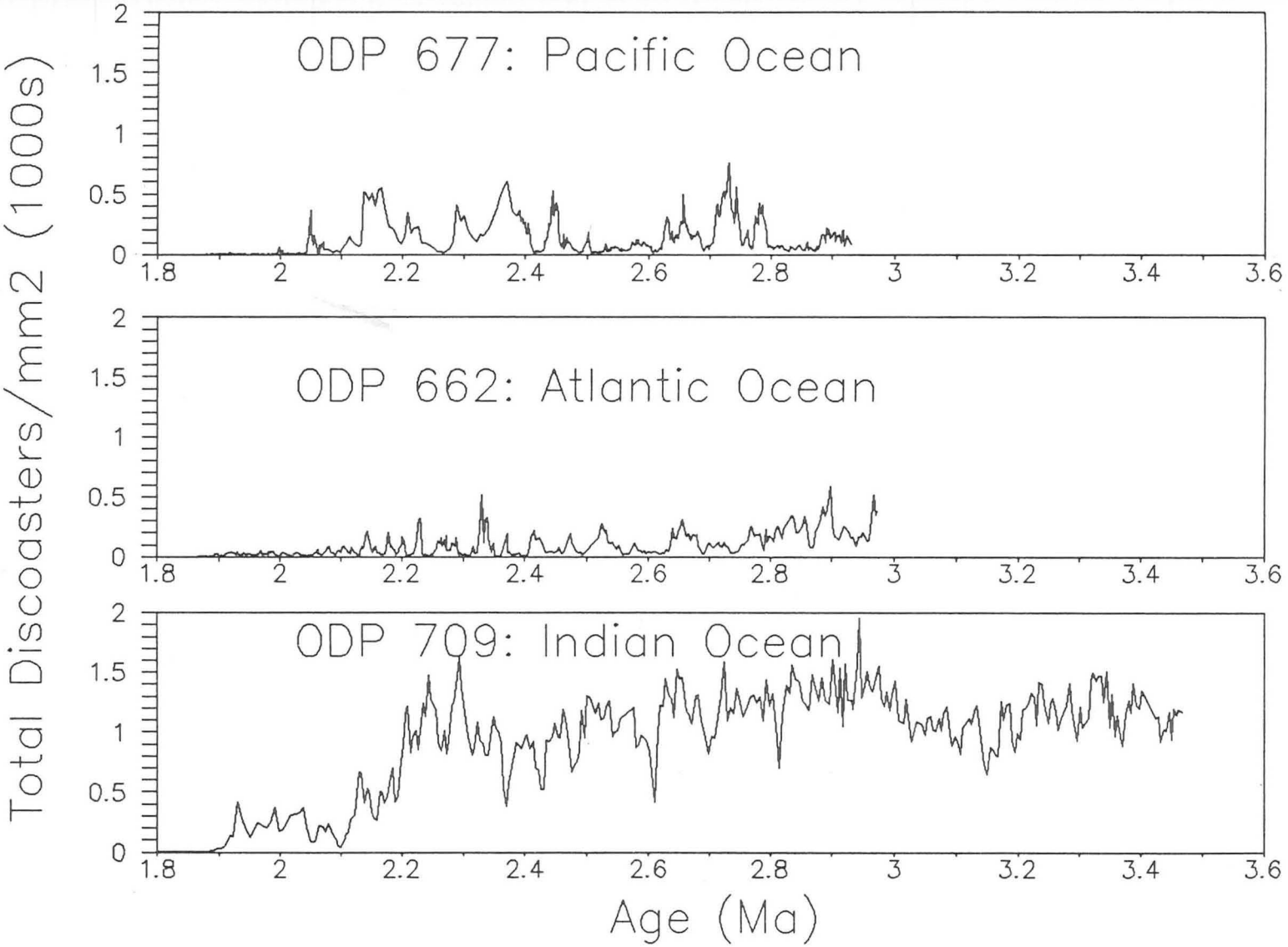

Figure 3:5a Abundance plots of total Discoaster assemblage at Sites 709, 662 and 677.

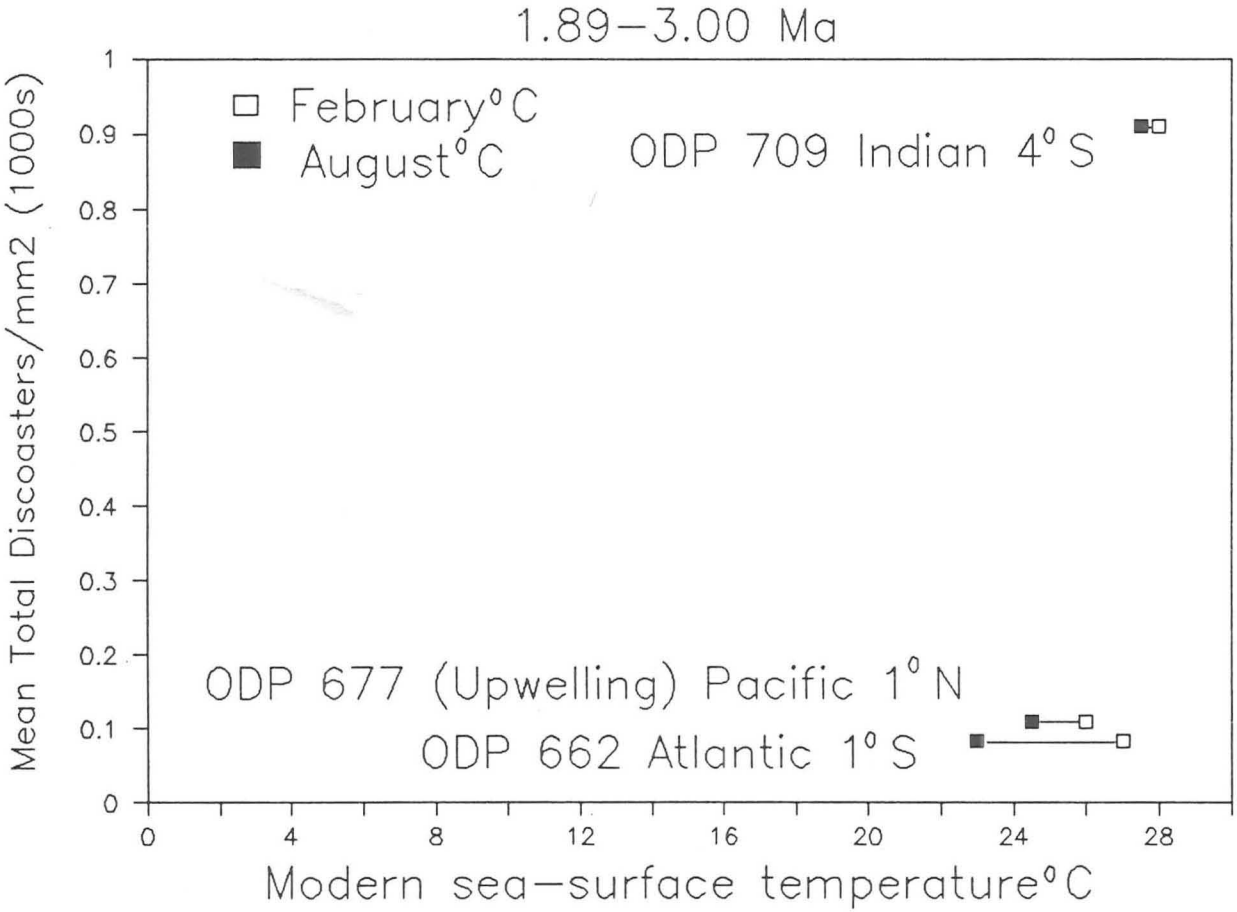

Figure 3:5b Mean Total Discoasters/mm2 versus modern sea–surface temperature at Sites 709, 662 and 677.

reduction in abundance through time. Site 677, however, does not display such an obvious trend.

Site 677 is exceptional in that it possesses such broad abundance peaks, despite the fact that it is composed of closely spaced samples with a better time resolution than any other site. This phenomenon is combined with several long time intervals of suppressed abundance between approximately 2.5-2.6 Ma and 2.8-2.9 Ma.

3:6 Spectral Analysis

In this chapter, spectral analysis is performed on datasets obtained by linear interpolation between the biostratigraphic control points selected for the age-models (Table 3:3:2c). No magnetostratigraphic data was available at the three equatorial sites. As explained in Chapter 2, the data sets have been divided into two time intervals 1.88-2.39 Ma and 2.39-3.00 Ma (Fig. 3:6).

This analysis is performed on the sum of all the Discoaster species as in Chapter 2. The order of magnitude change in the total Discoaster abundances and the apparent regularity of the abundance peaks suggested a large signal available for spectral analysis.

Between 1.88-2.39 Ma, D. brouweri is the only species present except for the brief acme of D. triradiatus between 1.89 and 2.07. At Site 662 and to a lesser degree Site 677 concentrations of variance around the frequencies of the orbital elements of eccentricity (100kα), obliquity (41kα) and precession (21kα) are

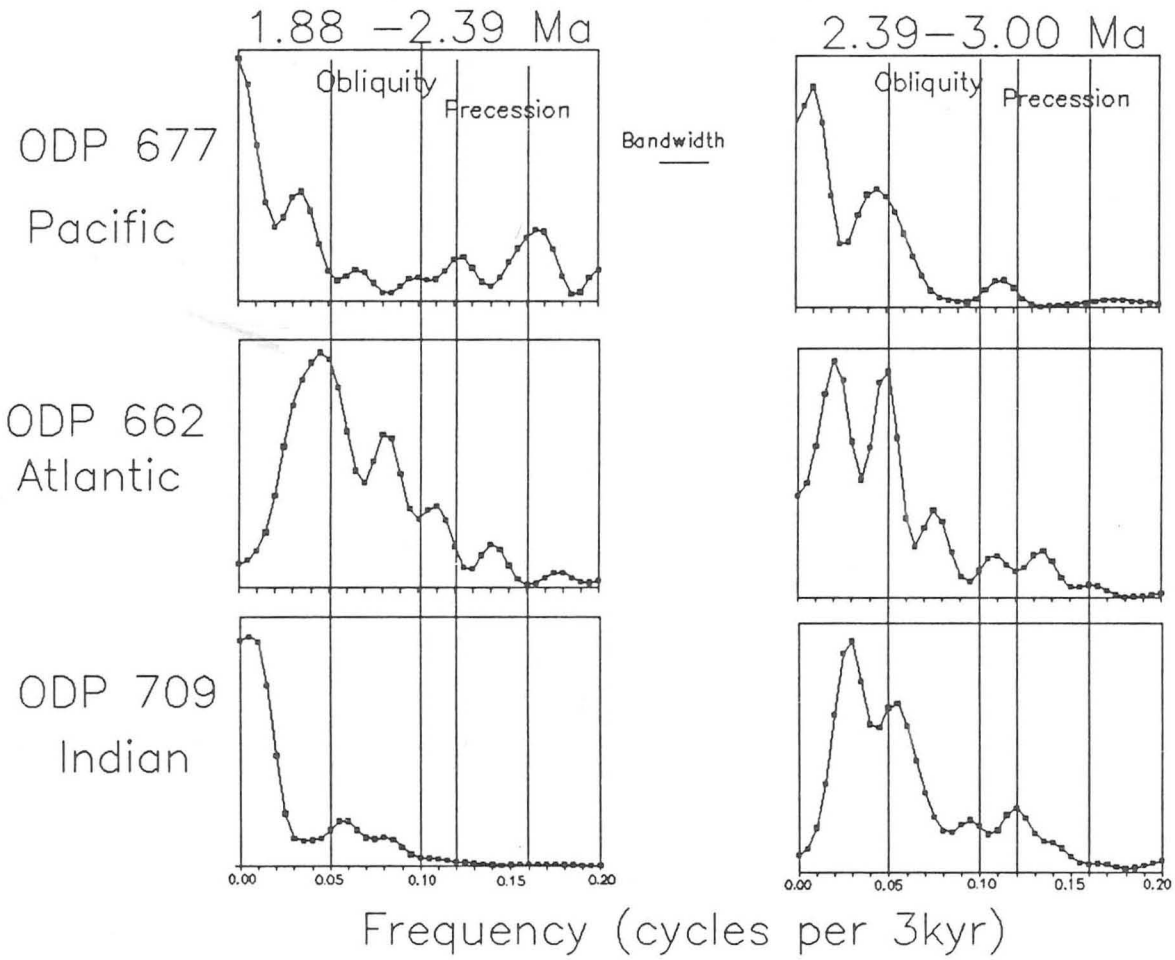

Figure 3:6 Spectral power density estimated on 2 time intervals of the total Discoaster data set at Sites 709, 662 and 677. B.W. indicates band width

distinguished. At Site 709, only a possible obliquity signal is noticeable.

During the time interval 2.39-3.00 Ma, a greater Discoaster diversity is present. There appears to be concentrations of variance around the frequencies of the three orbital elements at Sites 662 and 709. At Site 677, possible eccentricity and precessional periodicities are present, but less defined.

3:7 DISCUSSION

If one assumes that sea-surface temperatures at the equator were relatively constant during the upper Pliocene, why does the Discoaster record fluctuate so markedly ? If the sea-surface temperatures are only slightly different between sites, this cannot explain the differences in abundance between sites or through time.

Many studies in the past had concluded only that discoasters favoured warm water masses (e. g., Haq and Lohmann, 1976) and that their abundance decreased with increasing latitude. Numerous groups of nannoplankton have been shown to be restricted to specific temperature ranges (e. g., McIntyre, 1967; Okada and Honjo, 1973; Okada and McIntyre, 1979). Backman et al. (1986) and Backman and Pestiaux (1987) had shown that the Pliocene Discoaster record was affected by orbital forcing at ODP Site 606 and DSDP Site 552, but interpreted this in terms of sensitivity to sea surface temperature variability.

In Chapter 2, a five site latitudinal transect in the North Atlantic was

analysed, including Site 662 as the southernmost site and Site 552 as the northernmost site. The Discoaster abundance records in this transect were found by spectral analysis to indicate periodicities corresponding to orbital forcing. The sensitivity of the discoasters revealed especially by their cyclic fluctuations in the tropics pointed to the importance of another factor other than temperature which must have exerted strong influence on the pattern of observed Discoaster abundances.

Isotopic evidence (Shackleton, Berger and Peltier, in press) shows that at Site 677 the glacial/interglacial difference in surface water temperatures was similar in the late Pleistocene and the late Pliocene. The equatorial sites must have had temperature regimes which were consistently favourable for Discoaster reproduction during the Pliocene. In Chapter 2, a marked temperature threshold was demonstrated to exist in the North Atlantic. This threshold caused discoasters to decrease markedly in abundance crossing a palaeoisotherm between Sites 607 (41°) and 552 (56°).

When considering the combination of relatively low Discoaster abundances in high productivty areas and vice versa, it is suggested that the critical second factor causing low Discoaster abundances is related to productivity pressure. Discoasters are simply outcompeted by more opportunistic species or plankton groups during conditions of high nutrients. Satellite images from NASA (Lewis, 1989) show a global record of phytoplankton blooms e.g. between October to December, 1979 (Plate 4). Phytoplankton blooms are very prominent at the Pacific and Atlantic sites. In Pliocene times, this would

have suppressed Discoaster production. However, at Site 709 phytoplankton blooms are very low. This may explain why the discoasters thrived in this area due to the lack of productivity pressure. The three equatorial sites reveal major differences in productivity pressure between the oceans. Abundances of discoasters were high at Site 662 in a North Atlantic context. In comparison with Site 677 in a major upwelling area in the Pacific, Site 662 displays lower abundances and demonstrates the important affects of the equatorial divergence and South Equatorial Current. Discoasters flourished in the Indian Ocean at Site 709 in waters of lower productivity indicated by suppressed diatom abundances. Only in the Indian Ocean and Atlantic sites do all the species, except D. surculus reflect a long term temperature decline. The Pacific site, Site 677 probably manifests the best record of productivity pressure independent of sea-surface temperature of the three sites. All three sites however show an abundance decrease in discoasters between 2.40 and 2.42 Ma which is presumably linked to the initiation of glaciation in the North Atlantic at about 2.4 Ma (Shackleton et al., 1984).

The absence or very suppressed abundances of Discoaster pentaradiatus at Site 677 after 2.9 Ma reflects interesting information about its ecological limitations. Major abundances of diatoms were found to occur prior to 2.5 Ma (Appendix C) and this indication of high productivity pressure may have been responsible for the early "disappearance" of D. pentaradiatus in this area. Cores V28-179 and V32-127 in the Pacific Ocean (Backman and Shackleton, 1983) show the extinction of D. pentaradiatus occurred a short

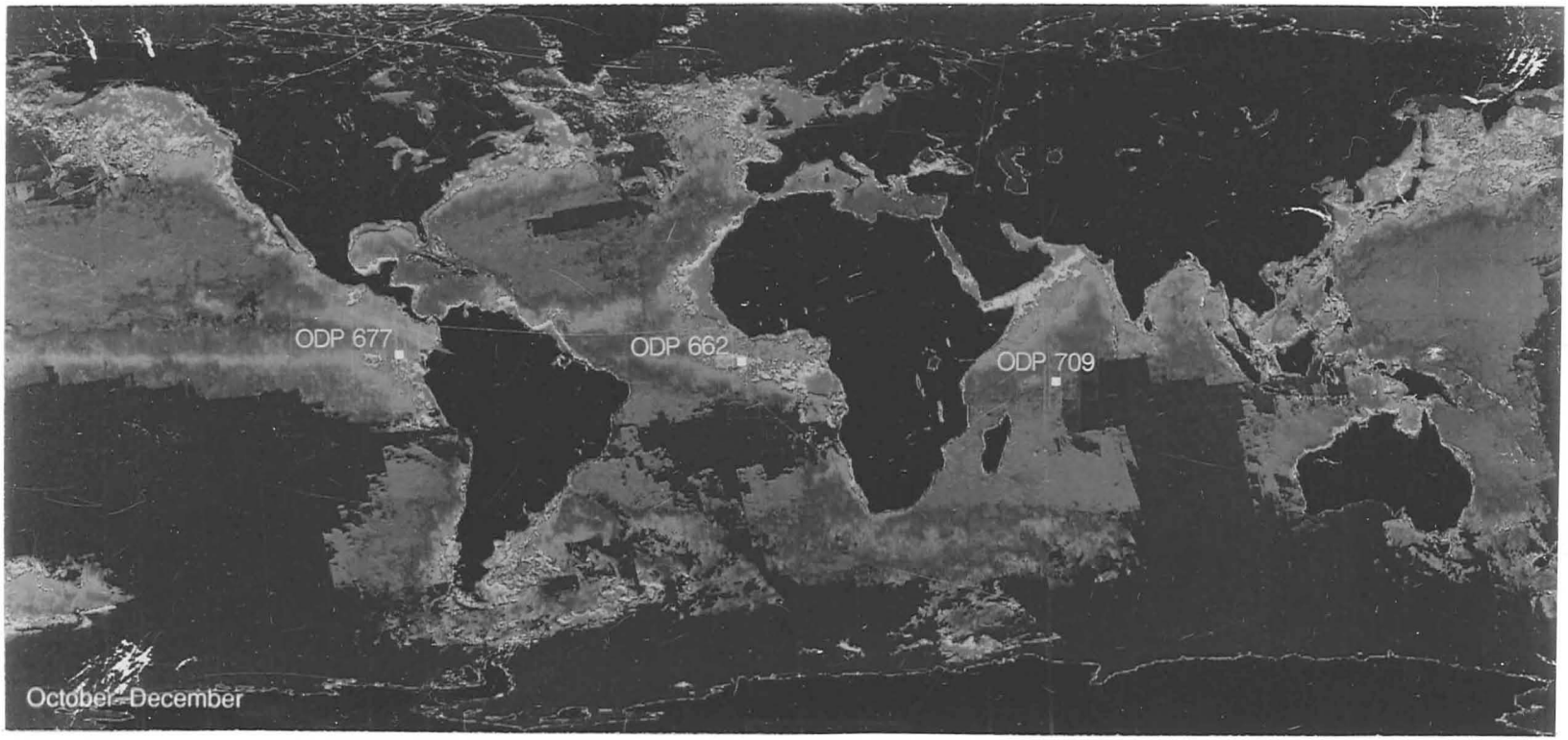

PLATE 4.

Equatorial sites located on satellite image of global phytoplankton concentration during October-December, 1979(after Lewis, 1989)

Purple- minimum phytoplankton concentration

red- maximum phytoplankton concentration

time interval after D. surculus.

Bukry (1978) observed that D. surculus appeared to favour the cooler end of the warm water spectrum. In Chapter 2, D. surculus was demonstrated to favour higher nutrient conditions in addition to cooler temperatures. At Site 709, D. surculus may occur in high absolute abundances, but relative to the total Discoaster assemblage, this species is only a significant component at Sites 662 and 677. Discoaster surculus is especially important at Site 677 which demonstrates its preference for nutrient rich waters which are probably associated with cooling. This species likewise appears to be less affected by the gradual decline of sea surface temperatures that is clearly superimposed on the other Discoaster species records.

In Chapter 2, the production of D. asymmetricus and D. tamalis was shown to increase as a percentage of the total Discoaster assemblage (especially relative to D. brouweri) with increasing latitude (i. e. cooler waters) in the North Atlantic. High nutrients however offset this trend as revealed by the upwelling site, Site 658.

Relative to the total Discoaster assemblage, the abundances of D. asymmetricus and D. tamalis were suppressed at all sites, though to a lesser extent at the higher productivity sites, Sites 662 and 677. Nevertheless, the relative abundances of these two species are still low due to the additional factor of productivity pressure. At Site 662, the lower productivity pressure and cooler waters were more favourable than the Pacific upwelling site, Site 677. Discoaster abundances in the future must always be considered

within the context of productivity pressure and not just sea surface temperature.

3:8 SUMMARY

1. The Discoaster abundance fluctuations at all sites reveals the importance of productivity pressure at the equator where relatively constant sea-surface temperatures would be expected.

2. Production of discoasters in the Indian Ocean (Site 709) is much greater than at the Pacific site, Site 677 (upwelling site) and the Atlantic site, Site 662 (affected by the South Equatorial Current and equatorial divergence).

3. Prior to 2.4 Ma, Discoaster brouweri forms the greatest component of the Discoaster assemblage at the Pacific site, Site 677.

4. Discoaster pentaradiatus forms a major component of the Discoaster assemblage at Sites 662 and 709, but is virtually absent after 2.9 Ma at Site 677.

5. Discoaster surculus forms its largest component of the Discoaster assemblage at Site 677, followed closely by Site 662 which are both influenced

by higher productivity in spite of the greater absolute abundances at Site 709.

6. Discoaster asymmetricus and Discoaster tamalis are present in greatest abundances at Site 709, but relative to the total Discoaster assemblage (and especially D. brouweri) they are more significant at the higher productivity sites, Sites 662 and 677. The relationship of these two species with D. brouweri is especially apparent in the cooler, lower productive waters of Site 662.

7. Spectral analysis reveals that marked fluctuations in the abundance of discoasters at the equator are in the range of earth orbital fluctuations.

CHAPTER 4: COMPARISON OF DISCOASTER ABUNDANCE VARIATIONS AT SITES 709 AND 716 IN THE INDIAN OCEAN; OPTIMUM CONDITIONS VERSUS MONSOONALLY INDUCED PRODUCTIVITY PRESSURE.

4:1 Introduction

In comparison to the Atlantic and Pacific Ocean Basins, the palaeoceanography of the Indian Ocean is still relatively unexplored. Previous knowledge of pre-Pleistocene palaeoceanography and stratigraphy in the tropical Indian Ocean is based on material recovered from DSDP Legs 22 through 25 in 1972. Much of this DSDP material is of poor quality since the conventonal rotary coring device was in use disturbing the softer sediments. ODP Sites 709 and 716 from Leg 115 are of very high quality drilled with the Advanced Piston Corer.

Sites 709 and 716 are located in warm water masses of similar sea-surface temperature today, approximately 28°C in February and August (CLIMAP, 1981) (Table 4:1). According to Bé and Hutson (1977) they are both in the Equatorial Water Mass. This corresponds with a faunal province defined by planktonic foraminifera. In this chapter, the Discoaster abundances at these two sites are compared back to 3.5 Ma.

All the sites analysed in this thesis, except Site 716, were drilled at a water depth of over 2000 metres. Site 716 was drilled at 533 metres. This is the first chapter attempting to correlate abundance peaks between sites within the framework of biostratigraphic age-models.

CHAPTER 4: COMPARISON OF DISCOASTER ABUNDANCE VARIATIONS AT SITES 709 AND 716 IN THE INDIAN OCEAN; OPTIMUM CONDITIONS VERSUS MONSOONALLY INDUCED PRODUCTIVITY PRESSURE.

4:1 Introduction

In comparison to the Atlantic and Pacific Ocean Basins, the palaeoceanography of the Indian Ocean is still relatively unexplored. Previous knowledge of pre-Pleistocene palaeoceanography and stratigraphy in the tropical Indian Ocean is based on material recovered from DSDP Legs 22 through 25 in 1972. Much of this DSDP material is of poor quality since the conventonal rotary coring device was in use disturbing the softer sediments. ODP Sites 709 and 716 from Leg 115 are of very high quality drilled with the Advanced Piston Corer.

Sites 709 and 716 are located in warm water masses of similar sea-surface temperature today, approximately 28°C in February and August (CLIMAP, 1981) (Table 4:1). According to Bé and Hutson (1977) they are both in the Equatorial Water Mass. This corresponds with a faunal province defined by planktonic foraminifera. In this chapter, the Discoaster abundances at these two sites are compared back to 3.5 Ma.

All the sites analysed in this thesis, except Site 716, were drilled at a water depth of over 2000 metres. Site 716 was drilled at 533 metres. This is the first chapter attempting to correlate abundance peaks between sites within the framework of biostratigraphic age-models.

CHAPTER 4: COMPARISON OF DISCOASTER ABUNDANCE VARIATIONS AT SITES 709 AND 716 IN THE INDIAN OCEAN; OPTIMUM CONDITIONS VERSUS MONSOONALLY INDUCED PRODUCTIVITY PRESSURE.

4:1 Introduction

In comparison to the Atlantic and Pacific Ocean Basins, the palaeoceanography of the Indian Ocean is still relatively unexplored. Previous knowledge of pre-Pleistocene palaeoceanography and stratigraphy in the tropical Indian Ocean is based on material recovered from DSDP Legs 22 through 25 in 1972. Much of this DSDP material is of poor quality since the conventonal rotary coring device was in use disturbing the softer sediments. ODP Sites 709 and 716 from Leg 115 are of very high quality drilled with the Advanced Piston Corer.

Sites 709 and 716 are located in warm water masses of similar sea-surface temperature today, approximately 28°C in February and August (CLIMAP, 1981) (Table 4:1). According to Bé and Hutson (1977) they are both in the Equatorial Water Mass. This corresponds with a faunal province defined by planktonic foraminifera. In this chapter, the Discoaster abundances at these two sites are compared back to 3.5 Ma.

All the sites analysed in this thesis, except Site 716, were drilled at a water depth of over 2000 metres. Site 716 was drilled at 533 metres. This is the first chapter attempting to correlate abundance peaks between sites within the framework of biostratigraphic age-models.

CHAPTER 4: COMPARISON OF DISCOASTER ABUNDANCE VARIATIONS AT SITES 709 AND 716 IN THE INDIAN OCEAN; OPTIMUM CONDITIONS VERSUS MONSOONALLY INDUCED PRODUCTIVITY PRESSURE.

4:1 Introduction

In comparison to the Atlantic and Pacific Ocean Basins, the palaeoceanography of the Indian Ocean is still relatively unexplored. Previous knowledge of pre-Pleistocene palaeoceanography and stratigraphy in the tropical Indian Ocean is based on material recovered from DSDP Legs 22 through 25 in 1972. Much of this DSDP material is of poor quality since the conventonal rotary coring device was in use disturbing the softer sediments. ODP Sites 709 and 716 from Leg 115 are of very high quality drilled with the Advanced Piston Corer.

Sites 709 and 716 are located in warm water masses of similar sea-surface temperature today, approximately 28°C in February and August (CLIMAP, 1981) (Table 4:1). According to Bé and Hutson (1977) they are both in the Equatorial Water Mass. This corresponds with a faunal province defined by planktonic foraminifera. In this chapter, the Discoaster abundances at these two sites are compared back to 3.5 Ma.

All the sites analysed in this thesis, except Site 716, were drilled at a water depth of over 2000 metres. Site 716 was drilled at 533 metres. This is the first chapter attempting to correlate abundance peaks between sites within the framework of biostratigraphic age-models.

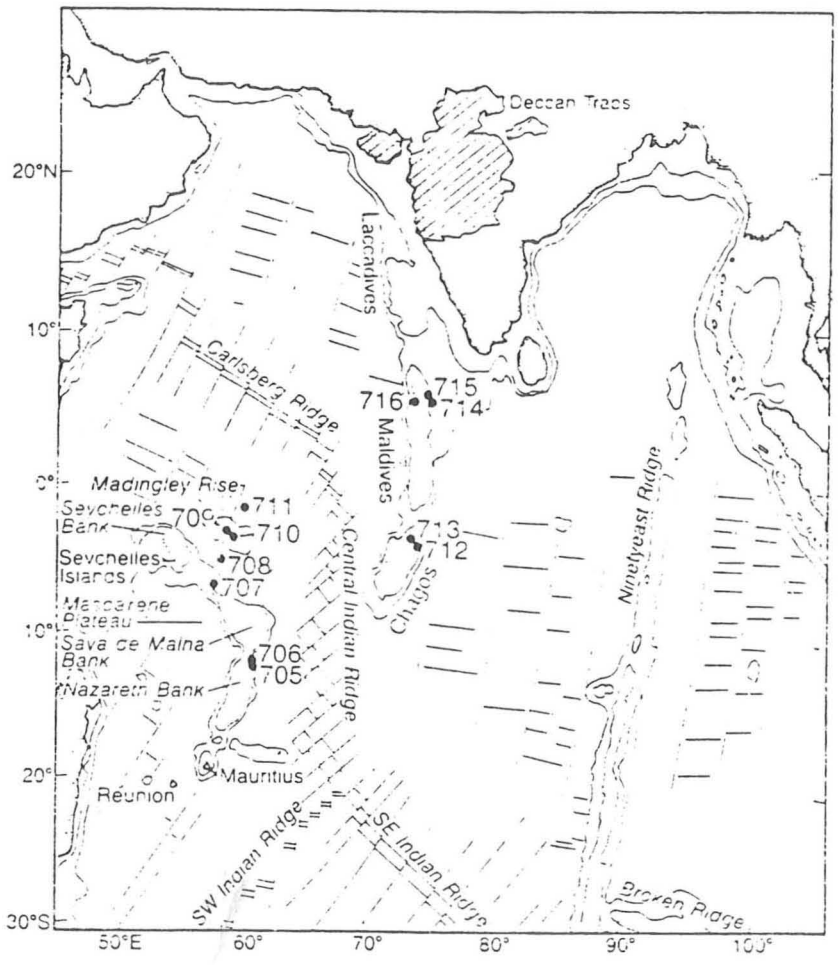

Figure 4:2 Location of Indian Ocean Sites 716 and 709.

TABLE 4:1

Modern sea-surface temperatures at Sites 709 and 716 (CLIMAP, 1981).

	February	August
Site 709	28°C	27.5°C
Site 716	28°C	28°C

TABLE 4:2

Indian Ocean sites, their geographic positions and water depth

HOLE	LOCATION	WATER DEPTH(M)	REFERENCE
709C	4°S 61°E	3,038	Backman, Duncan et al., 1988
716B	5°N 73°E	533	" "

TABLE 4:3 Summary of control points used in age-models

Hole 716B (Sampling interval=10cm)

Datum	Age (Ma)	Depth (mbsf)	Event	Sedimentation Rate
D. brouweri	1.89	62.60	Extinction	
				22.0cm/ka
D. pentaradiatus	2.38	73.40	Extinction	
				20.0cm/ka
G. atispira	2.95	84.80	Extinction	

Hole 709C (Sampling interval=5cm)

C. macintyrei	1.45	15.45	Extinction	
				5.6cm/ka
D. brouweri	1.89	17.90	Extinction	
				7.5cm/ka
D. triradiatus	2.07	19.25	Peak Abundance began	
				11.9cm/ka
D. surculus	2.39	23.05	Extinction	
				11.3cm/ka
D. tamalis	2.65	26.00	Extinction	
				9.4cm/ka
D. variabilis	2.90	28.35	Extinction	
				11.4cm/ka
R. pseudoumbilica	3.56	35.85	Extinction	

4:2 Background on Site 716.

Site 716 is located in the centre of the Maldives Ridge at 4°56'N and 73°17'E in a water depth of only 533.3m (Fig. 4:2, Table 4:2). The site lies in flat terrain on a broad, shallow basin which is filled with 1-1.5km of sediments and sedimentary rocks.

Aragonite, a less stable form of calcium carbonate is preserved at intermediate depths and has been found present throughout the entire sequence from petrographic observation and x-ray diffraction (XRD) results. Diatoms and radiolarians are reported as virtually absent which was confirmed during high resolution counting of the Discoaster component. The single lithologic unit is composed of foraminifer- bearing nannofossil ooze and foraminifer-bearing nannofossil calcareous ooze. These sediments consist of mostly unaltered and undisturbed, turbidite-free periplatform ooze. The carbonate content of sediment was always 90% or higher. Below the Pleistocene the nannofossils are poorly preserved. Sample spacing was at 10 cm intervals. (10cm ≈ 0·5ka)

4:3 Age-model for Site 716

As seen at Site 709, no magnetostratigraphic data were available at Site 716. The Discoaster species were found to be heavily overgrown, due to diagenetic recrystallization of calcite. All the 6-armed Discoaster species have been lumped

together and called "Discoaster brouweri" as a working hypothesis. This is the only 6-armed species covering the complete time interval and D. brouweri is the most abundant species, especially at low latitudes. The LAD's of Discoaster tamalis and D. triradiatus, to a lesser extent, are considered unreliable datums. These two species are poorly preserved and those identified occurred in low abundances. Discoaster asymmetricus was likewise poorly preserved and occurred in low abundances. The abundances of these species are thought not to be truly representative and are shown versus depth in Appendix B. Discoaster surculus and D. variabilis were beyond positive recognition and are probably a proportion of the 6-armed specimens counted as "D. brouweri" .

The age-model (Fig. 4:3, Table 4:3) was based on the LAD of "D. brouweri" , which fortunately was associated with a few recognisable specimens of D. triradiatus. G. altispira (S. Moody, Pers. Comm.) at 2.95 Ma provided a good datum. Discoaster pentaradiatus was the other distinct Discoaster datum, using the age of 2.38 Ma, originally ascertained from Site 659. This hardly caused any change in the sedimentation rate of 20cm/ka between 2.38-2.95 Ma to a slight increase of 22cm/ka between 1.89-2.38 Ma. No reliable datum was obtained for R. pseudoumbilica, though a few poorly preserved specimens were found at the bottom of core 11 (100.4 mbsf). The age-model was therefore extrapolated to cover the time interval below 2.95 Ma. Future work may define the LAD of R. pseudoumbilica, which was distinct at Site 709. The sedimentation rates at Site 716 are high and generally twice or more those found at Site 709. Information on background and age-model details of Site 709 is found in the previous chapter.

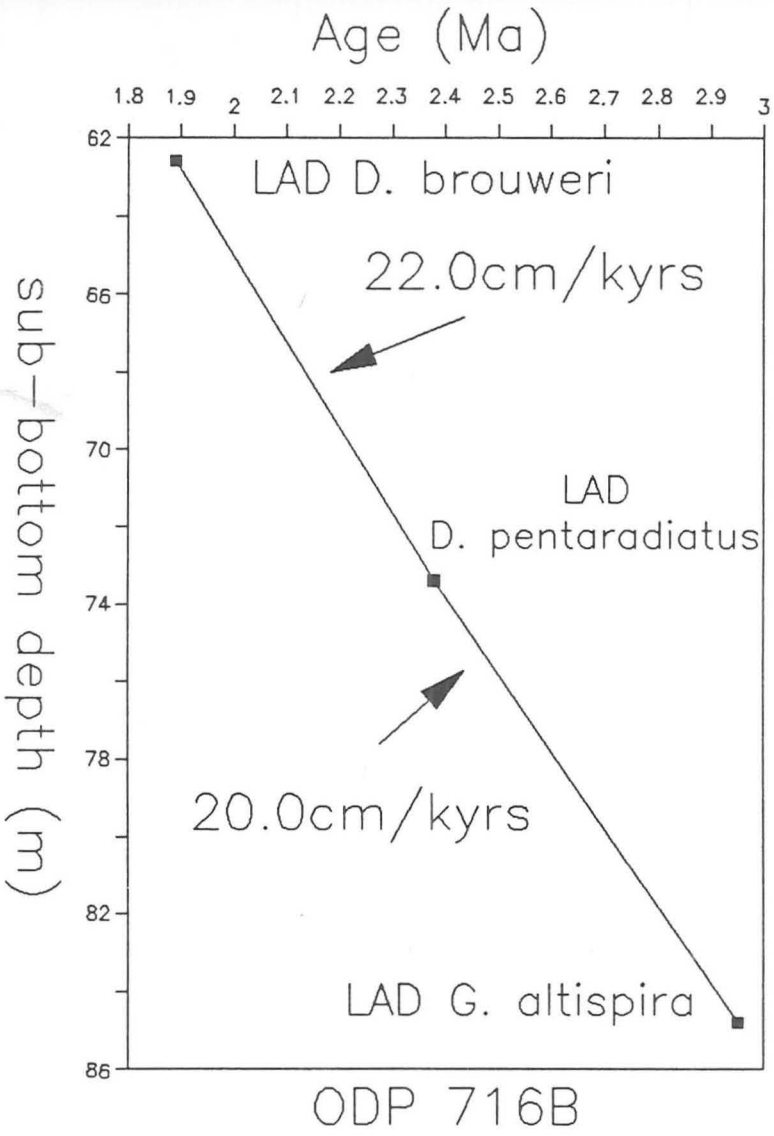

Figure 4:3 Age/depth relationships of biochronologic control points at Hole 716B

4:4 Discoaster species abundance patterns and relative abundances within the assemblage

Calcite overgrowth at Site 716 on the 6 armed Discoaster species caused identification problems, associated with the low occurrence of the other Discoaster species. Only "D. brouweri", D. pentaradiatus and total Discoaster abundances are compared between Sites 716 and 709. Twenty fields of view were counted at both sites at a view field diameter of 0.3 mm.

4:4:1 Discoaster brouweri

Discoaster brouweri is the only species covering the complete time interval. Abundances at Site 709 are approximately five times those found at Site 716 (Fig. 4:4:1a). A number of the abundance peaks appear to correlate approximately between 2.2 and 2.8 Ma, prior to which correlation breaks down. The major abundance peak at 2.3 Ma is clearly recognisable at both sites.

Site 716 shows a clearer trend of reduction in abundance through time. D. brouweri is a major component of the complete Discoaster assemblage at both sites (Fig. 4:4:1b). Although, D. brouweri appears to be a greater component prior to 2.4 Ma at Site 716, the difference between the sites may be represented by unidentifiable D. surculus lumped in the "D. brouweri" category. Both sites, nevertheless, display a distinct increase in the relative abundance of D. brouweri towards 2.4 Ma.

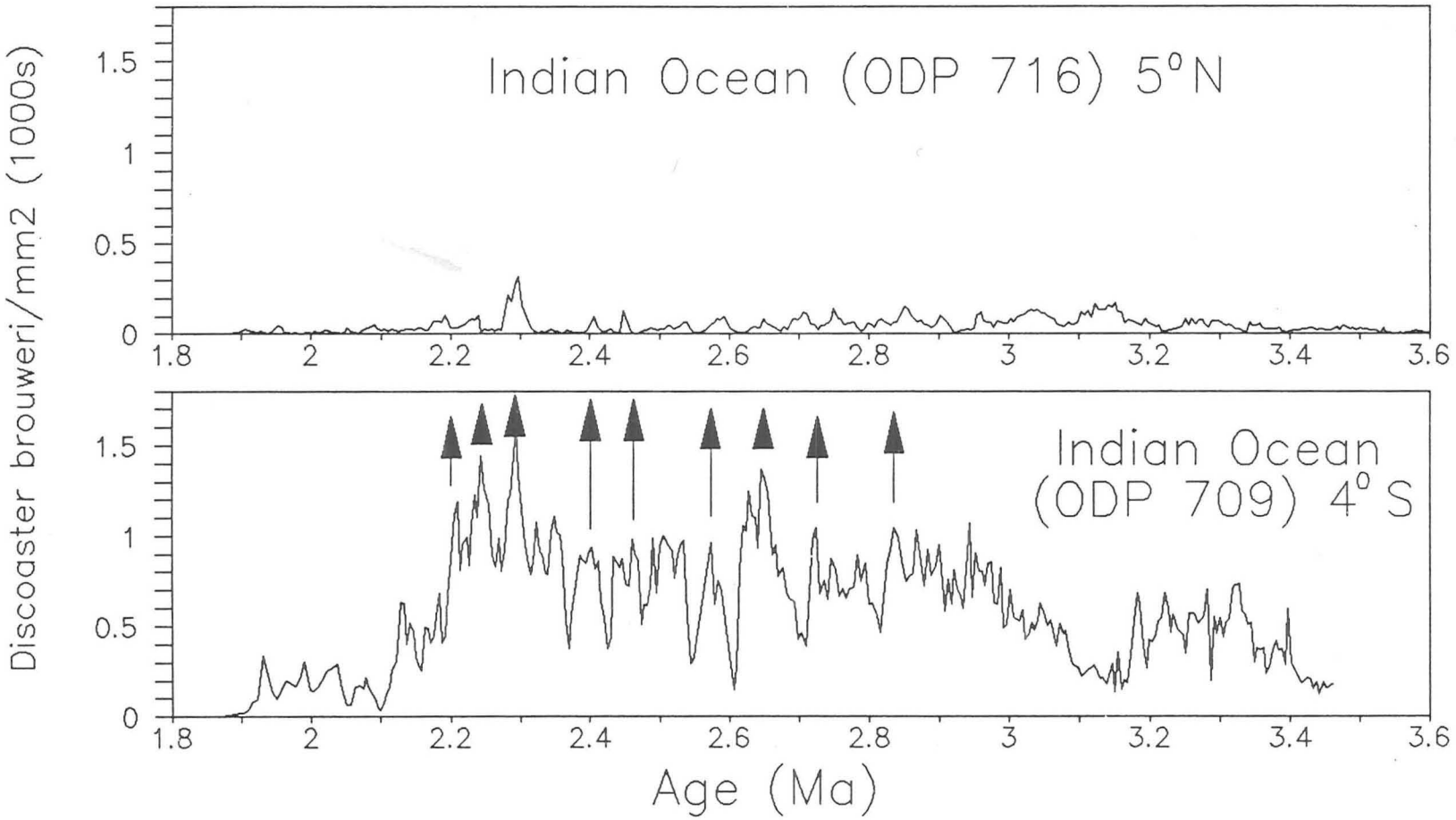

Figure 4:4:1a Abundance plots of D. brouweri at Indian Ocean Sites 709 and 716. Arrows indicate possible correlation between sites

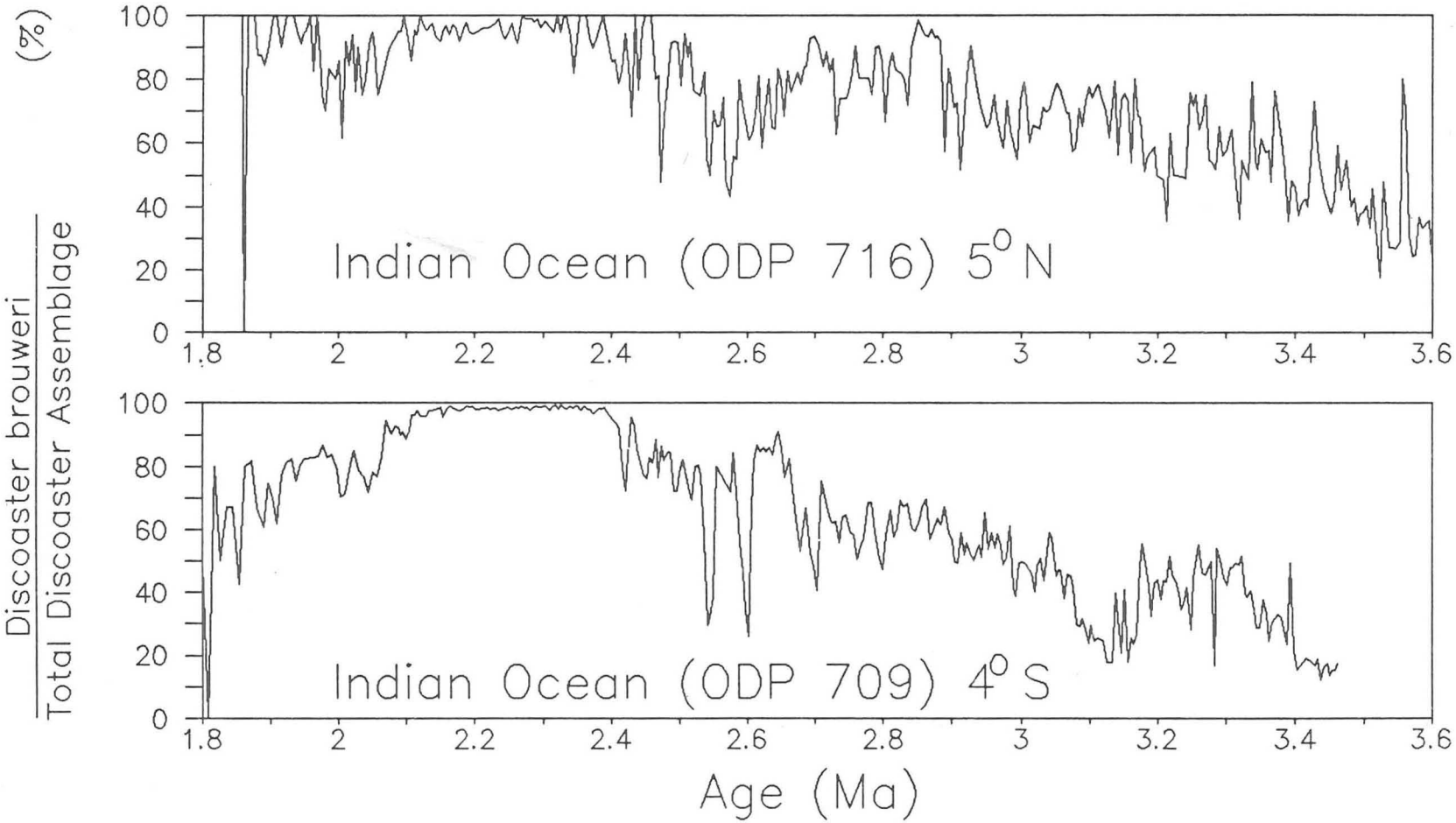

Figure 4:4:1b Percentage abundance plots of D. brouweri at Indian Ocean Sites 709 and 716.

4:4:2 Discoaster pentaradiatus

This species was easily identifiable at Site 716. Site 709 shows far greater abundances than at Site 716 (Fig. 4:4:2a), although both display a trend of abundance reduction up to the exinction event at 2.38 Ma. Very few abundance peaks appear to be easily correlated, except the largest peaks at approximately 2.6 and 3.1 Ma.

If D. pentaradiatus is represented as a percentage of the complete Discoaster assemblage, the relative abundances are similar (Fig. 4:4:2b). The trend of abundance reduction through time is further emphasised. Discoaster pentaradiatus forming similarly high relative abundances was found in Chapter 2 across a transect of five sites with a wide latitudinal range and upwelling versus non-upwelling conditions in the North Atlantic.

4:5 Total Discoaster Abundance

At Site 716, this is effectively the sum of "D. brouweri" and D. pentaradiatus (Fig. 4:5), but appears virtually identical with the abundance plots of "D. brouweri" (Fig. 4:4:1a). Site 709 displays abundances of the order six to seven times that of Site 716 prior to 2.4 Ma, though modern sea-surface temperatures are similar and this is probably also true in the upper Pliocene . The difference in total Discoaster abundance between the sites cannot be explained by dilution

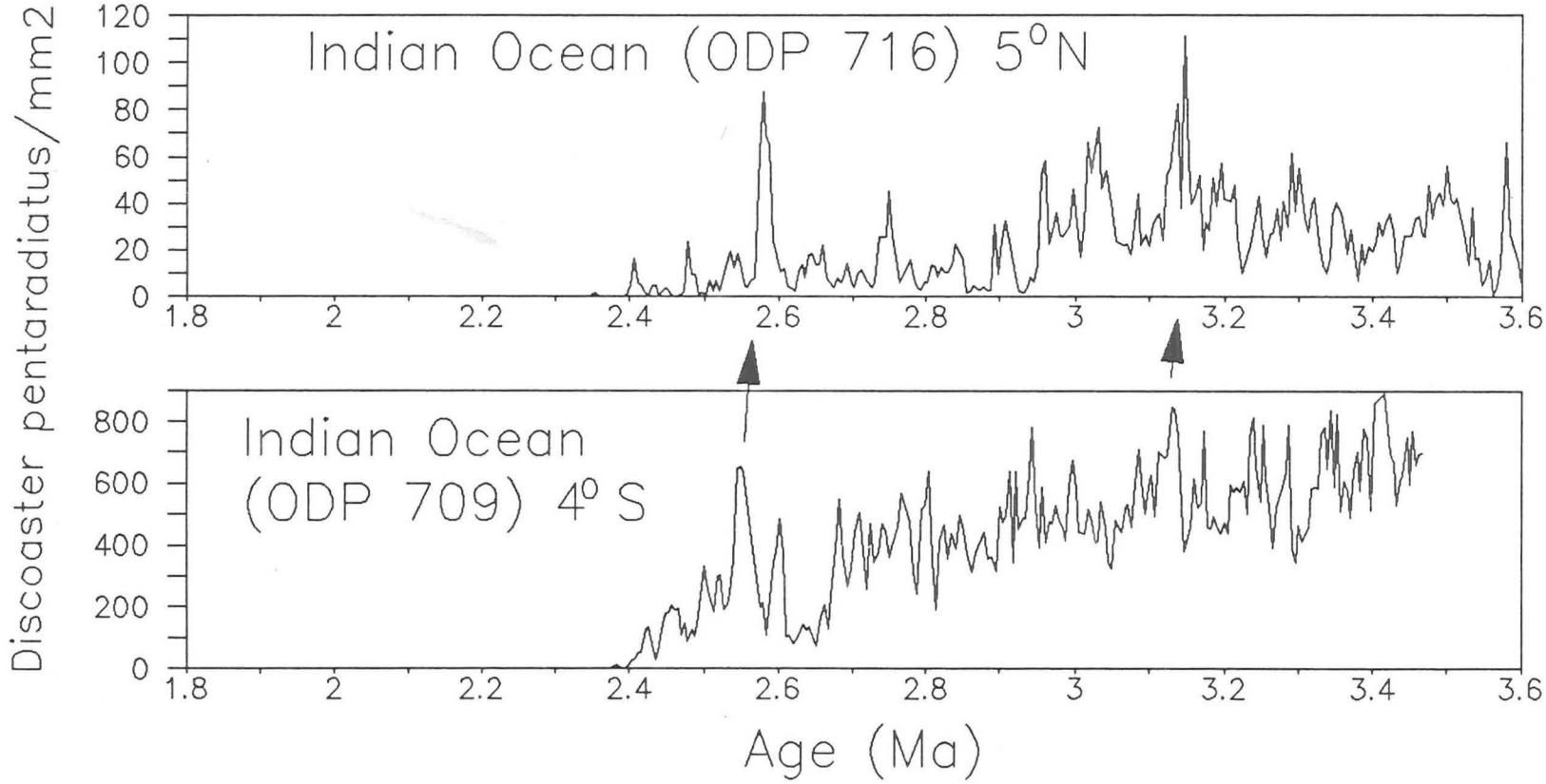

Figure 4:4:2a Abundance plots of D. pentaradiatus at Indian Ocean Sites 709 and 716. Notice the difference in abundance scales. Arrows indicate possible correlation between greatest peaks

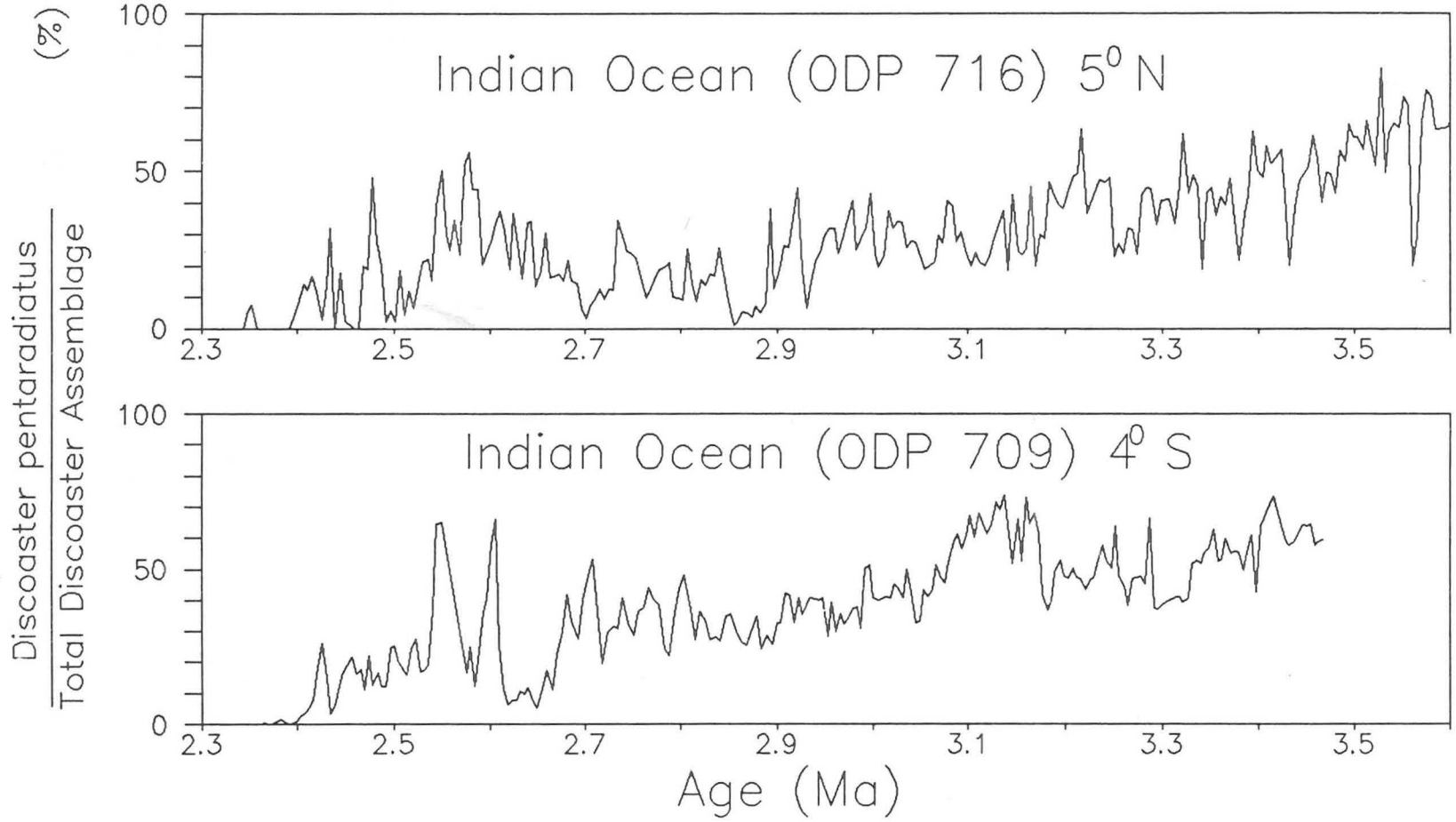

Figure 4:4:2b Percentage abundance plots of D. pentaradiatus at Indian Ocean Sites 709 and 716

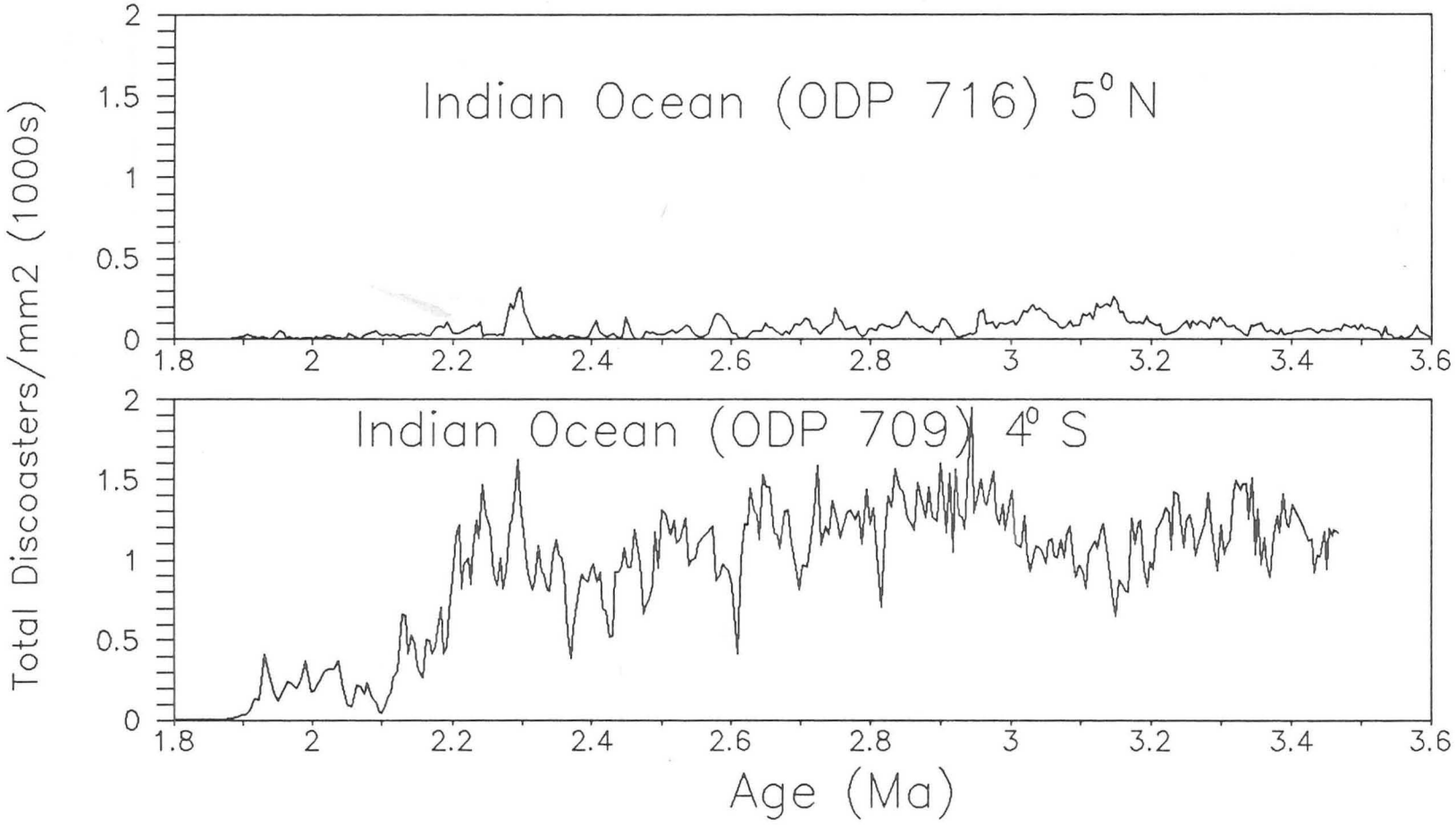

Figure 4:5 Abundance plots of Total Discoasters at Indian Ocean Sites 709 and 716.

of the Discoaster component at Site 716 which has a sedimentation rate at least twice that of found at Site 709. Site 709 is located above the calcite lysocline (3500-4000m) and little or no dissolution is generally observed in planktonic calcitic sediments, which consist mainly of coccoliths and foraminifer tests (Peterson and Prell, 1985a). The robust Discoaster component is therefore not enhanced by dissolution of planktonic foraminifera or placoliths (Lohman and Carlson, 1981). Productivity pressure must be considered to explain the difference in Discoaster abundance between these two sites.

4:6 Spectral Analysis

In this study, spectral analysis is based on linear interpolation between the biostratigraphic control points selected for the age-models (Table 4:3). No magnetostratigraphic data were available. The data sets have been divided into three time intervals: from 1.88 to 2.39 Ma, from 2.39 to 3.00 Ma and 3.00 to 3.50 Ma, approximately 0.5 Ma intervals. As in Chapters 2 and 3, spectral analysis is performed on the sum of all the Discoaster species. Figure 4:5 shows that there is a large signal at both sites for spectral analysis.

During the time interval from 1.89 to 2.39 Ma, D. brouweri is effectively the only species present. At Site 716, concentrations of variance around the frequencies of the orbital elements of eccentricity (100 ka) and obliquity (41 ka) are present, but no precession (21 ka) is distinguished (Fig. 4:6). Site 709 displays a possible obliquity periodicity.

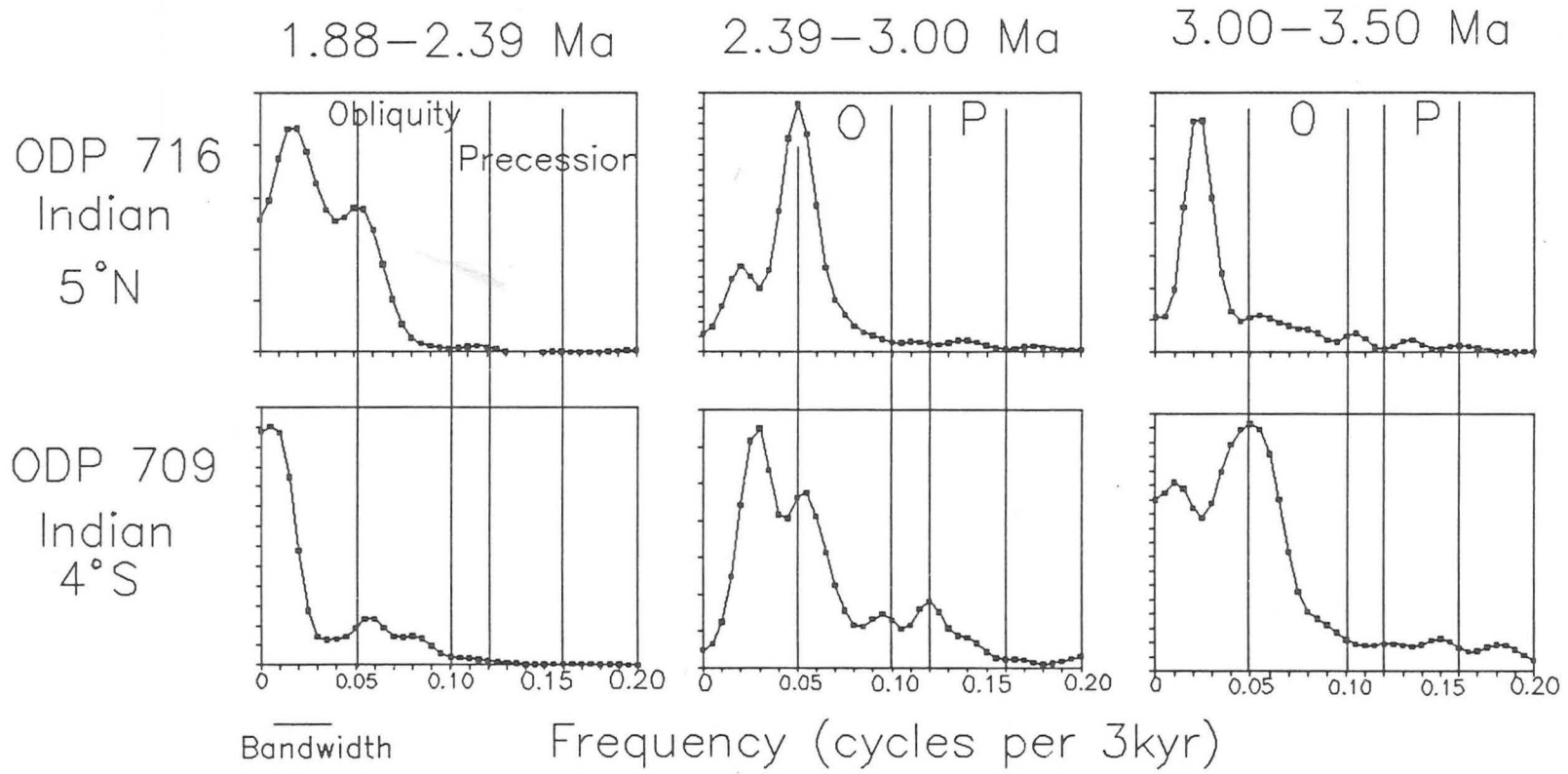

Figure 4:6 Spectral power density estimated on 3 time intervals of the total Discoaster data set at Sites 716 and 709. B.W. indicates band width

Between 2.39 and 3.00 Ma, when a greater Discoaster assemblage occurs, possible eccentricity and obliquity periodicities occur at both sites. Only Site 709 shows a tentative precessional periodicity. In the time interval between 3.00 and 3.50 Ma, all the Discoaster species are present, but the age-models are weakest interpolating/extrapolating over the longest time interval with the fewest control points at Sites 709 and 716 respectively. Nevertheless, possible eccentricity periodicities are present at both sites. An obliquity periodicity may be present at Site 709, but no precessional periodicities can be distinguished at either site.

4:7 Discussion

The first question to be addressed is why should these two sites display such marked differences in Discoaster abundances if they are located in water masses of such similar sea-surface temperature? The fact that Sites 716 and 709 are located in such contrasting depths of 533m and 3038m respectively should not be significant. Site 716 has aragonite preserved at these intermediate depths, but according to Droxler et al. (in press), this averages only 15% of the total sediment between 2.0 and 3.5 Ma, and hence is not important. At Site 709, carbonate dissolution is not a problem since it is above the calcite lysocline.

Productivity pressure was found in the North Atlantic (Chapter 2) and across the Equator (Chapter 3) to be a major factor. Diatoms can reflect high nutrient levels, but these were poorly represented at both sites. The next question is how subtle does the productivity pressure have to be before the Discoaster

abundances are suppressed? Site 709 is believed to be located in warm, low-nutrient waters. However, Site 716 is affected by high-nutrient waters of the monsoon gyre. The evidence for this can be seen from satellite imaging by NASA in Plate 5 (Lewis, 1989). Strong summer southwesterly monsoon winds generate upwelling of nutrient rich water, leading to the development of bloom conditions. This is clearly seen in the Maldives, but not in the Mascarene Plateau area. Under these conditions, the production of discoasters are suppressed by the competition of more successful plankton.

Discoaster pentaradiatus once again reveals itself as a highly flexible species in its ecological requirements. At both sites which reflect contrasting high and low productivity for the discoasters, D. pentaradiatus occurs in significant abundances and forms an important proportion of the complete Disco aster assemblage.

4:8 Summary

1. Very high Discoaster abundances at Site 709 indicate minimal productivity pressure, whereas lower Discoaster abundance at Site 716 reveals major suppression caused by productivity pressure. This is linked with upwelling caused by summer southwesterly winds as seen in the NASA images of phytoplankton concentration.

2. There is a gradual increase in the significance of D. brouweri within the complete Discoaster assemblage at Sites 709 and 716 between 3.5 and 2.4 Ma.

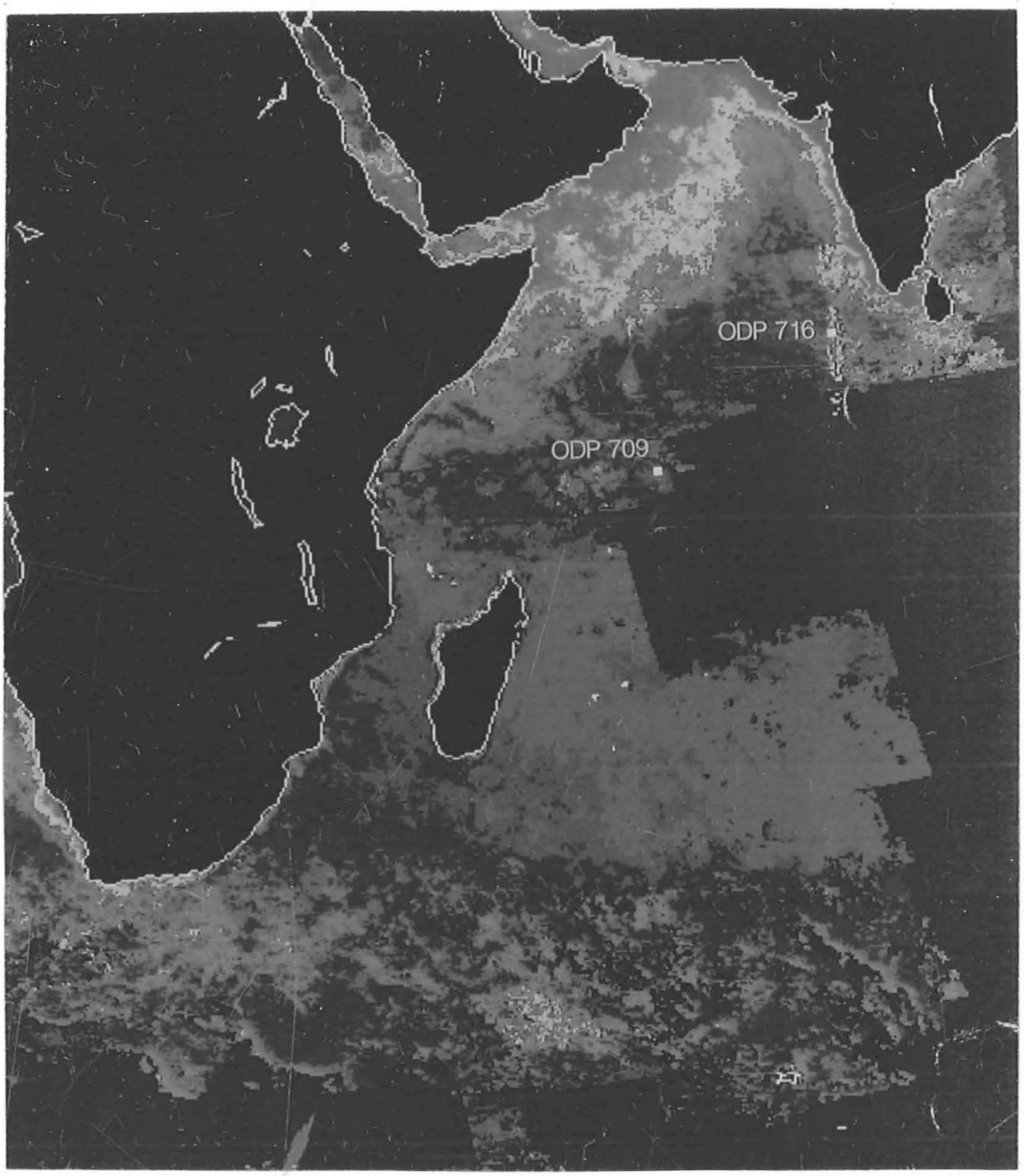

PLATE 5

Indian ocean sites located on satellite image of phytoplankton concentration in September–October, 1979 (after Lewis, 1989).

Purple– minimum phytoplankton concentration
red–maximum phytoplankton concentration

Conversely, the relative abundance of D. pentaradiatus shows the opposite trend.

3. Tentative correlation is possible between the two sites using D. brouweri abundance peaks, and D. pentaradiatus abundance peaks to a lesser degree.

4. Orbital forcing is indicated at both sites through spectral analysis, but the timescales need to be improved to refine the periodicities.

CHAPTER 5: RELATIONSHIPS WITHIN THE GENUS DISCOASTER IN THE UPPER PLIOCENE; SIX SPECIES OR THREE SPECIES ?

5:1 Introduction

In this chapter, the relationships between the six Discoaster species are investigated, following on from the work of Backman and Shackleton (1983). It has already been shown that by representing each individual species as a proportion of the total Discoaster assemblage or a group of species, we can convey valuable palaeoecological information. However, apparently similar palaeoecological records given by two species may be due to close taxonomic affinities. The high resolution data gathered in Chapter 2 (North Atlantic transect) and Chapter 3 (Equatorial transect) is ideal for addressing this question.

The first strong evidence pointing towards taxonomic affinity in the Discoaster group is the simultaneous extinction at 1.89 Ma of Discoaster brouweri and Discoaster triradiatus, preceded by an acme of D. triradiatus back to 2.07 Ma. This was observed to be a constant relationship between these two species at all the sites. In Chapters 2 and 3, we found that Discoaster asymmetricus and Discoaster tamalis show strong co-variation and increase relative to D. brouweri with cooler water conditions, but are suppressed by high productivity. An inverse relationship between the abundance of Discoaster pentaradiatus and Discoaster surculus had been frequently observed at the sites, but not analysed in any detail. In Chapter 2, however, Figure 2:4:2i shows that D. surculus increases as a proportion of the sum of itself and D. pentaradiatus as a function of higher

productivity and cooler sea-surface temperatures. We also investigate here, the relationship between D. brouweri and D. surculus, and D. brouweri and D. pentaradiatus to see if these are distinct species. This chapter deals firstly with relationships in the Discoaster group at individual sites, and secondly compares between sites to add to our palaeoecological interpretation. All the sites are examined, except Site 716, where preservation was very poor (see Chapter 4) to investigate if these relationships hold true on a global scale. In examining individual sites, we follow the sequence of the North Atlantic transect (Chapter 2), from highest latitude to lowest latitude, followed by the two other equatorial sites in the Pacific and Indian Oceans (Chapter 3).

To compare Discoaster species, we have selected shorter time intervals for analysis in much greater detail than seen before, and represent the data on scatter diagrams. Each point on the diagram represents the relative abundance of two species of Discoaster at one moment in time. The number of points reflects the length of the time interval and the time resolution. A scatter diagram is a convenient way of displaying results, but it is necessary to decide whether there is a significant correlation. To measure correlation, statisticians use the correlation coefficient, r, which is given by the equation:

$$r = \frac{\text{sum}((x-\bar{x}) (y-\bar{y}))}{\sqrt{(\text{sum } (x-\bar{x})^2 \ \text{sum}(y-\bar{y})^2)}}$$

In this expression, one variable (i.e. species A) is represented by x , the other by y (i.e. species B); $\bar{x}$ and $\bar{y}$ are the means of the two sets of variables. The terms $(x-\bar{x})$ and $(y-\bar{y})$ are deviations from the mean. The term sum ($(x-\bar{x})(y-\bar{y})$) above the line shows that for each sample, one measures the deviation of x from the mean $\bar{x}$, and the deviation of y from the mean $\bar{y}$, and multiplies these two deviations together. The term below the line $\surd$ (sum $(x-\bar{x})^2$ sum$(y-\bar{y})^2$) contains the sums of the squares of deviations in x and in y, and is related to the variances of x and y taken separately. Basically, the equation for r expresses the relationship between x (species A) and y (species B) in terms of the variances within x and within y.

We make assumptions that D. brouweri was closely related with D. triradiatus, and that D. asymmetricus and D. tamalis were closely related. Similarly, we believed there existed some taxonomic affinity between D. brouweri and D. asymmetricus and D. tamalis, but not between these species and D. pentaradiatus and D. surculus. Furthermore, we did not believe there to have been any taxonomic affinity between D. pentaradiatus and D. surculus. We thought that we could indicate any affinities from their correlation coefficients. The correlation coefficient can range between +1 and -1. If it is +1, correlation is perfect and positive; a value of -1 means perfect negative correlation; zero means no correlation. The correlation coefficients between the Discoaster species are shown in Table 5:1a. Tables 5:1b-i show the significance of the correlation coefficients between the Discoaster species at the .01 significance level from Table 7 of Fisher and Yates: Statistical Tables for Biological, Agricultural and

	1.89–2.07 Ma	2.65–3.00 Ma *						2.38–3.00 Ma *
SITES	D. brouweri + D. trirodiatus	D. asymmetricus + D. tamalis	D. brouweri + (D. asymmetricus + D. tamalis)	D. brouweri + D. pentaradiatus	D. pentaradiatus + (D. asymmetricus + D. tamalis)	D. brouweri + D. surculus	D. surculus (D. asymmetricus + D. tamalis)	D. pentaradiatus + D. surculus
ATLANTIC DSDP 552 (56^0N)	.74	.54	.64	−.16	−.28	−.03	.33	.05
ATLANTIC DSDP 607 (41^0N)	.92	.96	.89	.43	.37	.35	.17	.08
ATLANTIC Upwelling ODP 658 (20^0N)	.85	.77	.22	.02	.24	.06	.19	.14
ATLANTIC ODP 659 (18^0N)	.94	.99	−.09#	−.01	.20	.47	−.32	−.02
ATLANTIC Upwelling ODP 662 (1^0S)	.39	.84	.15	.40	.66	.14	.25	.42
PACIFIC ODP 677 (1^0N)	.88	.82	.24	−.11	.10	.75	.21	.06
INDIAN ODP 709 (4^0S)	.80	.64	−.40	−.05	.37	−.02	.23	.25
Mean species Correlation Coefficient	.79	.80	.24	.08	.24	.25	.15	.14

TABLE 5:1a Correlation coefficients between Discoaster species (* Time interval at ODP 709 extends back to 3.5 Ma)

correlation coefficient 0.69 between 2.8–3.05 Ma

SITES	D. brouweri + D. triradiatus	degrees of freedom (n−1)	correlation coefficient at .01 level	S= significant NS= not significant
ATLANTIC DSDP 552 (56°N)	.74	25	.49	S
ATLANTIC DSDP 607 (41°N)	.92	56	.32	S
ATLANTIC ODP Upwelling 658 (20°N)	.85	85	.27	S
ATLANTIC ODP 659 (18°N)	.94	57	.32	S
ATLANTIC ODP Upwelling 662 (1°S)	.39	98	.25	S
PACIFIC ODP 677 (1°N)	.88	100	.25	S
INDIAN ODP 709 (4°S)	.80	25	.49	S

Table 5:1b.
Correlation coefficients and significance between
D. brouweri and D. triradiatus

SITES	D. asymmetricus and D. tamalis	degrees of freedom (n−1)	correlation coefficient at .01 level	S= significant NS= not significant
ATLANTIC DSDP 552 (56°N)	.54	35	.42	S
ATLANTIC DSDP 607 (41°N)	.96	83	.28	S
ATLANTIC ODP Upwelling 658 (20°N)	.77	129	.25	S
ATLANTIC ODP 659 (18°N)	.99	114	.25	S
ATLANTIC ODP Upwelling 662 (1°S)	.84	93	.27	S
PACIFIC ODP 677 (1°N)	.82	158	.25	S
INDIAN ODP 709 (4°S)	.64	166	.25	S

Table 5:1c
Correlation coefficients and significance between
D. asymmetricus and D. tamalis

SITES	D. brouweri / (D. aymmetricus + D. tamalis)	degrees of freedom (n−1)	correlation coefficient at .01 level	S= significant NS= not significant
ATLANTIC DSDP 552 (56°N)	.64	35	.42	S
ATLANTIC DSDP 607 (41°N)	.89	83	.28	S
ATLANTIC ODP Upwelling 658 (20°N)	.22 #	129	.25	NS
ATLANTIC ODP 659 (18°N)	−.09	114	.25	NS
ATLANTIC ODP Upwelling 662 (1°S)	.15	93	.27	NS
PACIFIC ODP 677 (1°N)	.24	158	.25	NS
INDIAN ODP 709 (4°S)	−.40	166	.25	S

Table 5:1d

Correlation coefficients and significance between D. brouweri and the sum of D. aymmetricus and D. tamalis

correlation coefficient 0.69 between 2.8−3.05 Ma is significant at the .01 level (= .28, 78 d.o.f)

SITES	D. brouweri + D. pentaradiatus	degrees of freedom (n−1)	correlation coefficient at .01 level	S= significant NS= not significant
ATLANTIC DSDP 552 (56°N)	−.16	35	.42	NS
ATLANTIC DSDP 607 (41°N)	.43	83	.28	S
ATLANTIC ODP Upwelling 658 (20°N)	.02	129	.25	NS
ATLANTIC ODP 659 (18°N)	−.01	114	.25	NS
ATLANTIC ODP Upwelling 662 (1°S)	.40	93	.27	S
PACIFIC ODP 677 (1°N)	−.11	158	.25	NS
INDIAN ODP 709 (4°S)	−.40	166	.25	S

Table 5:1e

Correlation coefficients and significance between D. brouweri and D. pentaradiatus

SITES	D. pentaradiatus + (D. asymmetricus + D. tamalis)	degrees of freedom (n−1)	correlation coefficient at .01 level	S= significant NS= not significant
ATLANTIC DSDP 552 (56°N)	−.28	35	.42	NS
ATLANTIC DSDP 607 (41°N)	.37	83	.28	S
ATLANTIC ODP Upwelling 658 (20°N)	.24	129	.25	NS
ATLANTIC ODP 659 (18°N)	.20	114	.25	NS
ATLANTIC ODP Upwelling 662 (1°S)	.66	93	.27	S
PACIFIC ODP 677 (1°N)	.10	158	.25	NS
INDIAN ODP 709 (4°S)	.37	166	.25	S

Table 5:1f
Correlation coefficients and significance between D. pentaradiatus and the sum of D. asymmetricus and D. tamalis

SITES	D. brouweri + D. surculus	degrees of freedom (n−1)	correlation coefficient at .01 level	S= significant NS= not significant
ATLANTIC DSDP 552 (56°N)	−.03	35	.42	NS
ATLANTIC DSDP 607 (41°N)	.35	83	.28	S
ATLANTIC ODP Upwelling 658 (20°N)	.06	129	.25	NS
ATLANTIC ODP 659 (18°N)	.47	114	.25	S
ATLANTIC ODP Upwelling 662 (1°S)	.14	93	.27	NS
PACIFIC ODP 677 (1°N)	.75	158	.25	S
INDIAN ODP 709 (4°S)	−.02	166	.25	NS

Table 5:1g
Correlation coefficients and significance between D. brouweri and D. surculus

SITES	D. surculus (D. asymmetricus + D. tamalis)	degrees of freedom (n−1)	correlation coefficient at .01 level	S= significant NS= not significant
ATLANTIC DSDP 552 (56°N)	.33	35	.42	NS
ATLANTIC DSDP 607 (41°N)	.17	83	.28	NS
ATLANTIC ODP Upwelling 658 (20°N)	.19	129	.25	NS
ATLANTIC ODP 659 (18°N)	−.32	114	.25	S
ATLANTIC ODP Upwelling 662 (1°S)	.25	93	.27	NS
PACIFIC ODP 677 (1°N)	.21	158	.25	NS
INDIAN ODP 709 (4°S)	.23	166	.25	NS

Table 5:1h
Correlation coefficients and significance between
D. surculus and the sum of D. asymmetricus
and D. tamalis

SITES	D. pentaradiatus + D. surculus	degrees of freedom (n−1)	correlation coefficient at .01 level	S= significant NS= not significant
ATLANTIC DSDP 552 (56°N)	.05	62	.32	NS
ATLANTIC DSDP 607 (41°N)	.08	153	.25	NS
ATLANTIC ODP Upwelling 658 (20°N)	.14	241	.25	NS
ATLANTIC ODP 659 (18°N)	−.02	191	.25	NS
ATLANTIC ODP Upwelling 662 (1°S)	.42	170	.25	S
PACIFIC ODP 677 (1°N)	.06	332	.25	NS
INDIAN ODP 709 (4°S)	.25	223	.25	NS

Table 5:1i
Correlation coefficients and significance between
D. pentaradiatus and D. surculus

Medical Research.

5:2 Relationships between the Discoaster species

5:2:1 Co-variation between D. brouweri and D. triradiatus

We examine here in detail the time interval only of the D. triradiatus acme between 1.89 and 2.07 Ma (i.e. a time interval of only 180 ka) when these were the only Discoaster species present. Prior to 2.07 Ma, D. triradiatus occurs in very subdued abundances. A high positive correlation between the two species can be seen at most of the sites (Figs. 5:2:1a-g, Tables 5:1a & b).

At Site 552 (Fig. 5:2:1a), a low sedimentation rate and a temporally coarse sampling interval reduces the number of data points covering this short time interval, but a positive correlation is still evident. This is important when one considers how reduced the abundances are at high latitudes (56°N), and the statistical error that is possible.

At Site 607 (Fig. 5:2:1b), the sedimentation rate is four times greater (4.8cm/kα) than Site 552 giving us a higher time resolution at this high latitude site (41°N). There is a high positive correlation between D. brouweri and D. triradiatus, which is enhanced by the long interval of suppressed abundances between 1.94 Ma and 2.03 Ma. It is noticeable that the two most prominent peaks are separated by approximately 100 ka.

At Site 658 (Fig. 5:2:1c), the higher sedimentation rate at this upwelling site (7.9cm/kα) produces a more detailed record with obviously more data pairs to correlate. There is still a high positive correlation, but as seen at Site 607, this is still enhanced by long intervals of suppressed abundances. Nevertheless, the main

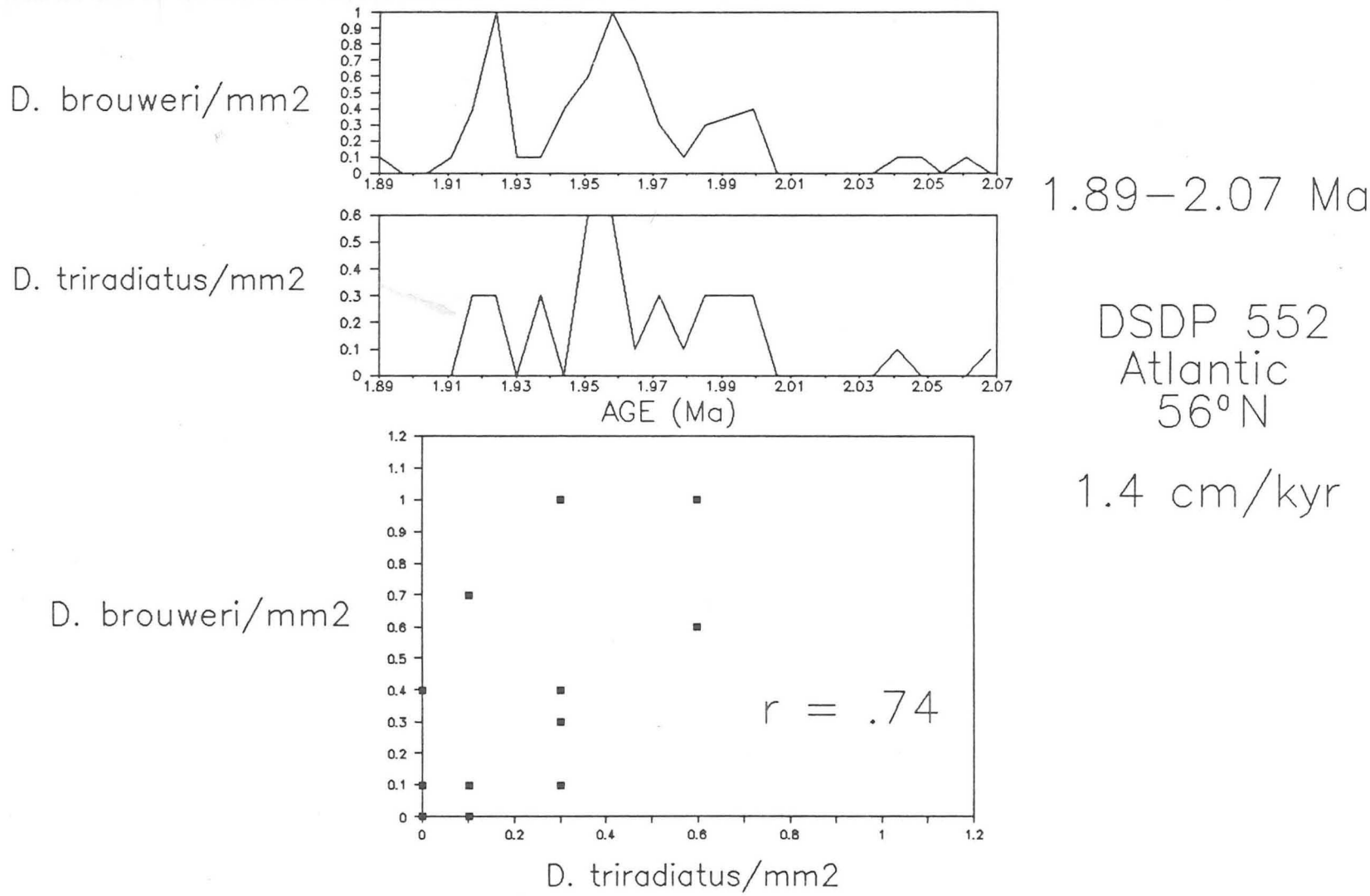

Figure 5:2:1a Abundance of D. brouweri and D. triradiatus/mm2 at DSDP 552 between 1.89–2.07 Ma.

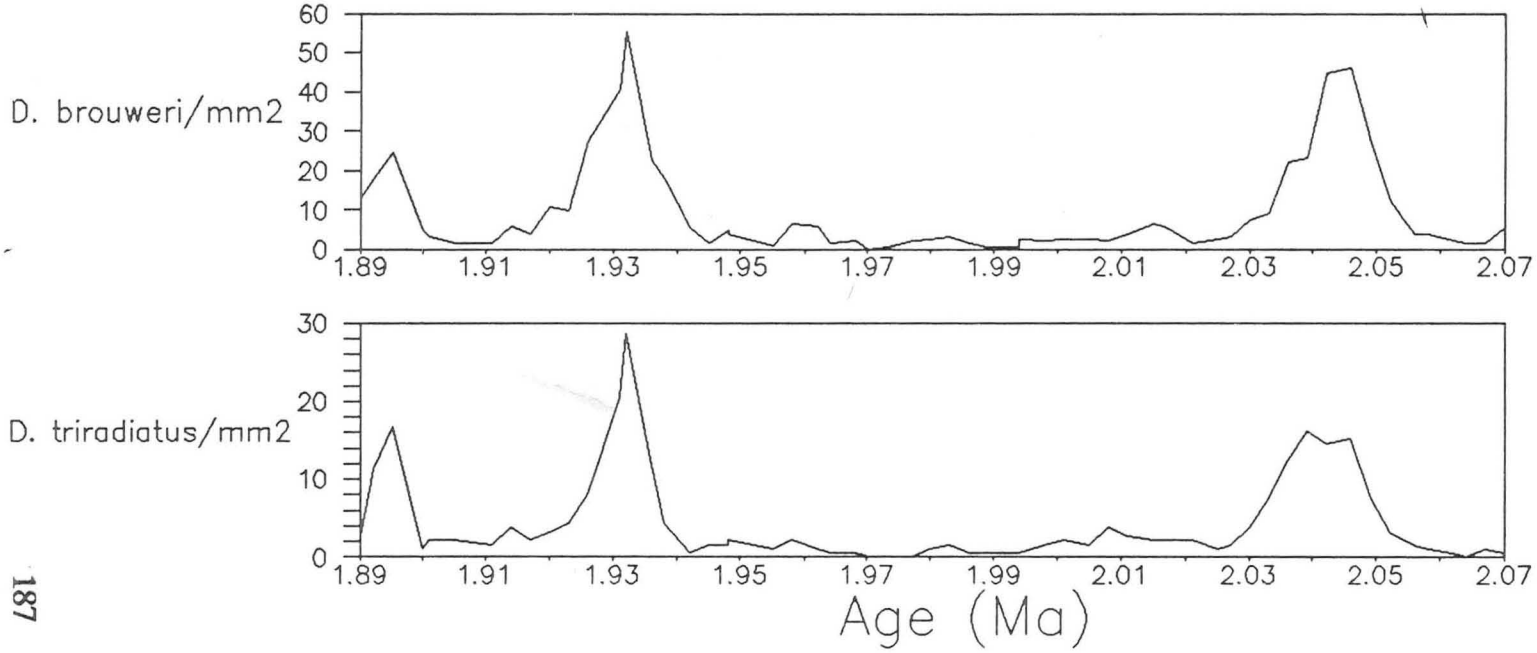

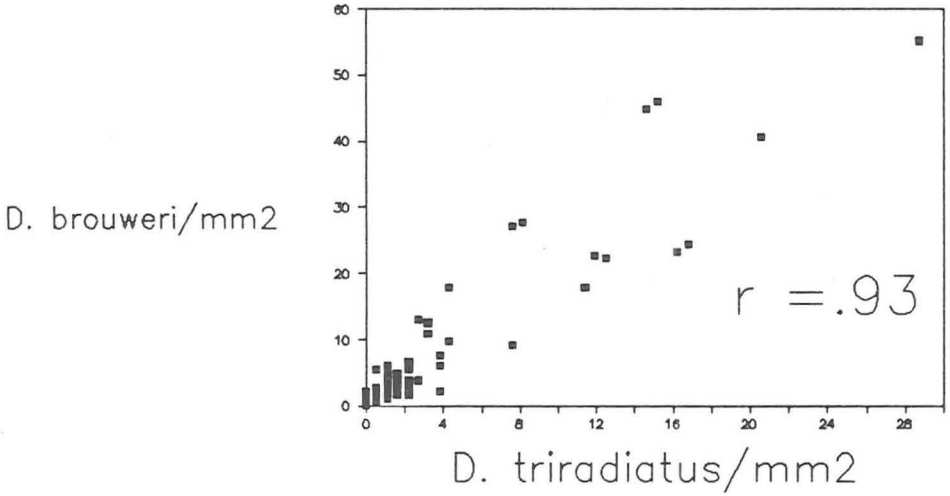

1.89–2.07 Ma

DSDP 607
Atlantic
41°N

4.8 cm/kyr

Figure 5:2:1b Abundance of D. brouweri and D. triradiatus/mm2 at DSDP 607 between 1.89–2.07 Ma.

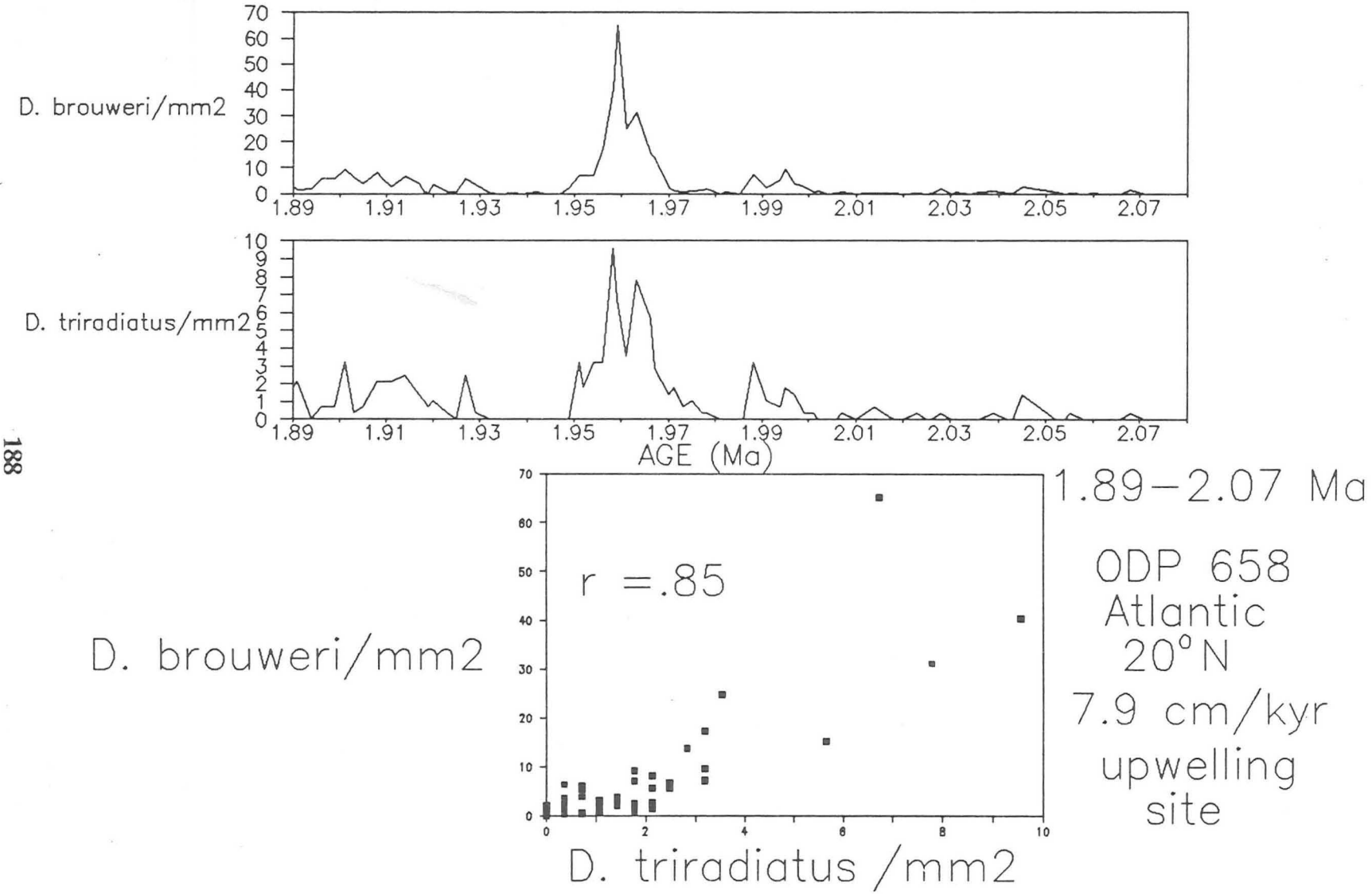

Figure 5:2:1c Abundance of D. brouweri and D. triradiatus/mm2 at ODP 658 between 1.89–2.07 Ma.

feature of high abundance between 1.95 and 1.97 Ma marks an interval of lower suppression.

At Site 659 (Fig. 5:2:1d), in close proximity to Site 658, there is similarly a high positive correlation between D. brouweri and D. triradiatus. The abundances may be much higher than already seen, but prior to 1.96 Ma and after 1.92 Ma, the abundances are suppressed by comparison to the main peaks. It is possible that the two main peaks together at Site 659 at approximately 1.93 and 1.95 Ma respectively are synchronous with those observed independently at Sites 607 and 658.

The correlation is poorest at the equatorial Atlantic site, Site 662 (Fig. 5:2:1e). This is a very low abundance interval of D. brouweri preceding its extinction, whereas the abundances prior to this time interval have been generally very high (see Fig. 2:4:1e). A correlation does exist, but it is probably weakened by reworking of D. brouweri through this interval, since this site is known to be affected by slumping. There is no source, prior to 2.07 Ma, for D. triradiatus to be reworked from. This would explain why low abundances of D. triradiatus are associated with high abundances of D. brouweri, but the reverse is not possible. A clear linear relationship is visible if these anomalously high D. brouweri abundances associated with low D. triradiatus abundances are ignored.

At Site 677 (Fig. 5:2:1f), in the Pacific Ocean, the correlation coefficient is higher than would be expected from the scatter diagram. The scatter diagram gives the impression of very few data points and potentially two linear relationships. It must be remembered that Site 677 is an upwelling site with an

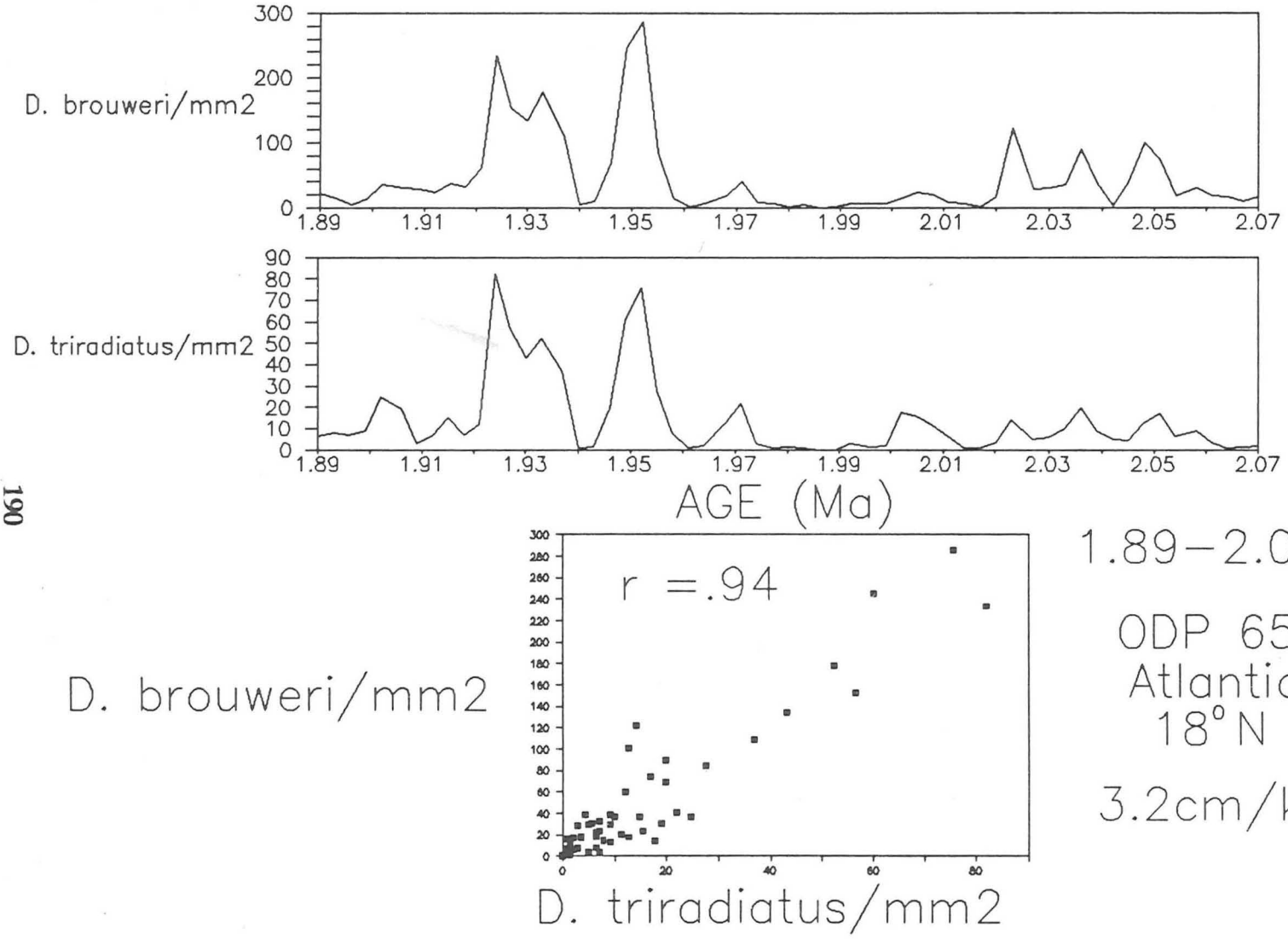

Figure 5:2:1d Abundance of D. brouweri and D. triradiatus/mm2 at Site 659 between 1.89–2.07 Ma.

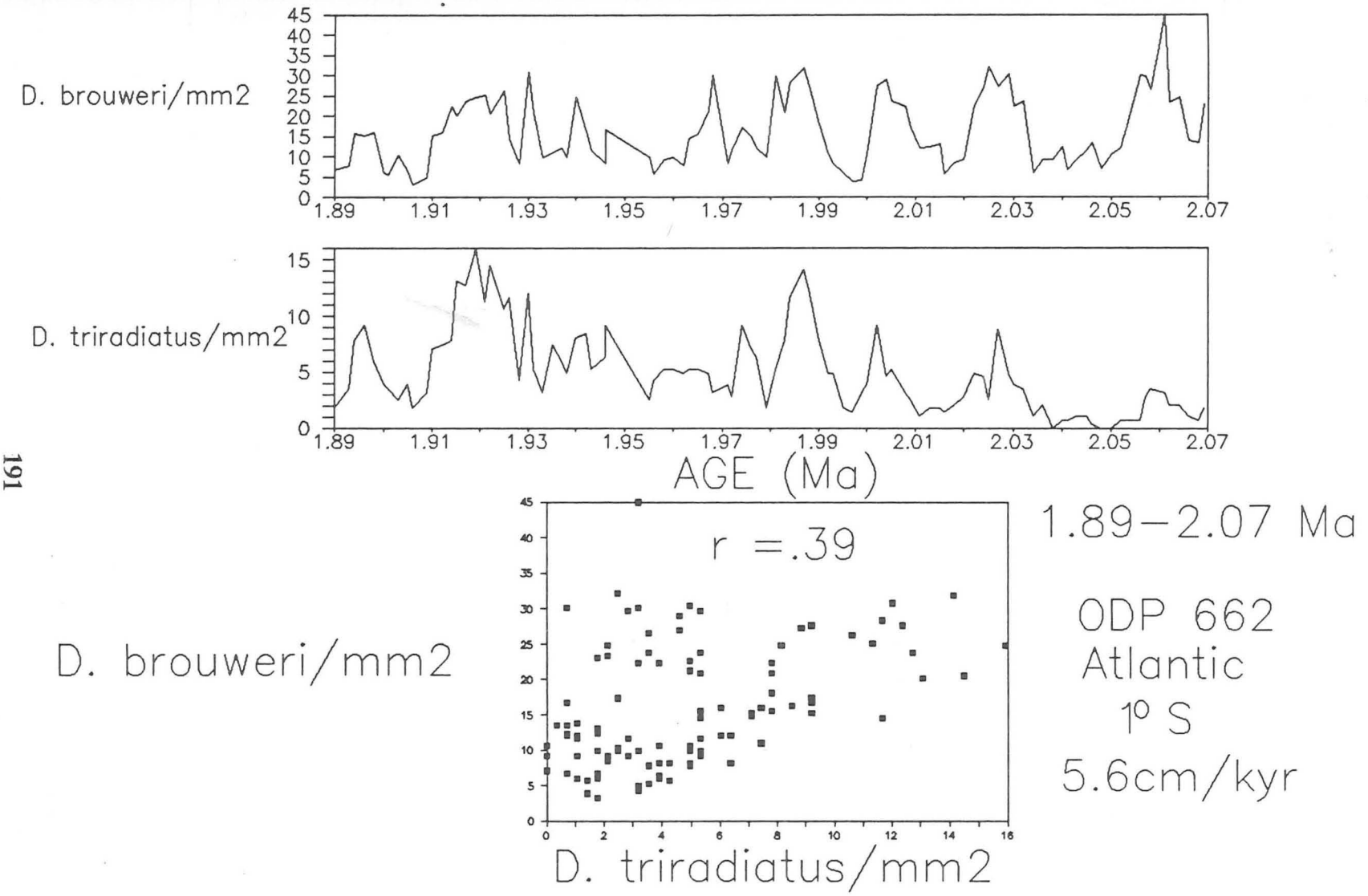

Figure 5:2:1e Abundance of D. brouweri and D. triradiatus/mm2 at Site 662 between 1.89–2.07 Ma.

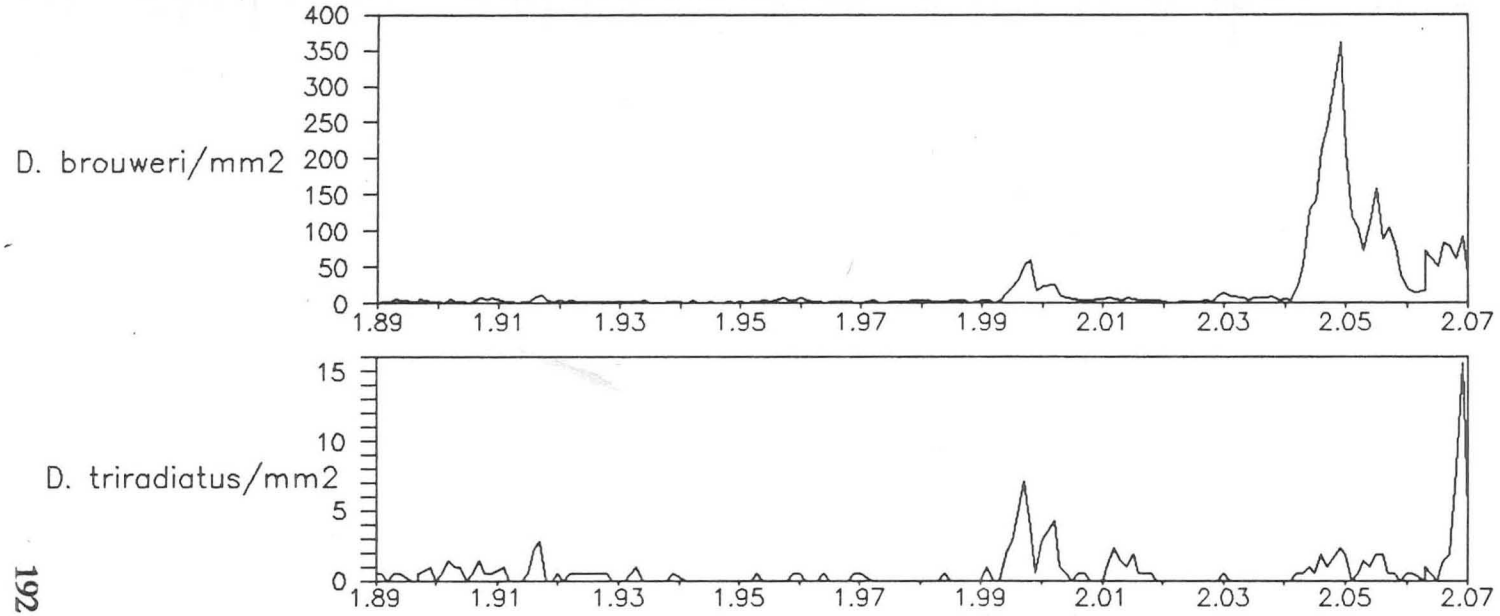

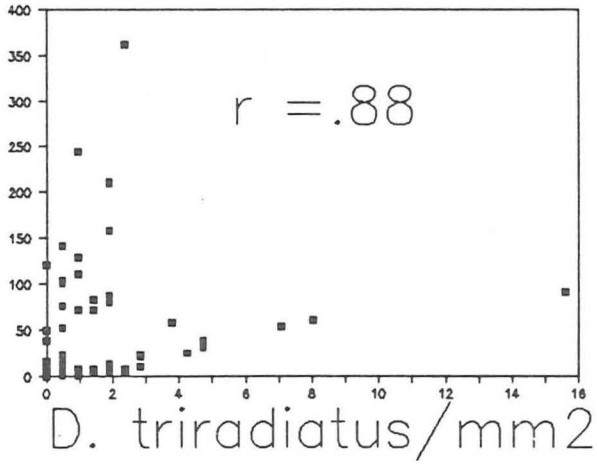

1.89–2.07 Ma

ODP 677
Pacific
1° N
93.4cm/kyr
upwelling
site

Figure 5:2:1f Abundance of D. brouweri and D. triradiatus/mm2 at Site 677 between 1.89–2.07 Ma.

extremely high sedimentation rate through this time interval of 93.4cm/ka and very suppressed abundances. It is the mutually low abundances of D. brouweri and D. triradiatus which give the high positive correlation. There are two short time intervals of increased abundance for both species at approximately 2.00 and 2.05 Ma. The two linear trends are the result of D. triradiatus being more abundant at the lower D. brouweri abundance interval than the distinctive high D. brouweri abundance interval. This is not to be expected.

In the equatorial Indian Ocean at Site 709 (Fig. 5:2:1g), there is a relatively high positive correlation between D. brouweri and D. triradiatus. However, there are subtle differences such as the drop in abundance of D. triradiatus at 2.03 Ma, corresponding with a D. brouweri peak. In addition to this, a distinctive peak of D. triradiatus between 1.91 and 1.92 Ma does not correspond with any noticeable peak in the D. brouweri record. Although the abundances of these two species are very high during this time interval compared to the other sites, this is a low abundance interval at Site 709, preceding the extinction event.

To summarise, the relationship between D. brouweri and D. triradiatus has a high positive correlation regardless of the several orders of magnitude difference between the lowest and highest abundance sites.

5:2:2 Co-variation between D. asymmetricus, D. tamalis and D. brouweri ?

Discoaster brouweri is the only species covering the complete time interval in this

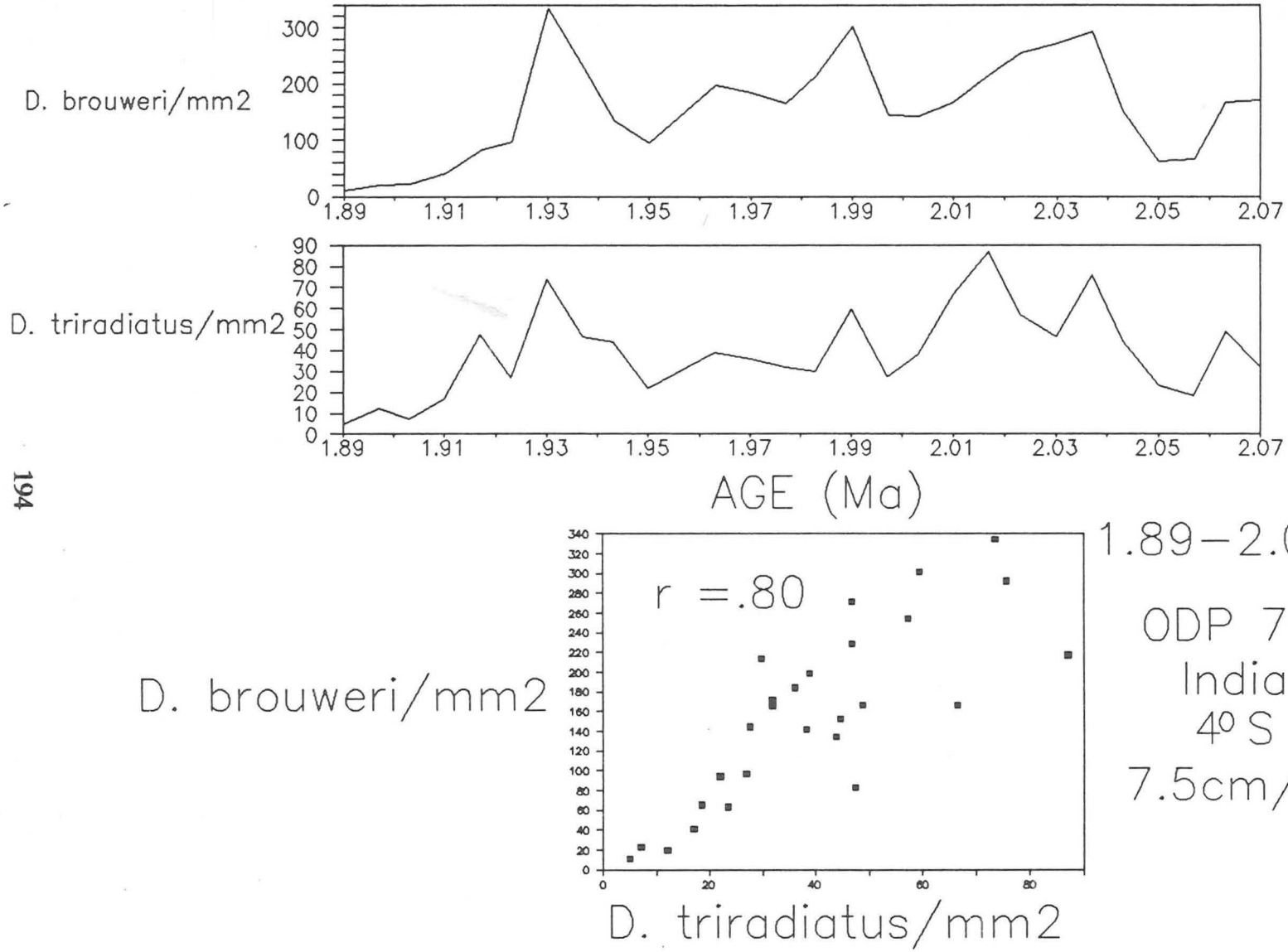

Figure 5:2:1g Abundance of D. brouweri and D. triradiatus/mm2 at Site 709 between 1.89–2.07 Ma.

study as shown in Chapters 2 and 3, and always occurs in much higher abundances than Discoaster asymmetricus and Discoaster tamalis, except at high latitudes. At 2.65 Ma, the LAD of D. tamalis occurs which corresponds coincidentally with an abrupt abundance decline in D. asymmetricus. This is the first piece of evidence that these two species may be related. We examine here the time interval prior to 2.65 Ma (i.e. 2.65 -3.00 Ma) when all the species are present. This is almost twice the time interval being examined before i.e. 350 ka. Only at Site 709 is the time interval extended back beyond 3 Ma to approximately 3.5 Ma. We have already assumed that a very close relationship exists between D. asymmetricus and D. tamalis. The sum of these two species is plotted against the abundance of D. brouweri at all the sites.

In Table 5:1, it is shown that a high positive correlation coefficient exists between D. asymmetricus and D. tamalis at all the sites, but it is very variable between D. brouweri and the sum of D. asymmetricus and D. tamalis away from the high latitudes.

At Site 552 (Fig. 5:2:2a), there may be problems associated with low abundances or temporally coarse sampling, but the correlation coefficients are much higher between these three species than between these species and the other Discoaster species. In the D. tamalis record, abundances are so low that gaps appear, but this is probably an artifact which may be resolved by counting more than 100 view fields. At such a low abundance site, a greater correlation would be expected of D. brouweri with the sum of D. tamalis and D. asymmetricus, than with these two species independently.

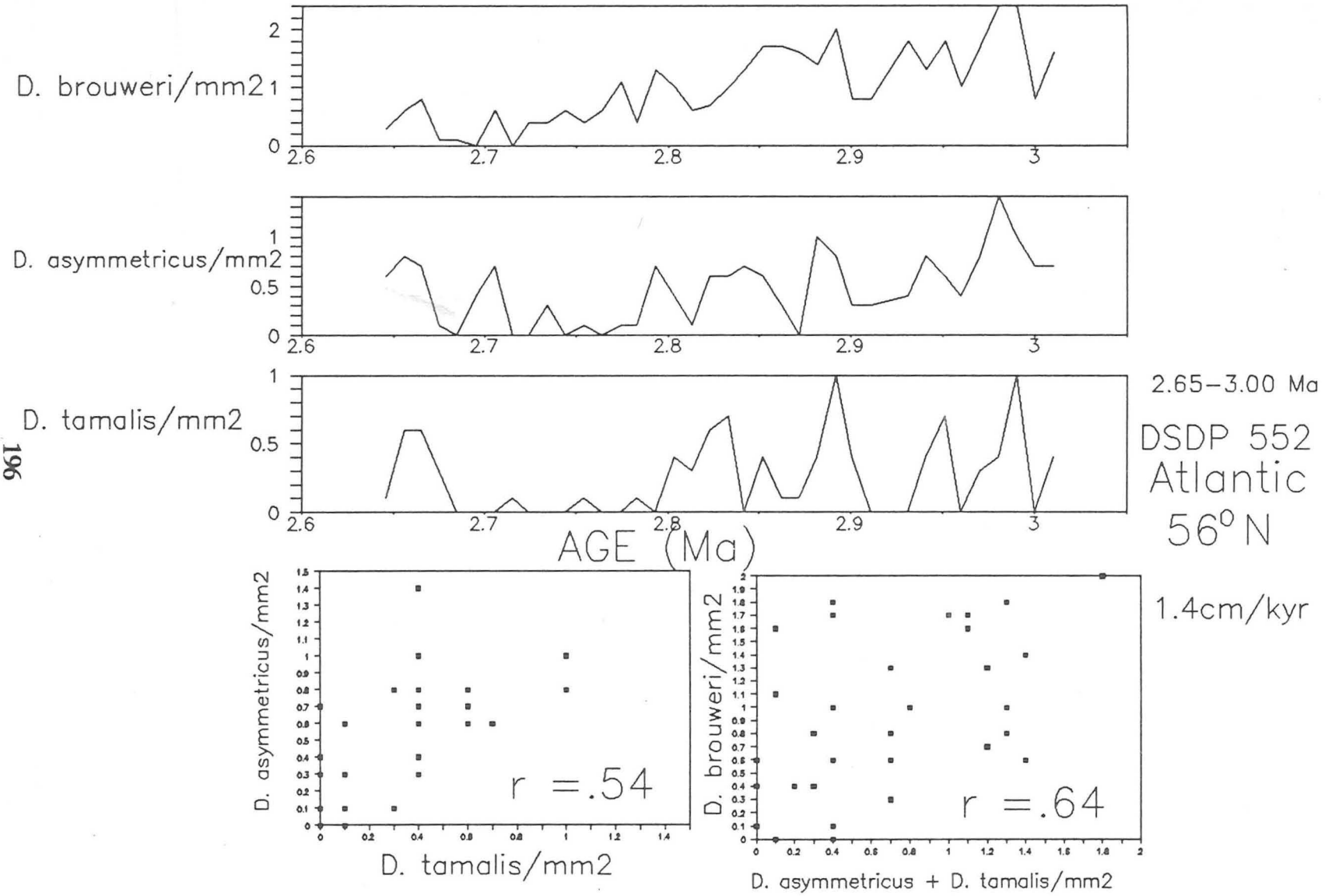

Figure 5:2:2a Abundance of D. brouweri, D. asymmetricus and D. tamalis/mm2 at Site 552 between 2.65–3.00 Ma.

At Site 607 (Fig. 5:2:2b), there is a very high correlation between these three species. It can be argued that at high latitudes, climatic changes induced by orbital forcing such as sea-surface temperature fluctuations are going to be stronger than at low latitudes. However, although D. brouweri, D. asymmetricus and D. tamalis co-vary strongly, there is much less correlation between them and the other species (Table 5:1a).

At the upwelling site, Site 658 (Fig. 5:2:2c), the correlation between D. asymmetricus and D. tamalis is still strong, but it begins to break down between D. brouweri and the sum of D. asymmetricus and D. tamalis. The abundances of all these species are suppressed at this site, but especially D. asymmetricus and D. tamalis. Abundance peaks of D. asymmetricus and D. tamalis correlate with D. brouweri abundance peaks, but not the main abundance peaks. These two species are frequently produced in lower abundances during the higher D. brouweri abundance intervals. It appears that since D. asymmetricus and D. tamalis correlate with the minor D. brouweri peaks, their ecological ranges overlap, but this is during sub-optimum conditions for D. brouweri, if they were thought to be separate species.

At Site 659 (Fig. 5:2:2d), the non-upwelling site in relative close proximity to Site 658, there is similarly a strong correlation coefficient for the relationship between D. asymmetricus and D. tamalis. However, from the correlation coefficient for the relationship between D. brouweri and the sum of D. asymmetricus and D. tamalis, one would believe there to be no relationship. From the records for the three species, there is clearly a high correlation. D.

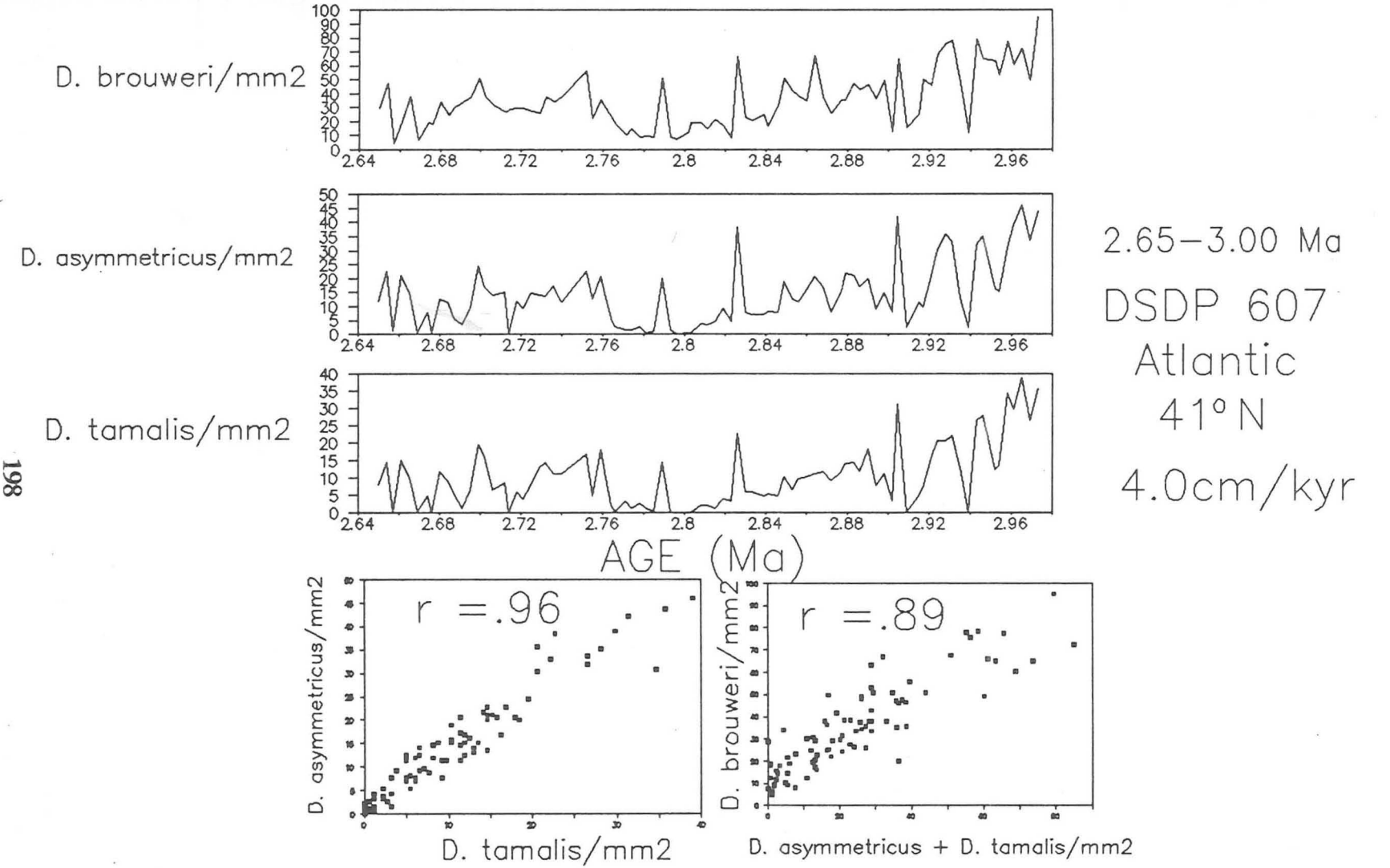

Figure 5:2:2b Abundance of D. brouweri, D. asymmetricus and D. tamalis/mm2 at Site 607 between 2.65–3.00 Ma.

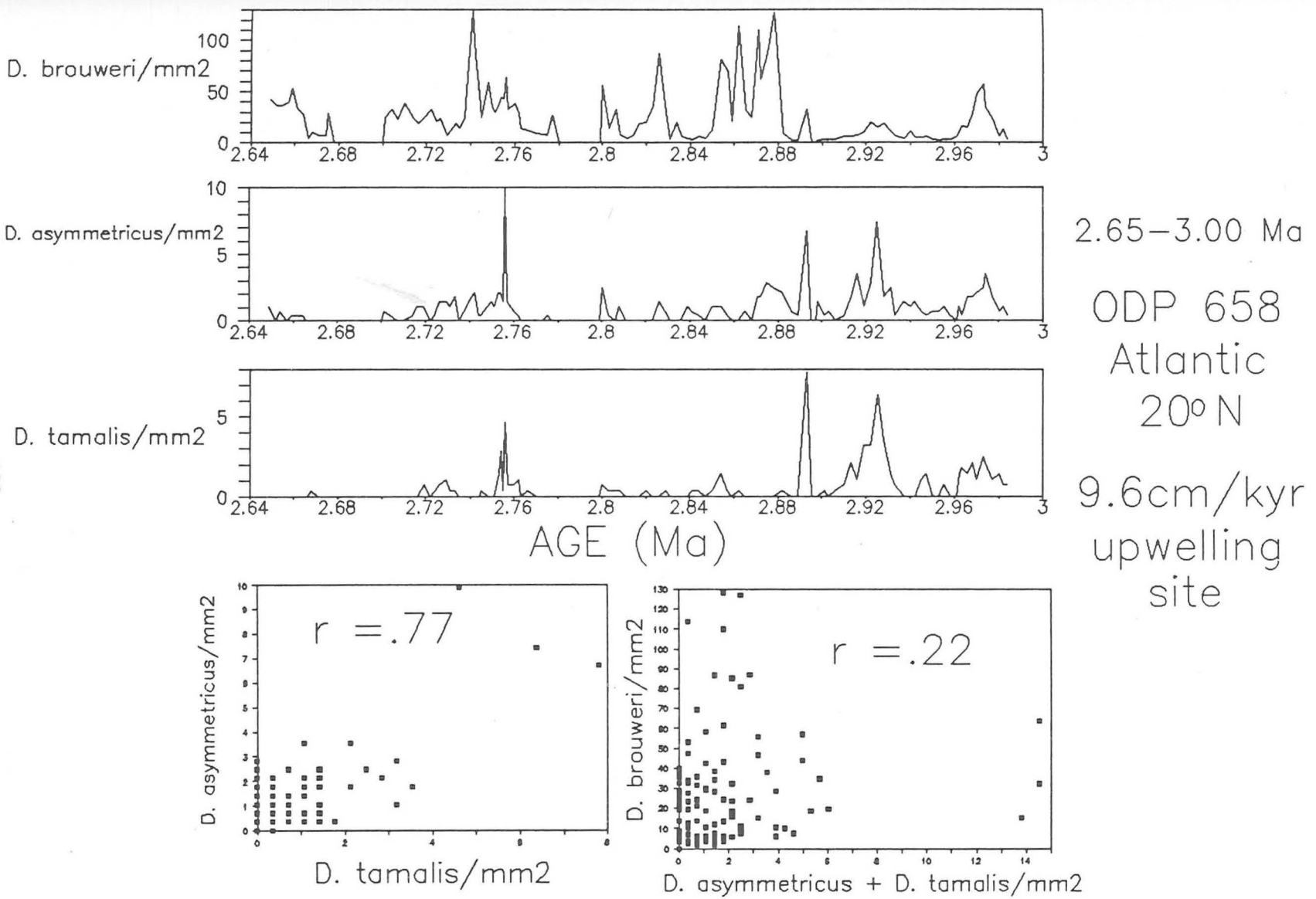

Figure 5:2:2c Abundance of D. brouweri, D. asymmetricus and D. tamalis/mm2 at Site 658 between 2.65–3.00 Ma.

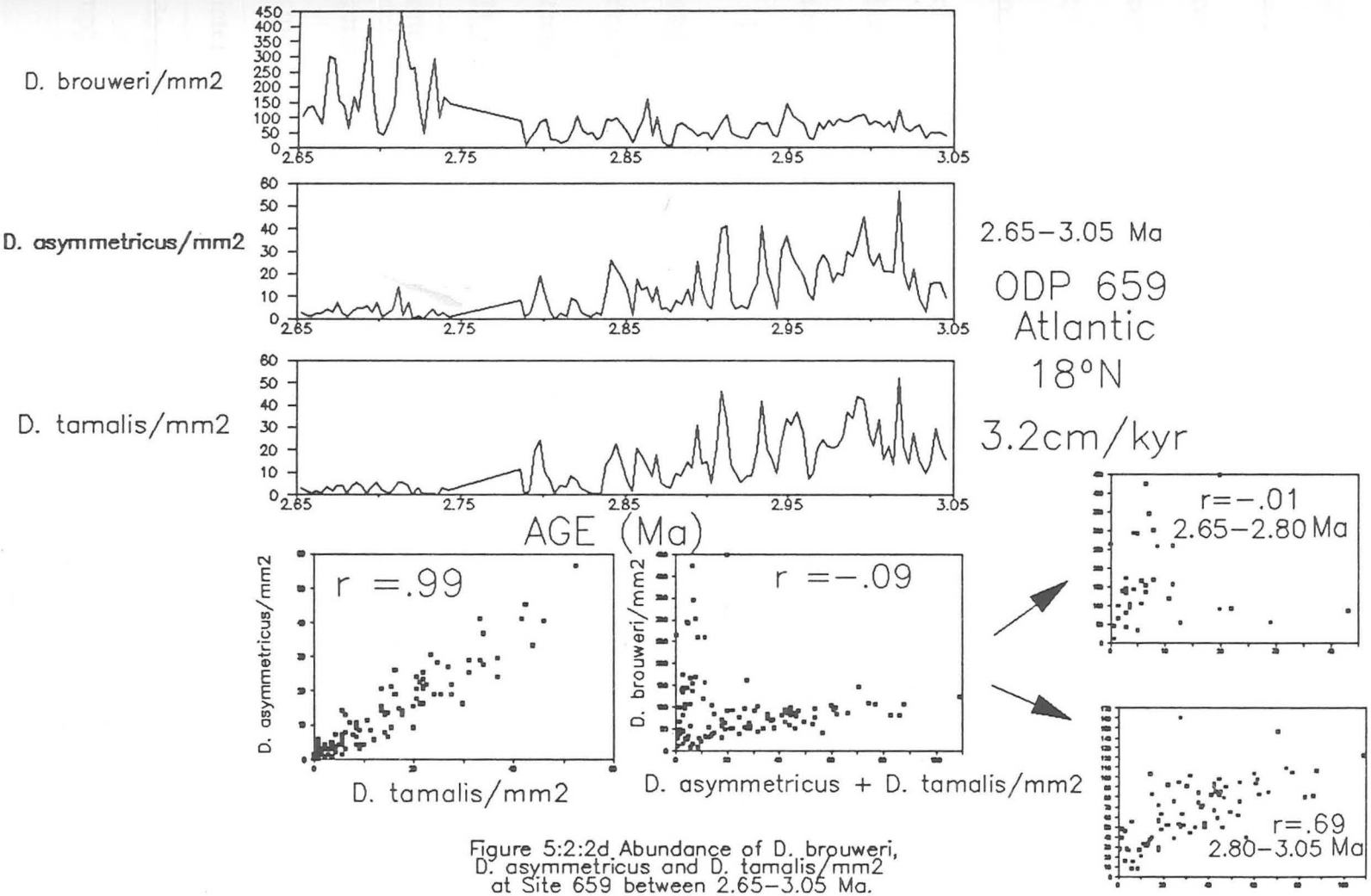

Figure 5:2:2d Abundance of D. brouweri, D. asymmetricus and D. tamalis/mm2 at Site 659 between 2.65–3.05 Ma.

brouweri abundance increases through time, whereas D. asymmetericus and D. tamalis show the opposite trend. In the time interval 2.65-2.74 Ma, minor abundances of D. asymmetricus and D. tamalis approximately correlate with high abundance peaks of D. brouweri. This is the upper linear trend in the scatter diagram. However, in the time interval 2.80-3.05 Ma, with a correlation coefficient of 0.69, the higher D. asymmetricus and D. tamalis abundance peaks correlate well with the less major abundance peaks of D. brouweri. This linear trend is clearly shown in the lower part of the scatter diagram. Minor abundance peaks of D. asymmetricus and D. tamalis correlating with high abundance peaks of D. brouweri and vice versa was similarly shown at Site 658. This example indicates that scatter diagrams and correlation coefficients must not be taken at face value, but can be an aid to interpretation.

In the equatorial Atlantic at Site 662 (Fig. 5:2:2e), the relationship between D. asymmetricus and D. tamalis is still very strong, but appears to have broken down further between the sum of these species and D. brouweri. All three records indicate a decline in abundance towards 2.65 Ma. D. asymmetricus and D. tamalis are more suppressed and D. brouweri has increased in this time interval when compared with Site 659. As shown at Sites 658 and 659, there is a general correlation between the records of the three species, which produces the confusing two linear relationships in the scatter diagram. For most of the time interval 2.65-2.90 Ma, the peaks of D. asymmetricus and D. tamalis, though low, do correlate with the much higher D. brouweri abundance peaks, which is the upper linear trend. Subtle increases of D. asymmetricus are noticeable during low

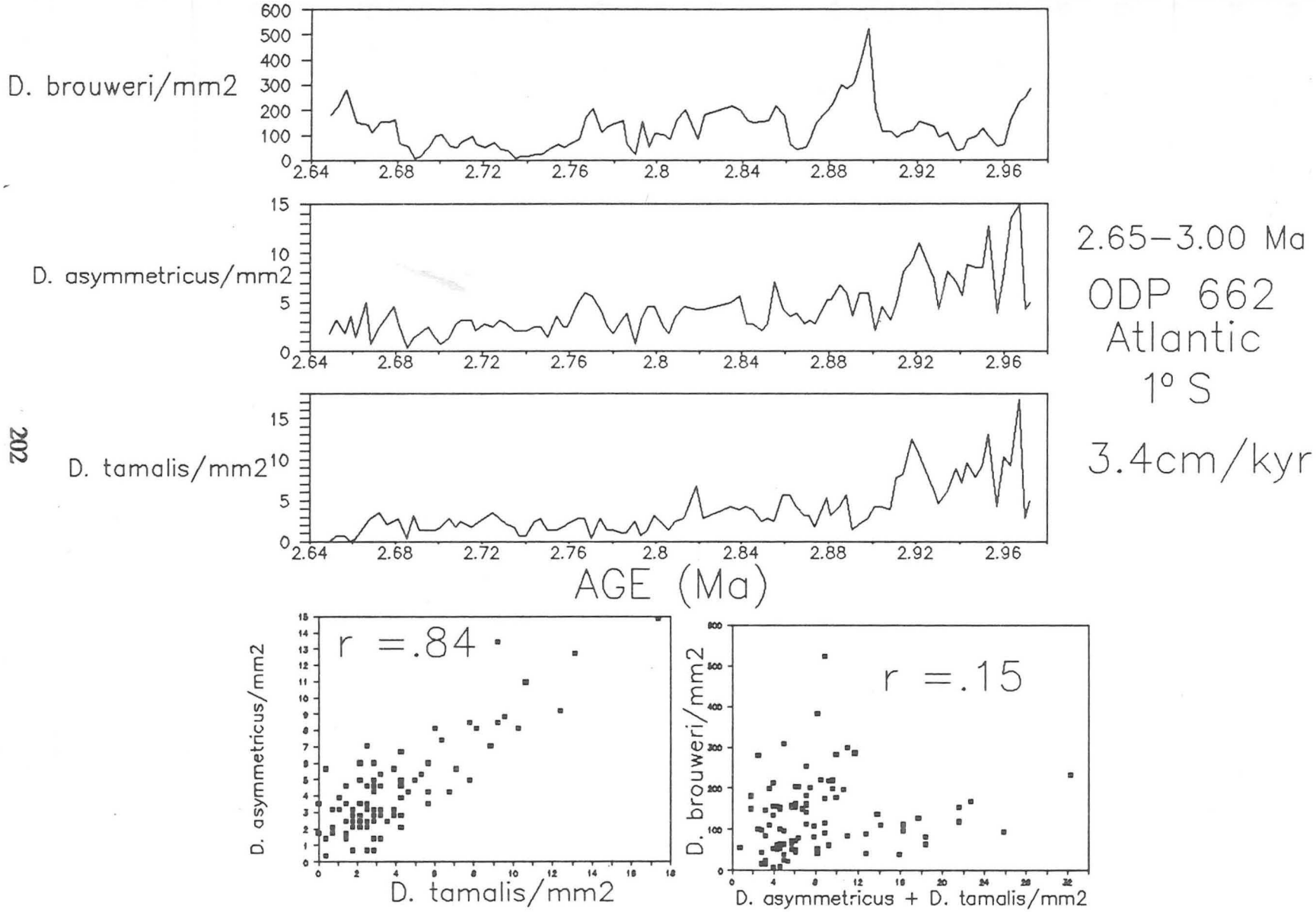

Figure 5:2:e Abundance of D. brouweri, D. asymmetricus and D. tamalis/mm2 at Site 662 between 2.65–3.00 Ma.

abundance intervals of D. brouweri at e.g. 2.74 and 2.80 Ma. Reworking of D. asymmetricus and D. tamalis through this interval would be undetectable from comparing each other since they occur in such similar abundances. The most noticeable interval of higher abundances of D. asymmetricus and D. tamalis corresponding with low abundances of D. brouweri is prior to 2.90 Ma, though the peaks can still be crudely correlated. This is the lower linear trend on the scatter diagram. It is suspicious that only during this low abundance D. brouweri interval that D. asymmetricus and D. tamalis significantly increase but not in later intervals. Are the abundances of D. asymmetricus and D. tamalis a reworking trickle after 2.90 Ma or are they suppressed because of warmer waters associated with equatorial divergence ?

At Site 677 (Fig. 5:2:2f), the upwelling site in the Pacific Ocean, a strong correlation exists between D. asymmetricus and D. tamalis, though this may be enhanced by the long intervals of suppressed abundance. However, once again, the correlation breaks down between D. brouweri and the sum of D. asymmetricus and D. tamalis. D. asymmetricus and D. tamalis occur in supressed abundances at upwelling sites as shown in Chapters 2 & 3. Increases in these two species at this major upwelling site are noticeable in low abundance intervals of D. brouweri. There are exceptions though such as at approximately 2.80 and 2.86 Ma, when all three species are suppressed possibly by intervals of intensive upwelling. There is limited correlation between the D. brouweri abundance peaks and the abundance peaks of D. asymmetricus and D. tamalis, though a few peaks such as at 2.71 Ma clearly correlate well. At Site 677, variations in the intensity

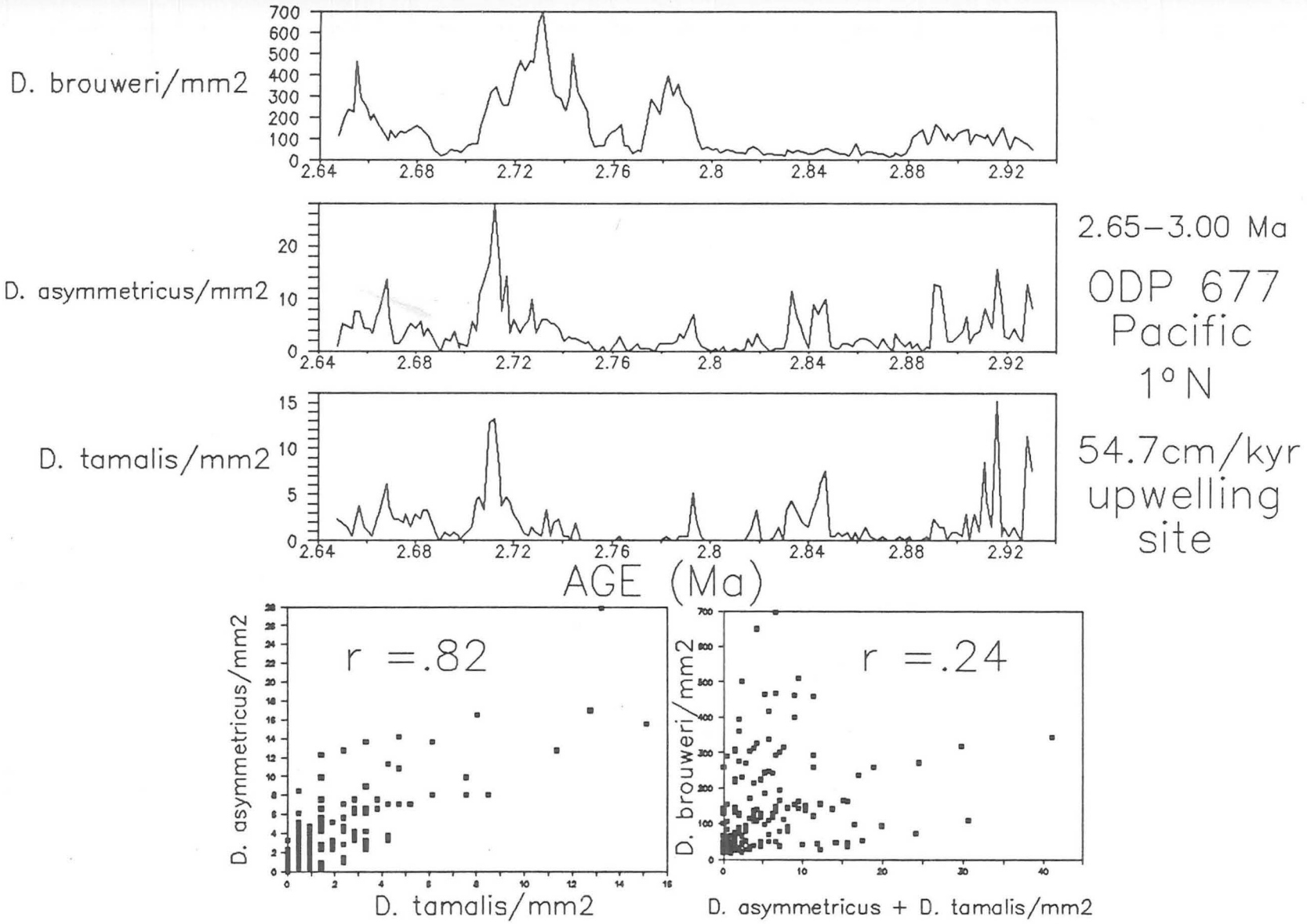

Figure 5:2:2f Abundance of D. brouweri, D. asymmetricus and D. tamalis/mm2 at Site 677 between 2.65–3.00 Ma

of upwelling may impose conditions favouring D. brouweri, or D. asymmetricus and D. tamalis (associated with a low stock of D. brouweri) or none of these species at different times. We will consider the range of these conditions later on and how fixed are the ecological requirements for a Discoaster species globally and through time?

In the Indian Ocean at Site 709 (Fig. 5:2:2g), there is a reasonable correlation between D. asymmetricus and D. tamalis, and a fairly low, but perhaps significant negative correlation between the sum of these species and D. brouweri. This site in the Indian Ocean overshadows all the others for favouring the production of D. brouweri. It is very apparent that there is an increase in abundance of D. brouweri through time, whereas D. tamalis, but especially D. asymmetricus decrease towards 2.65 Ma. If one assumes that this site represents close to optimum ecological conditions for D. brouweri, D. asymmetricus and D. tamalis generally increase during troughs and low peak abundances of D. brouweri, and not during high abundance intervals. D. asymmetricus and D. tamalis only form a minor fraction of the total Discoaster assemblage at this site (see Chapter 3). A noticeable inconsistency is an event at approximately 3.1 Ma, which suppresses all three species, when D. asymmetricus and D. tamalis would be thought to increase.

In conclusion, D. asymmetricus and D. tamalis demonstrate a strong 1:1 relationship regardless of different environmental conditions. Their relationship with D. brouweri decreases away from high latitudes, since D. asymmetricus and D. tamalis favour cooler, low productivity waters. Peaks can nevertheless be

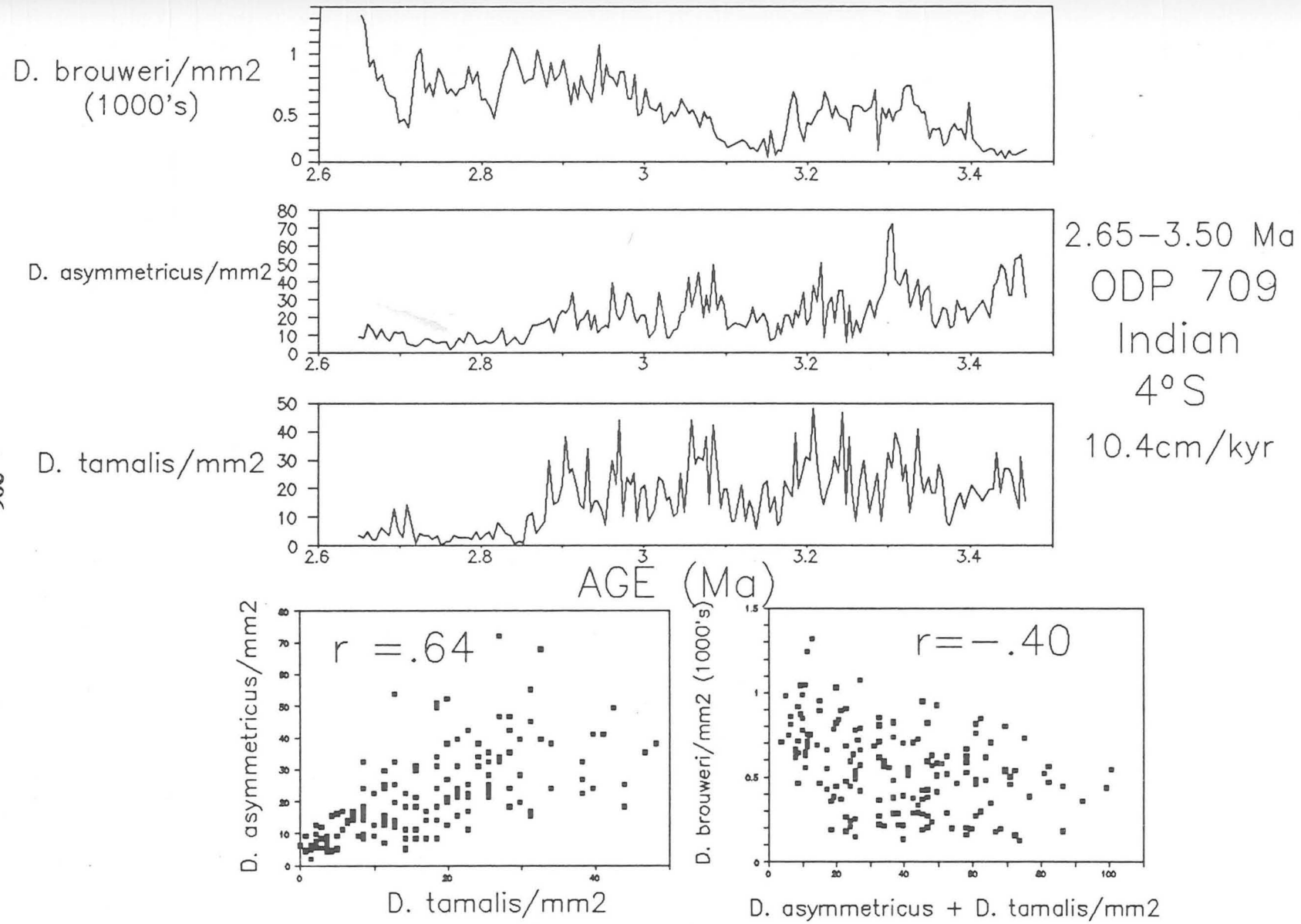

Figure 5:2:2g Abundance of D. brouweri, D. asymmetricus and D. tamalis/mm2 at Site 709 between 2.65–3.50 Ma.

matched up, since the same organism probably produced these three morphospecies, but never producing more than one pair of D. asymmetricus and D. tamalis for a single D. brouweri.

5:2:3 Relationships between D. pentaradiatus and D. brouweri or with the sum of D. asymmetricus and D. tamalis ("D. asyta") ?

In the previous section, we showed there to be a strong relationship globally between D. asymmetricus and D. tamalis independent of differences in latitude or upwelling versus non-upwelling conditions. From here on, we shall treat the sum of these two species as effectively "one species" and refer to it in this chapter as "Discoaster asyta". A strong relationship does exist between D. brouweri and "D. asyta" at high latitudes, but at lower latitudes and in upwelling conditions, it is apparent that they favour different ecological conditions, though their ranges overlap. We shall continue treating these as different species, though the assumption is that the plankton species producing low abundances of D. brouweri under sub-optimal conditions switches to favouring the production of "D. asyta" and vice versa, since the abundance peaks can be so easily matched up. Here, we now examine the same time interval i.e. prior to 2.65 Ma, and compare the relationship of D. pentaradiatus with D. brouweri, and D. pentaradiatus with "D. asyta".

At Site 552 (Fig. 5:2:3a), the highest latitude site, there is no visible relationship between D. pentaradiatus and D. brouweri. A very minor negative relationship

may be inferred between D. pentaradiatus and "D. asyta", since the major peak in the D. pentaradiatus record at approximately 2.75 Ma occurs during a major trough of "D. asyta". A record with higher time resolution may resolve if there is any genuine negative relationship. D. pentaradiatus does not show the gradual decline in abundance as shown in D. brouweri and "D. asyta".

At Site 607 (Fig. 5:2:3b), also a high latitude site (41°N), with a good time resolution, stronger correlations are produced between D. pentaradiatus and D. brouweri, and D. pentaradiatus and "D. asyta". These are much lower, however, than between D. asymmetricus and D. tamalis, or D. brouweri with "D. asyta" at this site. Nevertheless, climatic forcing is stronger at higher latitudes, and many peaks correlate well with all "3" species e.g. at approximately 2.82 and 2.90 Ma. However, major inconsistencies include high abundances of D. pentaradiatus at approximately 2.72 and 2.80 Ma corresponding with troughs in the records of D. brouweri and "D. asyta". As seen at Site 552, these troughs are especially clear in the "D. asyta" record. A decline in abundance through time is not apparent in the D. pentaradiatus record in this interval.

At Site 658 (Fig. 5:2:3c), with a high time resolution, there is little correlation between D. pentaradiatus and D. brouweri. D. pentaradiatus favours intervals of low D. brouweri abundance. The correlation between D. pentaradiatus and "D. asyta" may seem higher, but this is largely influenced by the mutually low abundances. It can be observed at e.g. 2.92 Ma, that "D. asyta" increases in lower abundance intervals of both D. brouweri and D. pentaradiatus. There is a subtle interplay between these "three" species. Some rare events, however, are important

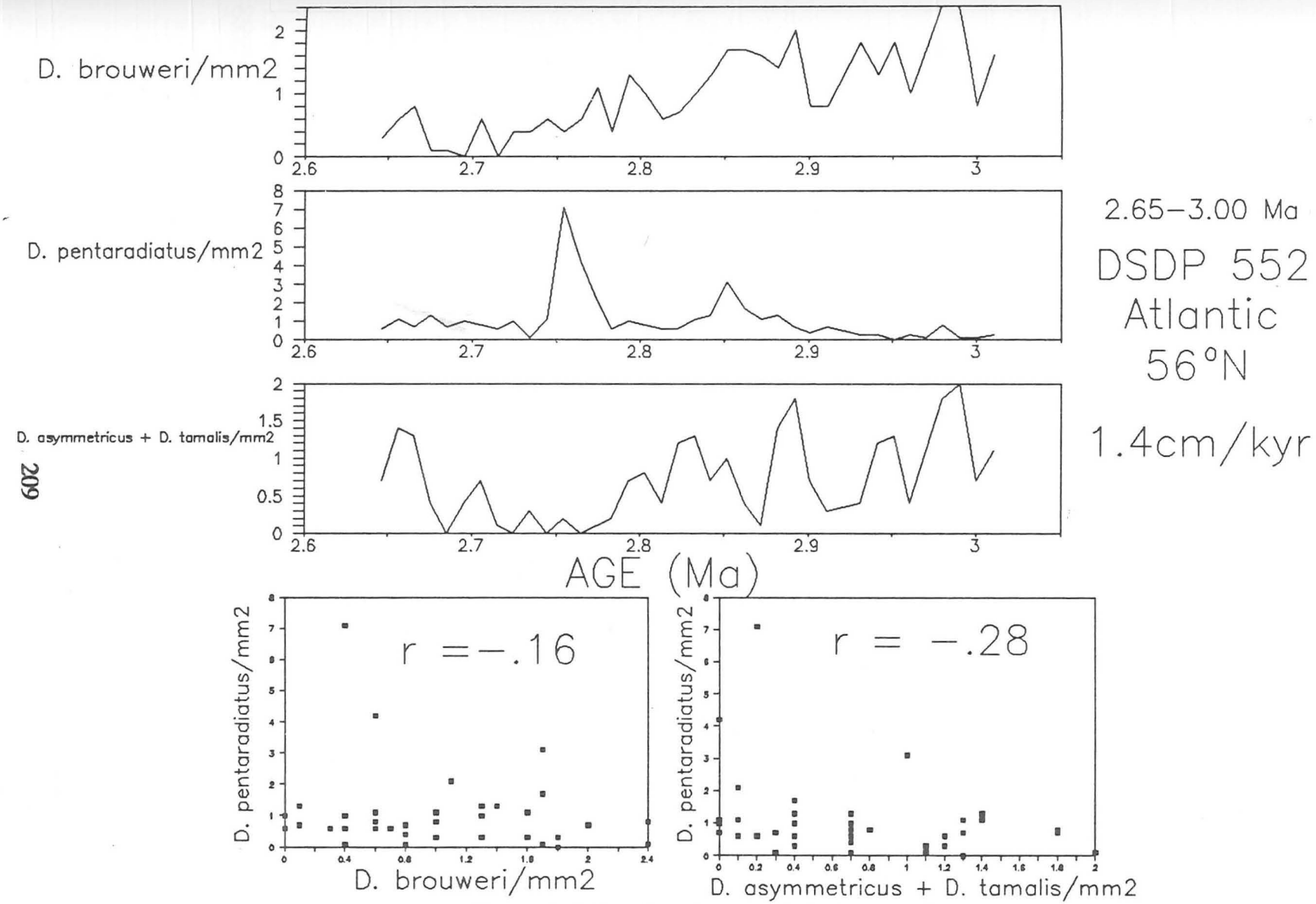

Figure 5:2:3a Abundance of D. brouweri, D. pentaradiatus and the sum of D. asymmetricus and D. tamalis/mm2 at Site 552 between 2.65–3.00 Ma

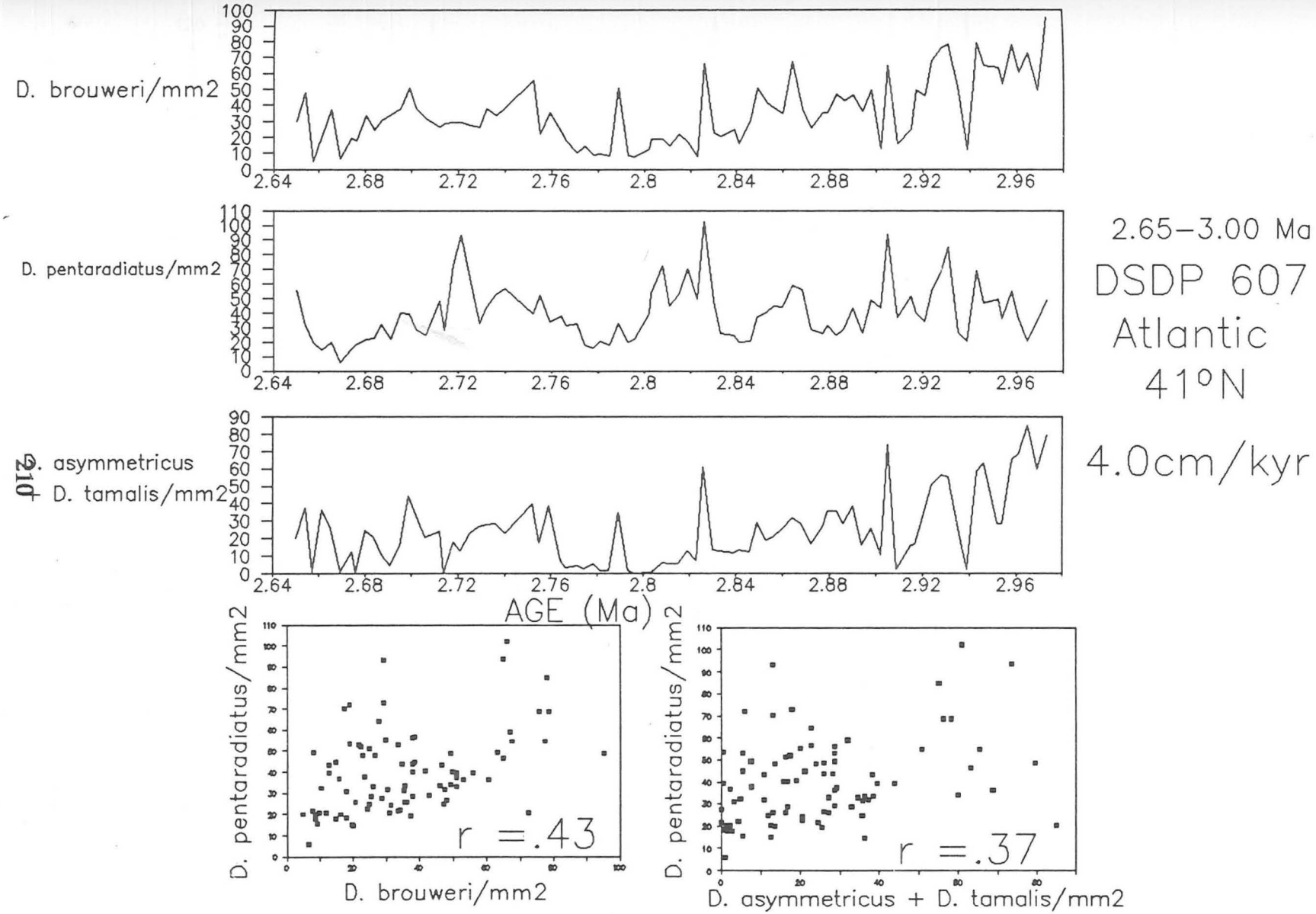

Figure 5:2:3b Abundance of D. brouweri, D. pentaradiatus and the sum of D. asymmetricus and D. tamalis/mm2 at Site 607 between 2.65–3.00 Ma.

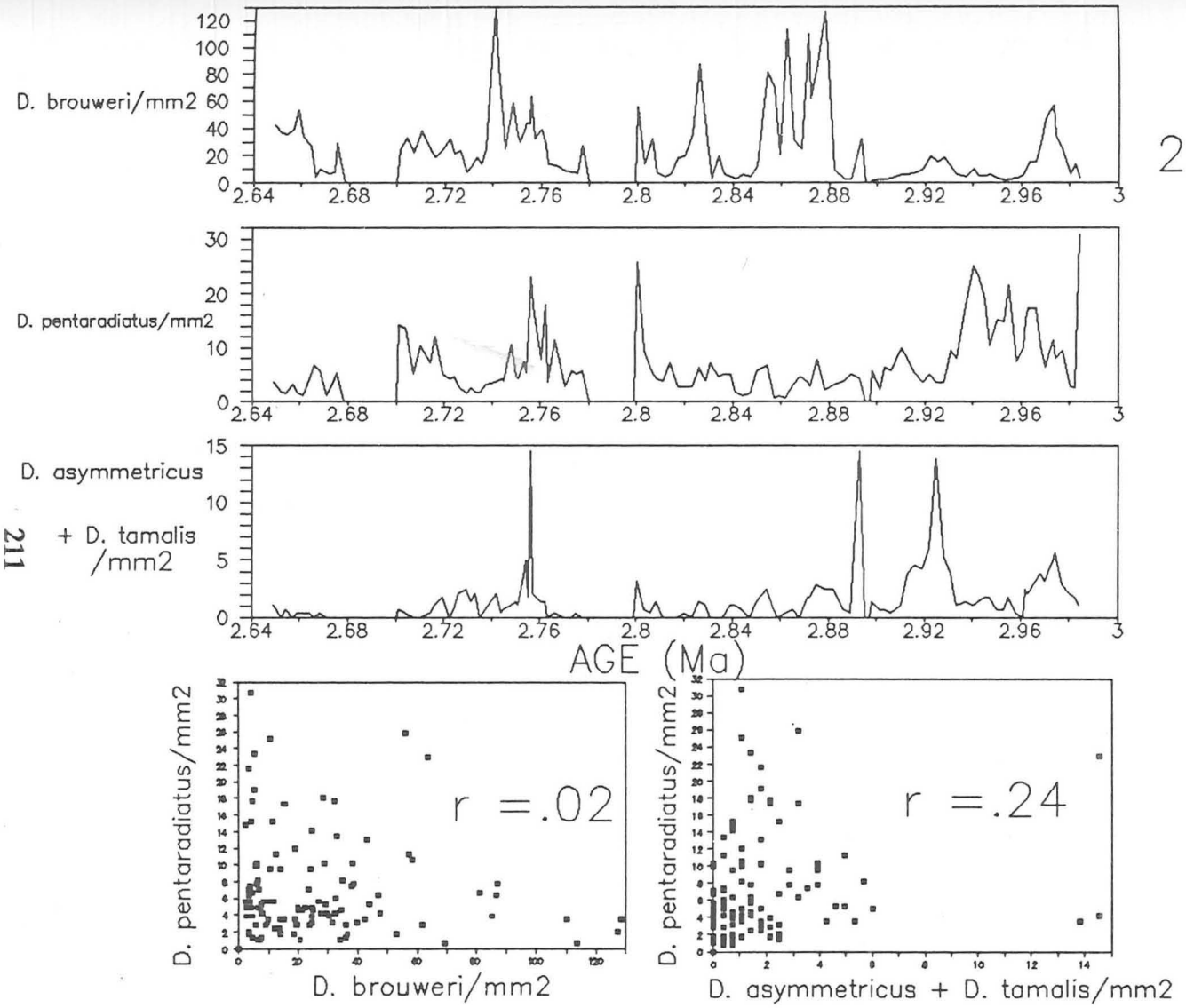

2.65–3.00 Ma

ODP 658
Atlantic
20°N

9.6cm/kyr
upwelling
site

Figure 5:2:3c Abundance of D. brouweri, D. pentaradiatus and the sum of D. asymmetricus and D. tamalis/mm2 at Site 658 between 2.65–3.00 Ma.

enough to favour all "three" species e.g. at approximately 2.76 Ma. Upwelling sites do not favour the production of discoasters in the first place, and all these species are suppressed.

In close proximity, Site 659 (Fig. 5:2:3d), the correlation coefficients reveal little information concerning the interplay between the "three" species, favouring different ecological conditions. D. pentaradiatus favours intervals of lower D. brouweri abundance. An inverse relationship between the abundance of these species can be observed in the time interval 2.65-2.90 Ma. Prior to 2.90 Ma, D. pentaradiatus shows some strong co-variation with D. brouweri, especially between approximately 2.90-2.95 Ma. However, increases in the D. pentaradiatus abundance peaks are matched by decreases in the D. brouweri abundance peaks. There is more correlation between D. pentaradiatus and "D. asyta". In the same interval of approximately 2.90-2.95 Ma, there is strong correlation in the abundance peaks, but increases in "D. asyta" abundance peaks are accompanied by decreases in the D. pentaradiatus abundance peaks. Between 2.65-2.90 Ma and 2.95-3.05 Ma, "D. asyta" generally favours average abundance intervals of D. pentaradiatus, especially if this is coupled with lower abundance intervals of D. brouweri, e.g. prior to 2.95 Ma.

At Site 662 (Fig. 5:2:3e), close to the equator, there are surprisingly higher correlation coefficients than expected, especially for the relationship between D. pentaradiatus and "D. asyta". Even the correlation coefficient between D. pentaradiatus and D. brouweri is much higher than was found between D. brouweri and "D. asyta". We know that this site is affected by reworking as

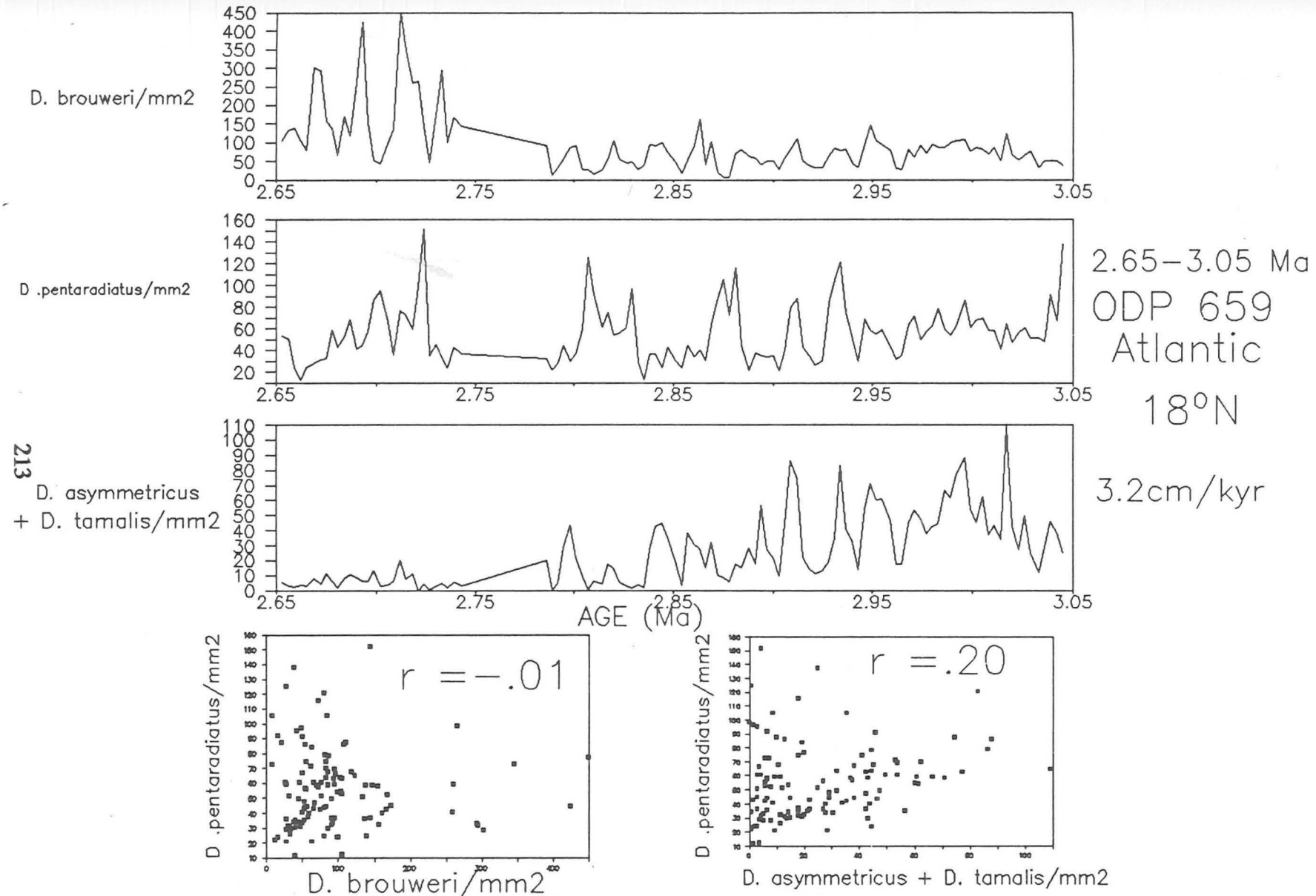

Figure 5:2:3d Abundance of D. brouweri, D. pentaradiatus and the sum of D. asymmetricus and D. tamalis/mm2 at Site 659 between 2.65–3.05 Ma.

shown by the relatively high abundances of D. pentaradiatus beyond its extinction event (see Chapter 2 , Fig. 2:4:2a). The broad correlation between peaks may have little to do with reworking events, but this site lacks the defined ecological relationships as seen in the other Atlantic sites. The record for D. pentaradiatus in this interval shows a similar declining trend in abundance through time as seen clearly in the records of D. brouweri and "D. asyta". Is it possible that at this site ecological conditions were such that D. pentaradiatus had to co-exist generally in the same intervals as D. brouweri and "D. asyta"? Comparison with D. surculus later on may shed more light on this.

At Site 677 (Fig. 5:2:3f), in the Equatorial Pacific, one cannot make genuine correlations, because it is difficult to assess if the suppressed abundances of D. pentaradiatus after 2.88 Ma are real or a background reworking level. This is the only site where this phenomenon is observed and probably is related to the intensity of upwelling. It is interesting to note that a major suppression of D. brouweri and "D. asyta" also occurs at approximately the same time. Though there is only a short interval of D. pentaradiatus, prior to 2.88 Ma to be examined, a familiar phenomenon is observed. This occurs during a D. brouweri low abundance interval, when "D. asyta" is on the increase. There is generally an inverse relationship between the abundance of D. pentaradiatus and "D. asyta", as shown clearly by the highest abundance peak of D. pentaradiatus corresponding with a trough in the "D. asyta" record.

At Site 709 (Fig. 5:2:3g), in the equatorial Indian Ocean, D. pentaradiatus shows a low negative correlation with D. brouweri and an inverse abundance

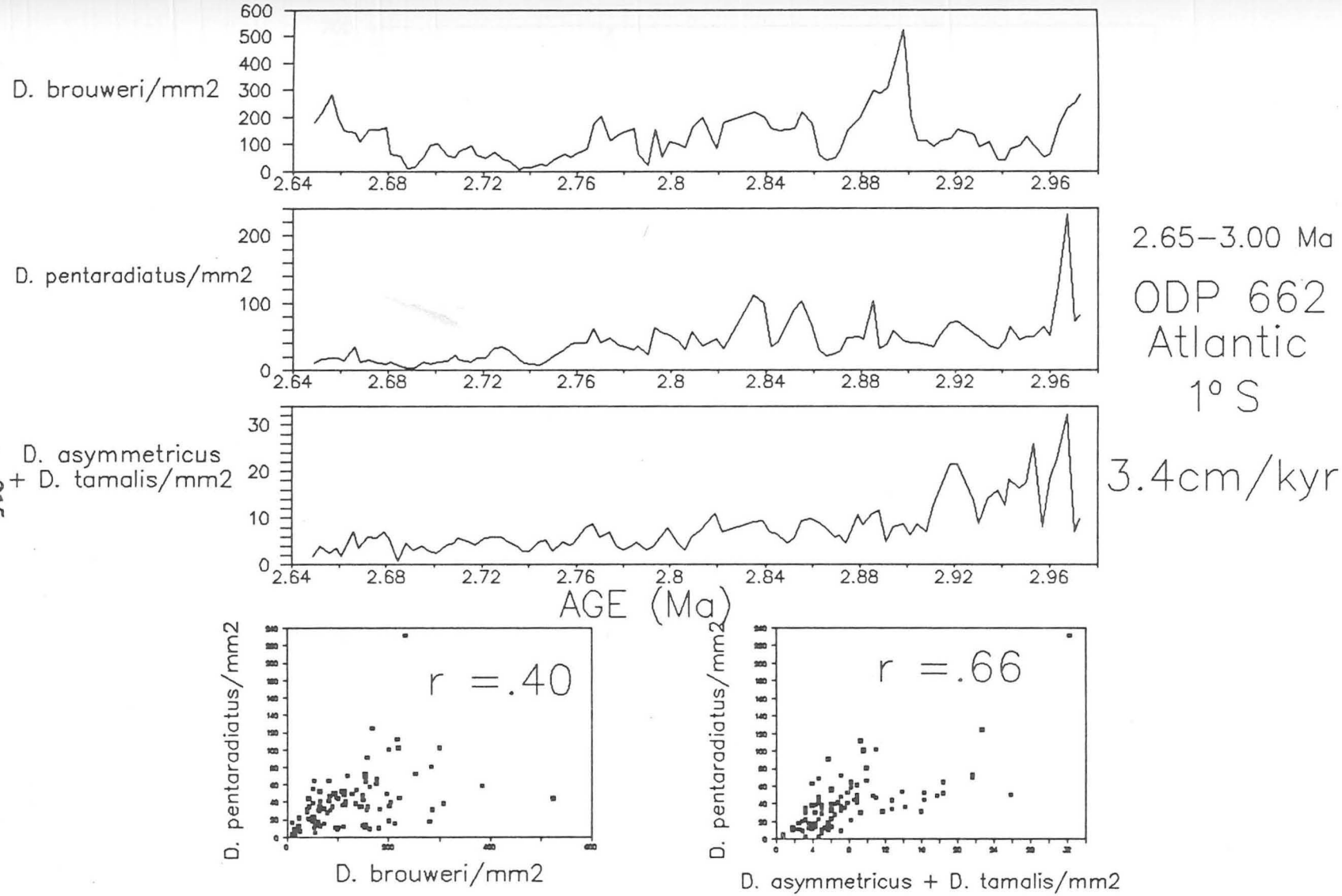

Figure 5:2:3e Abundance of D. brouweri, D. pentargdiatus and the sum of D. asymmetricus and D. tamalis/mm2 at Site 662 between 2.65–3.05 Ma.

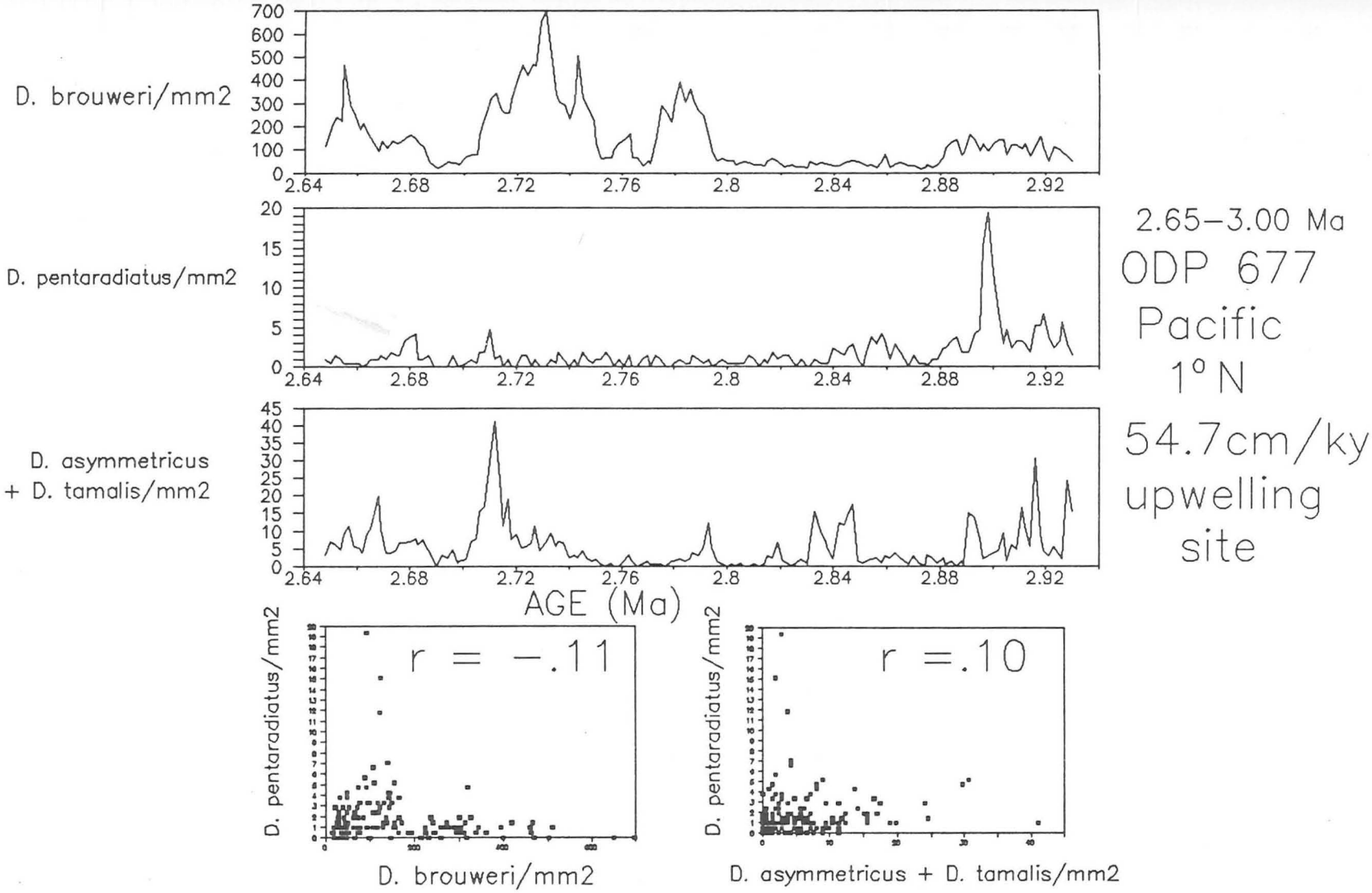

Figure 5:2:3f Abundance of D. brouweri, D. pentaradiatus and the sum of D. asymmetricus and D. tamalis/mm2 at Site 677 between 2.65–3.00 Ma.

relationship is very apparent. Upon this is superimposed a gradual decline in abundance of D. pentaradiatus through time, which is less steep than the increase of D. brouweri abundance through time. The largest abundances of D. pentaradiatus coincide with the lowest abundances of D. brouweri at approximately 3.1 and 3.4 Ma. There is a low positive correlation between D. pentaradiatus and "D. asyta", which both decline through time. The relationship between D. pentaradiatus and "D. asyta" cannot be considered independently of D. brouweri. Both D. pentaradiatus and D. brouweri occur in so much larger abundances than the other sites, that it is generally only when one or both these species shows any major reduction that "D. asyta" increases e.g. at approximately 3.2 and 3.3 Ma.

D. pentaradiatus appears to favour a wider temperature range than "D. asyta", but both prefer areas of modest productivity.

5:2:4 Relationships between D. surculus and D. brouweri or with the sum of D. asymmetricus and D. tamalis ("D. asyta")?

In this section, using the same time interval as before, we now examine the relationship with D. surculus.

At Site 552 (Fig. 5:2:4a), at 56°N in the North Atlantic there is a very minor negative correlation between D. surculus and D. brouweri. Although the abundances are very suppressed for both species and the time resolution is low, there may be an inverse abundance relationship, especially noticeable between 2.9

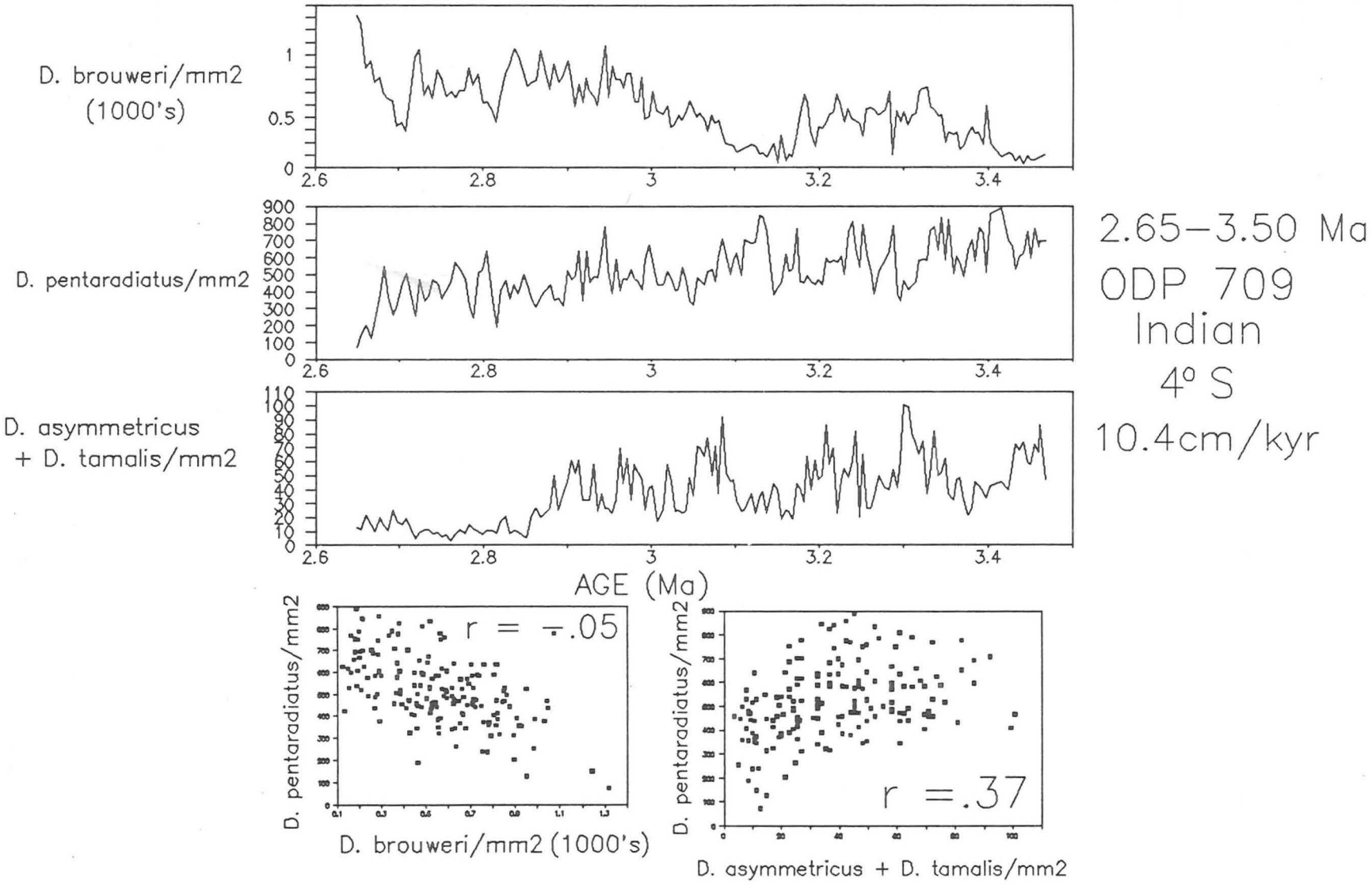

Figure 5:2:3g Abundance of D. brouweri,
D. pentaradiatus and the sum of D. asymmetricus
and D. tamalis/mm2 at Site 709 between 2.65–3.50 Ma.

and 3.0 Ma. D. surculus shows no trend of abundance decline with time. However, D. surculus does show a low positive correlation with "D. asyta". There may be some crude correlation between the abundance peaks at e.g. 2.65, 2.80, 2.95 and 2.98 Ma, but these also correlate with D. brouweri. Basically, there are less inverse abundance relationships than with D. brouweri. This correlation is too low to be significant, though "D. asyta" and D. surculus overlap in their preference for cooler waters.

At Site 607 (Fig. 5:2:4b), there would appear to be a low positive correlation between D. surculus and D. brouweri. One must consider the relationship between D. pentaradiatus and D. brouweri concurrently to compare the differences. It soon becomes apparent that D. surculus displays frequently an inverse abundance relationship with D. brouweri. This applies also with the relationship of D. surculus with "D. asyta" to a greater extent. The strong correlation peaks between D. pentaradiatus, D. brouweri and "D. asyta" at approximately 2.70, 2.82, 2.90 and 2.93 Ma coincide with abundance troughs in the D. surculus record. Nevertheless, there are some peaks and troughs correlating between D. surculus, D. pentaradiatus, D. brouweri and "D. asyta" at approximately 2.75, 2.79 and 2.87 Ma. These occur generally during less defined lower D. pentaradiatus peak abundances. The record of D. surculus does not demonstrate any clear trend of abundance decline, which is a possible indicator that it was not responding to the drop in sea-surface temperatures heralding the approach of northern hemisphere glaciation. However, in the time interval 2.76-2.84 Ma, when D. surculus demonstrates a minor trend of increasing abundance

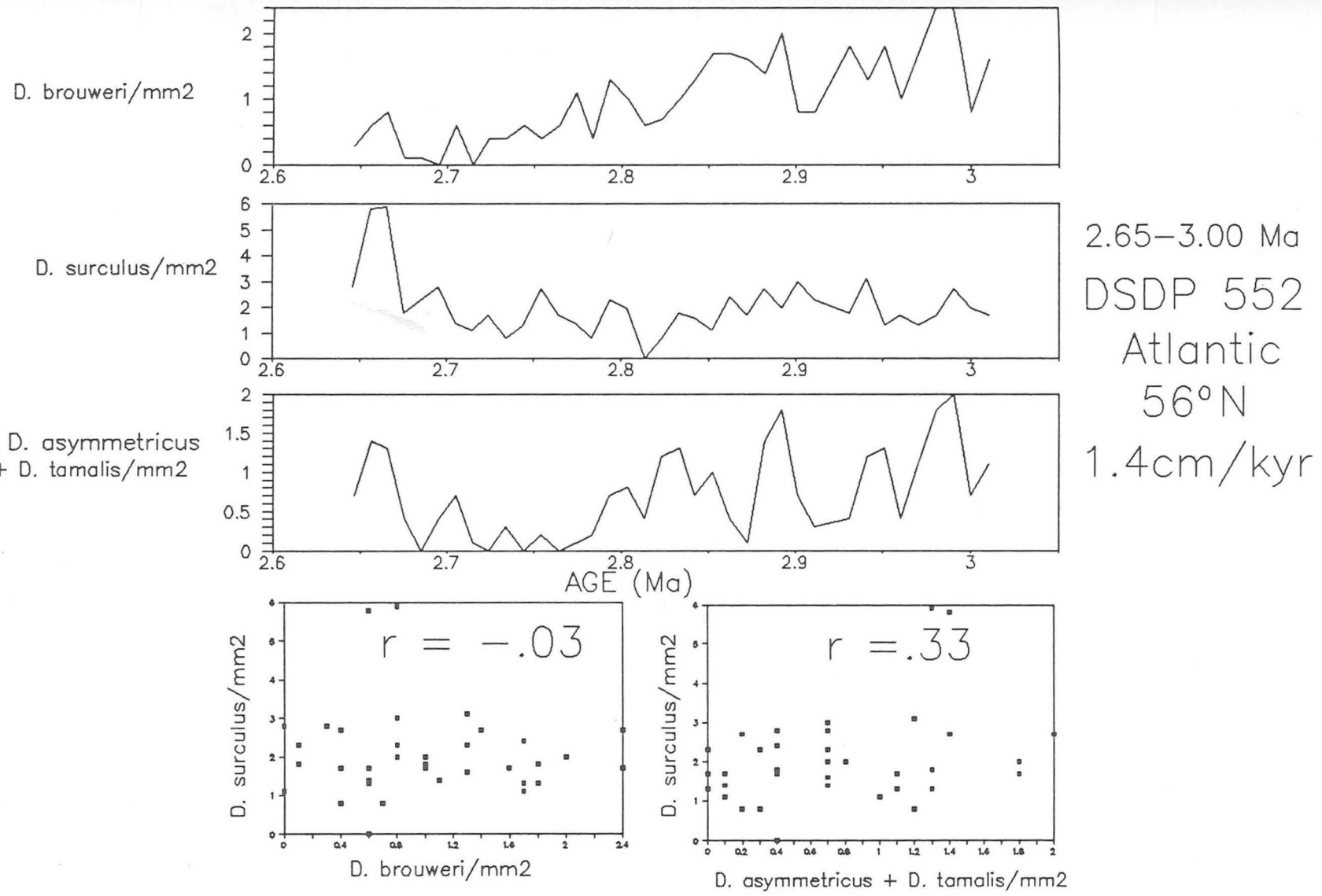

Figure 5:2:4a Abundance of D. brouweri, D. surculus and the sum of D. asymmetricus and D. tamalis/mm2 at Site 552 between 2.65–3.00 Ma.

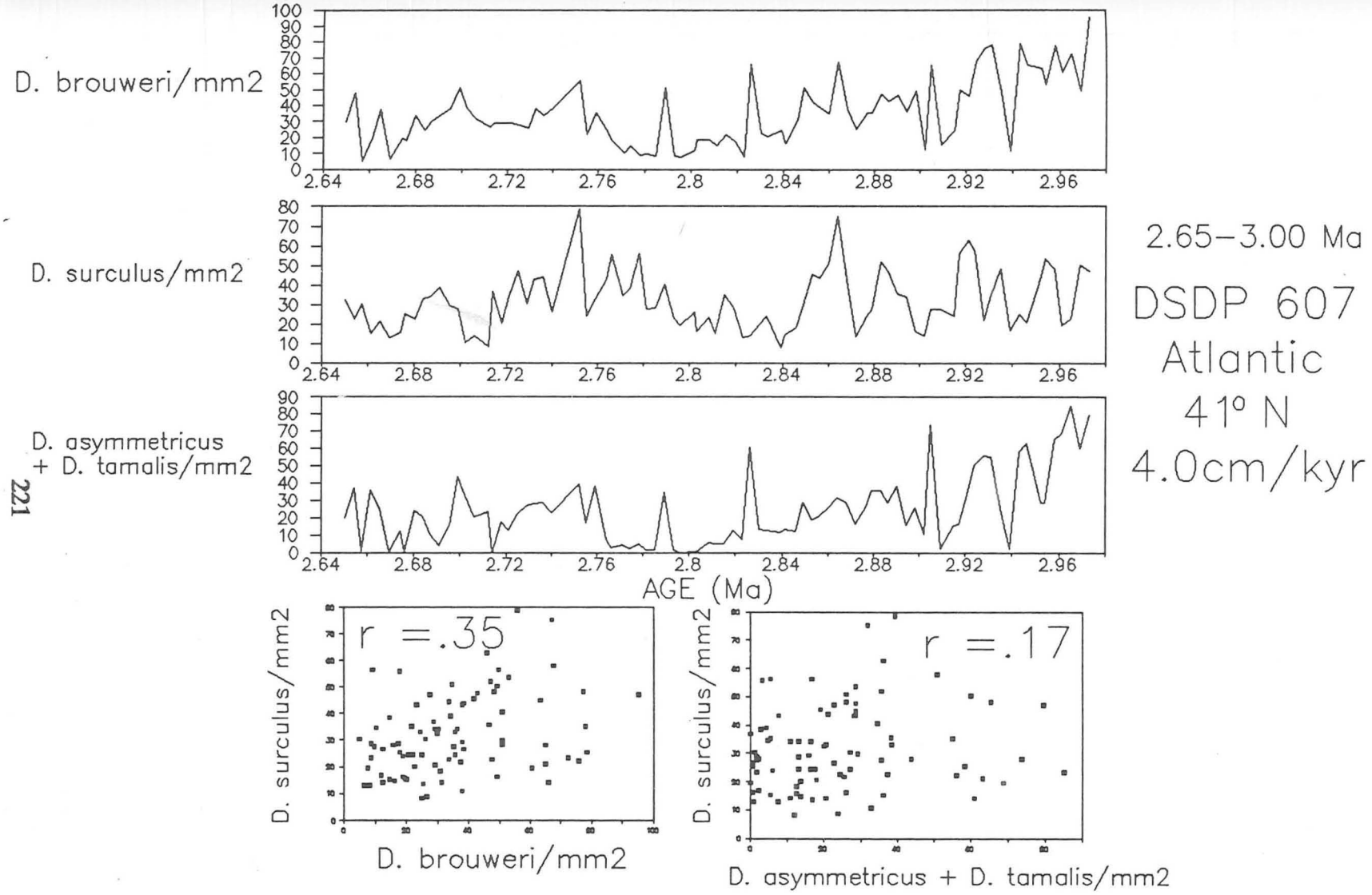

Figure 5:2:4b Abundance of D. brouweri, D. surculus and the sum of D. asymmetricus and D. tamalis/mm2 at Site 607 between 2.65–3.00 Ma.

after a major abundance decline, this coincides with suppressed abundances of "D. asyta".

At Site 658 (Fig. 5:2:4c), the upwelling site, this is an ideal location for demonstrating clearly the ecological relationship between D. surculus and D. brouweri, and with "D. asyta". D. surculus is thought to favour upwelling conditions (see Chapters 2 & 3). The scatter diagrams reveal little of the interplay between these species. After 2.88 Ma, the increasing abundance trend of D. surculus through time is accompanied by a decreasing abundance trend in D. brouweri. D. surculus clearly manifests an inverse abundance relationship with D. brouweri displaying peak abundances in low abundance intervals of D. surculus at e.g. approximately 2.74, 2.82 and 2.88 Ma. As D. surculus increases, "D. asyta" appears very suppressed. A peak abundance in the "D. asyta" record at approximately just after 2.76 Ma, corresponds with a trough between two closely spaced abundance peaks in the D. surculus record. Common peaks, not inversely proportional, between D. surculus and D. brouweri are rare if one excludes peaks at core boundaries i.e. 2.68-2.70 Ma, 2.78-2.80 Ma. Prior to 2.88 Ma, a distinctive common peak to D. surculus, D. brouweri and "D. asyta" is located close to a core boundary and may be the product of reworking, though a peak at 2.97 Ma correlates between these species. In this early time interval, both D. brouweri and D. surculus are suppressed, with "D. asyta" increasing with a peak abundance at 2.92 Ma, corresponding with a distinct trough in D. surculus abundance. Prior to 2.92 Ma, D. pentaradiatus was shown to increase at the expense of the other Discoaster species.

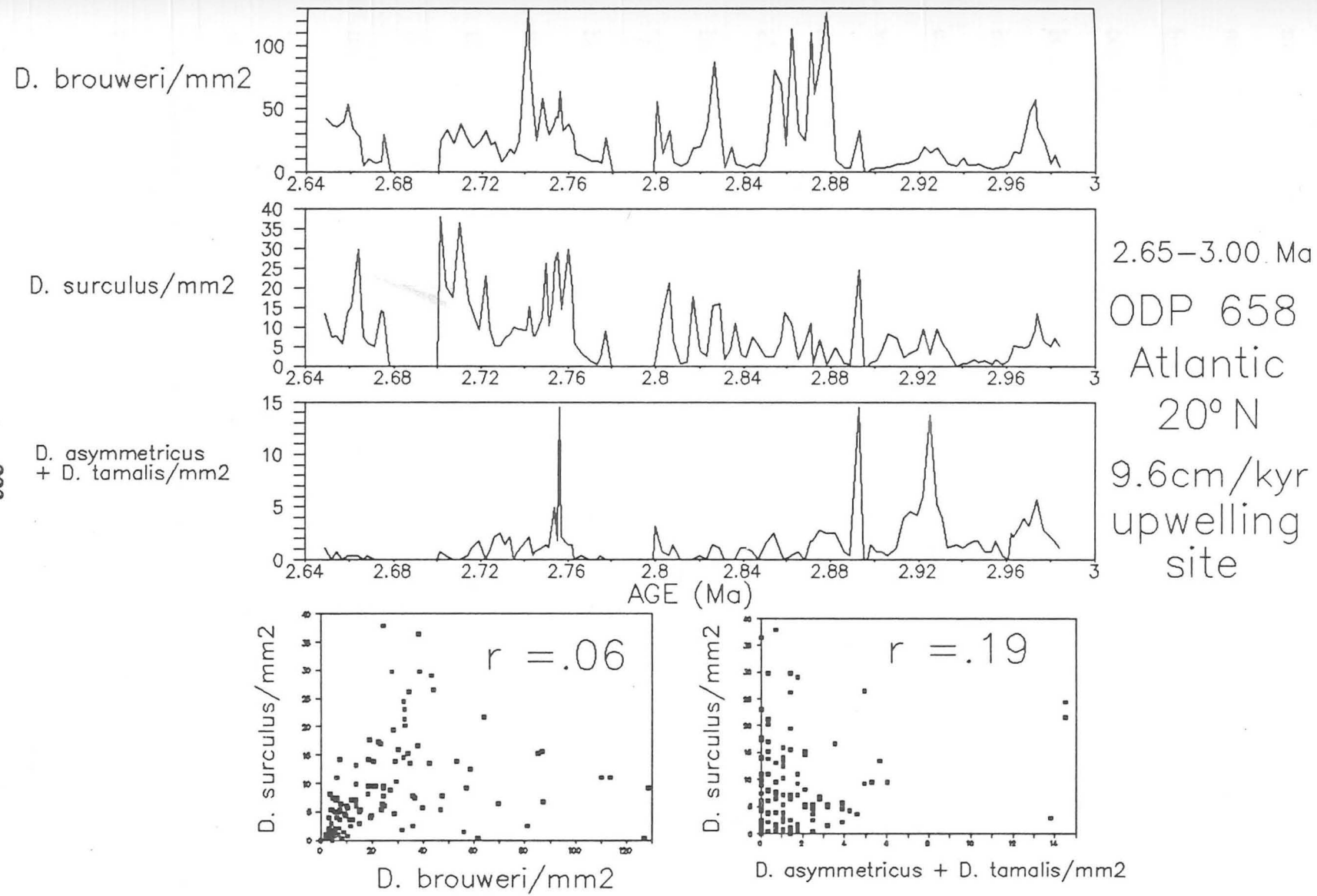

Figure 5:2:4c Abundance of D. brouweri, D. surculus and the sum of D. asymmetricus and D. tamalis/mm2 at Site 658 between 2.65–3.00 Ma.

At Site 659 (Fig. 5:2:4d), in close proximity to Site 658, the patterns between the D. surculus, D. brouweri and "D. asyta" are quite different. D. brouweri is a more dominant species at this site in relation to D. surculus. There is a fairly noticeable positive correlation between D. brouweri and D. surculus. Both D. brouweri and D. surculus increase with time, and broadly speaking the peaks correspond, with more definition in the D. surculus record. After 2.75 Ma, there is a striking fourfold abundance increase in D. brouweri, whereas D. surculus only increases by twice its abundance. It is noticeable that though the peaks roughly correspond, D. surculus increases in the lower D. brouweri abundance peaks and vice versa. The greater definition in the D. surculus record still results in inverse abundance relationships with D. brouweri e.g., at 2.83 Ma a D. surculus abundance peak corresponds with a decline in the D. brouweri record. In the high abundance interval of D. surculus and D. brouweri between 2.65-2.75 Ma, "D. asyta" is completely reduced. There is a fairly low negative correlation between D. surculus and "D. asyta", as the trends in declining abundance are in opposite directions, with "D. asyta" decreasing towards 2.65 Ma. It is apparent that the peaks in the "D. asyta" record correlate broadly with the D. surculus record, with decreases in the D. surculus peaks being matched generally by increases in the "D. asyta" peaks. Prior to 2.97 Ma, when D. surculus shows a major abundance decline, "D. asyta" demonstrates a major increase with a few noticeable inverse abundance correlations, especially between 3.0-3.05 Ma.

At Site 662 (Fig. 5:2:4e), D. brouweri is even more of a dominant species in relation to D. surculus, which occurs in rather suppressed abundances. The

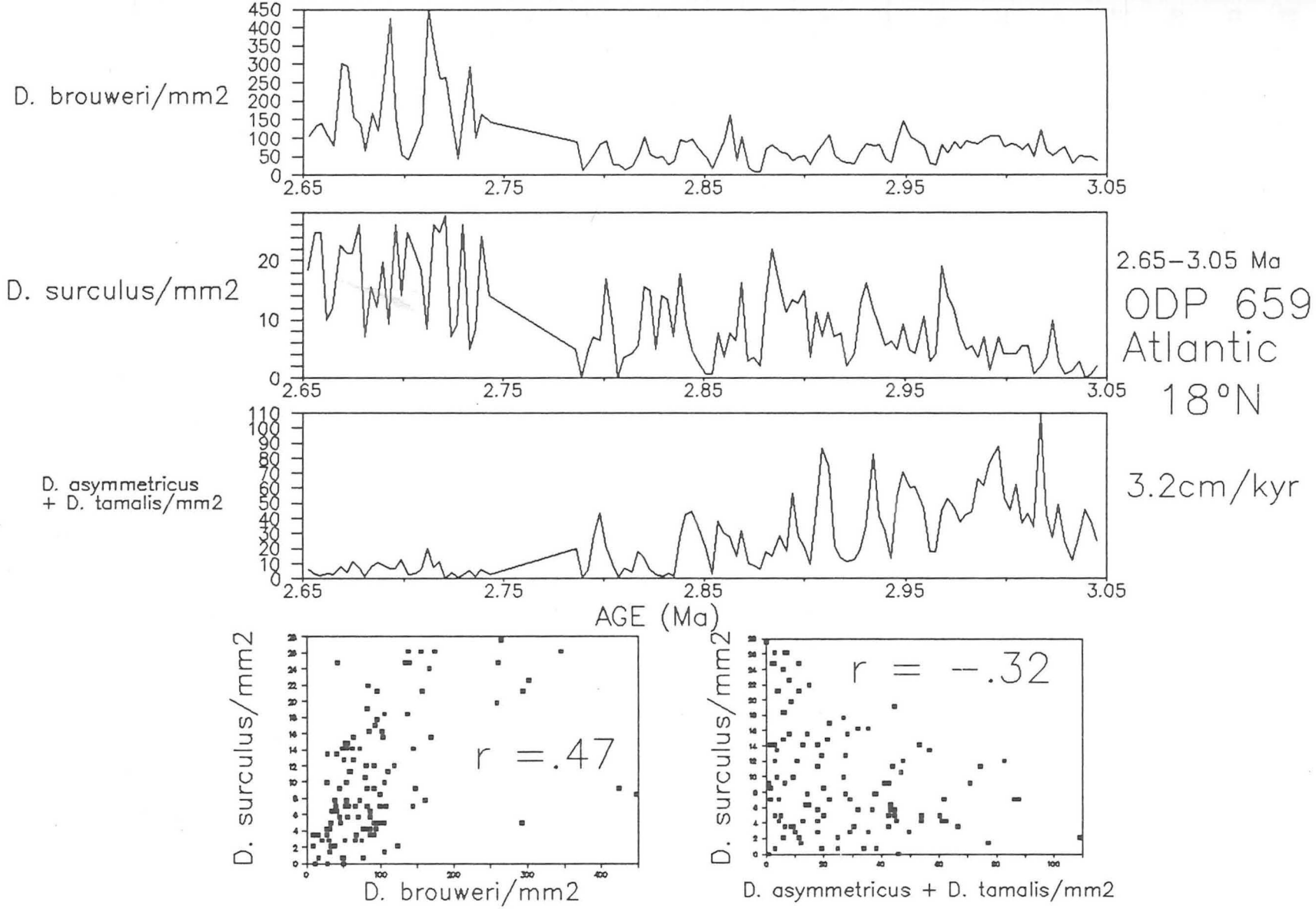

Figure 5:2:4d Abundance of D. brouweri, D. surculus and the sum of D. asymmetricus and D. tamalis/mm2 at Site 659 between 2.65–3.05 Ma.

correlation coefficient is low, but in view of the reduced abundances of D. surculus, there is generally a good correspondence of the abundance peaks and troughs with the D. brouweri record. Three D. surculus abundance peaks at approximately 2.66, 2.72 and 2.8 Ma, appear to tentatively correlate with troughs in the D. brouweri record. The correlation of D. surculus with "D. asyta" is also very low, but the situation is made difficult by "both species" occurring in such reduced abundances, coupled with the suspicion of possible reworking. There is no trend of abundance decline in the D. surculus record through time. The rise in abundance of "D. asyta", prior to 2.90 Ma, corresponds with no dramatic abundance decrease in the D. surculus record, or the D. pentaradiatus record as seen previously.

At Site 677 (Fig. 5:2:4f), there is a strong correlation between D. surculus and D. brouweri abundance, especially between 2.65 and 2.80 Ma, with the abundance peaks being largely proportional. Between 2.80 and 2.87 Ma, both species are largely suppressed, except for a high abundance peak of D. surculus at approximately 2.81 Ma. The D. brouweri record prior to 2.87 Ma is characterised by a minor increase, and this is accompanied by a marked increase in D. surculus abundance. Although, D. brouweri may be still be the dominant species at this upwelling site, it shows there are intervals when conditions are favourable for both these species, D. surculus (accompanied by very suppressed abundances of D. brouweri) or extremely suppressed abundances of both these species at e.g. approximately 2.70 and 2.84 Ma. D. brouweri does not occur in high abundances in this time interval independent of a corresponding increase in D.

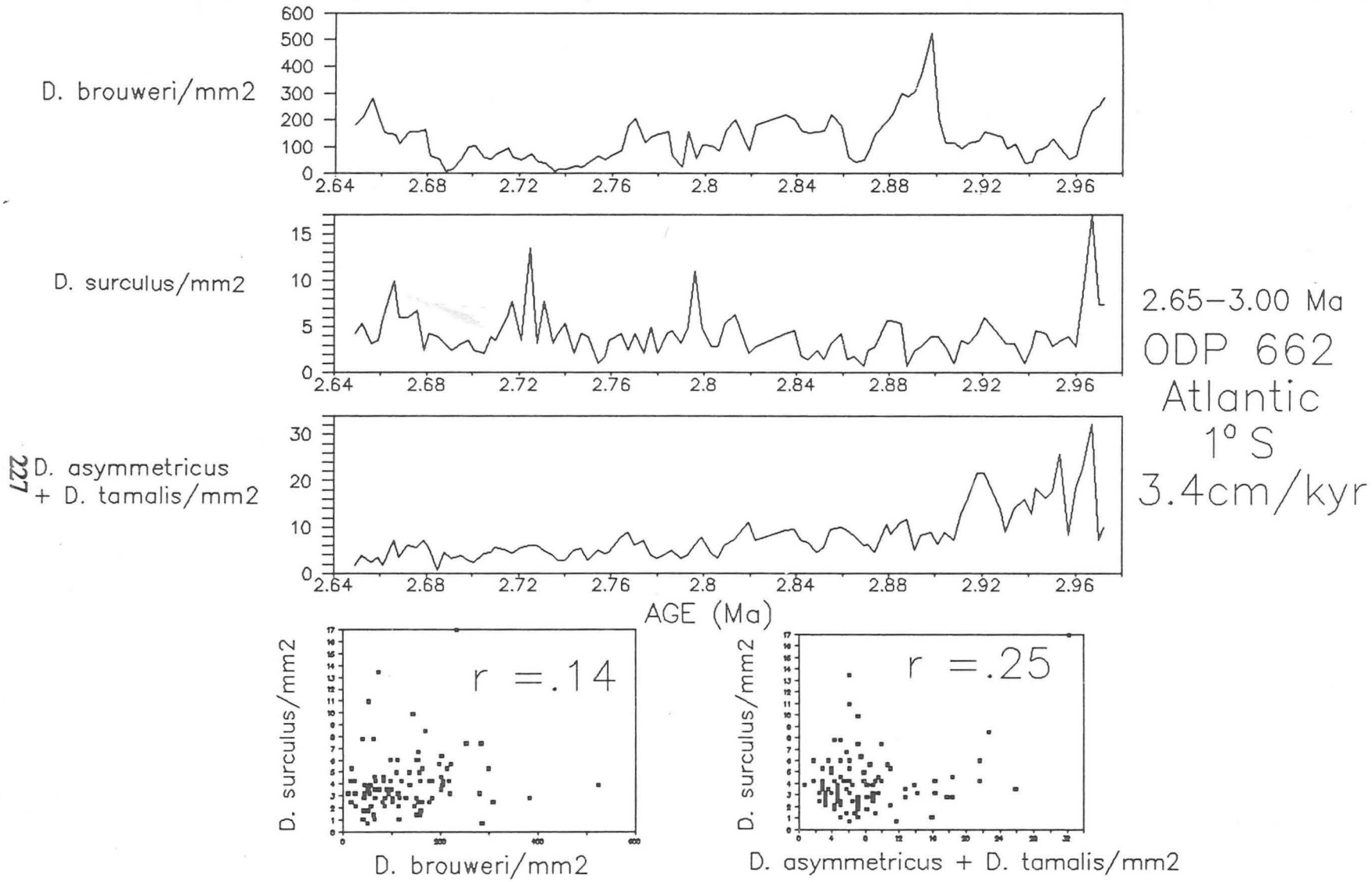

Figure 5:2:4e Abundance of D. brouweri, D. surculus and the sum of D. asymmetricus and D. tamalis/mm2 at Site 662 between 2.65–3.00 Ma.

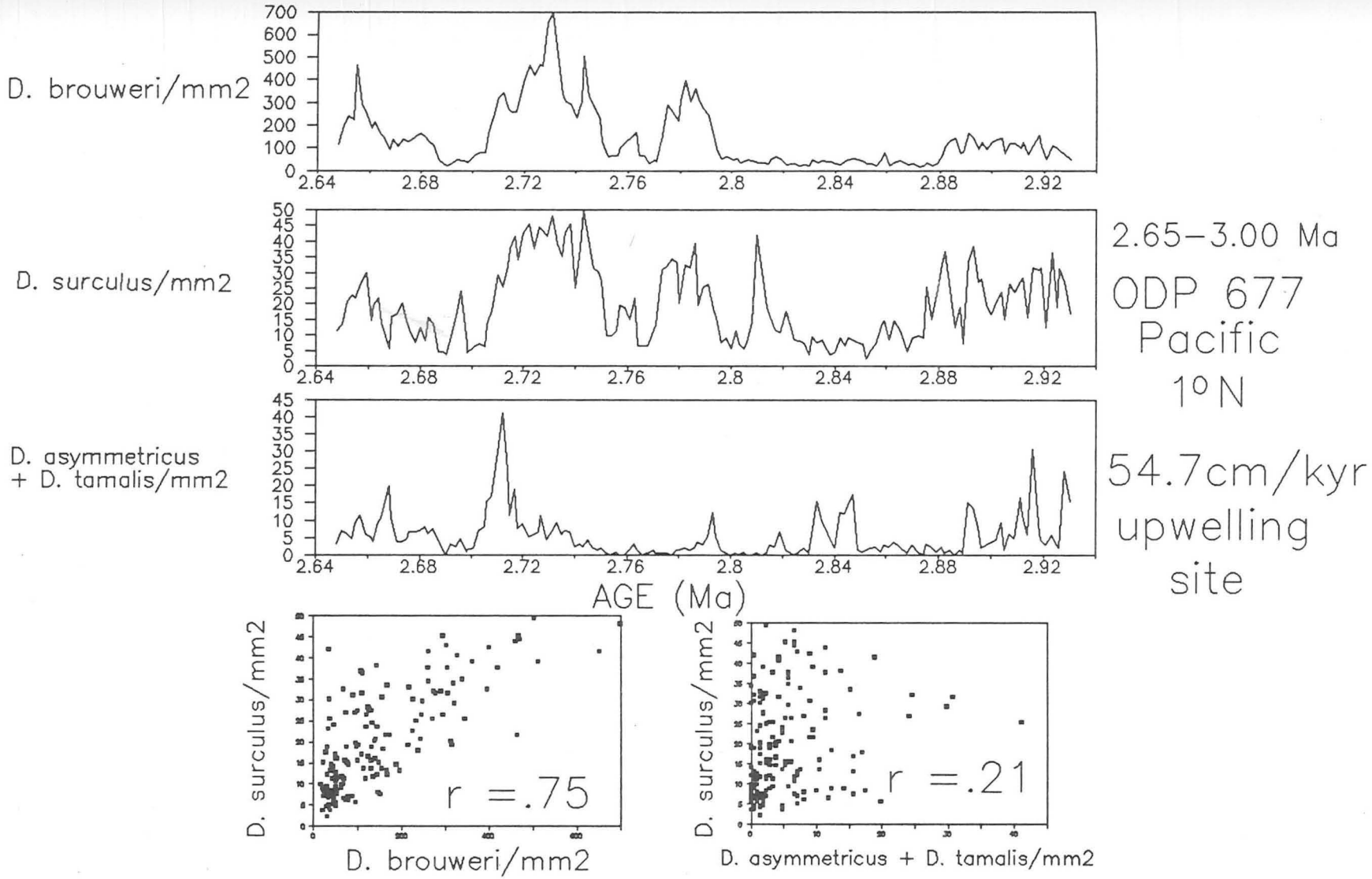

Figure 5:2:4f Abundance of D. brouweri,
D. surculus and the sum of D. asymmetricus
and D. tamalis/mm2 at Site 677 between 2.65 and 3.00 Ma

surculus abundance. The D. surculus record does not show an abundance decline trend through time.

The correlation of D. surculus abundance with "D. asyta" abundance is very low, and cannot be considered independently of D. brouweri abundance. "D. asyta" abundance is very suppressed at upwelling sites, but slight increases are apparent in intervals of low D. brouweri and D. surculus abundance, but especially the former species. A distinctive abundance peak of "D. asyta" at approximately 2.71 Ma, corresponds with a minor trough in a high abundance interval of D. surculus, but a high abundance peak of D. brouweri, so inconsistencies do exist when conditions were briefly favourable for all "3 species".

At Site 709 (Fig. 5:2:4g), in the Indian Ocean D. surculus shows a very low negative correlation with D. brouweri abundance. The D. surculus record manifests a weak abundance decline with time in contrast to the striking abundance increase of D. brouweri. It soon becomes apparent that most D. surculus abundance peaks correspond with troughs in the D. brouweri record. As mentioned earlier, this site is the most favourable for the production of discoasters, especially D. brouweri. D. surculus demonstrates particularly high abundances in the low D. brouweri abundance intervals i.e. approximately 3.1 and 3.45 Ma.

D. surculus shows a low positive relationship with "D. asyta", partly due to the fact that both records decline in abundance with time, though not with very defined trends. D. surculus generally shows an inverse abundance relationship with "D. asyta" which increases in low abundance intervals of D. surculus as seen

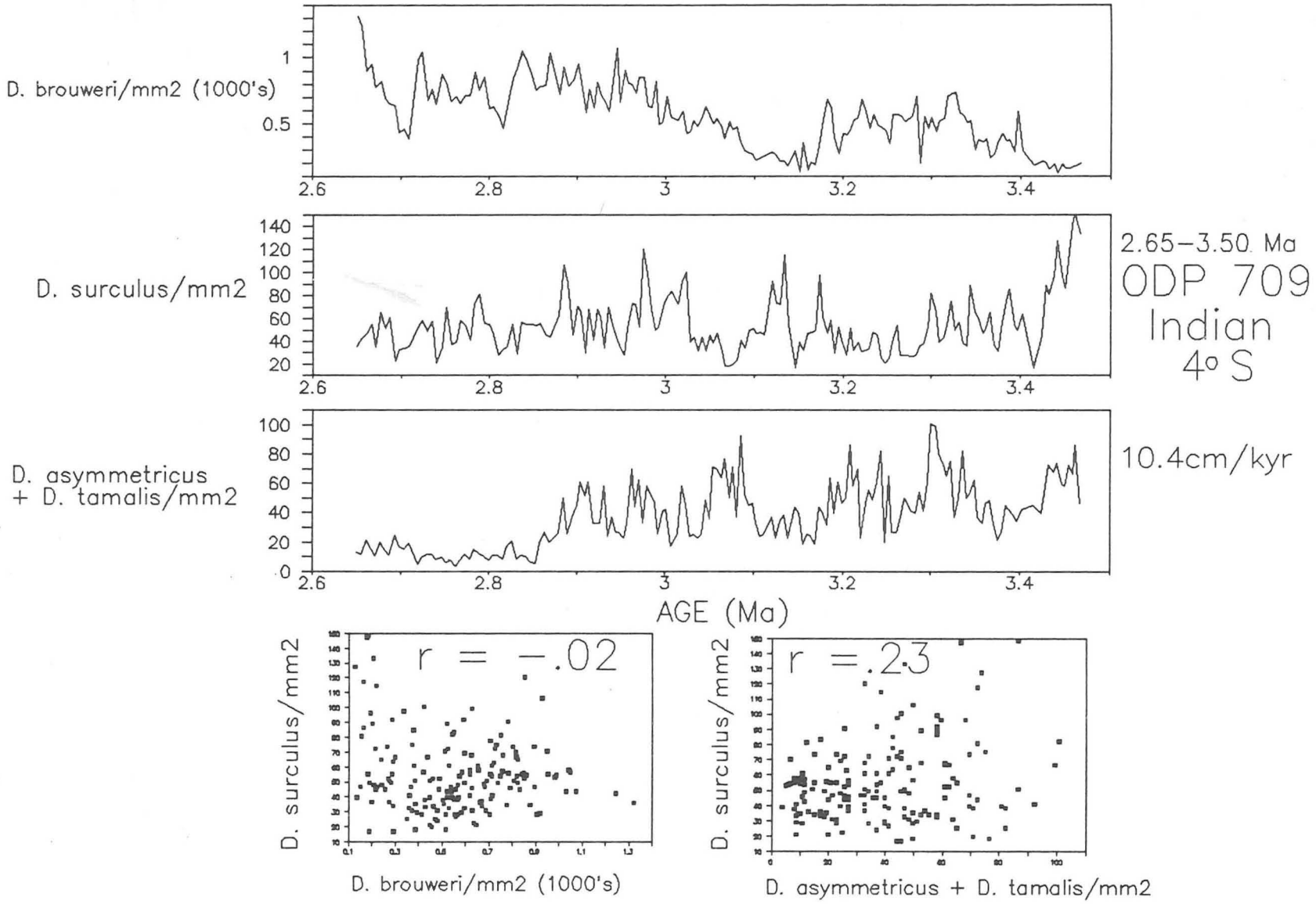

Figure 5:2:4g Abundance of D. brouweri, D. surculus and the sum of D. asymmetricus and D. tamalis/mm2 at Site 709 between 2.65–3.50 Ma.

at e.g. approximately 3.05 and 3.2 Ma. However, decreases in D. brouweri are also very significant, as demonstrated by an increase of "D. asyta" prior to 3.4 Ma, during a high abundance interval of D. surculus, but a low abundance interval of D. brouweri. "D. asyta" probably favoured brief cooler episodes, not accompanied by productivity increases, but D. surculus is thought to favour cooler waters associated with more nutrients. How brief or subtle were these changes in productivity or temperature in order to favour D. surculus and "D. asyta" species in what is generally a very warm site of modest productivity?

5:2:5 The relationship between D. surculus and D. pentaradiatus?

In this section, we are examining the time interval prior to 2.38 Ma i.e. the LAD of D. pentaradiatus, followed closely by the LAD of D. surculus at 2.39 Ma. Effectively, we have now doubled the time interval being analysed to approximately 620 ka. This is the last piece of the ecological jigsaw within the upper Pliocene discoasters, by comparing the global picture of D. surculus with D. pentaradiatus. These two species are thought to display the clearest inverse abundance relationship (Backman and Shackleton, 1983), so it will be interesting to see how this holds up on a global basis.

At Site 552 (Fig. 5:2:5a), the highest latitude site, there is virtually no positive correlation between D. surculus and D. pentaradiatus, except for the one major peak in the D. pentaradiatus record at approximately 2.75 Ma, corresponding with a minor peak in the D. surculus record. These peaks may appear to correlate, but this could be a function of such a low sedimentation rate. The

other peaks in the D. pentaradiatus record correlate with low abundances in the D. surculus record.

At Site 607 (Fig. 5:2:5b), D. pentaradiatus and D. surculus has the lowest correlation coefficient of all the Discoaster relationships at this site. This may be significant since if climatic forcing is so pronounced at high latitudes, forcing species to respond to the conditions imposed, this may indicate that these two species had the greatest ecological differences. High abundance peaks of D. pentaradiatus correspond with troughs in the D. surculus record and vice versa, and if peaks do happen to correspond, the peaks are disproportionate e.g. approximately 2.88 Ma.

At Site 658 (Fig. 5:2:5c), the upwelling site with high time resolution, a minor positive correlation coefficient is observed between D. surculus and D. pentaradiatus. However, this largely reflects correlations due to reworking close to the core breaks. If the records are analysed in detail, an intricate relationship is portrayed between D. surculus and D. pentaradiatus, with one species increasing during lower abundance intervals of the other. Intervals of increasing D. pentaradiatus in relation to declining D. surculus abundance i.e. prior to 2.92 Ma, or after 2.45 Ma, may mark episodes of increasing sea-surface temperature, perhaps associated with a decrease in the intensity of upwelling.

At Site 659 (Fig. 5:2:5d), in close proximity to Site 658, D. surculus manifests a very low negative correlation coefficient with D. pentaradiatus. Detailed observation of the two records once again reveals an intricate inverse abundance relationship between these two species, with high abundances of D. pentaradiatus

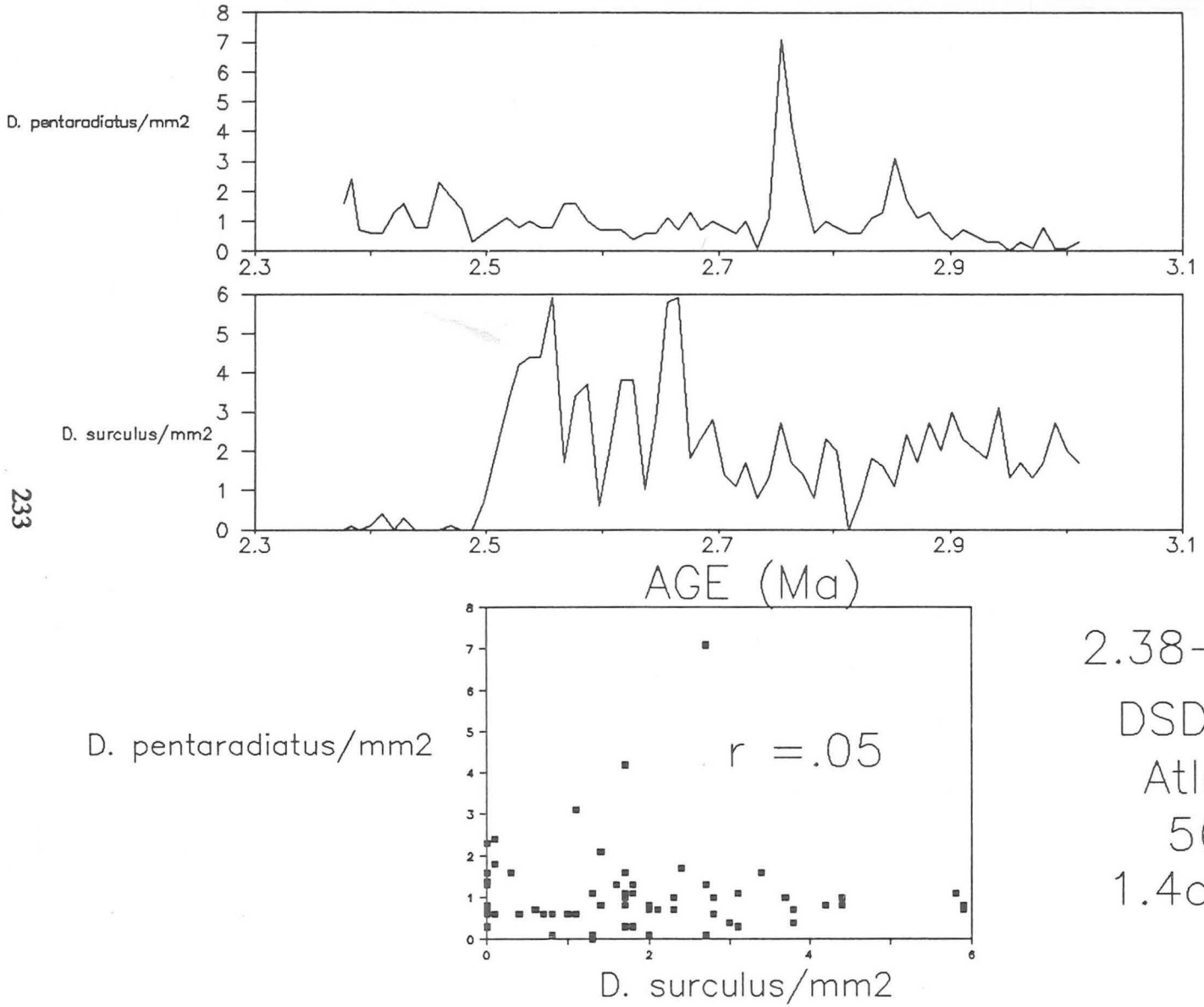

Figure 5:2:5a Abundance of D. pentaradiatus and D. surculus/mm2 at Site 552 between 2.38–3.00 Ma.

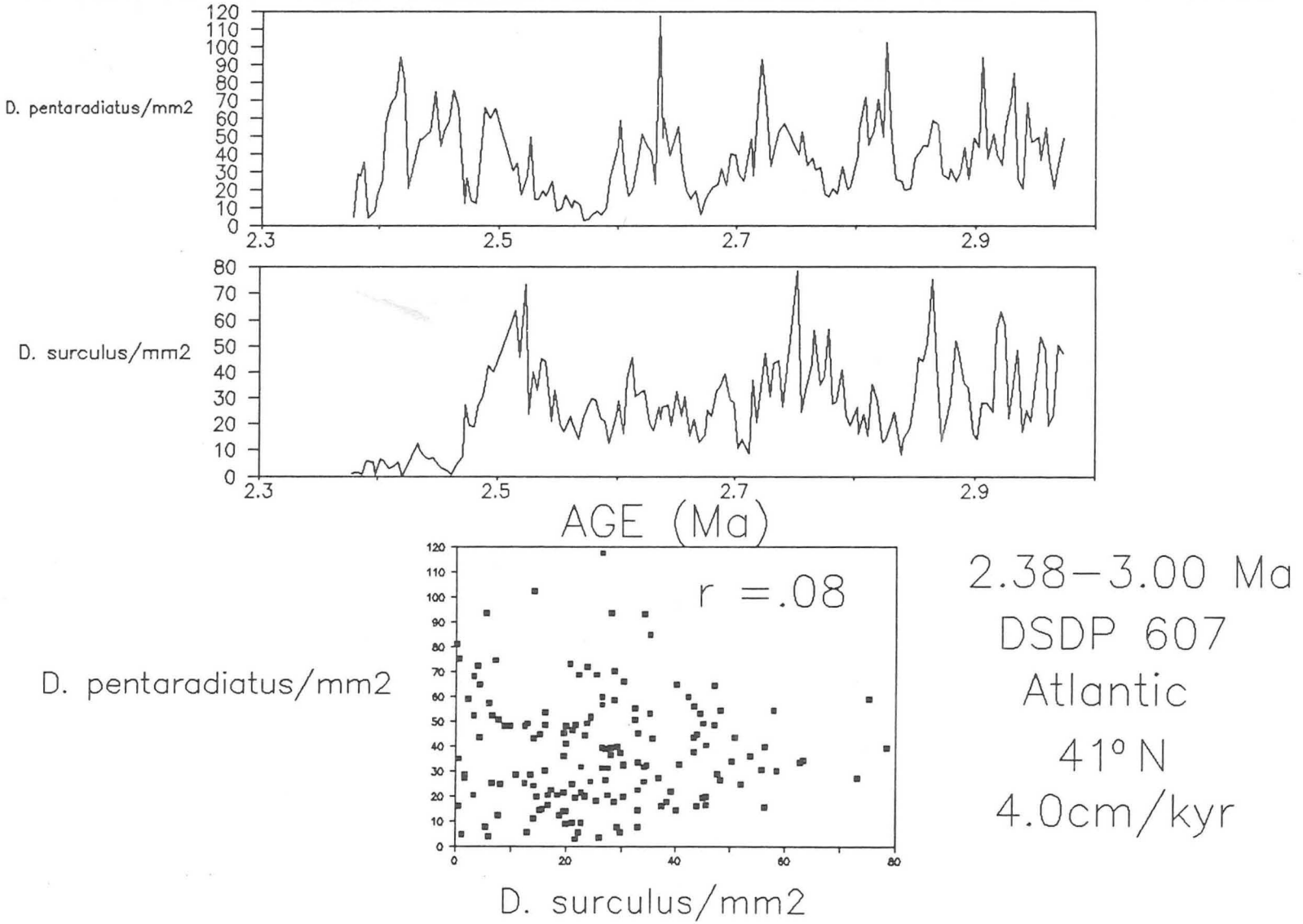

Figure 5:2:5b Abundance of D. pentaradiatus and D. surculus/mm2 at Site 607 between 2.38–3.00 Ma.

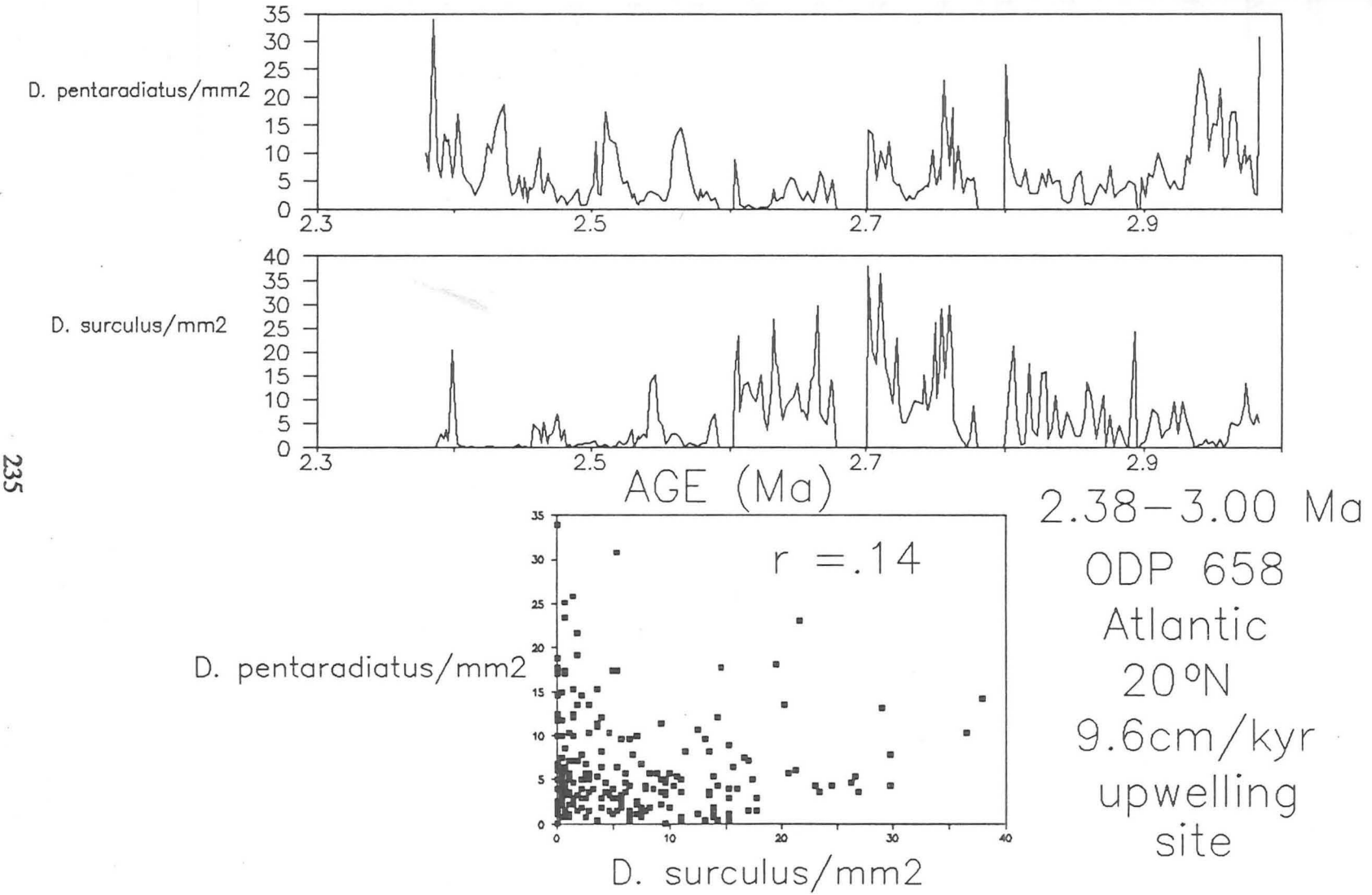

Figure 5:2:5c Abundance of D. pentaradiatus and D. surculus/mm2 at Site 658 between 2.38–3.00 Ma.

corresponding with low abundances of D. surculus and vice versa. A short high abundance interval of D. surculus between 2.50 and 2.65 Ma, corresponding with a low abundance interval of D. pentaradiatus may reflect a cooling in sea-surface temperature, perhaps associated with an increase in productivity. Prior to 2.65 Ma, D. surculus occurs in largely suppressed abundances, whereas the conditions favour D. pentaradiatus, which may indicate warmer sea-surface temperatures.

In the equatorial Atlantic at Site 662 (Fig. 5:2:5e), the inverse abundance relationship between D. pentaradiatus and D. surculus is not well defined and there is an unexpectedly high positive correlation coefficient between these species. D. pentaradiatus is the more dominant species at this site, whereas D. surculus occurs in very subdued abundances. At approximately 2.55 Ma, and especially 2.60 Ma, minor abundances in the D. pentaradiatus record correspond with distinct D. surculus abundance peaks. Most other peaks, however, can be correlated between the two records, and one becomes suspicious about reworking, such as the striking abundance peaks of D. surculus and D. pentaradiatus at 2.95 Ma. The drop in abundance of D. pentaradiatus after 2.75 Ma does not correspond with a major increase in D. surculus and the peaks can still be correlated. This may now prove unfortunately that this site is majorly affected by reworking, when these two species correlate so well.

In the equatorial Pacific at Site 677 (Fig. 5:2:5f), it is not possible to compare between the two species, since D. pentaradiatus occurs in such suppressed abundances after 2.9 Ma. It may indicate that the upwelling conditions were highly favourable for D. surculus, but they had reached a threshold when D.

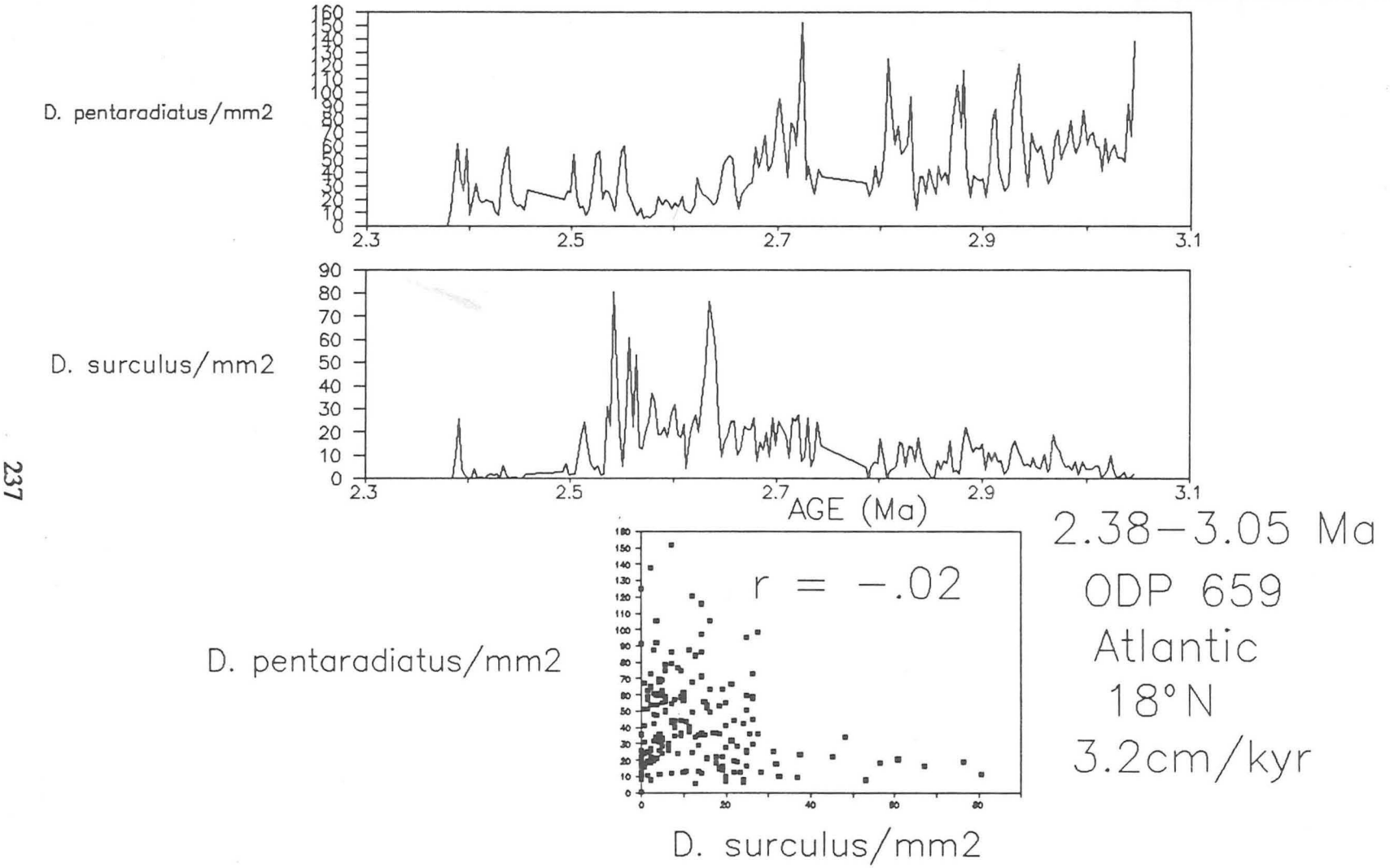

Figure 5:2:5d Abundance of D. pentaradiatus and D. surculus/mm2 at Site 659 between 2.38−3.05 Ma.

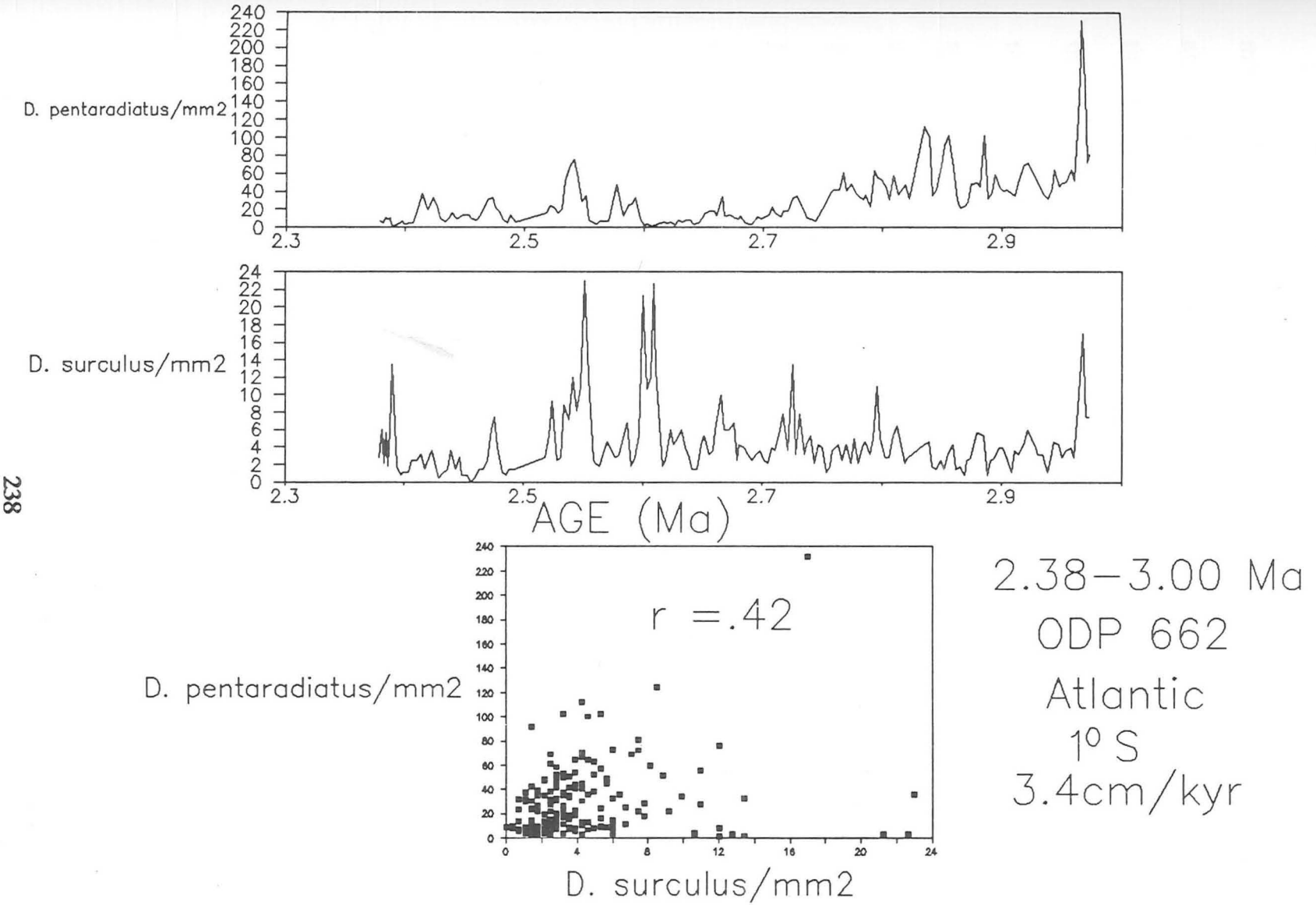

Figure 5:2:5e Abundance of D. pentaradiatus and D. surculus/mm2 at Site 662 between 2.38–3.00 Ma.

pentaradiatus could no longer exist. The distinctive abundance peak of D. pentaradiatus at 2.90 Ma, occurs in a trough in the D. surculus record.

In the equatorial Indian Ocean at Site 709 (Fig. 5:2:5g), there appears to be a minor positive correlation between the two records. This is a reflection that the abundances of both D. pentaradiatus and D. surculus decline through time, and that a number of peaks do correlate between the two species. However, generally there is an inverse abundance relationship between the two species, with peaks in the D. surculus record correlating with troughs in the D. pentaradiatus record and vice versa e.g. at approximately 2.62, 2.78, 2.89 and 3.3 Ma. Nevertheless, some peaks correspond well between the two species at e.g. approximately 2.5, 2.6 and 3.12 Ma. It must be remembered that this is a site dominated by high D. brouweri and D. pentaradiatus abundances on a major scale compared to all other sites, and the troughs in these records still represent high abundances compared to D. surculus. It is maybe not surprising that against this constant high background of D. brouweri and D. pentaradiatus, which show an inverse abundance relationship, and a similar relationship shown between D. surculus and D. brouweri, that D. surculus and D. pentaradiatus should occasionally overlap and display a number of peaks in common. These peaks are normally disproportionate i.e. high peaks of D. surculus abundance at approximately 2.98 and 3.02 Ma, corresponding with less substantial peaks in the D. pentaradiatus record.

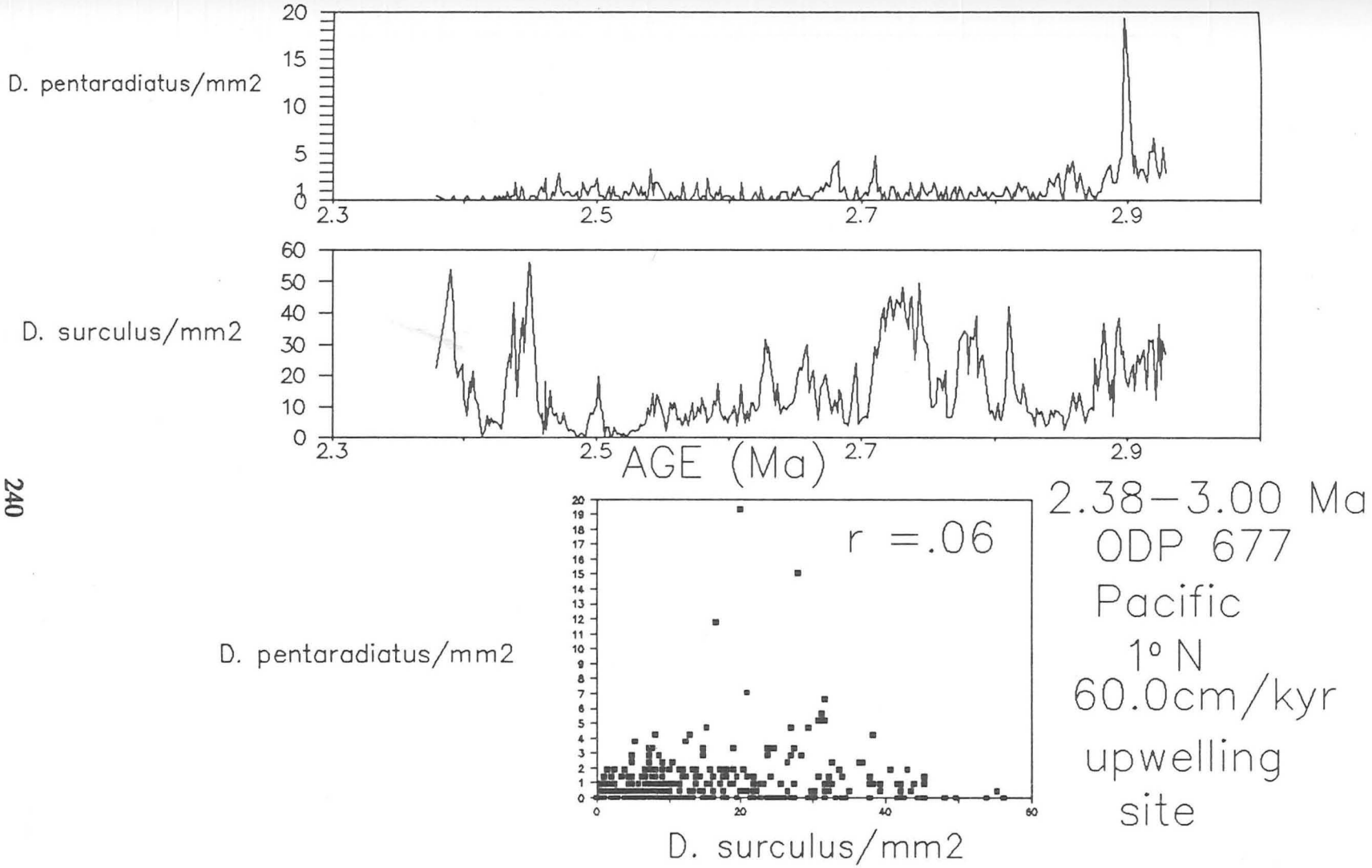

Figure 5:2:5f Abundance of D. pentaradiatus and D. surculus/mm2 at Site 677 between 2.38–3.00 Ma.

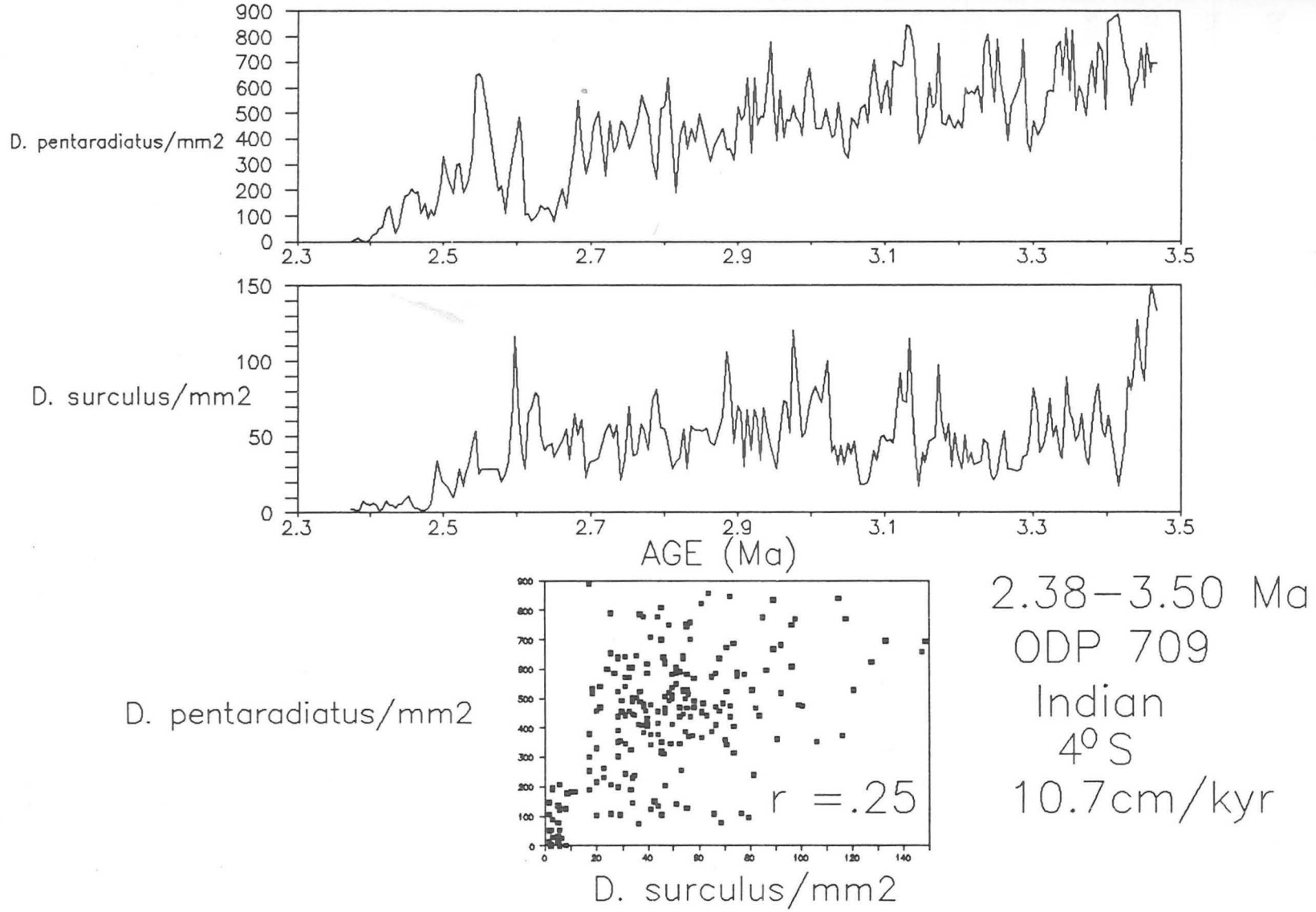

Figure 5:2:5g Abundance of D. pentaradiatus and D. surculus/mm2 at Site 709 between 2.38–3.50 Ma.

5:3 DISCUSSION

The means of the correlation coefficients for the Discoaster relationships of all the sites are given in Table 5:1a. Even without Site 662 in the calculation, if we believe it is majorly affected by reworking, the mean correlation coefficients were not significantly different. The mean species correlation coefficients reveal strong correlation between D. brouweri and D. triradiatus, and between D. asymmetricus and D. tamalis globally. However, the relationships between the other Discoaster species, including D. brouweri and "D. asyta" receive low correlation coefficients. This does not mean there is not a strong relationship between D. brouweri, and "D. asyta", as we have shown there is. However, this statistical method is not adequate to cope with the intricate relationships amongst the Discoaster species through time in such a wide range of oceanographic conditions. It is a tool that can be used in combination with the detailed records, but it is the unique records themselves which really reveal the relationships between the Discoaster species, be they ecological, taxonomic or both.

The mean site correlation coefficients may indicate additional information. If we ignore Site 552, due to its low abundances and coarse temporal spacing, Site 607, the next highest latitude site with a good time resolution, has the highest mean site correlation coefficient. This is to be expected since high latitude sites are affected most by climatic forcing. Further evidence for Site 662 being affected greatly by reworking is that it has the second highest mean site correlation coefficient. Species which were shown to have defined ecological ranges at other sites have abundance peaks roughly corresponding at Site 662. Even the

recognised global event, the D. triradiatus acme, has a poor correlation coefficient, because of D. brouweri being reworked (with D. pentaradiatus) into this restricted interval.

This study allows us to speculate about the taxonomic affinities and ecological preferences of the different species. There is a global relationship between D. brouweri and D. triradiatus, between 1.89-2.07, at all the sites independent of latitude or upwelling conditions. D. brouweri may be suppressed in cooler waters (e.g Site 552) or under intense upwelling conditions (e.g. Site 677), but D. triradiatus will be present, though affected to the same extent, since they are most certainly the same species. D. asymmetricus and D. tamalis (i.e. "D. asyta"), occurring in very similar abundances demonstrate this relationship, independent of latitude or upwelling conditions. They are produced especially in cooler, lower productivity waters as seen at Site 607, with abundance peaks corresponding closely with D. brouweri abundances. Away from high latitudes, a strong correlation still exists, but "D. asyta" does not appear to favour upwelling or warmer water conditions, though the peaks still correspond with the D. brouweri record. Low abundance peaks of D. brouweri with high abundance peaks of "D. asyta" may indicate cooler, low productivity waters. Conversely, high abundance peaks of D. brouweri with low abundance peaks of "D. asyta" may indicate warm, low productivity waters. "D. asyta" decreases in abundance away from high latitudes, but tends to increase in low abundance intervals of D. pentaradiatus and D. surculus. D. pentaradiatus appears to favour warmer waters and was a highly successful species at Site 709 in the Indian Ocean, which had very little

productivity pressure. Generally, D. pentaradiatus is a flexible species forming a major component of the Discoaster assemblage, regardless of latitude or upwelling conditions. At the upwelling site, Site 658, D. pentaradiatus shows suppressed abundances and a clear inverse abundance relationship with D. surculus, but it was still a significant component of the complete Discoaster assemblage. However, at Site 677, which displays very intense upwelling, the conditions were intolerable for D. pentaradiatus after 2.90 Ma, and abundances were almost completely suppressed. This may indicate that although D. pentaradiatus ideally favours warm waters, it still extends significantly into higher latitudes and that high productivity pressure may be the main limiting factor.

D. brouweri appears to manifest a high ecological flexibility, thriving in warm waters of low productivity, diminishing in abundance towards the high latitudes, but can still survive, though suppressed, in intense upwelling areas such as Site 677. At Site 677, D. brouweri largely covaries with D. surculus. D. brouweri appears therefore to be able to withstand a wider range of productivity pressure and temperature than D. pentaradiatus.

Since D. surculus generally demonstrates an inverse abundance relationship with "D. asyta", they may prefer different temperature ranges of cooler waters. However, it seems more probable that since "D. asyta" is suppressed at upwelling sites, D. surculus favours higher productivity areas in addition to cooler sea-surface waters.

D. surculus and D. pentaradiatus are probably the most different species (second lowest mean species correlation coefficient after D. brouweri and D.

pentaradiatus), because they represent the extremes of ecological conditions. D. surculus appears to favour cooler, high productivity waters and D. pentaradiatus ideally favours warmer, low productivity waters, though it still can be relatively flexible in its temperature tolerance, as shown at high latitudes. D. brouweri is especially tolerant, and bridges the ecological gap between these two species.

The D. surculus records display that this species is largely unaffected by sea-surface temperatures declining, because D. surculus is responding to productivity pressure. The abundance trends in the records of D. brouweri, "D. asyta" and D. pentaradiatus to a lesser extent, especially away from intense upwelling sites, are more obvious since they are linked to the gradual sea-surface temperature decline. Even the D. brouweri record at Site 677 is overshadowed by productivity pressure and does not record an obvious abundance decline linked to temperature.

Ecological tolerances must change in different populations of the same species from locality to locality. This study has revealed greater flexibility in certain species i.e. D. brouweri. Presumably, if the same conditions in operation during a peak abundance of D. brouweri at Site 677 were suddenly transferred to Site 709, there might occur a sudden drop in the population before D. brouweri had time to adapt to the new conditions of higher productivity and lower temperature.

Different ecological conditions are known to impose the production of different types of coccoliths in the same living coccolithophorids (Parke and Adams, 1960; Okada and McIntyre, 1979). The evidence here supports the theory that the same organism produced discs of D. brouweri, D. asymmetricus, D. tamalis and D.

triradiatus in its structure. D. asymmetricus and D. tamalis were probably produced in equal abundances in this structure under conditions of cooler temperatures and lower productivity, but never produced in greater abundance than D. brouweri. A threshold was reached at 2.65 Ma, when D. tamalis ceased to be produced which is not understood, and D. asymmetricus similarly showed an abundance decline at 2.65 Ma. After 2.65 Ma, D. asymmetricus was produced in very low abundances and this does not appear to be of any ecological significance, but probably just a random error in the mechanism for producing the six-rayed D. brouweri disc in the enigmatic organism. D. brouweri has revealed its ecological flexibility and superiority by surviving an extra 500 ka after D. pentaradiatus and D. surculus faced extinction respectively at 2.38 and 2.39 Ma.

5:4 SUMMARY

1. D. brouweri and D. triradiatus showed strong co-variation globally during the time interval 1.89-2.07 Ma. D. asymmetricus and D. tamalis occurred in similar abundances, displaying strongest co-variation with D. brouweri during cooler, low productivity episodes.

2. D. brouweri exhibits the widest ecological tolerance, favouring warm water, low productivity sites, but able to survive in intense upwelling conditions. Its ecological flexibility may have been the secret of its long term success.

3. D. pentaradiatus is a relatively flexible species in relation to sea-surface temperatures, favouring warmer waters preferably, but it has a lower tolerance for productivity pressure than D. brouweri, as shown at the upwelling site, Site 677.

4. D. surculus displays a well defined inverse abundance relationship with D. pentaradiatus, since the former species is adapted to high productivity areas. Cooler temperatures may have been of secondary importance.

CHAPTER 6: OXYGEN ISOTOPE STRATIGRAPHY AND ORBITALLY TUNED TIMESCALES FOR DISCOASTER ABUNDANCE (WITH SPECIAL REFERENCE TO DSDP 607 AND ODP 677).

6:1 Introduction

One of our objectives was to look at Discoaster abundances within the framework of the best orbitally tuned timescale available and compare the result with a timescale based on biostratigraphy and/or magnetostratigraphy. To accomplish this, we needed a site where the Discoaster abundances manifested a strong relationship with the oxygen isotope record.

Oxygen isotope ratios in foraminifera from deep sea sediments have been used as palaeoclimatic indicators following Emiliani's original work (1955). Until recently, there were only a few high-quality continuous records of $\delta^{18}O$ variations covering over a million years (Shackleton and Opdyke, 1973, 1976; Shackleton et al., 1984), but higher resolution records were sought after.

$\delta^{18}O$ in foraminifera varies with $\delta^{18}O$ in the water from which the carbonate tests are deposited, but differs from the water value by an amount that is temperature dependent (Epstein et al., 1951). The water isotopic fluctuations largely record changes in northern hemisphere ice volume. As the record in planktonic foraminifera may be affected by differences in surface salinity, changing seasonal growth and depth habitat (Berger et al., 1978), benthic foraminifera have recently been preferred as they provide a less complicated record of global ice volume. However, benthic foraminifera are much rarer than

planktonic foraminifera in samples.

In the late Pliocene, a major change in the earth's climate occurred when continental size ice sheets began to grow and shrink over large areas of North America and Eurasia. This cooling began about 3.1 Ma, (Backman and Pestiaux, 1986; Raymo et al, 1986; Einarsson and Albertsson, 1988) leading to the accumulation of gradually larger ice sheets. This finally resulted in the first extensive episode of ice-rafting in the open North Atlantic at 2.4 Ma, which corresponds with a significant glacial event in the oxygen isotope record of DSDP 552 (Shackleton et al., 1984).

Oxygen isotope studies (e.g. Shackleton and Opdyke, 1973) have indicated that global ice volume varied mainly with a periodicity of 100 ka during the late Pleistocene Bruhnes chron (0 - 0.735 Ma). During the Matuyama chron (0.735 - 2.47 Ma), when the amplitude of the $\delta^{18}O$ signal was smaller than in the Bruhnes by about half, much of the variance was concentrated at higher frequencies (e.g. Shackleton and Opdyke, 1976).

For most of the sites at which Discoaster abundances were examined, oxygen isotope records were available. Site 552 has an important oxygen isotope record and magnetostratigraphic control for the upper Pliocene, but the time resolution is too low and the Discoaster abundances are extremely reduced (Shackleton et al., 1984; Backman et al., 1986). This revealed, however, that the LAD of D. brouweri was located in stage 72 and that the LAD's of D. pentaradiatus and D. surculus were close to stage 100, when the first major ice rafting was recognized off Britain.

A range of problems from reworking to core gaps have resulted in unfavourable oxygen isotope records for Sites 659, 709 and 662 in the time interval of interest i.e. 1.89-3.00 Ma (Shackleton, Pers. Comm.). Of these sites, only Site 659 had any magnetic data, but magnetic reversals were unambiguous only above the interval we were studying in Hole 659A. At Site 716, the foraminifera were severely overgrown, which has caused problems in obtaining the true oxygen isotope signal in this time interval (Droxler, Pers. Comm.). Site 658, the upwelling site off northwest Africa, revealed many gaps in the oxygen isotope record, when compared with the oxygen isotope record of Site 607 e.g. stages 89-95 were missing (Sarnthein and Thiedemann, 1989; Raymo et al., 1989). Nevertheless, Site 658 revealed that the LAD of D. brouweri occurred in stage 72 and that the LAD of D. surculus was very close to stage 100, which is when the first major ice-rafting was observed at Site 552 (Shackleton et al., 1984).

Two complete oxygen isotope records of high time resolution at Sites DSDP 607 and ODP 677 have recently become available (Ruddiman et al., 1986; Raymo et al., 1989; Shackleton and Hall, 1989; Shackleton, Berger and Peltier, in press), which extend back into the late Pliocene. At Site 677, the Pacific upwelling site (1°N), the Discoaster abundance record displayed very little relationship with the oxygen isotope record, because the abundances were overshadowed by a productivity pressure signal. Secondarily, Site 677 lacked magnetostratigraphy, which would have given us an independent reference to the selection of the biostratigraphic control points used in the age-models.

We required a site in the high latitude North Atlantic Ocean (above 40°N),

which showed a climatic behaviour controlled by fluctuations of the surrounding continental ice sheets. Under this situation, orbital forcing would affect the oxygen isotope and Discoaster abundance record similarly, and hence would provide the best orbitally tuned timescale for the Discoaster record. Northern latitude sites being largely affected by oscillations of the surrounding continental ice sheets has been supported in part by a general circulation model experiment. This isolated the regional climatic impacts uniquely due to northern hemisphere ice sheets (Manabe and Brocccoli, 1985). Site 607 suited all these requirements (Raymo et al., 1989). This site also had good magnetostratigraphic control.

6:2 Development of orbitally tuned timescale for the upper Pliocene at Site 607.

In the development of an orbitally tuned at Site 607 (Raymo et al., 1989), palaeomagnetic measurements still provide the primary stratigraphic control (Clement and Robinson, 1987). In this section we look at how Raymo et al. (1989) extend the oxygen isotope timescales developed in the late Pleistocene (Imbrie et al., 1984) and early Pleistocene (Ruddiman et al., 1986a; Ruddiman et al., 1989) back to 2.75 Ma, using the orbital tuning methods described by Imbrie et al. (1984).

Raymo et al. (1989) have built up a complete sediment record for this time interval at Site 607. Splices from the offset hole (Hole 607A) have been used across the core breaks in the main hole, Hole 607, where disturbance may have occurred. Ruddiman et al., (1986b) document in detail sediment disturbances that

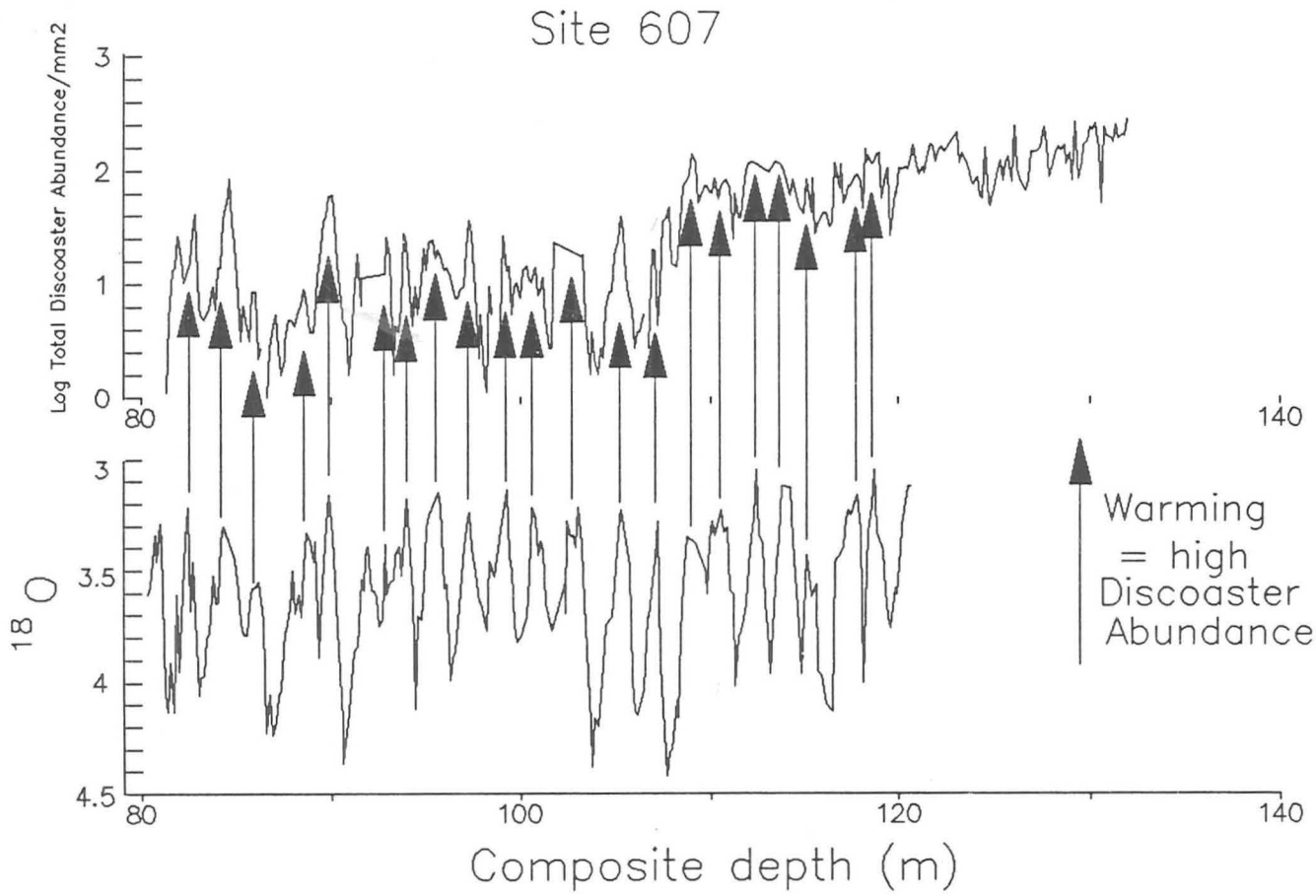

Figure 6:2a. Correlation of total Discoaster abundance with the oxygen isotope record at Site 607.

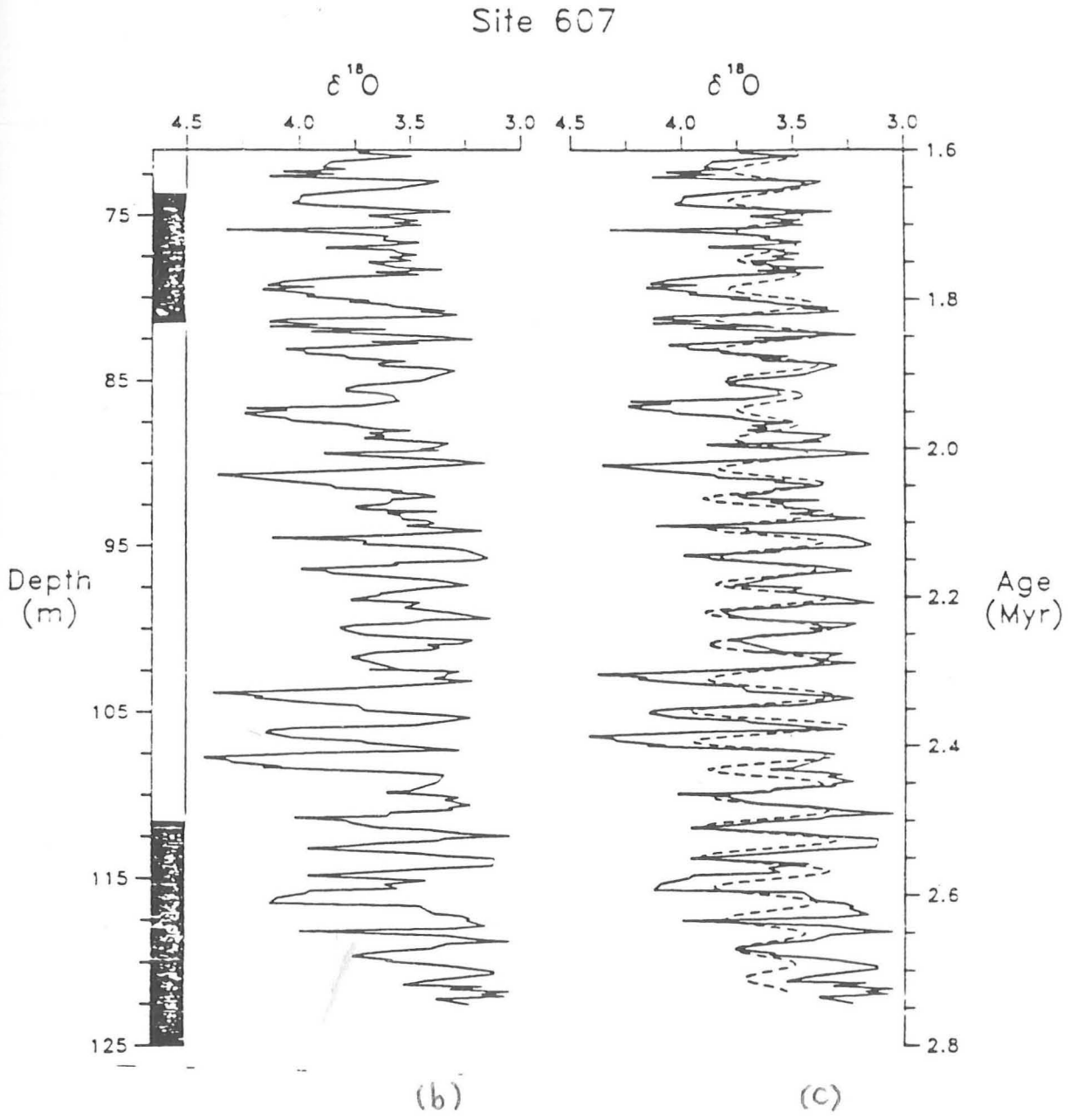

Figure 6:2b & c. Site 607 oxygen isotope record plotted to (b) composite depth (c) magnetic timescale. A 41 ka filter generated by spectral analysis of the data using the magnetic timescale is superimposed on the isotope record (dashed line). (After Raymo et al., 1989)

occurred during the hydraulic piston coring process. Our record of Discoaster abundance was only at Hole 607, and the splices that are used from Hole 607A across the core breaks (Raymo et al., 1989) are only short intervals. From here on, we adopt the composite depths used by Raymo et al. (1989). Figure 6:2a shows that in spite of the addition of splices from Hole 607A, there is a good agreement between the total Discoaster abundance peaks of Hole 607 with the oxygen isotope record of the composite depth section for Site 607.

In Figures 6:2b & 6:2c, the $\delta^{18}O$ record of Site 607 is plotted versus the composite depth and age. The ages were obtained by linear interpolation between the following magnetic events: Jaramillo (bottom=0.98 Ma), Olduvai (top=1.66 Ma), Matuyama/Gauss (2.47 Ma) and the Kaena (top=2.92 Ma). Spectral analysis by Raymo et al. (1989) on this age model has revealed that variations occur mainly at the 41 ka periodicity of obliquity. The filter of the 41 ka component of the record is superimposed on the raw data in Figure 6:2c. This indicates that prior to 2.0 Ma, the untuned data appears to vary mostly at the 41 ka obliquity rhythm. After 2.0 Ma, there is a more complex climatic response in the $\delta^{18}O$ record corresponding with more power concentrated at higher and lower frequencies.

Raymo et al. (1989) have assumed that individual $\delta^{18}O$ cycles in the data can be associated with specific orbital cycles using a fixed time lag. For "tilt" tuning, a 8 ka lag of $\delta^{18}O$ behind obliquity was used as demonstrated for the late Pleistocene (Imbrie et al., 1984). Similarly, a 5 ka lag (Imbrie et al., 1984) was used for "precession" tuning. In brief, Raymo et al. (1989) began by tuning

TABLE 6:2 Names, Ages and Depths of Late Pliocene ^{18}O Stages from 1.80–2.75 Ma (after Raymo et al., 1989).

^{18}O Stage	AGE (Ma)	Depth (m)	^{18}O Stage	AGE (Ma)	Depth (m)	^{18}O Stage	AGE (Ma)	Depth (m)
71	1.801	80.81	87	2.138	95.70	102	2.442	109.80
72	1.829	81.71	88	2.152	96.33	103	2.463	110.55
73	1.853	82.50	89	2.177	97.31	104	2.482	111.47
74	1.862	83.15	90	2.198	98.21	105	2.500	112.40
75	1.883	84.35	91	2.221	99.33	106	2.523	113.16
76	1.908	85.48	92	2.238	99.86	107	2.545	113.97
77	1.922	86.10	93	2.260	100.83	108	2.565	114.79
78	1.941	86.90	94	2.275	101.66	109	2.583	115.31
79	1.985	88.57	95	2.301	102.94	110	2.601	116.14
80	2.001	89.32	96	2.317	103.97	111	2.616	117.46
81	2.013	89.90	97	2.340	105.30	112	2.645	118.09
82	2.027	90.63	98	2.362	106.20	113	2.667	118.69
83	2.049	91.81	99	2.382	107.25	114	2.685	119.59
84	2.069	93.00	100	2.404	107.85	115	2.706	120.56
85	2.091	94.01	101	2.424	108.75	116	2.730	121.31
86	2.110	94.50						

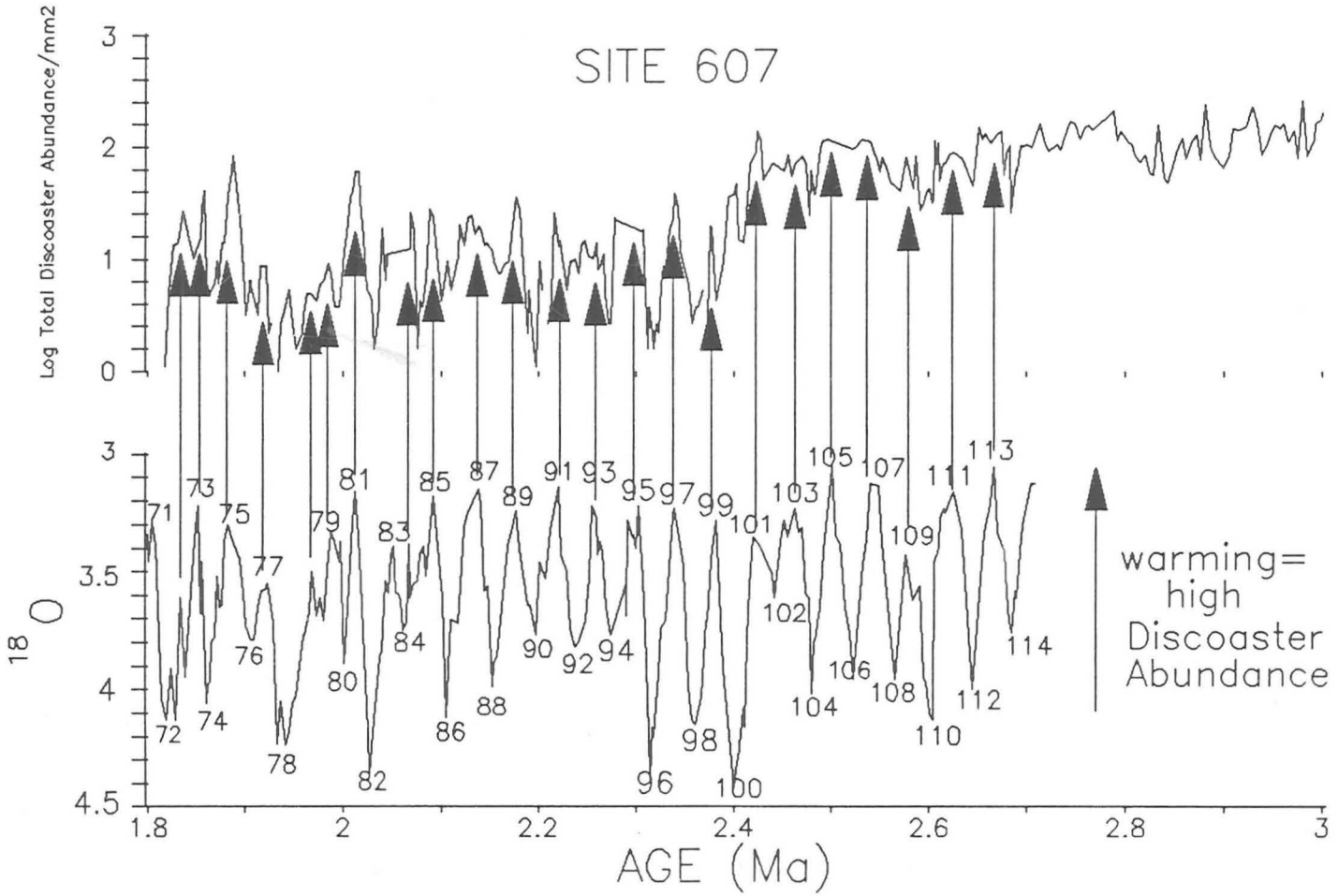

Figure 6:2d benthic
Total Discoaster Abundance versus the isotope record
on orbitally tuned timescale
(oxygen isotope stratigraphy after Raymo et al., 1989)

between 2.1 and 2.75 Ma, where each $\delta^{18}O$ maxima/minima is easily correlated to the tilt minima/maxima nearest in age (Berger, 1977). However, between 1.6 and 2.1 Ma, Raymo et al. (1989) adjusted the tuning strategy to take account of the effects of precessional forcing. This is accomplished by using a tuning target where precessional forcing is added to the obliquity forcing (still dominant), with the appropriate lags. For further details of this refer to Raymo et al. (1989).

This now provides us with a highly detailed age-model back to 2.73 Ma, beyond which we have extrapolated. The age control points are the midpoints of the isotope stages (Table 6:2, Fig. 6:2d). In Figure 6:2e, the LAD of D. brouweri and D. triradiatus is seen to occur within stage 72, as seen at Sites 552, 658 and 677. The base of the D. triradiatus acme is shown to occur within stage 82, as similarly demonstrated at Site 677 (Shackleton and Hall, 1989). Stages 72 and 82 are both relatively intense glacials. A dramatic drop in total Discoaster abundance occurs in stage 100, which is when the first major ice-rafting was observed at Site 552 (Shackleton et al., 1984). Raymo et al. (1989) date stages 72, 82 and 100 as 1.83, 2.03 and 2.4 Ma respectively.

In Figure 6:2f, the LAD of D. pentaradiatus at Site 607 is associated with stage 100, the first large glacial event. Although, Raymo et al. (1989) believe that the LAD of D. surculus is poorly constrained, the data here (and relative Discoaster abundances in Chapter 2) suggests that this similarly occurs during stage 100, as seen at Site 658 (Sarnthein and Thiedemann, 1989). The ages of the LAD's of D. pentaradiatus and D. surculus are not thought to be largely different from those suggested in Chapter 2 of 2.38 and 2.39 Ma respectively,

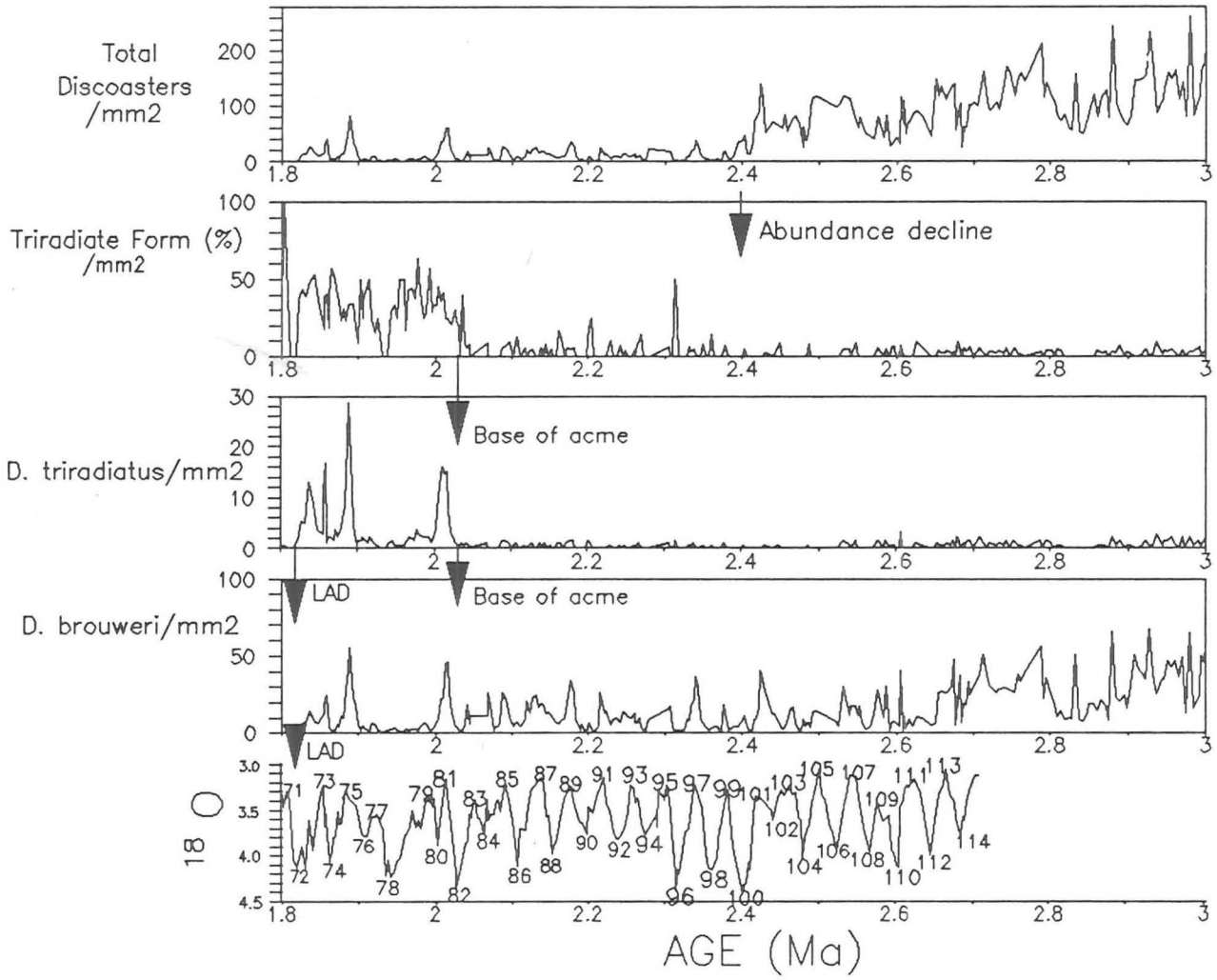

Figure 6:2e.
Abundance of D. brouweri, D. triradiatus and total Discoasters versus the benthic oxygen isotope record on an orbitally tuned timescale.

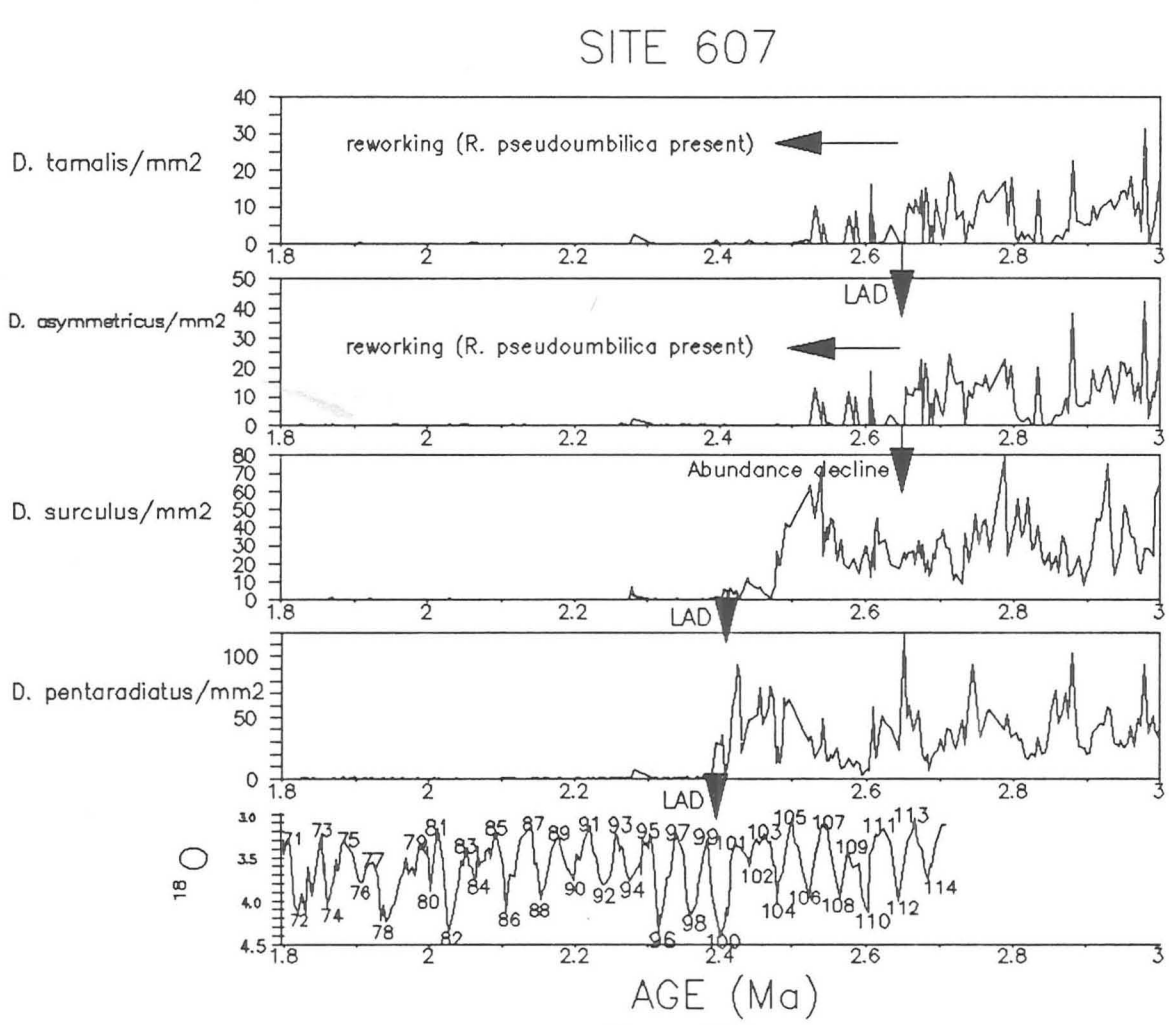

Figure 6:2f
Abundance of D. pentaradiatus, D. surculus
, D. asymmetricus and D. tamalis versus the
benthic oxygen isotope record on an orbitally tuned timescale

perhaps occurring 10-20 ka earlier on this new timescale.

The LAD and abundance decline of D. tamalis and D. asymmetricus respectively, occurs in stage 112 (Fig. 6:2f). This is still approximately at 2.65 Ma. Reworking after 2.65 Ma, is confirmed by D. tamalis and D. asymmetricus being associated with R. pseudoumbilica (LAD=3.56 Ma) (Jan Backman, Pers. Comm.). Raymo et al. (1989) suggested an age ranging from 2.62 to 2.72 Ma for the LAD of D. tamalis, but the data indicates strong evidence in support of an age of 2.65 Ma.

6:3 Orbitally tuned timescale compared with bio-magnetostratigraphic timescale at Site 607.

Here, the orbitally tuned timescale for total Discoaster abundance is compared with the timescale generated in Chapter 2, which is based on biostratigraphy and magnetostratigraphy (Fig. 6:3a). It is immediately apparent that the orbitally tuned timescale is more stretched out than the bio-magnetostratigraphic timescale, producing a younger datum for the extinction of D. brouweri at 1.83 Ma and extending the Discoaster record prior to 3.0 Ma. The Discoaster record with the bio-magnetostratigraphic timescale extends back to only approximately 2.95 Ma. The dramatic decrease in total Discoaster abundance at 2.4 Ma on the original timescale, occurs a little older at 2.41 Ma, on the orbitally tuned timescale. Spectral analysis on the two timescales (Fig. 6:3b) demonstrates the significance of obliquity in both time intervals. During approximately 1.8-2.4 Ma, obliquity is still the main component, but associated with lower and higher frequencies. In the orbitally tuned record, most of the power is associated with

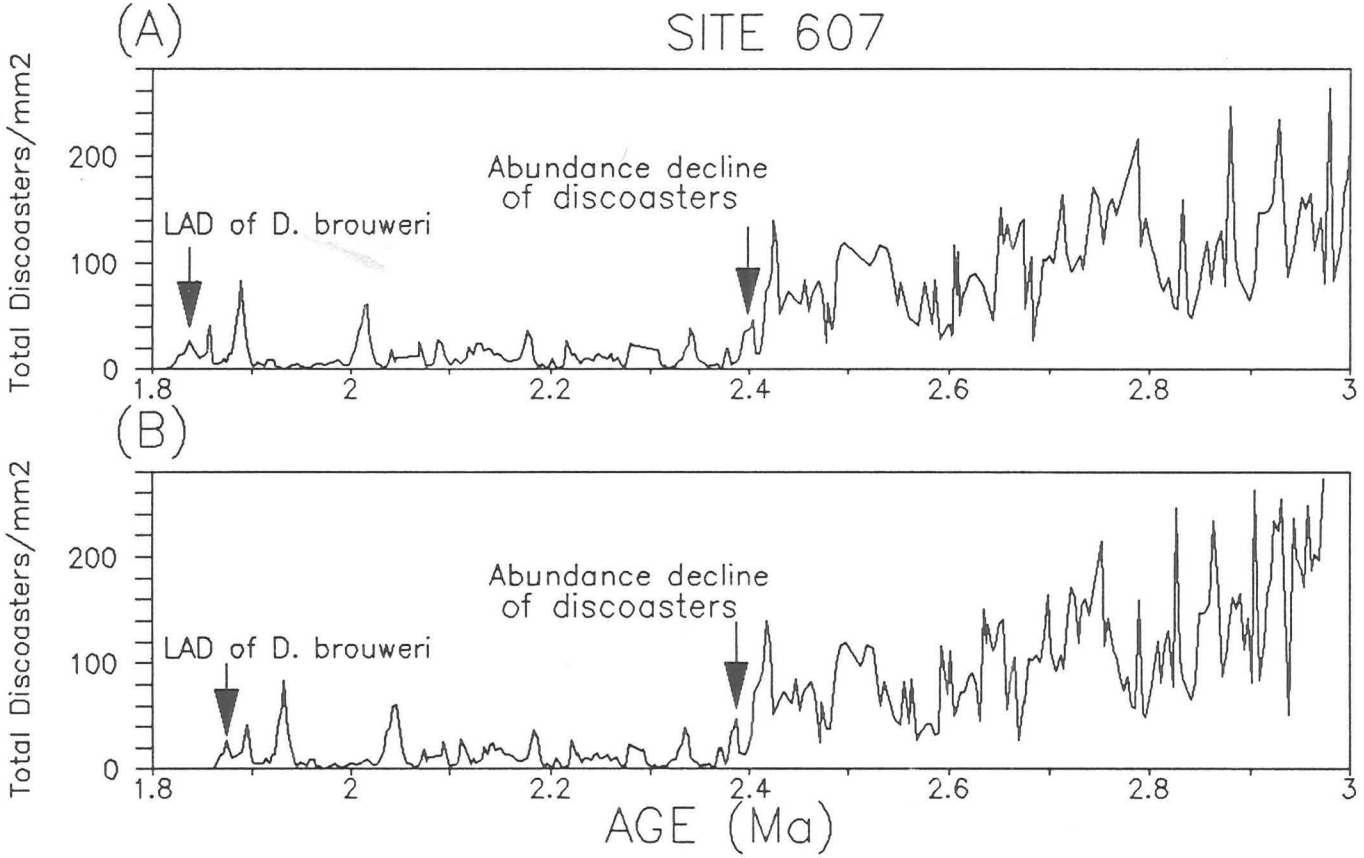

Figure 6:3a

Total Discoaster Abundance/mm2 compared at Site 607 versus age (A) orbitally tuned timescale (B) bio–magnetostratigraphic timescale

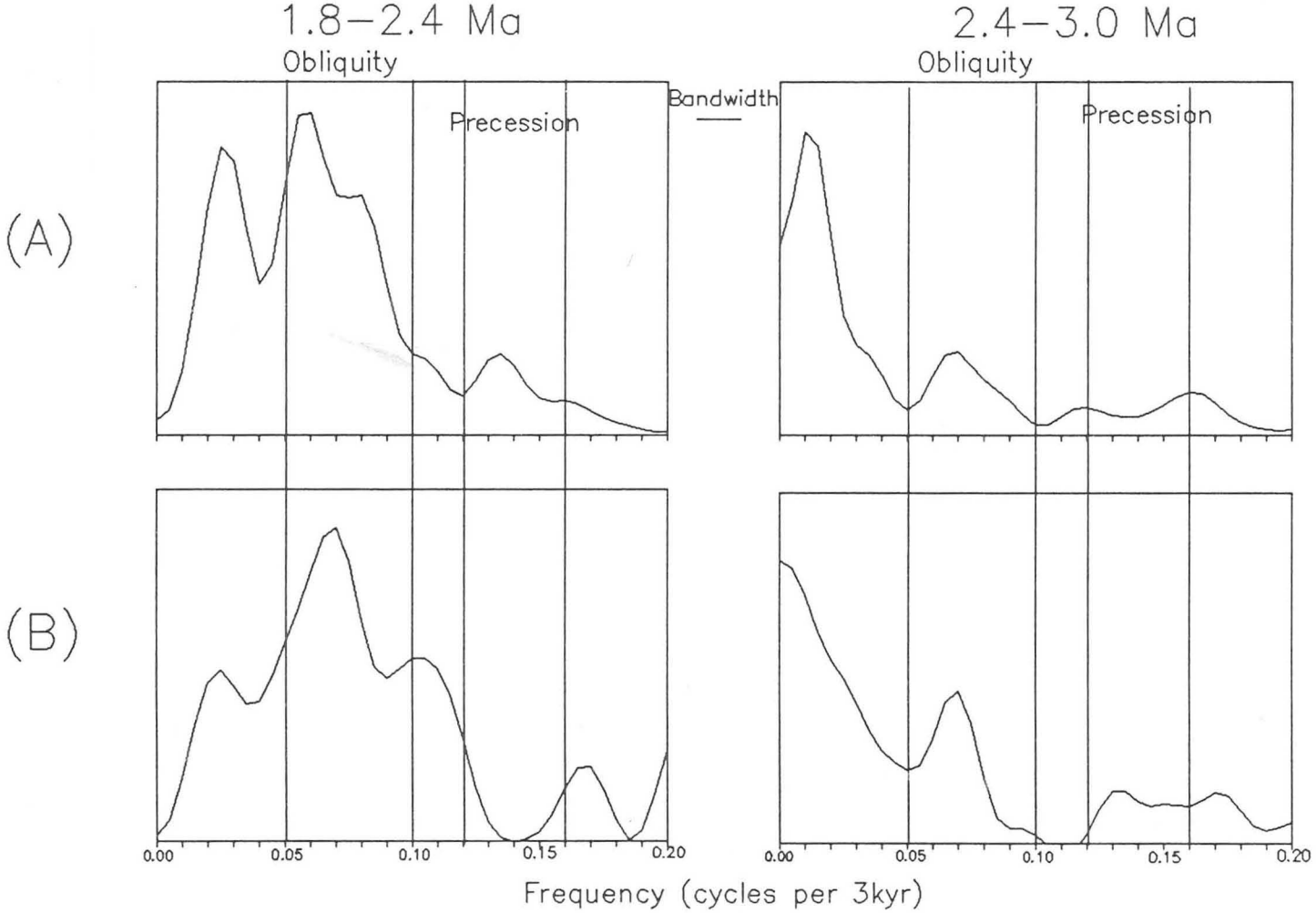

Figure 6:3b

Spectral power density compared on 2 time intervals of the total Discoaster data at Site 607 with two timescales : (A) Bio–magnetostratigraphic

(B) Orbitally tuned

variations occurring primarily at the 41 ka period of obliquity. However, even in the untuned record, the obliquity component is still seen to be an important component. Between approximately 2.4-3.0 Ma, nearly all the power is associated with the 41 ka period of obliquity. The orbitally tuned timescale accentuates the obliquity component even further in the Discoaster record.

6:4 Orbitally tuned timescales and the Discoaster record at Site 677

Correlation can be shown to be very limited between the oxygen isotope and the Discoaster record at Site 677 (Fig. 6:4a) in comparison to the relationship demonstrated at Site 607 (Fig. 6:2a). Frequently, Discoaster abundance peaks even correspond with intense glacials as manifested at e.g., 83m and 92m depth. It seems probable, therefore, that Discoaster abundance variation is responding mostly to a productivity pressure signal and not an ice volume signal.

In the interval between 1.6 and 2.6 Ma, Shackleton, Berger and Peltier, (in press) interpreted the sequence of obliquity cycles at Site 677 in the same way as Raymo et al. (1989) at Site 607. This means the interval between stages 71 and 104 are consistent between the two sites. However, the development of an orbitally tuned timescale at Site 677 (Shackleton, Berger and Peltier, in press) has produced some radical changes to the chronology of the Lower Pleistocene and Upper Pliocene. They have inferred an extra tilt cycle in the lower Bruhnes, and three precession peaks contained in stage 21, whereas Ruddiman et al. (1986) compressed this stage into a single tilt cycle. Lastly, Shackleton, Berger and

TABLE 6:1 Comparison of estimates from Shackleton, Berger and Peltier, (in press) and those previously obtained for selected magnetic reversal boundaries

Isotope Stage	Correlative reversal	Age[1] (Ma)	Age[2]	Age[3]
base 19	base Bruhnes	0.73	0.73	0.78
mid 27	top Jaramillo	0.92	0.90	0.99
mid 31	base Jaramillo	0.98	0.97	1.07
base 35	Cobb Mountain	1.10	1.10	1.19
base 63	top Olduvai	1.66	1.65	1.77
base 71	base Olduvai	1.88	1.82	1.95
104	top Gauss	2.47	2.48	2.60

[1] from Berggren et al. (1985) and Maniken and Gromme (1982)

[2] Ruddiman et al., 1989; Raymo et al., 1989

[3] Shackleton, Berger and Peltier (in press)

TABLE 6:1 Comparison of estimates from Shackleton, Berger and Peltier, (in press) and those previously obtained for selected magnetic reversal boundaries

Isotope Stage	Correlative reversal	Age[1] (ma)	Age[2]	Age[3]
base 19	base Bruhnes	0.73	0.73	0.78
mid 27	top Jaramillo	0.92	0.90	0.99
mid 31	base Jaramillo	0.98	0.97	1.07
base 35	Cobb Mountain	1.10	1.10	1.19
base 63	top Olduvai	1.66	1.65	1.77
base 71	base Olduvai	1.88	1.82	1.95
104	top Gauss	2.47	2.48	2.60

[1] from Berggren et al. (1985) and Maniken and Gromme (1982)

[2] Ruddiman et al., 1989; Raymo et al., 1989

[3] Shackleton, Berger and Peltier (in press)

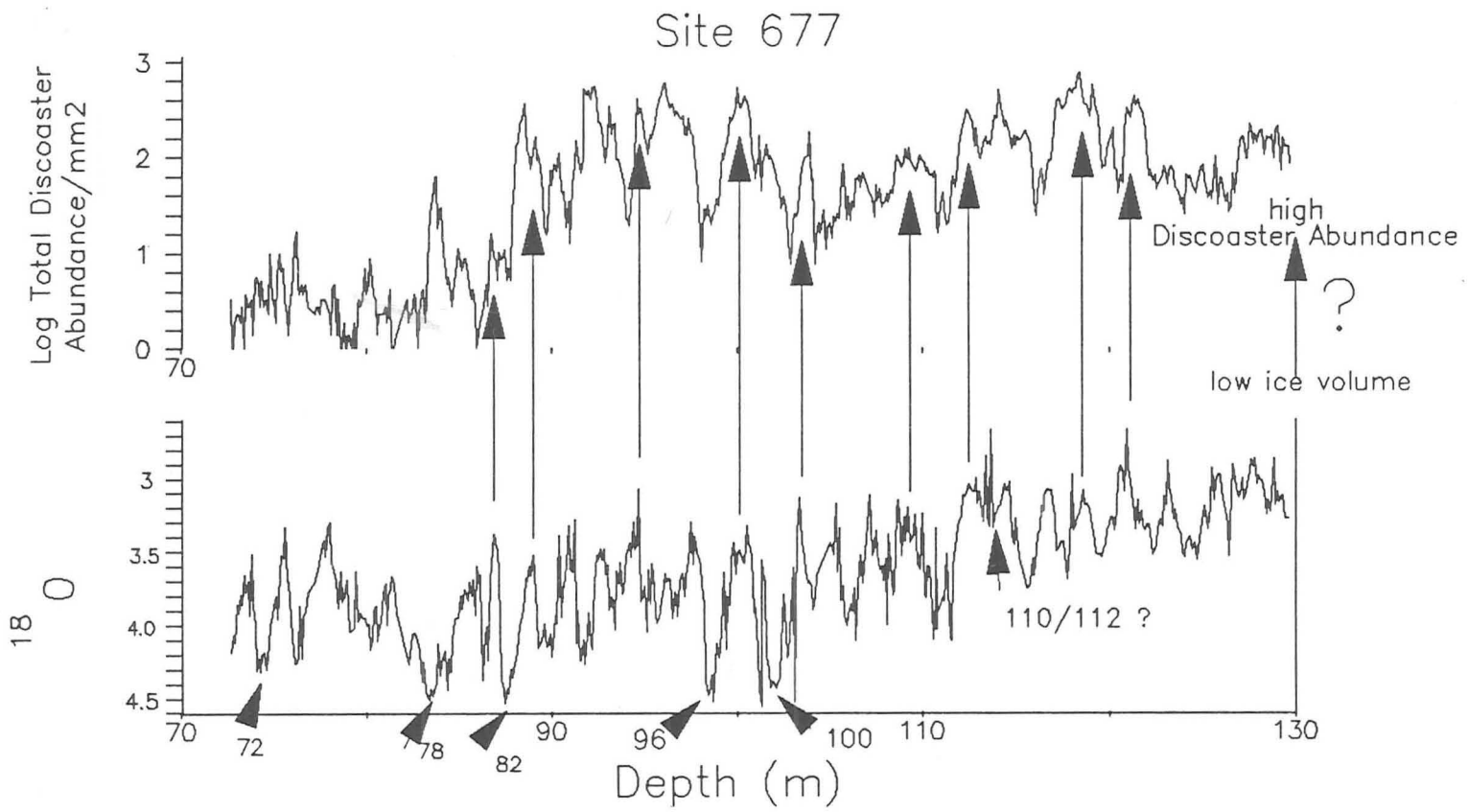

Figure 6:4a
The Discoaster record and the benthic oxygen isotope record at Site 677.

Peltier (in press) interpreted stage 35 as representing more than a single tilt cycle. This has resulted in the estimates for the ages of the last six major magnetic reversals being 5-7% older than the currently accepted values (Table 6:4). As a consequence our Discoaster datums will be greater by the same order of change. Although, the ages have changed in the new timescale for Site 677, the interval of time is essentially the same in the upper Pliocene as estimated by Raymo et al. (1989). This can be demonstrated for the estimate of the time interval between the top of the Gauss and the base of the Olduvai subchron being 0.66 Ma and 0.65 Ma at Sites 607 and 677 respectively (Table 6:4).

Figure 6:4b displays, total Discoaster abundance using the new age-model (Shackleton, Berger and Peltier, in press). The age-model on the new timescale extends back to 2.64 Ma, beyond which it has been extrapolated. In Figure 6:4c, the LAD of D. brouweri and D. triradiatus is seen to occur in stage 72 or the base of stage 71 and this has a new age of 1.96 Ma. The base of the D. triradiatus acme is shown to occur just after stage 82. No dramatic drop in total Discoaster abundance is apparent in stage 100, though this correlates with generally suppressed abundances. However, dramatic decreases in Discoaster abundance do correlate with stages 96 and 82, which are both intense glacials.

In Figure 6:4d, it is difficult to ascertain the LAD of D. pentaradiatus, since it occurs in such suppressed abundances. However, the orbitally tuned timescale reveals radical new information on the LAD of D. surculus. In Site 607, D. surculus was seen to disappear within stage 100, but at Site 677, the distinctive final abundance peak occurs approximately 50 ka after stage 96. This is highly

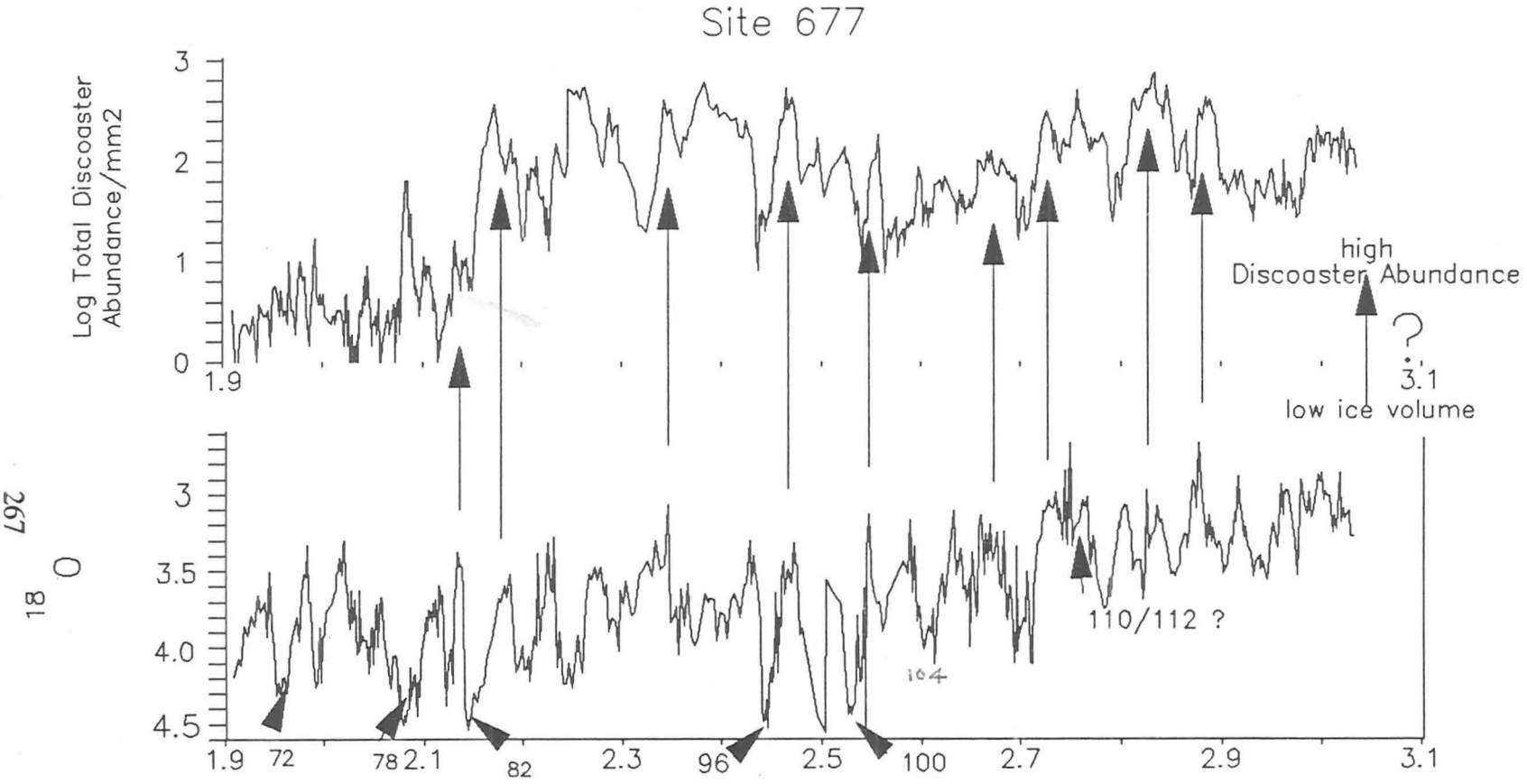

Figure 6:4b

benthic oxygen

Total Discoaster Abundance versus the isotope record on orbitally tuned timescale at Site 677.

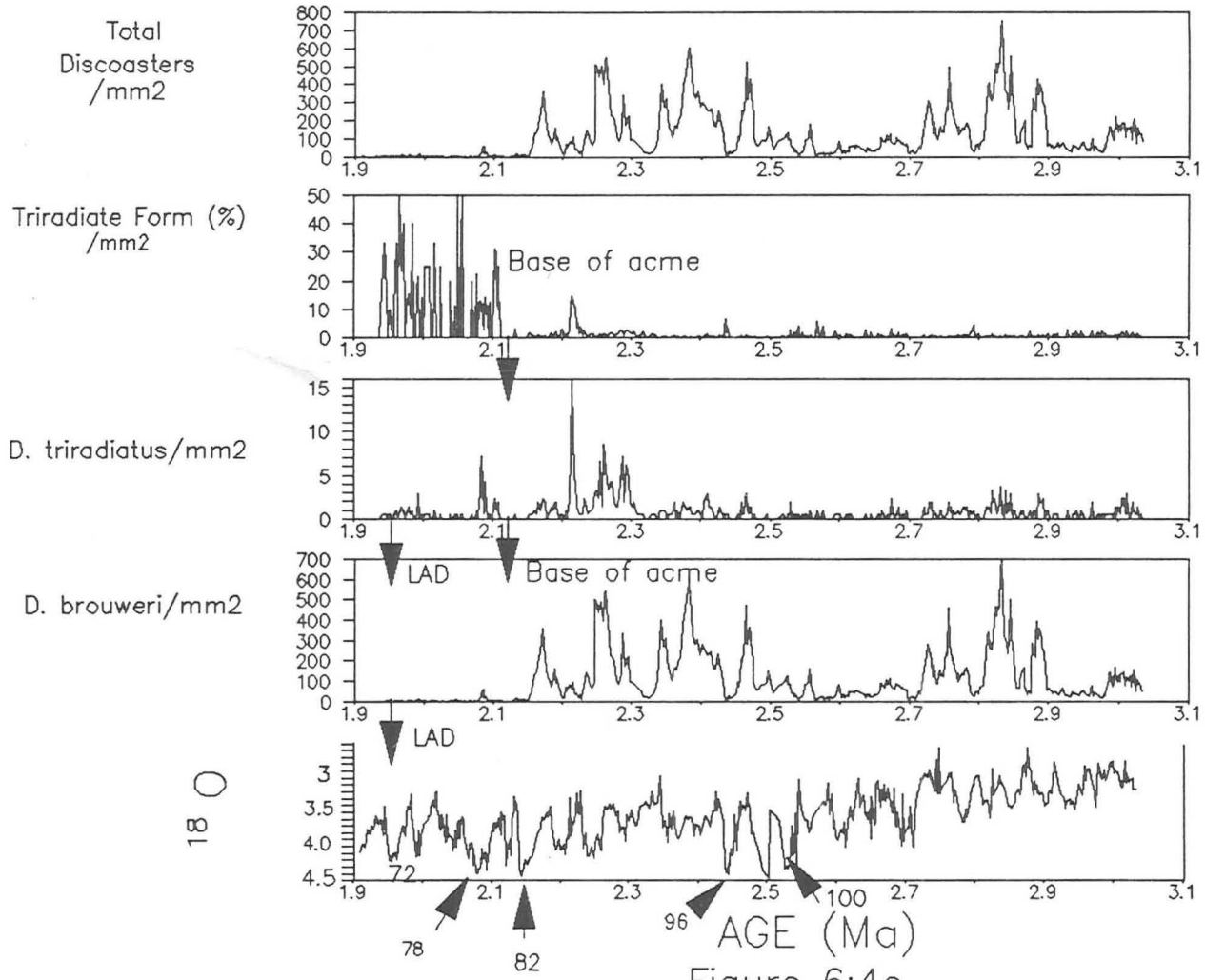

Figure 6:4c

Abundance of D. brouweri, D. triradiatus and total Discoasters versus the oxygen isotope record on an orbitally tuned timescale. at Site 677

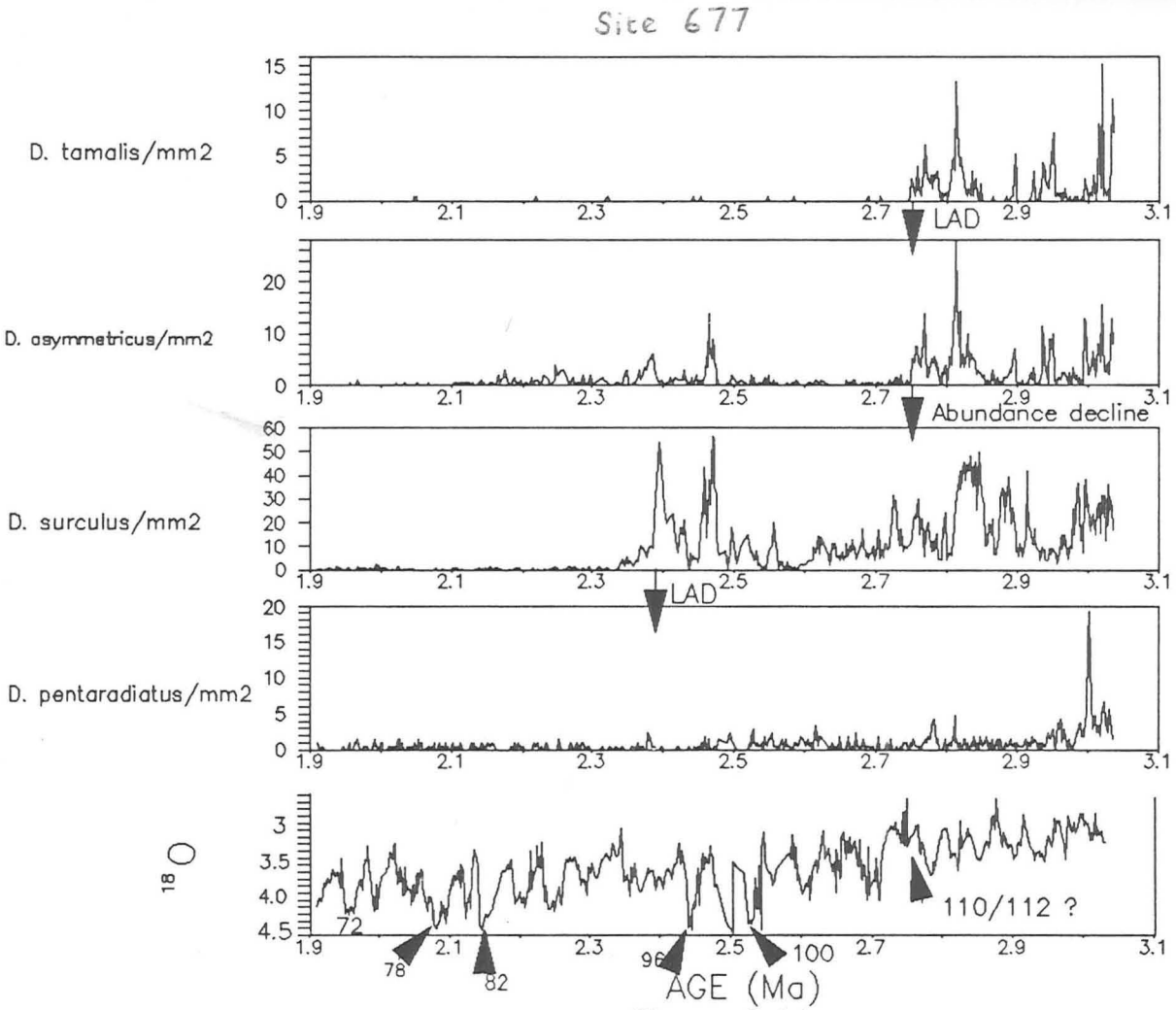

Figure 6:4d

Abundance of D. pentaradiatus, D. surculus , D. asymmetricus and D. tamalis versus the benthic oxygen isotope record on an orbitally tuned timescale

significant because it would mean that D. surculus disappears possibly 120 ka later at Site 677 than at Site 607. In the construction of our original age models, our assumption had been that the LAD of D. surculus was a synchronous global event. The LAD and abundance decline of D. tamalis and D. asymmetricus appears to correspond close to where stage 110/112 is located (N. J. Shackleton, Pers. Comm.), so this may be a globally synchronous event. Future work may confirm this.

6:5 Orbitally tuned timescale compared with biostratigraphic timescale at Site 677.

The orbitally tuned timescale for total Discoaster abundance is compared with the timescale in Chapter 3, which is based solely on biostratigraphy (Fig. 6:5a). The first feature is that the orbitally tuned timescale makes the record older by between 5% and 7%. Secondly, as seen at Site 607, there is more stretching overall of the Discoaster record with the orbitally tuned timescale, although the biostratigraphic timescale is noticeably more stretched in the time interval between 2.1 and 2.4 Ma. Much of the stretching occurs with the orbitally tuned timescale during the low Discoaster abundance interval after 2.2 Ma. At Site 607, the timescale produced a younger LAD for D. brouweri at 1.83 Ma, whereas the timescale for Site 677 (Shackleton, Berger and Peltier, in press) pushes the LAD of D. brouweri back to 1.96 Ma and our Discoaster record examined here beyond 3.00 Ma. The Discoaster record with the biostratigraphic timescale extends back to only approximately 2.94 Ma.

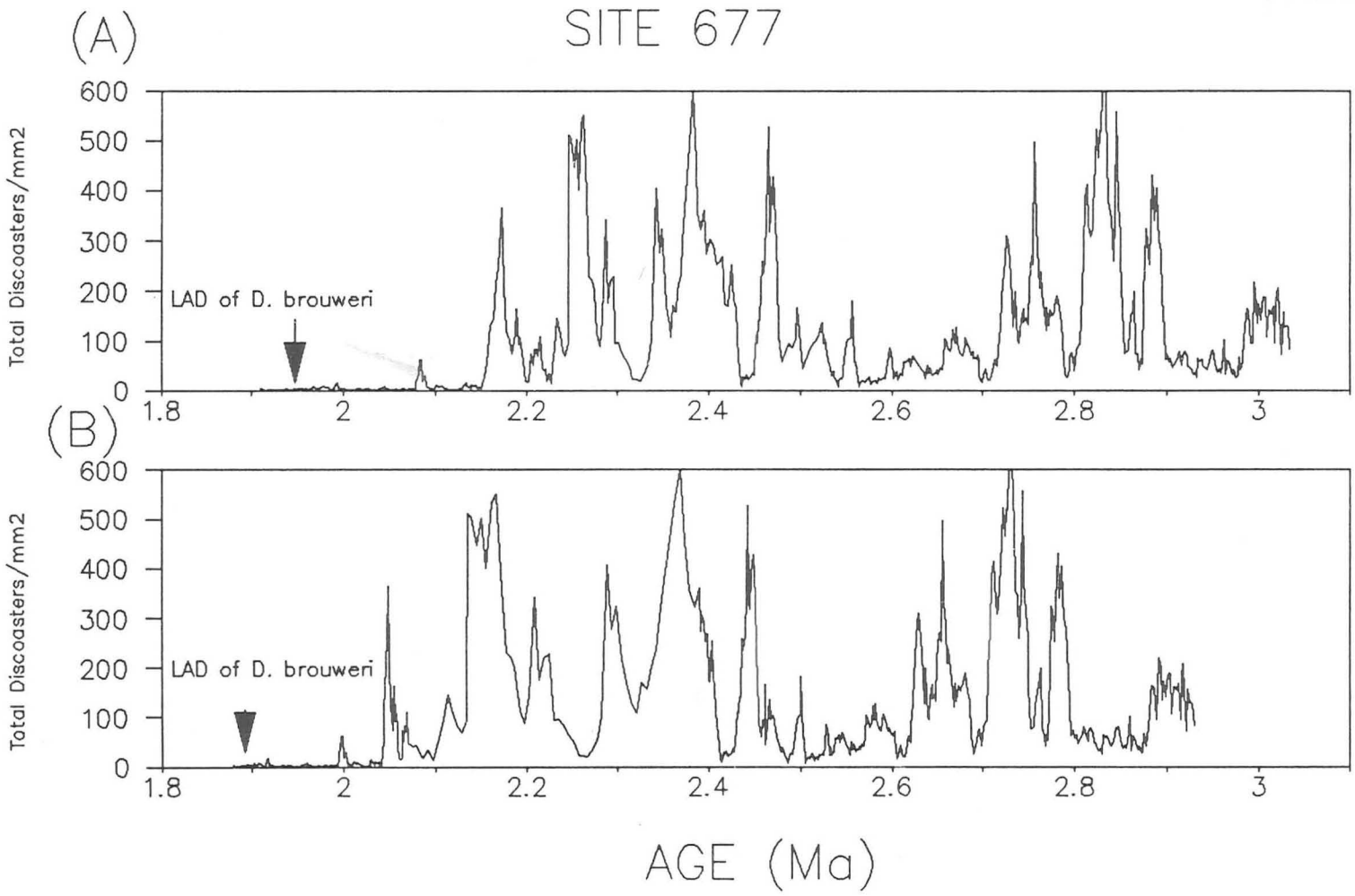

Figure 6:5a

Total Discoaster Abundance/mm2 compared at Site 677 versus age (A) orbitally tuned timescale
(B) biostratigraphic timescale

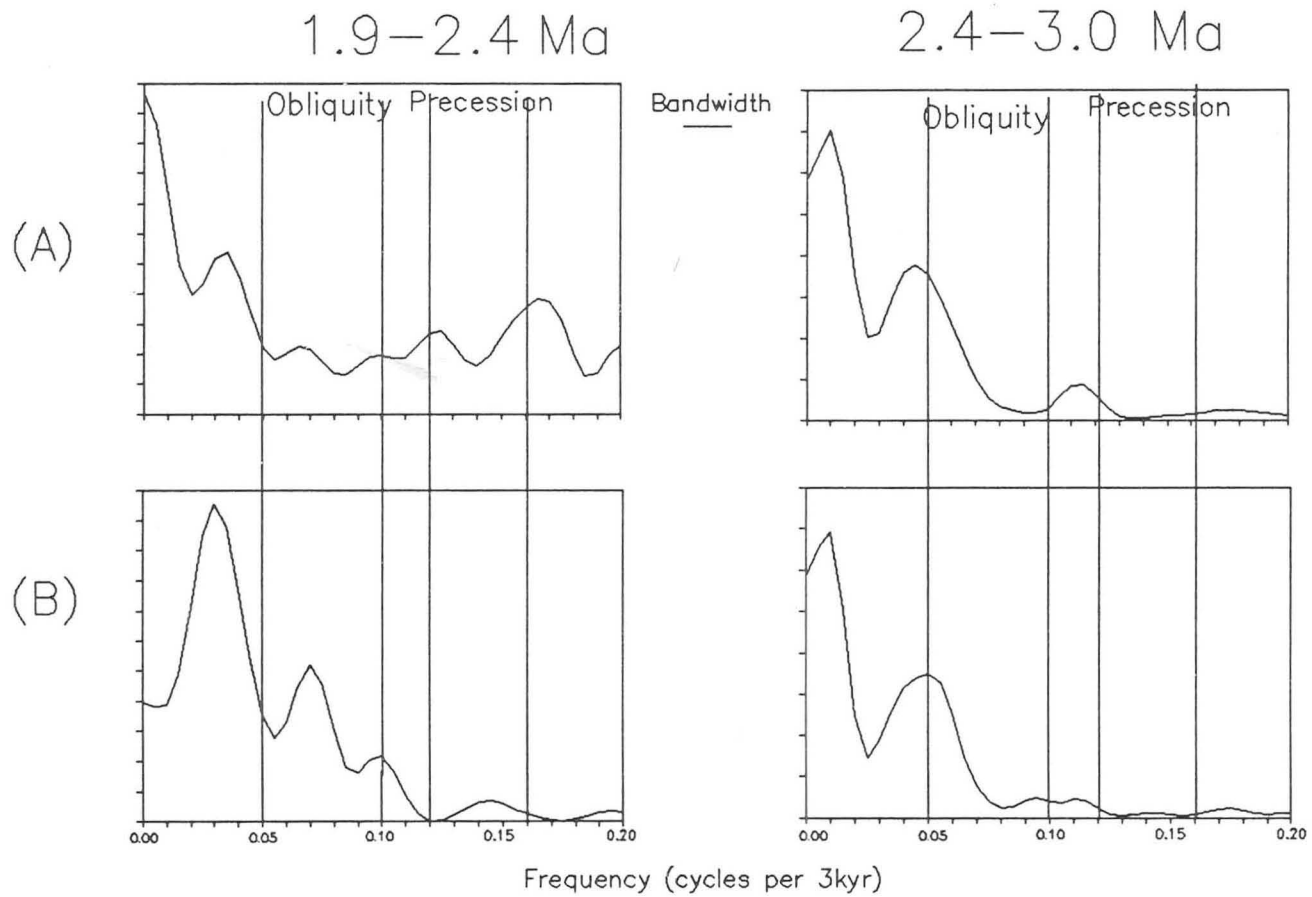

Figure 6:5b

Spectral power density compared on 2 time intervals of the total Discoaster data at Site 677 with two timescales : (A) Bio–magnetostratigraphic
(B) Orbitally tuned

Spectral analysis on the two timescales (Fig. 6:5b) reveals the importance of eccentricity and obliquity between 1.9-2.4 Ma on the orbitally tuned timescale. A minor peak associated with eccentricity occurs in the biostratigraphic record. Between 2.4 and 3.0 Ma, the orbitally tuned age model extends back to only 2.64 Ma, and this reveals a similar unrefined obliquity component as seen using the biostratigraphic age model.

6:6 Discussion

The Discoaster data represented at Site 607, in combination with the orbitally tuned timescale (Raymo et al., 1989) displays the most detailed evidence for the decline of discoasters in relation to the initiation of northern hemisphere glaciation. As mentioned earlier, Site 677, the equatorial Pacific upwelling site, preserved a more detailed record for oxygen isotopes and Discoaster abundances. This has also provided an orbitally tuned timescale for the upper Pliocene, but the discoasters respond inconsistently to the oxygen isotope signal. Site 677 has nevertheless furnished datums for the LAD's of D. surculus and D. tamalis. This has made it possible to assess the diachroneity of these species. It appears that D. surculus survived up to 120 ka longer at Site 677 than Site 607. The constant upwelling conditions at Site 677 may have extended the longevity of D. surculus in the Pacific. Ironically, though D. surculus favoured cooler water conditions, declining temperatures may have hastened its demise, especially at high latitudes, but it was buffered from changes in sea-surface temperatures at the equator, associated with the favourable upwelling conditions of Site 677. However, the diachroneity of D. surculus undermines the construction of our

original age models, which heavily relied upon the synchroneity of the LAD of D. surculus.

The large changes in Discoaster abundance at Site 607, especially prior to 2.4 Ma (Backman and Pestiaux, 1986), one assumes must be mostly due to the high variation in sea-surface temperature experienced at high latitudes. At Site 677, the variation in Discoaster abundance is probably mostly the result of fluctuating productivity pressure. At Site 607, a threshold was reached at stage 100, when only D. brouweri could survive the intense glacials afterwards. It is probably no coincidence that the extinction of D. pentaradiatus and D. surculus at Site 607 correlate with an intense glacial (stage 100), when the amplitude of the $\delta^{18}O$ signal first exceeded 1.00ppm. This cooling was associated with significant ice rafting as far south as 40°N in the open North Atlantic. At Site 677, however, D. surculus survived after stage 96. Nevertheless, it is interesting that most of the Discoaster events at Site 607 appear to correspond with intense glacials : the LAD of D. tamalis at stage 112; the base of the D. triradiatus acme at stage 82; the LAD's of D. brouweri and D. triradiatus at stage 72. These LAD's occur at approximately the same stages at Site 677.

The Discoaster data at Site 607 indicates that significant variation in northern hemisphere climate (and continental ice sheets) occurred prior to 2.4 Ma. Discoaster abundance variations reveal climatic oscillations occurring almost exclusively at the 41 ka period of obliquity. The abundance decline, prior to 2.4 Ma, reflects the gradual onset of northern hemisphere glaciation, which occurred over several hundred thousand years and resulted with a 30% increase

in average ice sheet size at 2.4 Ma. At Site 677, the Discoaster record appears to fluctuate similarly mostly at the obliquity periodicity, but this is less refined.

The fortunes of D. brouweri abundance at Site 607 (Fig. 6:2e) after 2.4 Ma are strongly linked to fluctuations in the size of the glacial ice sheets. The abundances are generally suppressed, but during warm interglacials (e.g. stages 75, 81 and 97), there are accompanying increases. From 2.3 to 2.1 Ma, when the $\delta^{18}O$ amplitude fell below 1.0ppm , D. brouweri abundances were less suppressed. It is thought that glacial ice sheets were as small as, or smaller than those observed prior to 2.4 Ma. After 2.1 Ma, the $\delta^{18}O$ record reached again glacial values as positive as those at 2.4 Ma, and some major suppression is observed in D. brouweri abundance, especially between 1.9-2.0 Ma (notably stage 78). At Site 677, abundances of D. brouweri after stage 100 are suppressed during stage 96 and after stage 82, but it is very difficult to relate the oxygen isotope record to the Discoaster record (Fig. 6:4c).

It is interesting that after 2.4 Ma at Site 607, some long wave component is apparent from the spectral analysis of the tuned and untuned D. brouweri abundance data. The intense glaciation at stage 82 (the base of the D. triradiatus acme) and the first significant glaciation at stage 100 (LAD of D. surculus and D. pentaradiatus) is separated by approximately 400 ka . This suggests that eccentricity may be a controlling factor. Some longwave component is also apparent from the tuned and untuned D. brouweri abundance data of Site 677 covering a similar time interval. Backman and Pestiaux (1986) discovered at Site 606 that Discoaster abundance variations appear to fluctuate at the 400 ka

eccentricity period between 3.6 and 2.0 Ma.

6:7 SUMMARY

1. Discoaster abundance variation is closely linked to the oxygen isotope record at Site 607. Warmer sea-surface temperatures (lower ice volume) corresponds with higher Discoaster abundances. Discoaster abundance is not closely linked to the oxygen isotope record at Site 677. Discoasters are probably responding to a productivity pressure signal.

2. A major abundance decline of discoasters occurs at stage 100 at Site 607, when the amplitude of the $\delta^{18}O$ signal first exceeded 1.0ppm. Stage 100 does coincide with suppressed Discoaster abundances at Site 677, but not a major decrease.

3. Major Discoaster events appear to correspond with intense glacials at Site 607

LAD's of D. brouweri and D. triradiatus	stage 72
Base of D. triradiatus acme	stage 82
LAD's of D. pentaradiatus and D. surculus	stage 100
LAD of D. tamalis	stage 112
D. asymmetricus abundance decline	stage 112

At Site 677, however, the LAD of D. pentaradiatus is indistinct and the LAD of D. surculus occurred after stage 96.

5. The obliquity periodicity was the main component in the Discoaster record prior to 2.4 Ma. After 2.4 Ma, obliquity is still dominant, but accompanied by higher and lower frequencies.

6. The orbitally tuned timescale of Site 677 will require a change to all future chronology in the lower Pleistocene and Upper Pliocene.

7. Further complete high resolution records are needed to establish the global synchroneity of Discoaster datums.

CHAPTER 7: DISCOASTER ABUNDANCE VARIATIONS; A GLOBAL PERSPECTIVE AND PALAEOCLIMATIC IMPLICATIONS.

7:1 Introduction

In this final chapter, a synthesis of our results is produced to create a global overview. The data represented here unequivocally is the best record of phytoplankton abundance today from the upper Pliocene. All the sites in this study are displayed on the CLIMAP maps of modern sea-surface temperature for February and August (CLIMAP, 1981) (Figs. 7:1a & 7:1b). Sea-surface temperatures in the upper Pliocene were probably not very different from today (Table 7:1), and this furnishes us a measure of the range and temperature contrasts between sites. Secondly, all the sites are displayed on the global satellite images of phytoplankton blooms for October-December (Lewis, 1989) to give a proxy indicator of productivity pressure (Plate 6). Our data suggests that discoasters were very susceptible to productivity pressure (Chepstow-Lusty et al., 1989). Using these two modern sources of information, we attempt to summarize the importance of sea-surface temperature and productivity pressure on discoasters as a group and on relative abundances of individual or groups of species.

This chapter uses Discoaster abundance data from two additional Pacific sites: Cores V28-179 and V32-127 from Backman and Shackleton (1983). The same age models have been used, which are based solely on magnetostratigraphy, but the sedimentation rate and hence time resolution are very low (approximately

CHAPTER 7: DISCOASTER ABUNDANCE VARIATIONS; A GLOBAL PERSPECTIVE AND PALAEOCLIMATIC IMPLICATIONS.

7:1 Introduction

In this final chapter, a synthesis of our results is produced to create a global overview. The data represented here unequivocally is the best record of phytoplankton abundance today from the upper Pliocene. All the sites in this study are displayed on the CLIMAP maps of modern sea-surface temperature for February and August (CLIMAP, 1981) (Figs. 7:1a & 7:1b). Sea-surface temperatures in the upper Pliocene were probably not very different from today (Table 7:1), and this furnishes us a measure of the range and temperature contrasts between sites. Secondly, all the sites are displayed on the global satellite images of phytoplankton blooms for October-December (Lewis, 1989) to give a proxy indicator of productivity pressure (Plate 6). Our data suggests that discoasters were very susceptible to productivity pressure (Chepstow-Lusty et al., 1989). Using these two modern sources of information, we attempt to summarize the importance of sea-surface temperature and productivity pressure on discoasters as a group and on relative abundances of individual or groups of species.

This chapter uses Discoaster abundance data from two additional Pacific sites: Cores V28-179 and V32-127 from Backman and Shackleton (1983). The same age models have been used, which are based solely on magnetostratigraphy, but the sedimentation rate and hence time resolution are very low (approximately

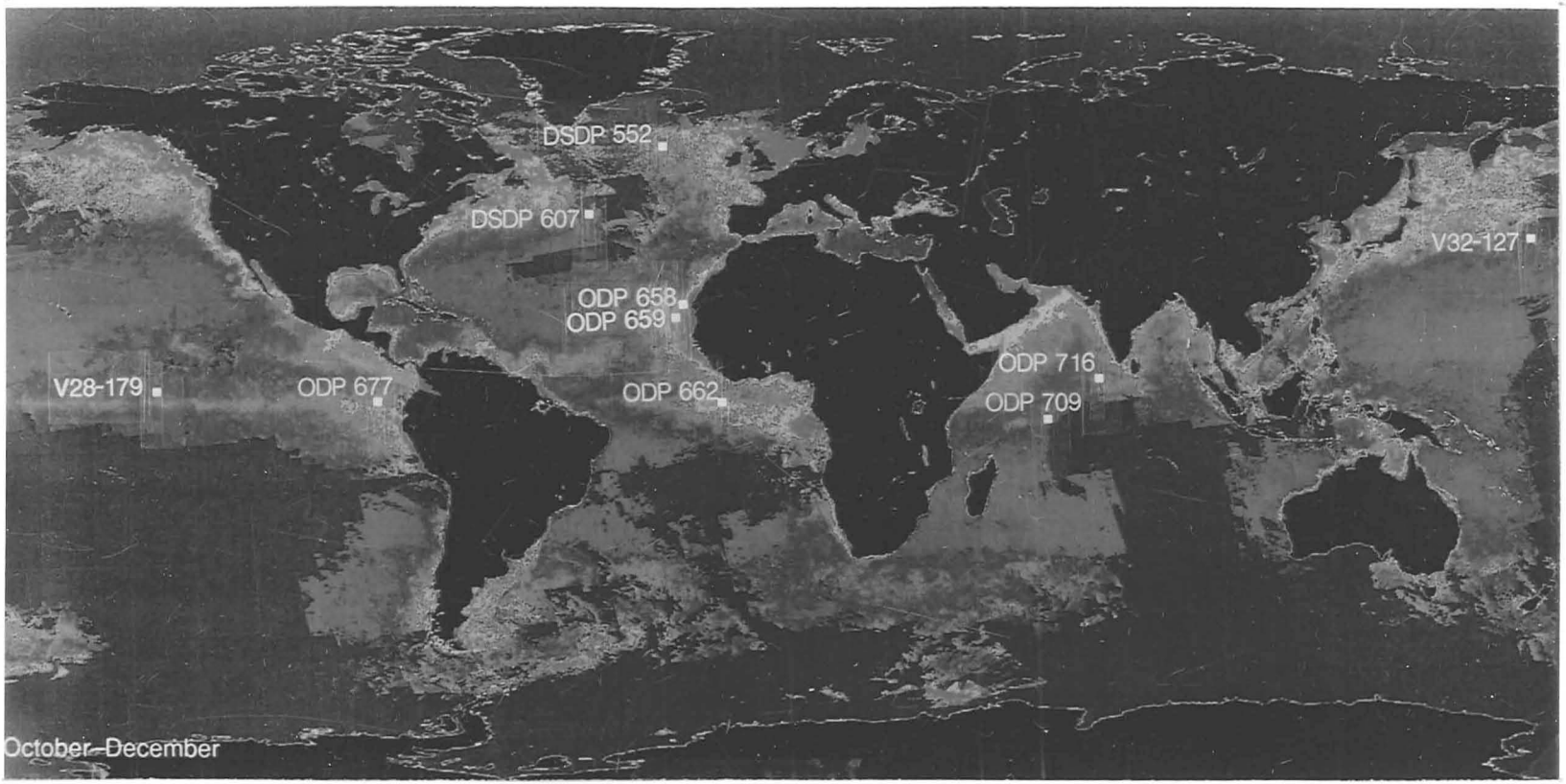

PLATE 6.

All sites in study located on global satellite image of phytoplankton concentrations during October–December, 1979 (after Lewis, 1989)

purple– minimum phytoplankton concentration
red– maximum phytoplankton concentration

TABLE 7:1

Modern sea-surface temperatures at sites in study (CLIMAP, 1981).

SITE	LOCATION	FEBRUARY	AUGUST
	ATLANTIC		
ODP 662	1°S 11°W	27°C	23°C
ODP 659	18°N 21°W	20°C	25°C
ODP 658	20°N 18°W	18°C	22°C
DSDP 607	41°N 33°W	13°C	23°C
DSDP 552	56°N 23°W	9°C	14°C
	INDIAN		
ODP 709	4°S 61°E	28°C	27.5°C
ODP 716	5°N 73°E	28°C	28°C
	PACIFIC		
ODP 677	1°N 84°W	26°C	24.5°C
V28-179	5°N 140°W	27°C	27°C
V32-127	35°N 178°E	16.5°C	25°C

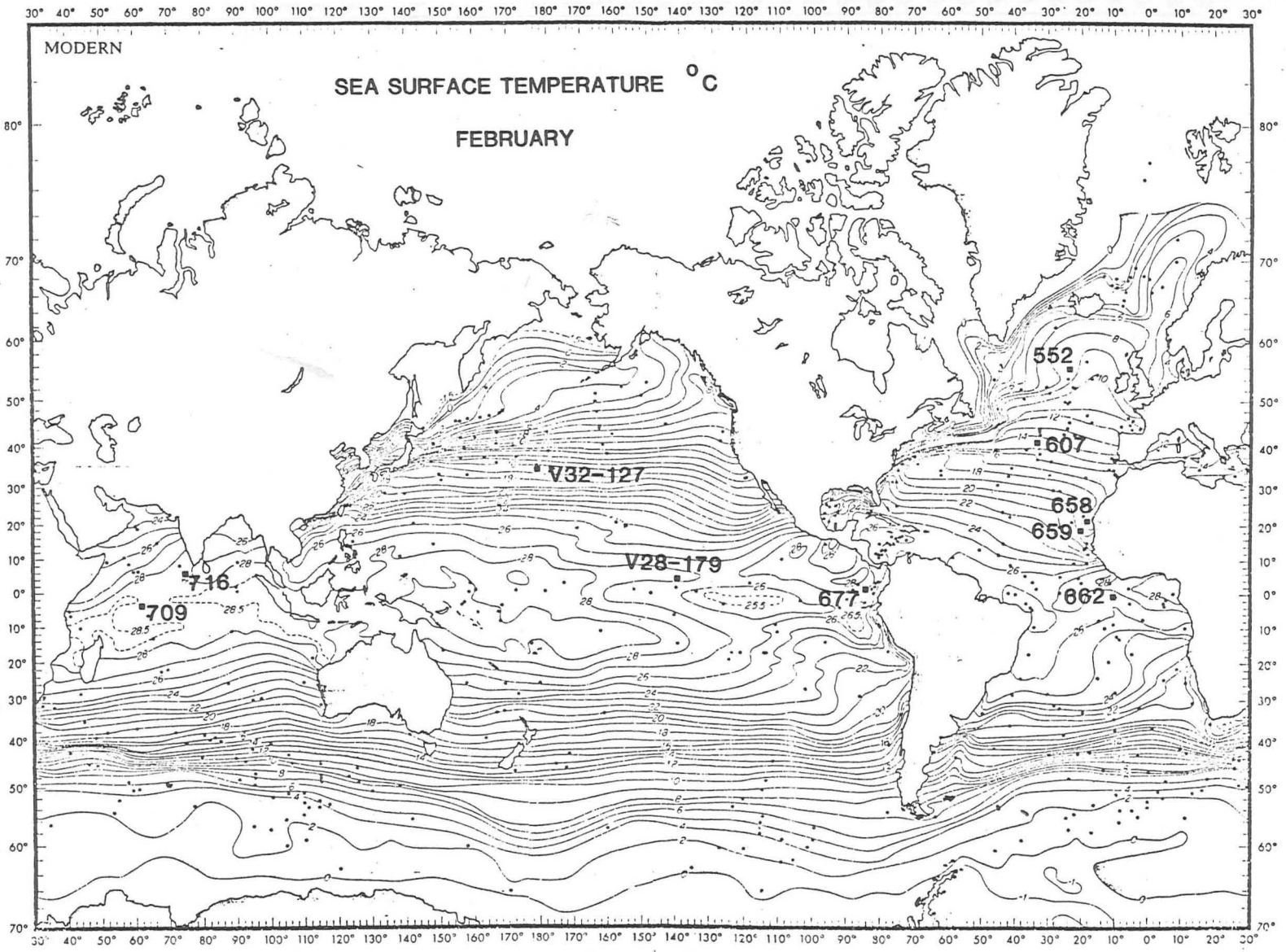

Figure 7:1a

Sites in study on modern sea-surface temperature map for February (after CLIMAP, 1981)

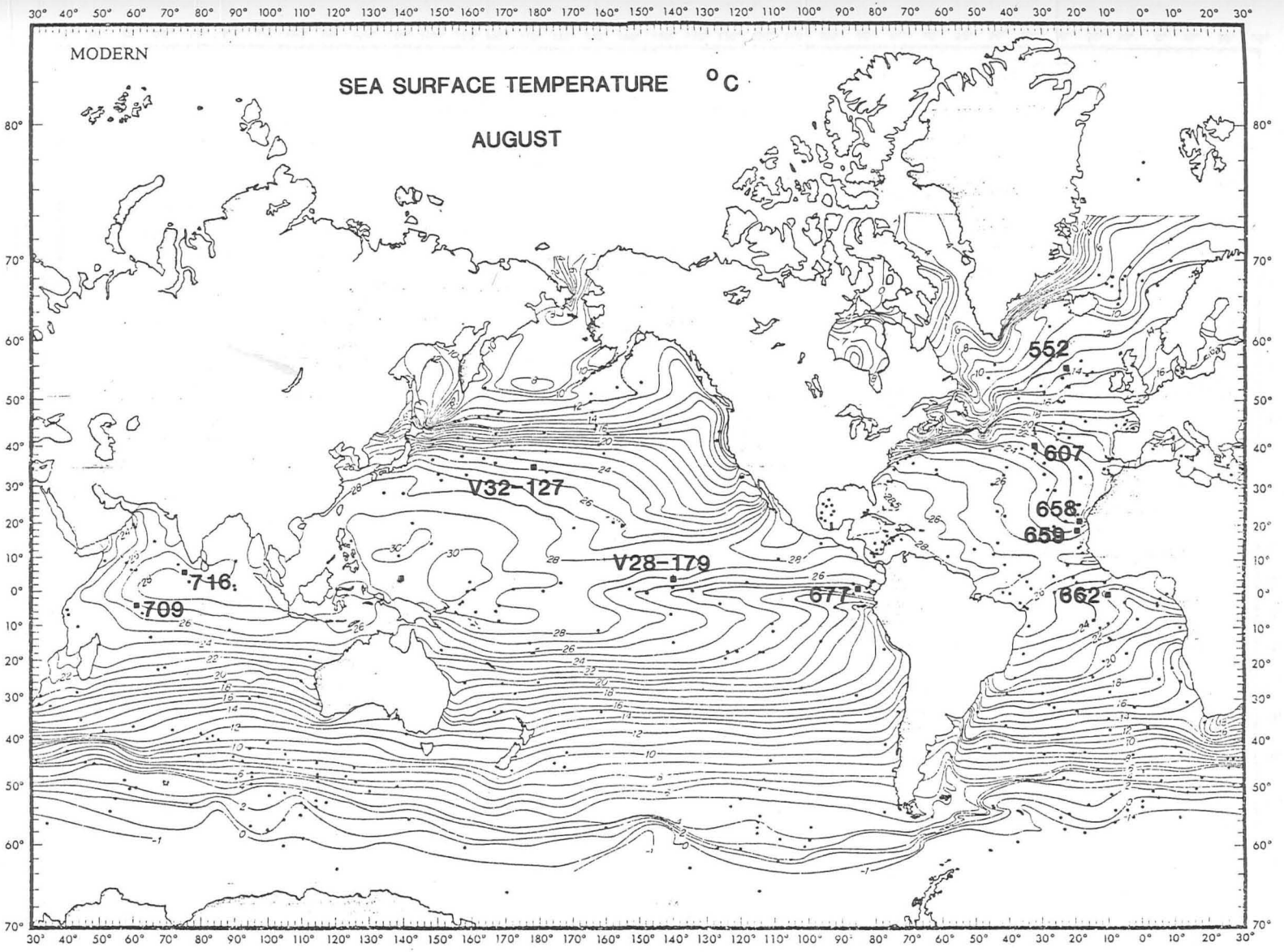

Figure 7:1b
Sites in study on modern sea-surface temperature map for August (after CLIMAP, 1981)

0.3cm/ka at V32-127 and 0.4cm/ka at V28-179). The abundances of the individual Discoaster species at Cores V28-179 and V32-127 are displayed in Appendix B. Here, are only shown the differences in total Discoaster abundance between V28-179, V32-127 and 677 to demonstrate the contrasts in the Pacific (Fig. 7:1d). This also indicates the distinct final abundance decline of D. surculus between 2.38 and 2.44 Ma at V32-127 and V28-179, which has provided important support for our previous age-models. These three sites represent our Pacific data base.

In the second part of this chapter, we compare the mean total Discoaster abundances at all the sites, prior to and after 2.4 Ma. 2.4 Ma marks a critical time when the oxygen isotope record reveals an abrupt cooling (high ice volume), associated with ice rafting at high latitudes in the North Atlantic (Shackleton et al., 1984). We address the question; did Discoaster abundances always decrease globally after 2.4 Ma?

7:2 Selected Palaeoclimatic Indicators

7:2a Global Abundance of Total Discoaster Assemblage

In Figure 7:2a, the mean of the total Discoaster assemblage over the whole time interval investigated for all sites is plotted versus the range of modern sea-surface temperatures. Abundance is on a logarithmic scale . At the extremes, lower temperatures do equate with lower abundances e.g. 552 and higher abundances are shown at the warmer sites e.g. 709 and V28-179. Summer sea-surface temperatures appear to be particularly important. However, modern sea-surface temperatures do not solely explain the similarities in Discoaster abundance

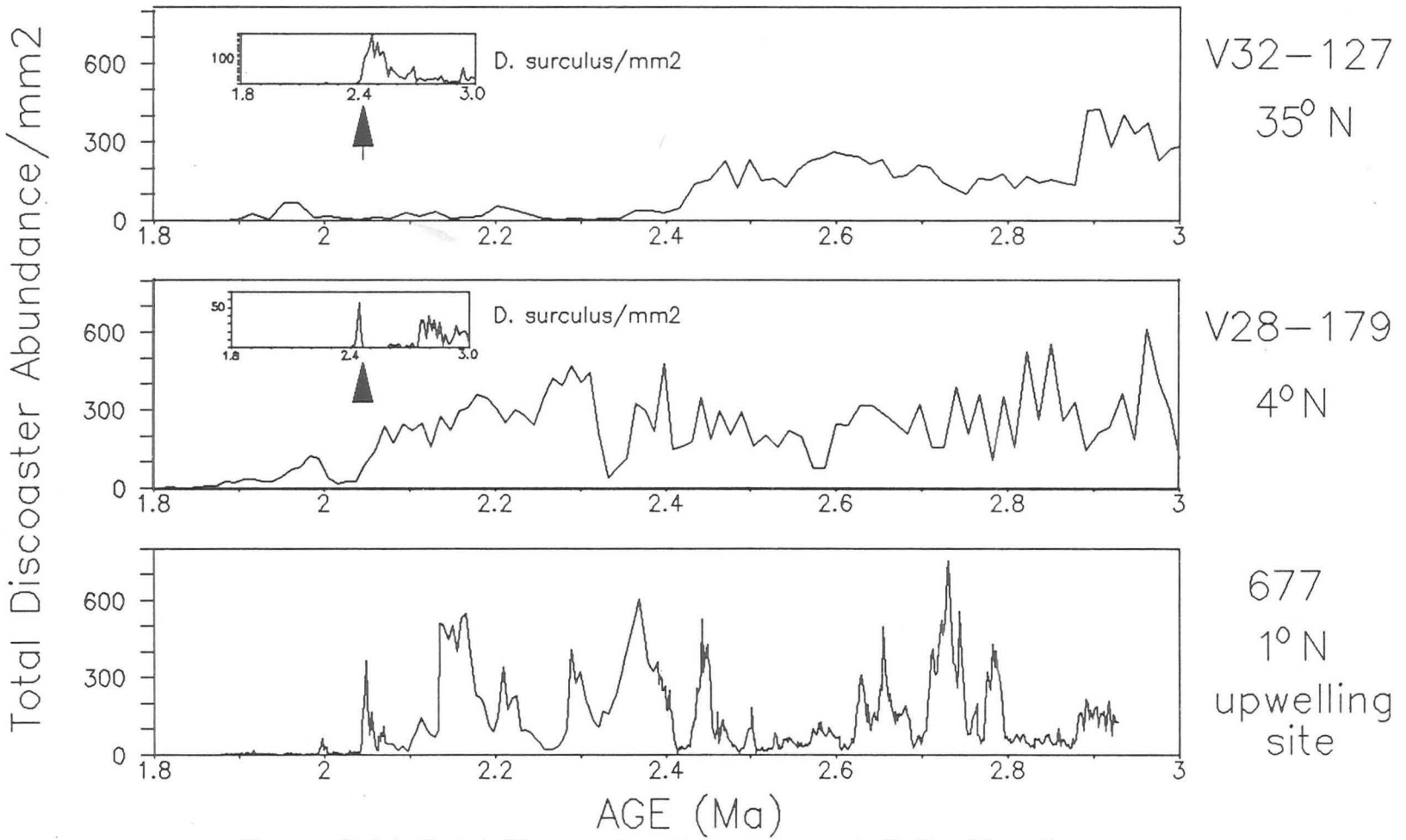

Figure 7:1d. Total Discoaster Abundance at 3 Pacific sites: ODP 677, Cores V28–179 and V32–127. The distinct final abundance of D. surculus at approximately 2.4 Ma is shown for Cores V28–179 and V32–127

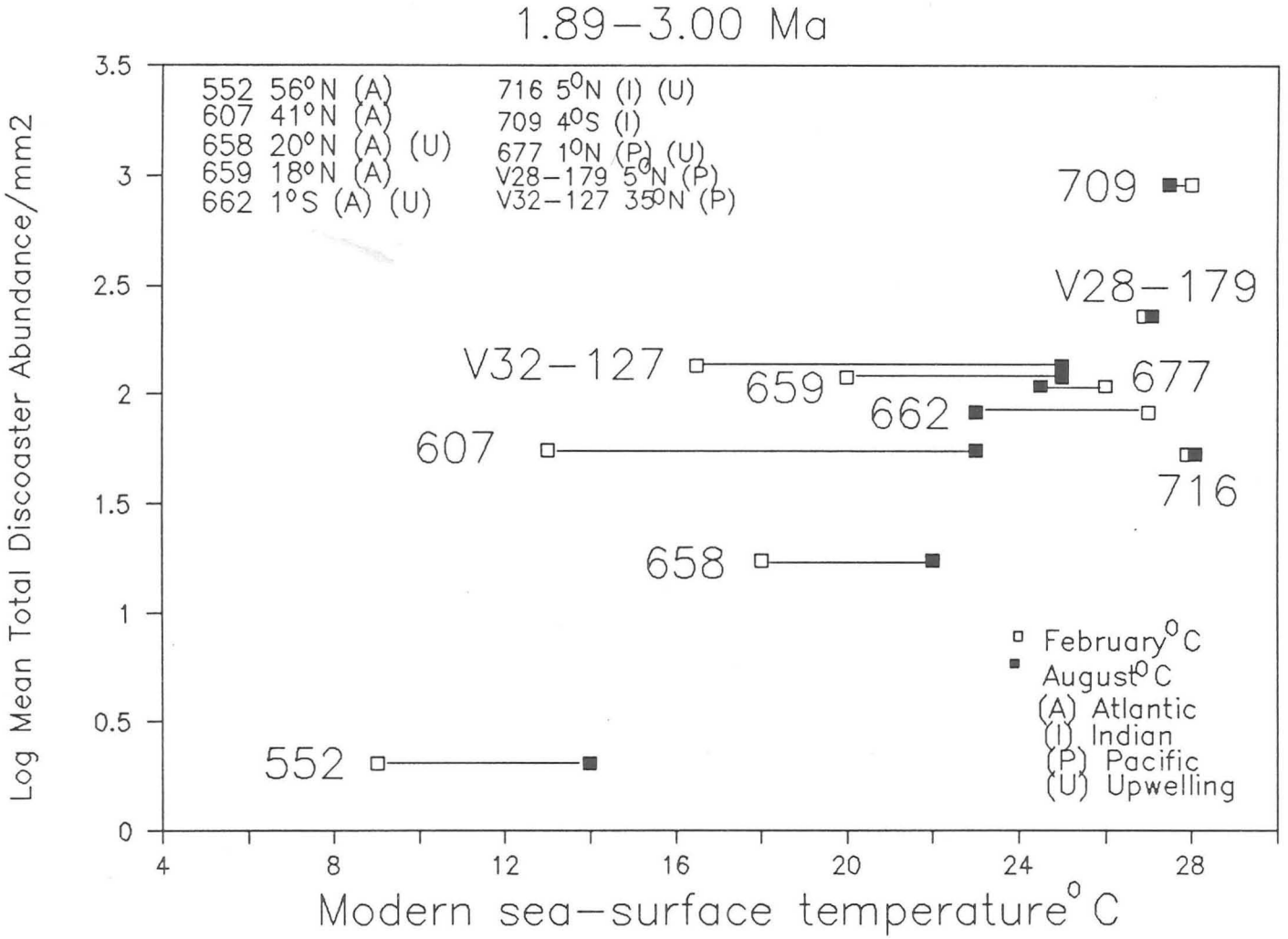

Figure 7:2a. Global synthesis of mean total Discoaster abundance versus modern sea--surface temperature between 1.89–3.00 Ma.

between some of the sites in between these extremes e.g., Sites 607 and 716. Therefore, it is necessary to investigate productivity pressure concurrently.

Sites 709 and V28-179, located on the satellite map of phytoplankton blooms (Plate 6) can be demonstrated to be located in areas of reduced productivity pressure. Upwelling reduces Discoaster abundances e.g. Site 658, but during episodes of reduced productivity pressure the discoasters are going to be produced in greater abundances, if the upwelling site is located in warm waters. This is manifested at Sites 662, 677 and 716, even though these sites are all affected by upwelling to some extent. This reveals the interplay between sea-surface temperature and fluctuations in productivity pressure.

7:2b Relative abundance of D. brouweri prior to 2.3 Ma

In Figure 7:2b, D. brouweri is clearly shown to form a smaller component of the Discoaster assemblage at lower sea-surface temperatures, when other Discoaster species became more important. This relationship is especially apparent with winter sea-surface temperatures. It appears that although upwelling reduces D. brouweri absolute abundance, it does not necessarily reduce the D. brouweri component, unless accompanied by reduced temperatures e.g. compare upwelling sites 658 and 677.

7:2c Relative abundance of D. pentaradiatus

In Figure 7:2c, D. pentaradiatus shows a constant proportion of the Discoaster assemblage at between 20-30% in the Atlantic and Indian oceans, regardless of temperature or productivity. There is a subtle increase in relative abundance of D. pentaradiatus with lower temperatures in the Atlantic. This ecologically

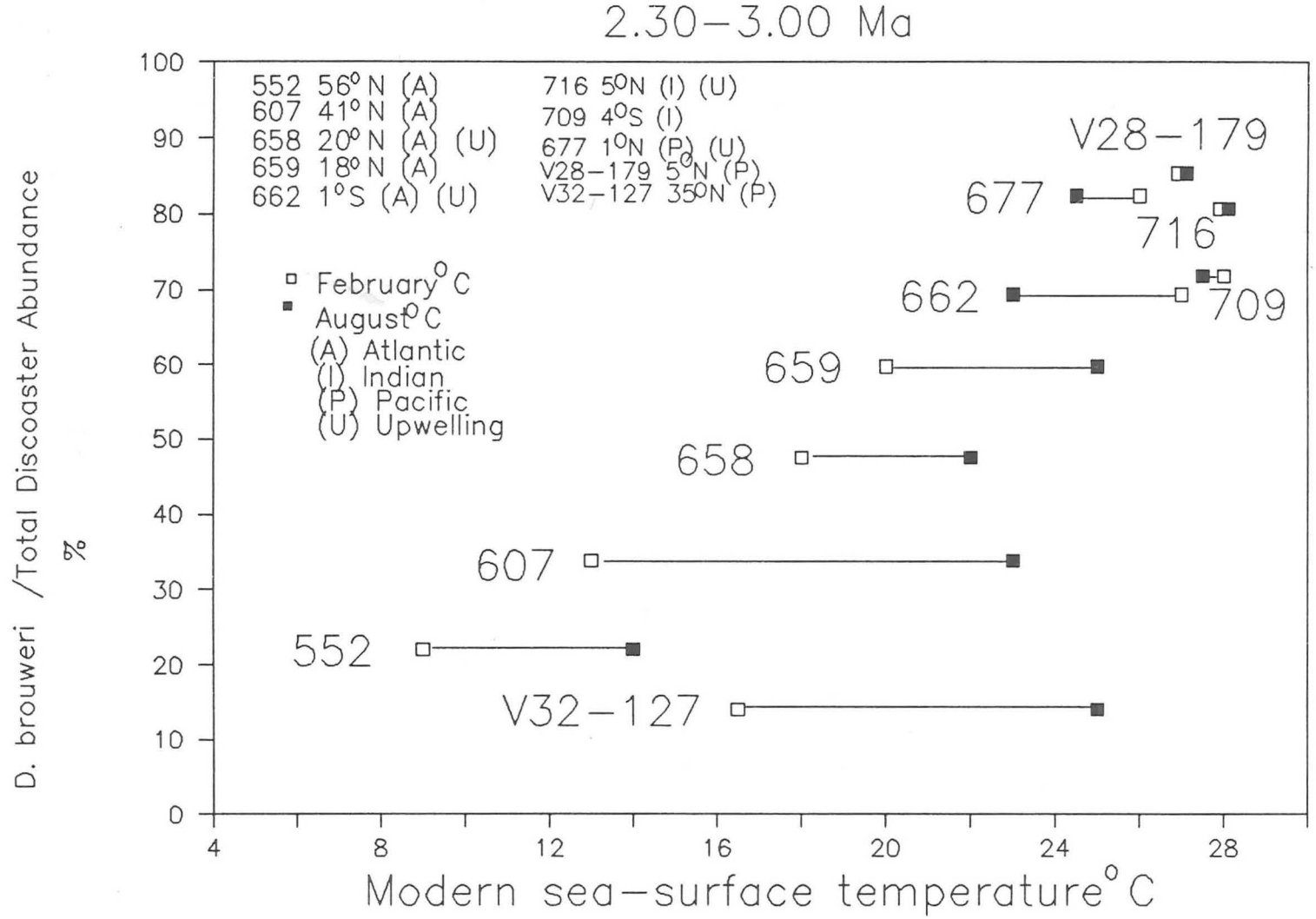

Figure 7:2b. Global synthesis of mean relative D. brouweri abundance versus modern sea–surface temperature between 2.30–3.00 Ma

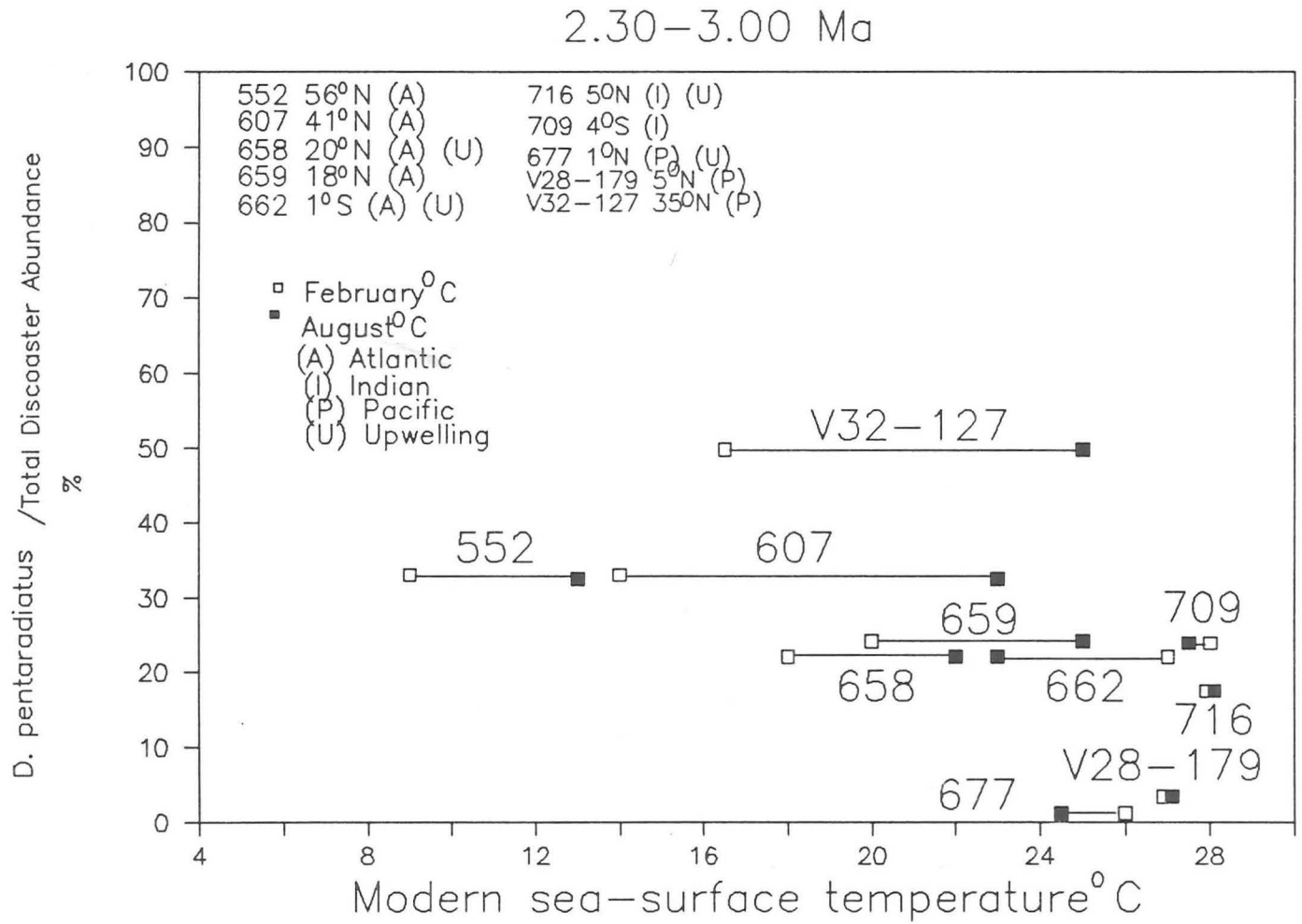

Figure 7:2c. Global synthesis of mean relative D. pentaradiatus abundance versus modern sea–surface temperature between 2.30–3.00 Ma.

flexible species demonstrates a different picture in the Pacific. At the upwelling site, Site 677, D. pentaradiatus occurred in very suppressed abundances. This may be because productivity pressure was too high, but a similar situation to a lesser extent was found at V28-179, where productivity pressure was probably minimal (Fig. 7:1c), and Discoaster abundances are generally high. Nevertheless, the relative abundance of D. pentaradiatus increases dramatically with cooler temperatures in the Pacific as seen at V32-127. It is possible that D. pentaradiatus is less flexible ecologically in the Pacific favouring cooler, low productivity waters.

7:2d Relative Abundance of D. surculus

Figure 7:2d clearly demonstrates that the relative abundance of D. surculus increases as a function of cooler temperatures (Bukry, 1978), especially winter sea-surface temperatures. A comparison of Site 677 (upwelling site) and V28-179 (non-upwelling site) in the Pacific suggests that relative abundance differences are secondarily the result of upwelling conditions. Warm, low productivity sites such as V28-179 and 709 have extremely reduced relative abundances of D. surculus.

7:2e Relative Abundance of D. asymmetricus, D. tamalis and D. brouweri.

In Figure 7:2e, the relative abundance of D. asymmetricus and D. tamalis, as a sum of these two species and D. brouweri, clearly documents an increase with decreasing temperature, not associated with high productivity pressure. Warm sites and upwelling sites display low relative abundances. As discussed in Chapter 5, we believe these three morphospecies are in fact one species, that produced

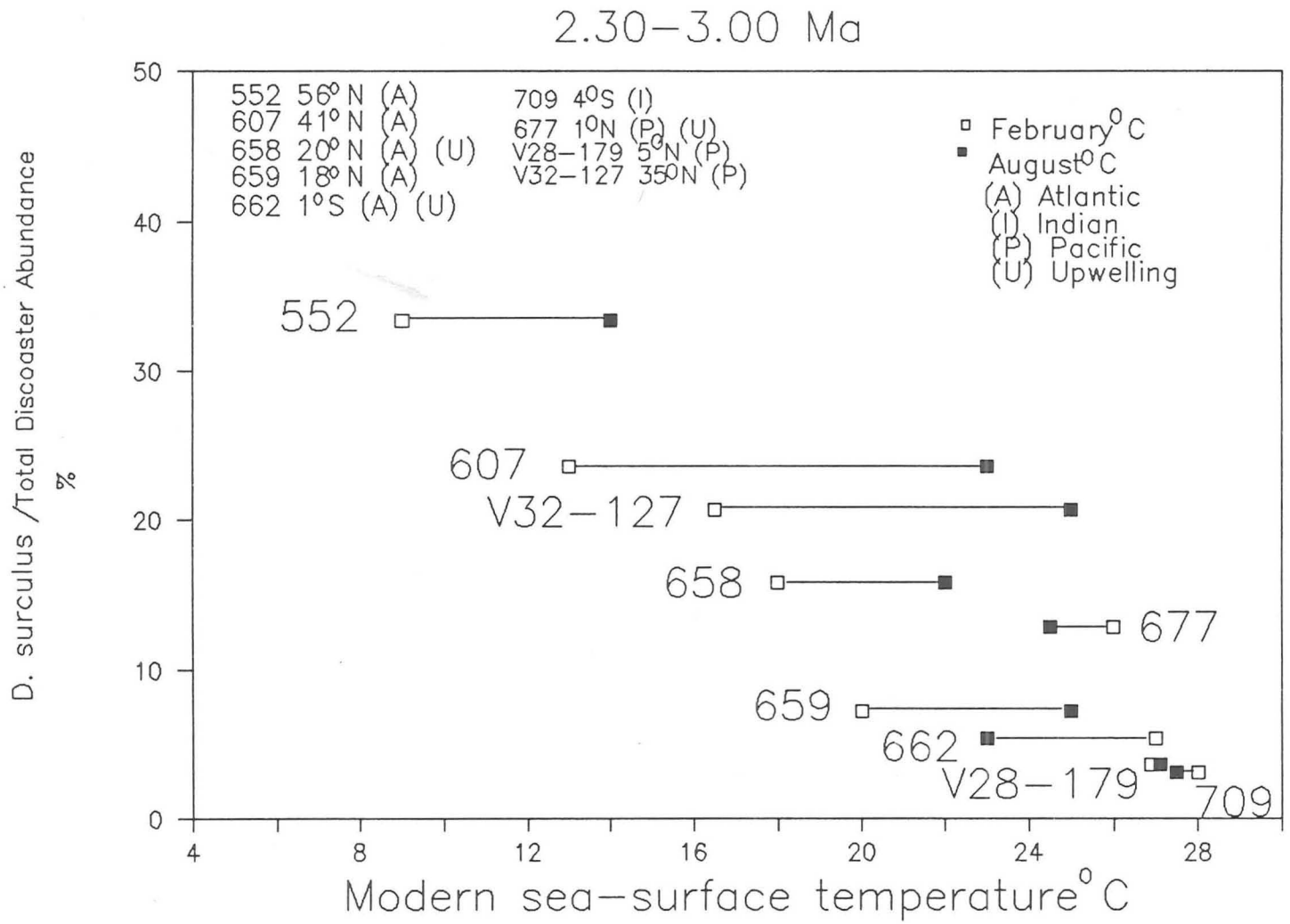

Figure 7:2d. Global synthesis of mean relative D. surculus abundance versus modern sea–surface temperature between 2.30–3.00 Ma.

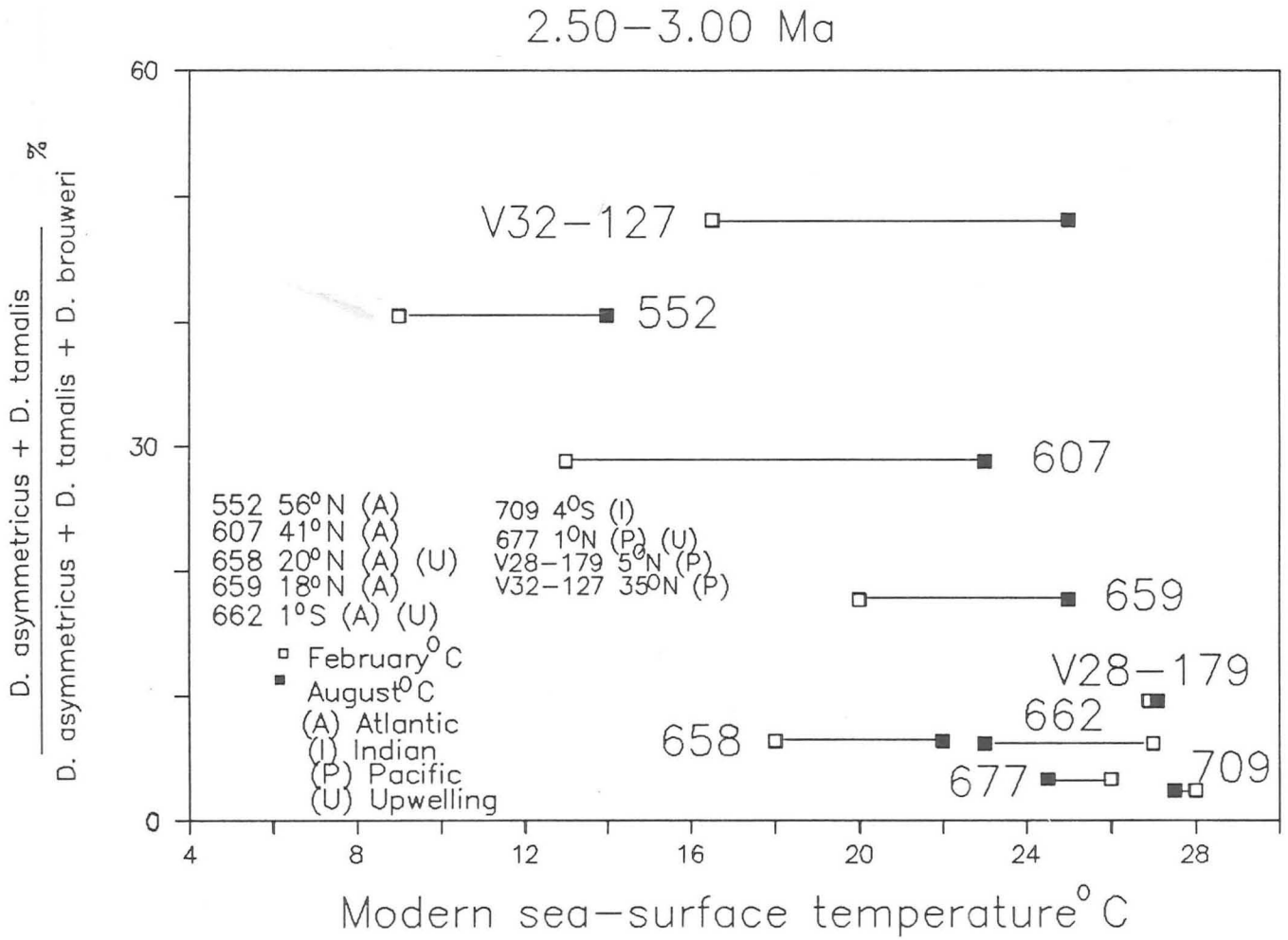

Figure 7:2e. Global synthesis of mean relative abundance of the sum of D. asymmetricus and D. tamalis as a percentage of these species and D. brouweri versus modern sea–surface temperature between 2.50–3.00 Ma.

more discs of "D. asymmetricus" and "D. tamalis" relative to "D. brouweri" at cooler temperatures and lower productivity.

7:3 Discoaster Abundance prior to and after 2.4 Ma.

2.4 Ma marks a significant episode of cooling and ice rafting in the North Atlantic (Shackleton et al., 1984). Figure 7:3 displays the mean abundances of total Discoaster abundance before and after 2.4 Ma. It is apparent that all sites portray a reduction in abundance after 2.4 Ma. The most dramatic changes in abundance occur at the higher latitude sites as expected and the tropical upwelling site, Site 658. The low latitude sites display subtler reductions in abundance, suggesting that the drop in sea-surface temperature was less significant at lower latitudes. This would be in accordance with sea-surface surface temperatures predicted at the last glacial (18 ka) and those observed today (CLIMAP, 1981).

7:4 FINAL DISCUSSION

Our Discoaster global database reveals important palaeoclimatic information concerning productivity pressure and sea-surface temperatures. Discoasters did thrive best in the tropics, especially in the absence of productivity pressure as seen at Site 709. The fluctuations in the tropics may be due to productivity pressure, but the longer trends, as demonstrated by comparing before and after 2.4 Ma, may indicate a long term temperature signal. Even intense upwelling sites such as Site 677, which mostly reflect a productivity signal in the Discoaster record, may still indicate the overall trend of abundance decline due to sea-

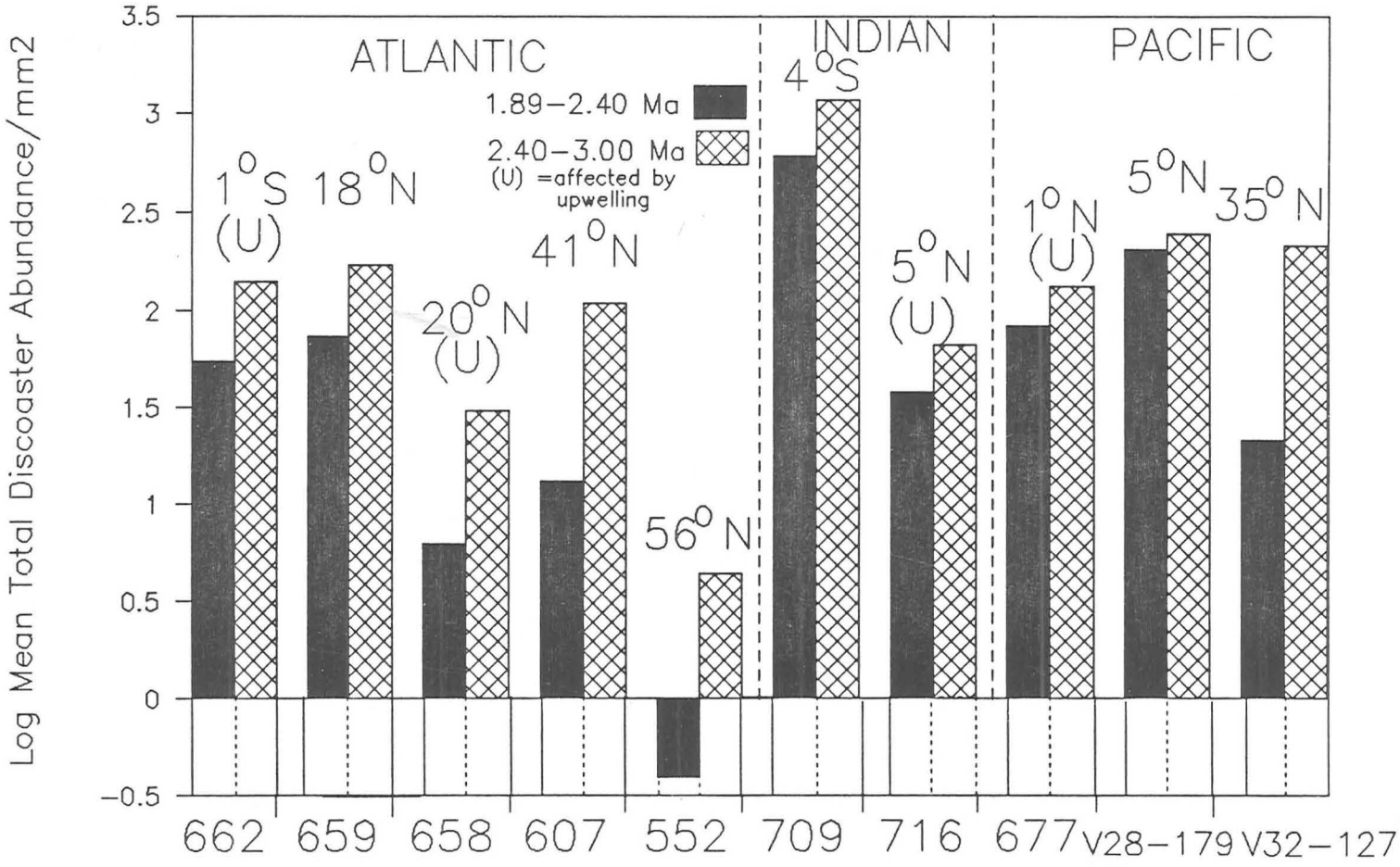

Figure 7:3. Global synthesis of mean total Discoaster abundance between 1.89−2.40 Ma and 2.40−3.00 Ma.

surface temperatures decreasing. Upwelling does suppress Discoaster abundance, but especially if this is coupled with lower sea-surface temperatures.

Between 41°N and 56°N in the Atlantic, a threshold was reached when discoasters rapidly decrease in abundance. At higher latitudes as seen at Site 607, the abundance fluctuations are probably more to do with sea-surface temperature (ice volume), upon which is superimposed a longer term declining Discoaster abundance trend which may be related to a temperature signal.

Individual species or groups of Discoaster species, especially relative to the total Discoaster assemblage, furnish significant palaeoclimatic indicators. Low relative abundances of D. brouweri prior to 2.3 Ma may indicate cooler, low productivity waters. D. asymmetricus and D. tamalis increase relative to D. brouweri under these conditions. D. brouweri is always a major component at low latitudes, even in intense upwelling conditions. D. pentaradiatus is a tolerant species in the Atlantic and Indian oceans favouring warm low productivity waters, but subtle increases in relative abundance may indicate decreases in sea-surface temperature. In the Pacific, available evidence suggests that D. pentaradiatus favoured cooler, low productivity waters. High relative abundances of D. surculus, however, is a good indicator of cooler and/or high productivity waters.

The oceanographic conditions at each site must always be considered using modern information (e.g. satellite maps of phytoplankton blooms and sea-surface temperature maps) and contemporaneous sources (e.g. oxygen isotope records and additional microfloral-faunal data such as diatom abundances) to obtain the

best picture.

7:5 FUTURE WORK

So far this has been a global story based on a few scattered locations - effectively a five site transect in the North Atlantic, two sites in the Indian Ocean and three sites in the Pacific Ocean. Age models for six out of ten of the sites lacked good magnetostratigraphy in the relevant time interval and had to be based solely on biostratigraphic events, mostly Discoaster events for internal consistency, by extrapolation from sites with good magnetostratigraphy (e.g. V28-179 and V32-127).

However the sites in this study contain the best marine Pliocene sequences at the present day and form the foundation for extending the global data base. For comparison now we need sites with good, undisturbed Pliocene sequences, high sedimentation rates and magnetostratigraphy from a number of areas:-

1. Western Pacific: Leg 127 has recently focused on the Ontong Java Plateau drilling a number of sites comprising a depth transect. This would not only be interesting for comparison with ODP Site 677, since these are warm water, non-upwelling sites but it would be very important to contrast a deep water site with a shallower site to assess the effects of dissolution at enriching the Discoaster component in relation to all other biogenic and non-biogenic components.

We may be able to show in the laboratory that our semi- quantitative counting technique reflects absolute abundances in the material, but we cannot

be sure that the original material has not already undergone dissolution enhancing the proportion of the more resistant Discoaster component. The Ontong-Java Plateau may confirm our hypothesis that D. pentaradiatus favoured cooler, low productivity waters in the Pacific if it is found to occur in subdued abundances by comparison with more northern sites such as V32-127.

2. Western North Atlantic and South Atlantic sites: Our North Atlantic transect was limited to the eastern side which has probably produced a biased picture. This needs to be extended to include a site on the western side and a site from the South Atlantic to give a wider overall view of the Atlantic.

3. Upwelling and/or Monsoonal Indian Ocean Site : Good localities exist in the Arabian Sea. It would be interesting to contrast a suitable site with ODP Sites 709 which was very poor in diatoms possibly indicating low productivity in the Upper Pliocene, and likewise compare with ODP Sites 677 and 658, upwelling sites from the Pacific and Atlantic Oceans respectively. Site 716, located in very shallow water, unfortunately showed very poor preservation of the Discoaster asssemblage because of overgrowth.

This would extend the axes of the global data base a little further in terms of Discoaster abundance patterns. However, discoasters are only a small component of all the biogenic and non-biogenic components and should not be considered in isolation:-

A. Other Coccolith Species: Coccolithus pelagicus was only counted at ODP Sites 709, 716 and 677, and Calcidiscus macintyrei at ODP Site 709 (Appendix

be sure that the original material has not already undergone dissolution enhancing the proportion of the more resistant Discoaster component. The Ontong-Java Plateau may confirm our hypothesis that D. pentaradiatus favoured cooler, low productivity waters in the Pacific if it is found to occur in subdued abundances by comparison with more northern sites such as V32-127.

2. Western North Atlantic and South Atlantic sites: Our North Atlantic transect was limited to the eastern side which has probably produced a biased picture. This needs to be extended to include a site on the western side and a site from the South Atlantic to give a wider overall view of the Atlantic.

3. Upwelling and/or Monsoonal Indian Ocean Site : Good localities exist in the Arabian Sea. It would be interesting to contrast a suitable site with ODP Sites 709 which was very poor in diatoms possibly indicating low productivity in the Upper Pliocene, and likewise compare with ODP Sites 677 and 658, upwelling sites from the Pacific and Atlantic Oceans respectively. Site 716, located in very shallow water, unfortunately showed very poor preservation of the Discoaster asssemblage because of overgrowth.

This would extend the axes of the global data base a little further in terms of Discoaster abundance patterns. However, discoasters are only a small component of all the biogenic and non-biogenic components and should not be considered in isolation:-

A. Other Coccolith Species: Coccolithus pelagicus was only counted at ODP Sites 709, 716 and 677, and Calcidiscus macintyrei at ODP Site 709 (Appendix

C). It would be useful to discover how these two species fluctuated in relation to Discoaster abundances across the five site North Atlantic transect. The ratio between Coccolithus pelagicus/Total discoasters% may prove to be an additional palaeoclimatic tool for indicating cool and/or nutrient rich waters (Appendix C).

B. Diatom Abundances: These can be an important indicator of productivity and should be considered concurrently with Discoaster abundances. Semi-quantitative counts were made at ODP Sites 709 and 716 where they were found to be a very minor component of the assemblage. At ODP Site 677, diatoms are extremely numerous prior to approximately 2.5 Ma, after which there is a sudden drop in production (Appendix C). No detailed semi- quantitative counts were made in the North Atlantic sites, but this transect will provide much useful palaeoclimatic information from the diatom abundances.

Comparison of sites using accumulation rates where the abundance of discoasters/unit area is multiplied by the sedimentation rate in the relevant interval must be used with caution. This becomes apparent if one considers comparing sites, ODP 677 and DSDP 552 which demonstrate the wide spectrum of high and low sedimentation rates and Discoaster abundances respectively. The use of relative abundances within the Discoaster assemblage is more useful in such an example.

One last question to be addressed is: what caused the global extinction of discoasters at 1.89 Ma and made it such a useful datum? We have evidence

from the isotopic records of Sites 607, 677, 658 and 552 that D. brouweri disappeared in stage 72 confirming the global synchroneity of this event. However, why did this glacial event coincide with the extinction and not any of the preceding glacials commencing at stage 100. Though some have tried to link it with a magnetic reversal, it is now well documented the extinction took place below the base of the Olduvai and it seems unlikely that discoasters could have predicted their own extinction and died out earlier than the possible cause! A more serious line of investigation may be ecological displacement by another coccolith group such as the rapidly evolving gephyrocapsids though this still has to be resolved.

BIBLIOGRAPHY

Backman, J., 1986. Accumulation patterns of Tertiary calcareous nannofossils around extinctions. Geologische Rundschau 75/1. 185-196. Stuttgart.

Backman, J., Pestiaux, P., Zimmerman, H., and Hermelin, O., 1986. Pliocene paleoclimatic and palaeo-oceanographic development in the North Atlantic: Discoaster abundance and coarse fraction data. Spec. Pap. Geol. Soc. London.

Backman, J., Duncan, R. A., et al., 1988. Proc. ODP, Init. Repts., 115: College Station, TX (Ocean Drilling Program).

Backman, J., and Shackleton, N. J., 1983. Quantitative biochronology of Pliocene and early Pleistocene calcareous nannofossils from the Atlantic, Indian and Pacific oceans. Mar. Micropaleontol., 8: 141-170.

Backman, J., and Pestiaux, P., 1987. Pliocene Discoaster abundance variations from DSDP Site 606: biochronology and paleoenvironmental implications. Init. Repts. DSDP 94.

Be, A. W. H. and Hutson, W. H., 1977. Ecology of planktonic foraminifera and biogeographic patterns of life and fossil assemblages in the Indian Ocean. Micropaleontol., 23 (4): 369-414.

Becker, K., Sakai, H., et al., 1988. Proc. ODP, Init. Repts. 111: College Station, TX (Ocean Drilling Program).

Berger, A., 1977. Support for the astronomical theory of climatic change. Nature, 268, 44-45.

Berger, A., 1978. Long term variations of daily insolation and Quaternary climatic changes. J. Atmospheric Sciences, 35 (12) 2362-2367.

Berger, W. H., Killingley, J. S. and Vincent, E., 1978. Stable isotopes in deep sea carbonates: Box core ERDC-92, West Equatorial Pacific. Oceanologica Acta 1, 203-216.

Berggren, W. A., Kent, D. V., Flynn, J. J. and Van Couvering, J. A., 1985a. Cenozoic geochronology. Geol. Soc. of Amer. Bull., 96, 1407-1418.

Berggren, W. A., Kent, D. V. and Flynn, J. J., 1985. Jurassic to Paleogene geochronology and chronostratigraphy. In Snelling, N. J. (ed), The Chronology of the Geological Record, Geol. Soc. Mem. 10, 141-195.

Bukry, D., 1973a. Coccolith stratigraphy, eastern equatorial Pacific, Leg 16 Deep Sea Drilling Project. Init. Repts. DSDP, 16: Washington (U.S. Govt. Printing Office), 653-711.

Bukry, D., 1973b. Low-latitude coccolith biostratigraphic zonation. Init. Repts. DSDP 15: Washington (U.S. Govt. Printing Office), 685-703.

Bukry, D., 1978. Biostratigraphy of Cenozoic marine sediment by calcareous nannofossils. Micropaleontol., 24: 44-60.

Chepstow-Lusty, A., Backman, J. and Shackleton, N. J., 1989. Comparison of upper Pliocene Discoaster abundance variations from North Atlantic Sites 552, 607, 659, 658 and 662: Further evidence for marine plankton responding to orbital forcing. In Init. Repts. ODP, 108: Washington (U.S. Govt. Printing Office), 121-141.

Clement, B., and Robinson, F., 1987. The Magnetostratigraphy of Leg 94 Sediments. In Init. Repts. DSDP, 94: Washington (U.S. Govt. Printing Office), 635-650.

CLIMAP project members, 1981. Seasonal Reconstructions of the Earth's Surface at the Last Glacial Maximum Geol. Soc. Am. Map and Chart Series no. MC-36.

Dowsett, H. J., 1989. Application of the Graphic Correlation method to Pliocene sequences. Mar. Micropaleontol., 14: 3-32.

Driever, B. W. M., 1988. Calcareous nannofossil biostratigraphy and paleoenvironmental interpretation of the Mediterranean Pliocene. Utrecht Micropaleontol. Bull. 36.

Droxler, A. W., Haddad, G. A., Mucciarone, D. A., and Cullen, J. L., (in press). Late Pliocene-Pleistocene periplatform aragonite cycles and supercycles in Holes 716B and 714A (The Maldives, Equatorial Indian Ocean) and Hole 633A (The Bahamas, western North Atlantic): an indicator of climatically induced $CaCO_3$ preservation and dissolution at intermediate water depths. In Init. Repts. ODP, 115.

Einarsson, T. and Albertsson, K. J., 1988. The glacial history of Iceland during The past three million years: evolution of climatic variability in the North Atlantic region, edited by N. J. Shackleton, R. G. West, and D. Q. Bowen, 227-234, University Press, Cambridge.

Emiliani, C., 1955. Pleistocene temperatures. J. Geol. 63, 538-78.

Epstein, S., Buchsbaum, R., Lowenstam, H. A., and Urey, H. C., 1951. Carbonate -water isotopic temperature scale. Bull. geol. Soc. Am. 62, 417-426.

Fisher, R. A., and Yates, F., 1963. Statistical Tables for Biological, Agricultural and Medical Research, Oliver & Boyd Ltd, Edinburgh.

Gartner, S., 1969. Correlation of Neogene planktonic foraminifera and calcareous nannofossil zones. Trans. Gulf Coast Assoc. Geol. Soc., 19: 585-599.

Haq, B. U., Lohmann, G. P., 1976. Early Cenozoic calcareous nannoplankton biogeography of the Atlantic Ocean. Mar. Micropaleontol., 1: 119-194.

Hays, J. D., Imbrie, J., and Shackleton, N. J., 1976. Variations in the Earth's orbit: Pacemaker of the ice ages. Science, 194: 1121-1132.

Honjo, S., 1977. Biogeography and Provincialism of living coccolithophorids in the Pacific Ocean, in Oceanic Micropaleontology, ed. A. T. S. Ramsay. New York: Academic Press. vol. 2, 951-972.

Houghton, S. D., 1989. Late Neogene calcareous nannofossil biostratigraphy and palaeoceanography of ODP Hole 677A, Panama Basin. In Becker, K., Sakai, H., et al., Init. Repts. ODP, 111: Washington (U.S. Govt. Printing Office), 277-285.

Imbrie, J. and Imbrie, K. P., 1979. Ice Ages, solving the Mystery. Enslow Publishers, Short Hills, New Jersey.

Imbrie, J., Hays, J., Martinson, D. G., McIntyre, A., Mix, A. C., Morley, J. J., Pisias, N. G., Prell, W. L., Shackleton, N. J., 1984. The orbital theory of Pleistocene climate: support from a revised chronology of the marine ^{18}O record. In : "Milankovitch and Climate", A. Berger, J. Imbrie, J. Hays, G. Kukla, B. Saltzman (Eds), D. Reidel Publ. Company, Dordrecht, Holland, 269-305.

Kamptner, E., 1967. Kalkflagellaten-Skelettreste aus Tiefseeschlamm des Sudatlantlantischen Ozeans. Ann. Naturhist. Mus. Wien, 71: 117-198.

Lewis, M. R., 1989. The variegated ocean: a view from space. New Scientist, 124 (1685), 37-42.

Lohmann, G. P., and Carlson, J. J., 1981. Oceanographic significance of Pacific late Miocene calcareous nannoplankton. Mar. Micropaleontol., 6: 553-579.

Manabe, S., and Broccoli, A. J., 1985. The influence of continental ice sheets on the climate of an ice age, J. Geophys. Res. 90, 2167.

Maniken, E. A., and Gromme, C. S., 1982. Paleomagnetic data from the Coso Range, California and current status of the Cobb Mountain normal Geomagnetic Polarity Event. Geophys. Res. Lett. 9, 1279-1282.

Martini, E., 1971. Standard Tertiary and Quaternary calcareous nannoplankton zonation. In: A. Farinacci (Editor), Proc. II Plakt. Conf. Roma 1970. Tecnoscienza, Roma, 2: 739-785.

Martini, E., and Bramlette, M. N., 1963. Calcareous nannoplankton from the experimental Mohole drilling. J. Paleontol., 37 (4): 845-856.

McIntyre, A., 1967. Coccoliths as paleoclimatic indicators of Pleistocene glaciation. Science, 158: 1314-1317.

Milankovitch, M. M., 1941. Kanon der Erdbestrahlung. Beograd. Koninglich Serbische Akademie, 484pp. (English translation, Canon of Insolation and the Ice Age Problem, by Israel Program for Scientific Translation and published for the U.S. Department of Commerce and the National Science Foundation).

Mitchell, J. M., 1976. An overview of climatic variability and its causal mechanisms. Quat. Res. 6, 481-493.

Moore, T. C., Heath, R. C., and Konsman, R. O., 1973. Biogenic sediments of the Panama Basin. J. Geol., 81: 458-472

Okada, H., and Honjo, S., 1973. The distribution of oceanic coccolithophorids in the Pacific. Deep-Sea Res., 20: 355-374.

Okada, H., and McIntyre, A., 1979. Seasonal distribution of modern coccolithophores in the western North Atlantic Ocean. Mar. Biol., 54: 319-328.

Parke, M., and Adams, I., 1960. The motile Crystallolithus hyalinus (Gaarder and Markali) and non-motile phase in the life history of Coccolthus pelagicus (Wallich) Schiller. J. Mar. Biol.,54, 319-328.

Perch-Nielsen, K., 1985. Cenozoic calcareous nannofossils. In: Bolli, H. M., Saunders, J. B., and Perch-Nielsen, K. (eds.) Plankton Stratigraphy. Cambridge University Press, 427-554.

Pestiaux, P., and Berger, A., 1984. An optimal approach to the spectral characteristics of deep-sea climate records. In: Milankovitch and Climate. Riedel Publishing Company, Bordrecht. 417-46.

Peterson, L. C., and Prell, W. L., 1985a. Carbonate dissolution in Recent sediments of the eastern equatorial Indian Ocean: Preservation and carbonate loss above the lysocline. Marine Geology, 64: 259-290.

Pisias, N. G., and Leinen, M., 1984. Milankovitch forcing of the oceanic system: Evidence from the northwest Pacific. In Berger, A., Imbrie, J., Hays, J., Kukla, G., and Saltzman, B. (Eds.), Milankovitch and Climate, 1: Dordrecht (D. Riedel Publ. Co.), NATO ASI Ser. C, 126: 307-330.

Raymo, M. E., Ruddiman, W. F. and Clement, B. M., 1986. Pliocene-Pleistocene palaeoceanography of the North Atlantic at DSDP Site 609. Init. Repts. DSDP, 94: Washington (U.S. Govt. Printing Office), 895-901.

Raymo, M. E., Ruddiman, W. F., Backman, J., Clement, B. M., and Martinson, D. G., 1989. Late Pliocene Variation in Northern Hemisphere Ice Sheets and North Atlantic Deep Water Circulation. Paleoceanography, 4 (4), 413-446.

Rio, D., 1982. The fossil distribution of coccolithophore genus Gephyrocapsa Kamptner and related Plio-Pleistocene chronostratigraphic problems. In: W.L. Prell, J.V. Gardner, et al., Init. Repts. DSDP,68: Washington (U.S. Govt. Printing Office), 325-343.

Roberts, D. G., Schnitker, D., et al., 1984. In Init. Repts. DSDP, 81: Washington (U.S. Govt. Printing Office), 31 - 234.

Ruddiman, W. F., Cameron, D. and Clement, B. M., 1986b. Sediment disturbance and correlation of offset holes drilled with the hydraulic piston corer: Init. Repts. DSDP, 94: Washington (U.S. Govt. Printing Office), 615-634.

Ruddiman, W. F., Kidd, R. B., Thomas, E., et al., 1983. Site 607: Background and Objectives. In Init. Repts. DSDP, 94: Washington (U.S. Govt. Printing Office), 75-147.

Ruddiman, W. F. and McIntyre, A., 1981. Oceanic mechanisms for amplification of the 23,000-year ice-volume cycle. Science, 212, 617-627.

Ruddiman, W. F., Raymo, M. and McIntyre, A., 1986a. Matuyama 41,000-year cycles: North Atlantic Ocean and northern hemisphere ice sheets, Earth and Planet. Sci. Lett., 80, 117-129.

Ruddiman, W. F., Raymo, M., Martinson, D. G., Clement, B. M., and Backman, J., 1989. Pleistocene Evolution: Northern Hemisphere Ice Sheets and North Atlantic Ocean. Paleoceanography, 4 (4), 353-412.

Ruddiman, W. F., Sarnthein, M., et al., 1988. In Init. Repts. ODP, 108: Washington (U.S. Govt. Printing Office).

Sarnthein, M. and Tiedemann, R., 1989. Toward a high-resolution isotope stratigraphy of the last 3.4 Million years: Sites 658 and 659 off Northwest Africa. In Ruddiman, W., Sarnthein M., et al., Init. Repts. ODP, 108: Washington (U.S. Govt. Printing Office), 167-185.

Schrader, H. J., 1971. Fecal Pellets: Role in sedimentation of pelagic diatoms. Science 174: 55-57.

Shackleton, N. J., Backman, J., Zimmerman, H. G., Kent, D. V., Hall, M. A., et al., 1984. Oxygen isotope calibration of the onset of ice-rafting and history of glaciation in the North Atlantic region. Nature, 307: 320-323.

Shackleton , N. J., Berger, A. and Peltier, W. R., (in press). An alternative astronomical calibration of the Lower Pleistocene timescale based on ODP Site 677. Trans. Roy. Soc. Edinburgh: Earth Sciences.

Shackleton, N. J. and Hall, M. A., 1983. Stable isotope record of Hole 504 sediments: High resolution record of the Pleistocene. In Cann, J. R., Langseth, M. G., Honnorez, J., Von Herzen, R. P., White, S. M., et al., Init. Repts. DSDP, 69: Washington (U.S. Govt. Printing Office), 431-442.

Shackleton, N. J. and Hall, M. A., 1989. Stable isotope history of the Pleistocene at ODP Site 677. In Becker, K., Sakai, H., et al., Init. Repts. ODP, 111: Washington (U.S. Govt. Printing Office), 295-316.

Shackleton, N. J. and Opdyke, N. D., 1973. Oxygen isotope and palaeomagnetic stratigraphy of equatorial Pacific Core V28-238: oxygen isotope temperatures and ice volumes on a 10^5 year and 10^6 year scale. Quat. Res. 3 (1), 39-55.

Shackleton, N. J. and Opdyke, N. D., 1976. Oxygen isotope and paleomagnetic stratigraphy of Pacific Core V28-239 late Pliocene to latest Pleistocene. Geol. Soc. Am. mem. 145, 449-464.

Shackleton, N. J. and Opdyke, N. D., 1977. Oxygen isotope and paleomagnetic evidence for early Northern Hemisphere glaciation. Nature, 270: 216-219.

Takayama, T., 1970. The Pliocene-Pleistocene boundary in the Lamont Core V21-98 and at le Castella, southern Italy. J. Mar. Geol, 6: 70-77.

Tan Sin Hok, 1927. Discoasteridae incertae sedis. Proc. Sect. Sc. K. Acad. Wet. Amsterdam, 30: 411-419.

Tauxe, L., Valet, J. P., and Bloemendal, J., 1989. Magnetostratigraphy of Leg 108 Advanced Hydraulic Piston Cores. In Init. Repts. ODP, 108: Washington (U.S. Govt. Printing Office), 429-440.

Weaver, P. P. E. and Raymo, M. E., 1989. Late Miocene to Holocene Planktonic foraminifers from the equatorial Atlantic, Leg 108. In Ruddiman, W., Sarnthein M., et al., Init. Repts. ODP, 108: Washington (U.S. Govt. Printing Office), 71-91.

Wei, W., Bergen, J. A. and Applegate, J., 1988. Cenozoic calcareous nannofossils from the Galicia Margin, ODP Leg 103. In Boillot, G., Winterer, E. L., et al., Init. Repts. ODP, 103: Washington (U.S. Govt. Printing Office), 279-291.

Zimmerman, H. B., et al., 1984. History of Plio-Pleistocene climate in the northeastern Atlantic: DSDP Site 552A. Init. Repts. DSDP, 81, 861-875.

APPENDIX A

Abundance of Discoaster species versus depth in the North Atlantic:

DSDP 552A
DSDP 607
ODP 658A
ODP 659A
ODP 662A

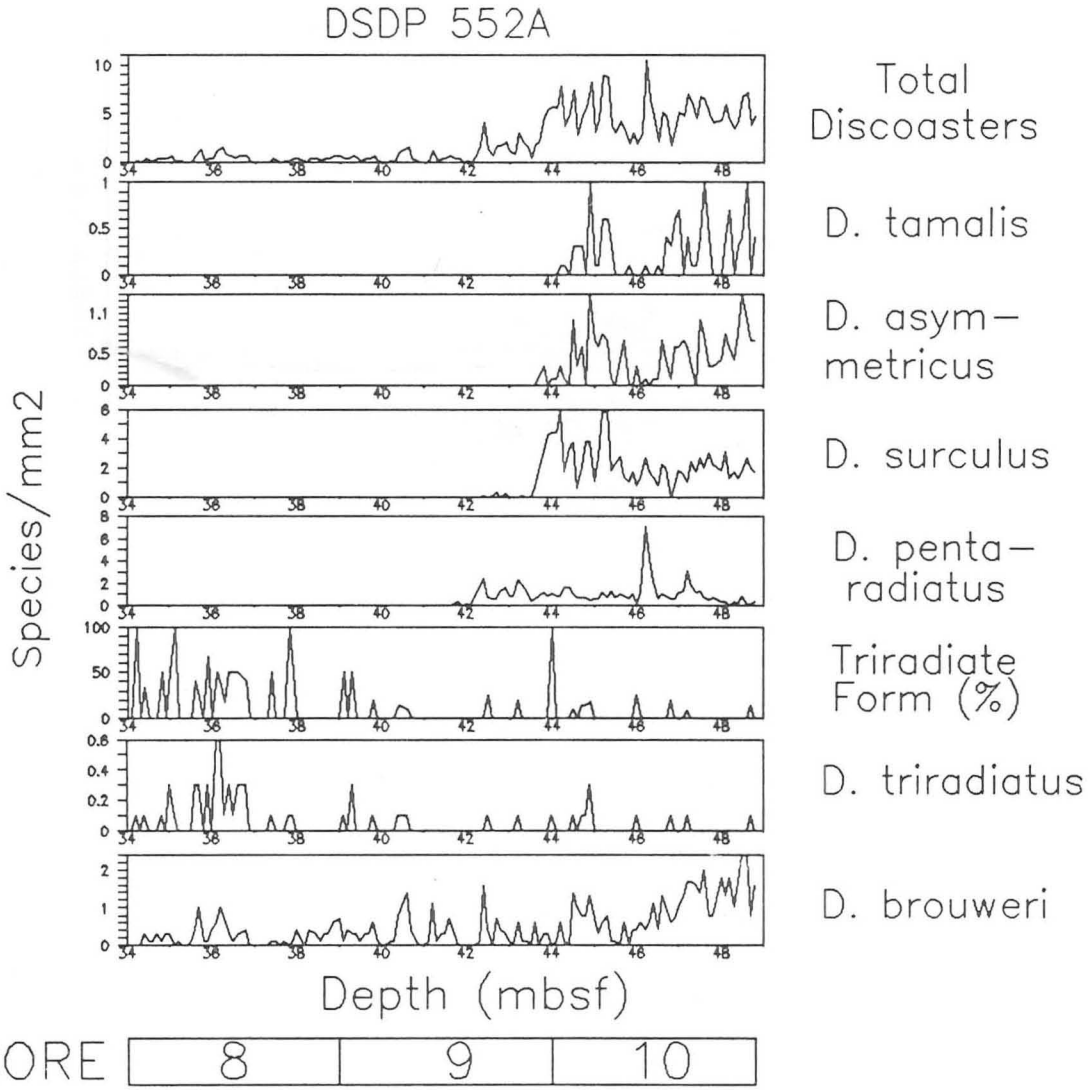

A1: Abundance of Discoaster species/mm2 versus depth at DSDP 552A

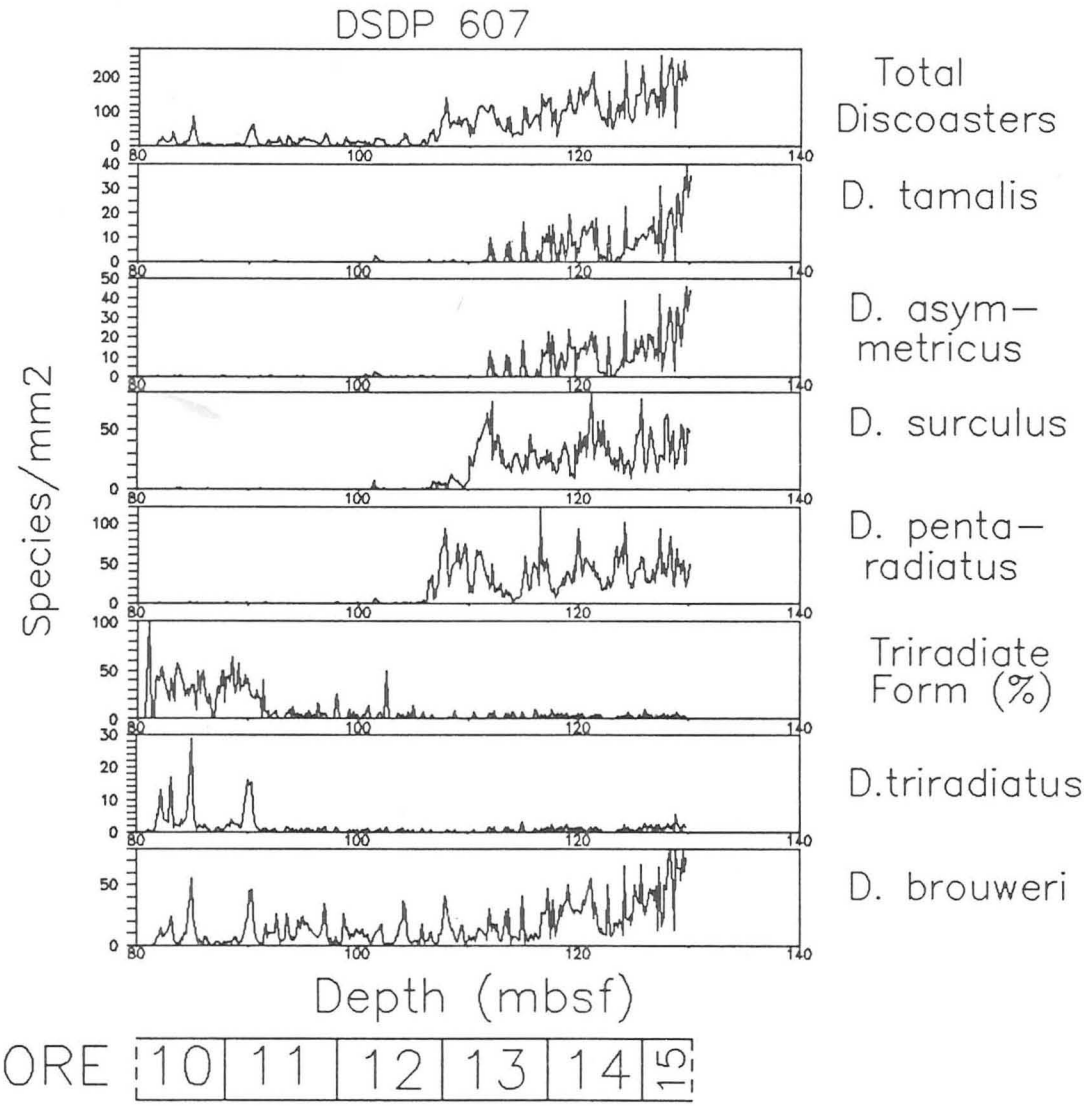

A2: Abundance of Discoaster species/mm2 versus depth at DSDP 607

A3: Abundance of Discoaster species/mm2 versus depth at ODP 658A

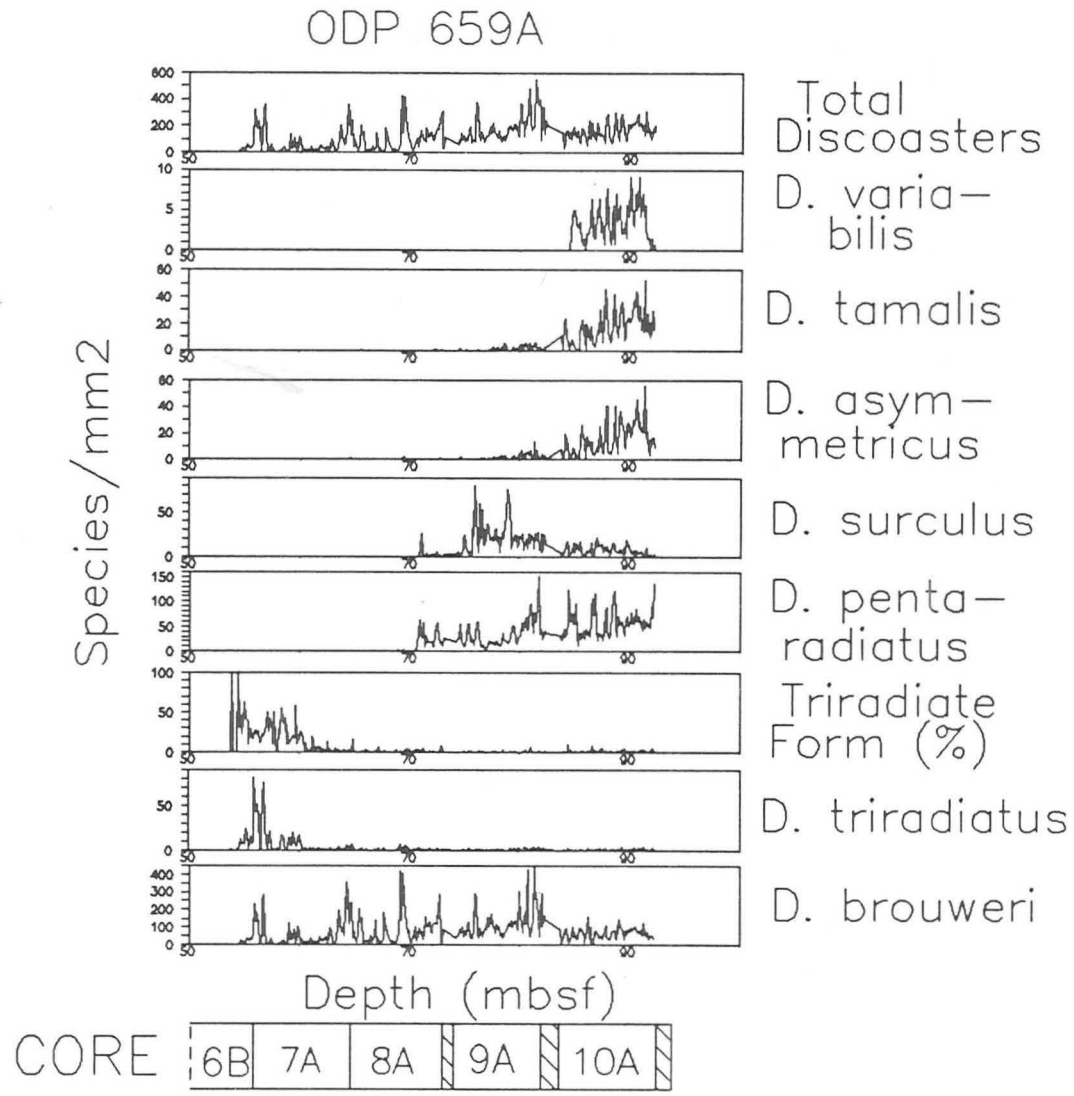

A4: Abundance of Discoaster species/mm2 versus depth at ODP 659A

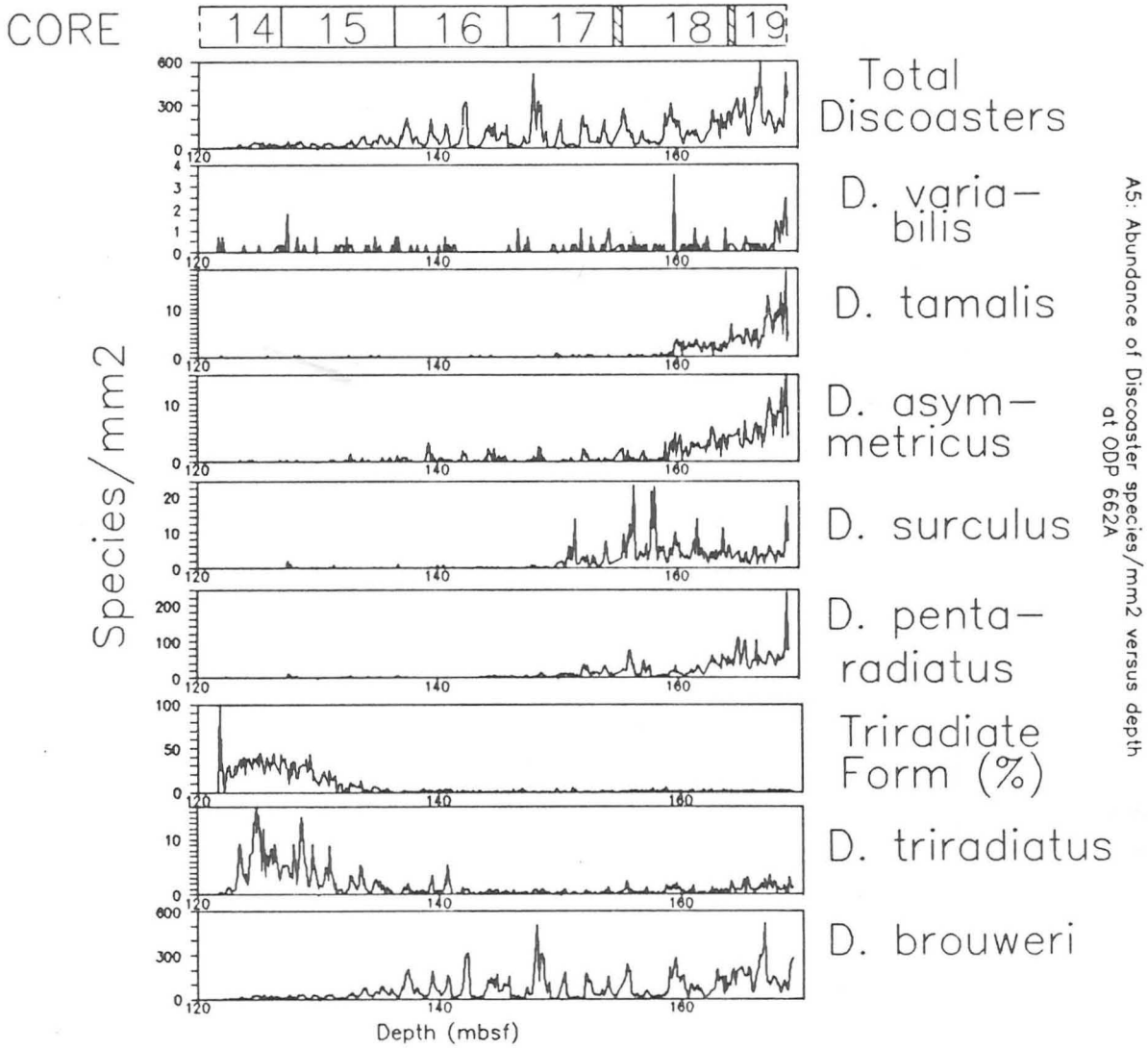

A5: Abundance of Discoaster species/mm2 versus depth at ODP 662A

APPENDIX B

Abundance of Discoaster species versus depth in the Indo-Pacific:

ODP 709C
ODP 716B
ODP 677A
V28-179
V32-127

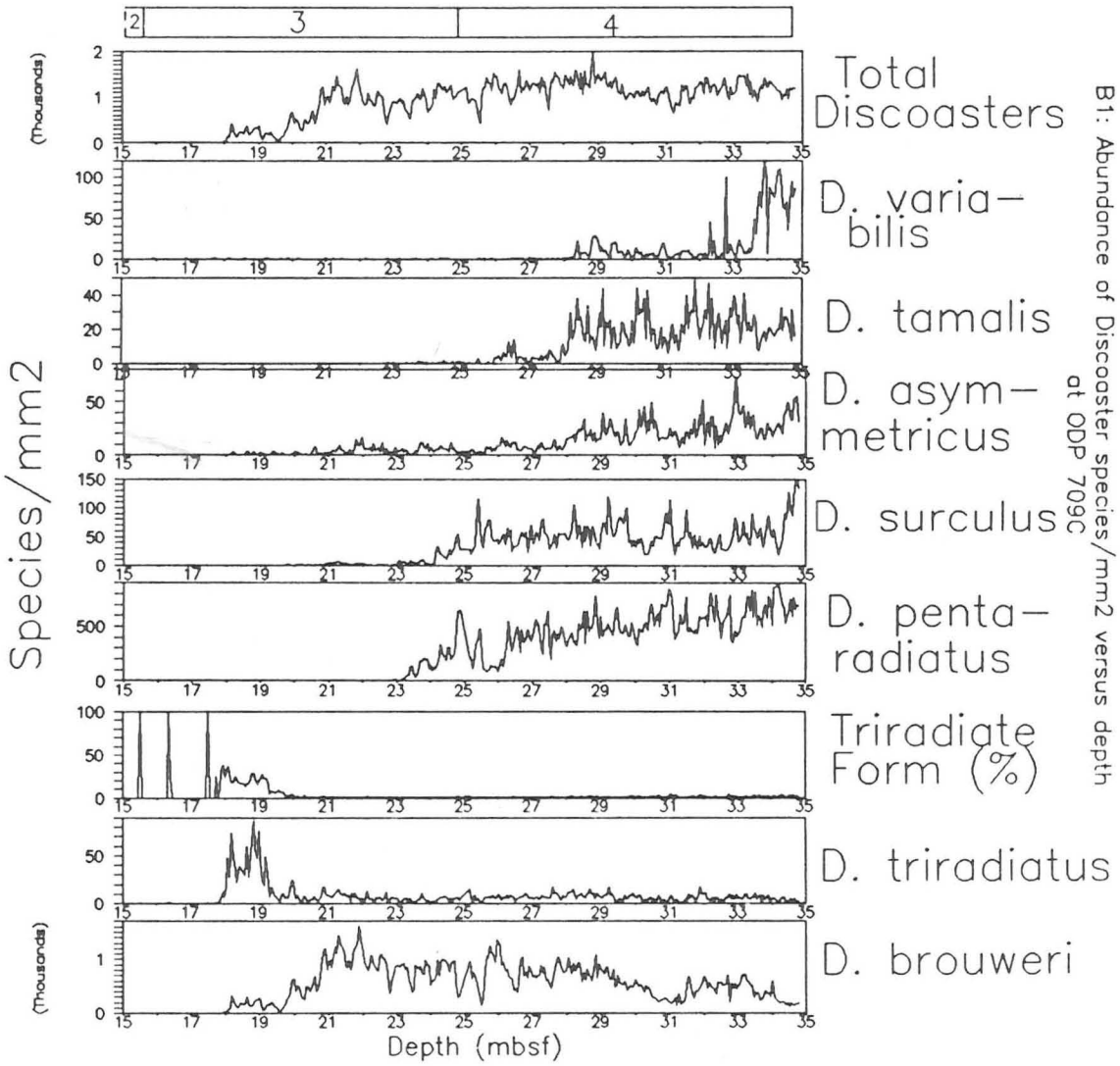

B1: Abundance of Discoaster species/mm2 versus depth at ODP 709C

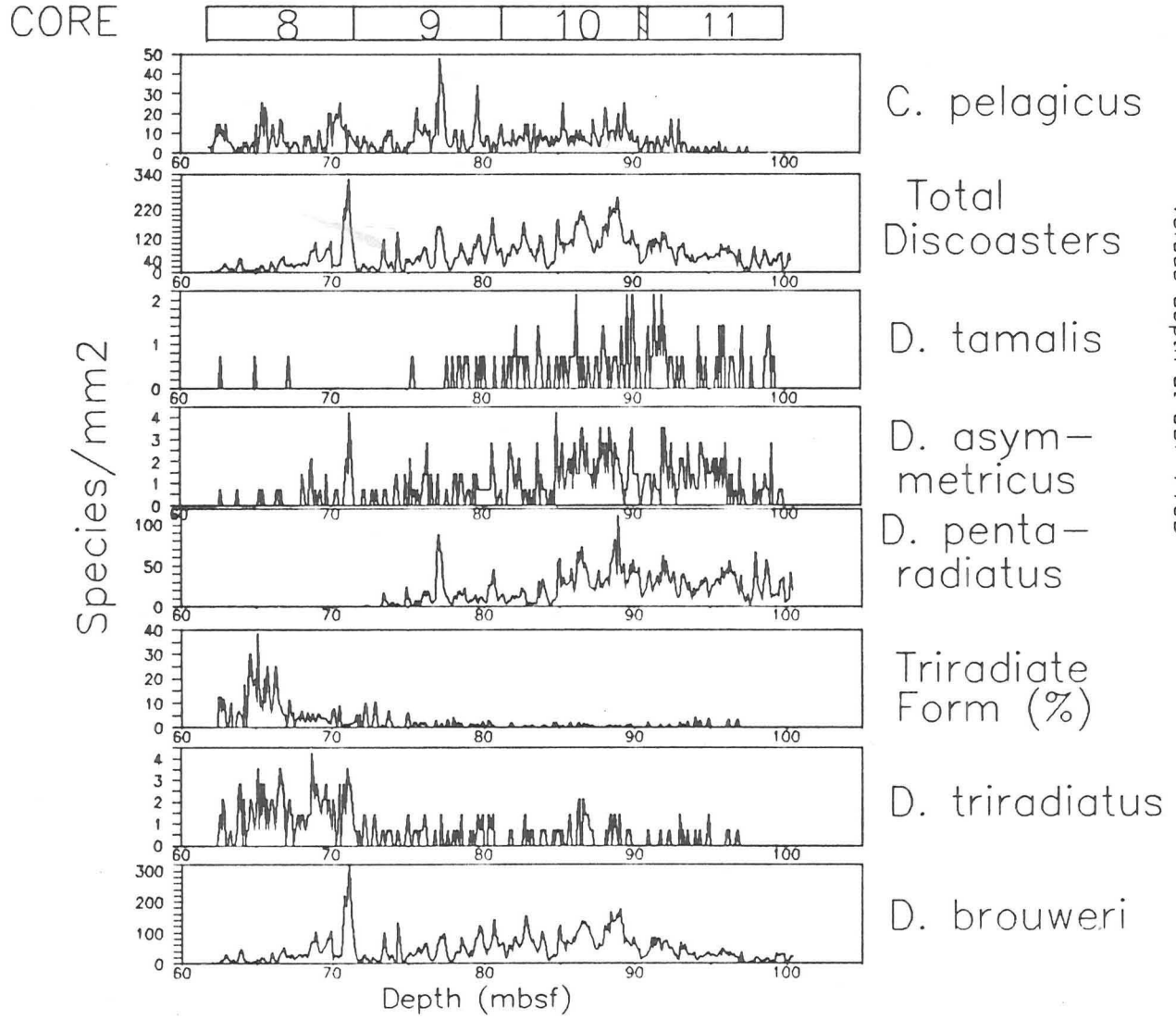

B2: Abundance of Discoaster species and C. pelagicus /MM2 versus depth at ODP 716B

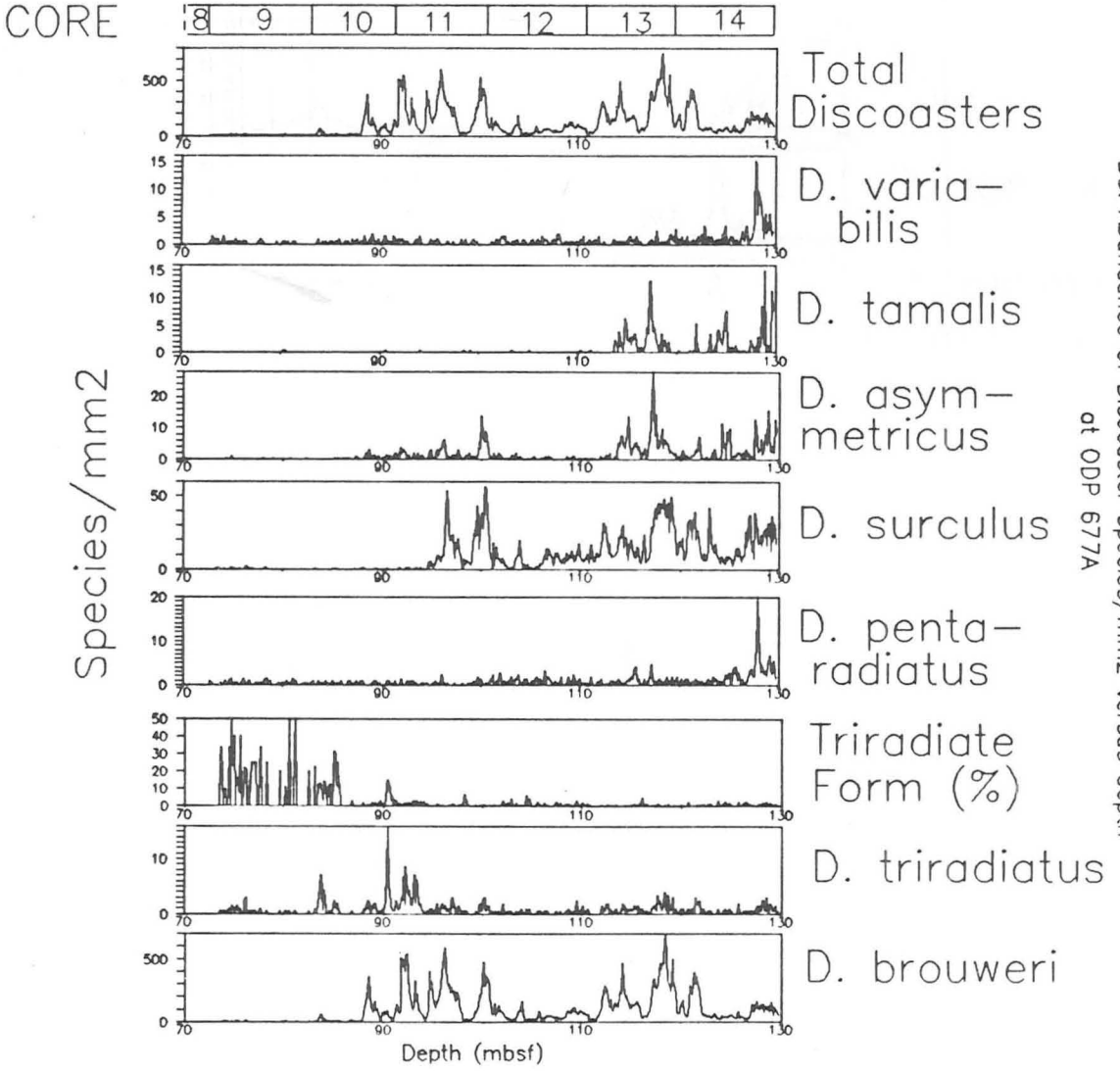

B3: Abundance of Discoaster species/mm2 versus depth at ODP 677A

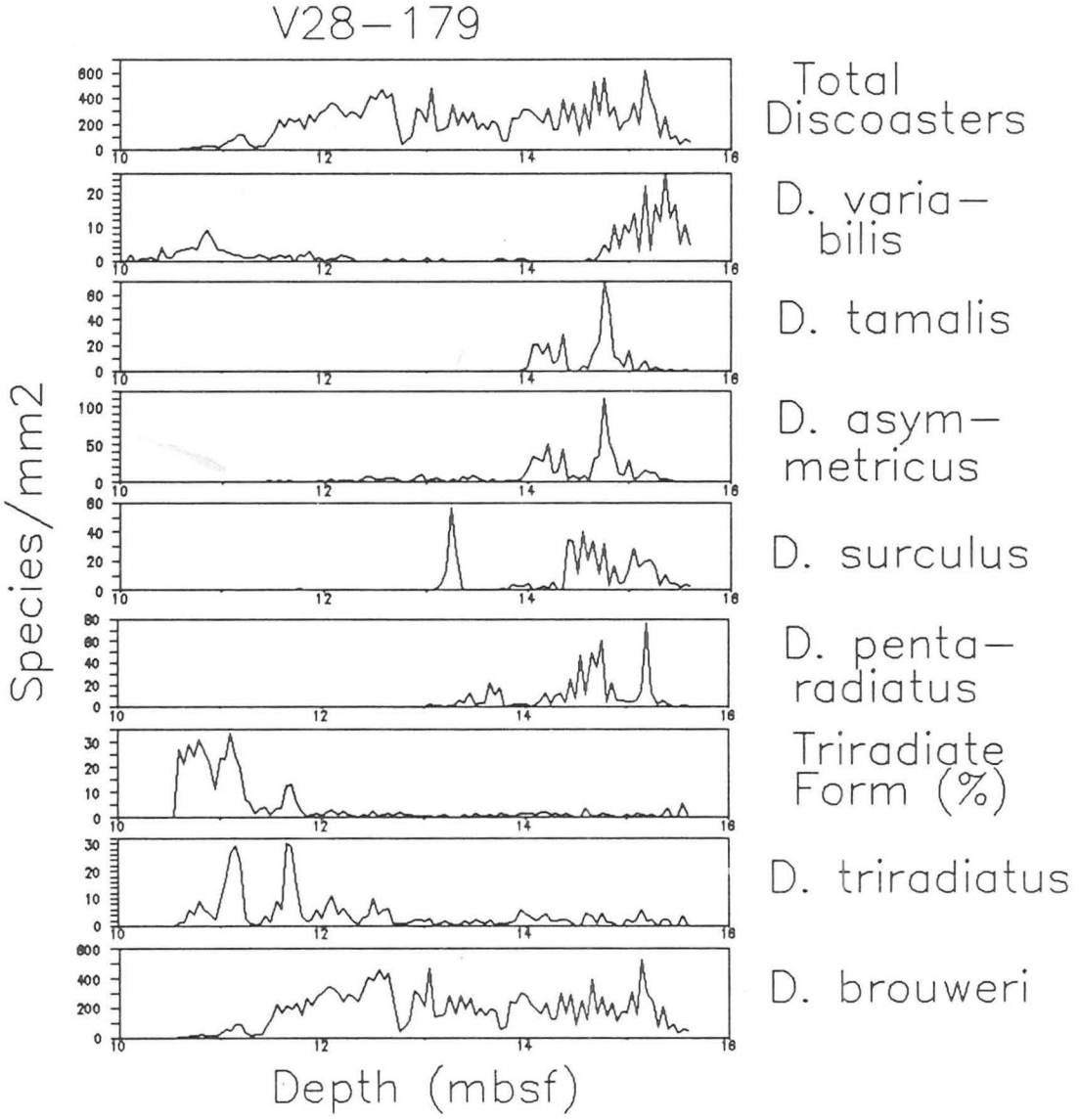

B4: Abundance of Discoaster species/mm2 versus depth at Core V28–179

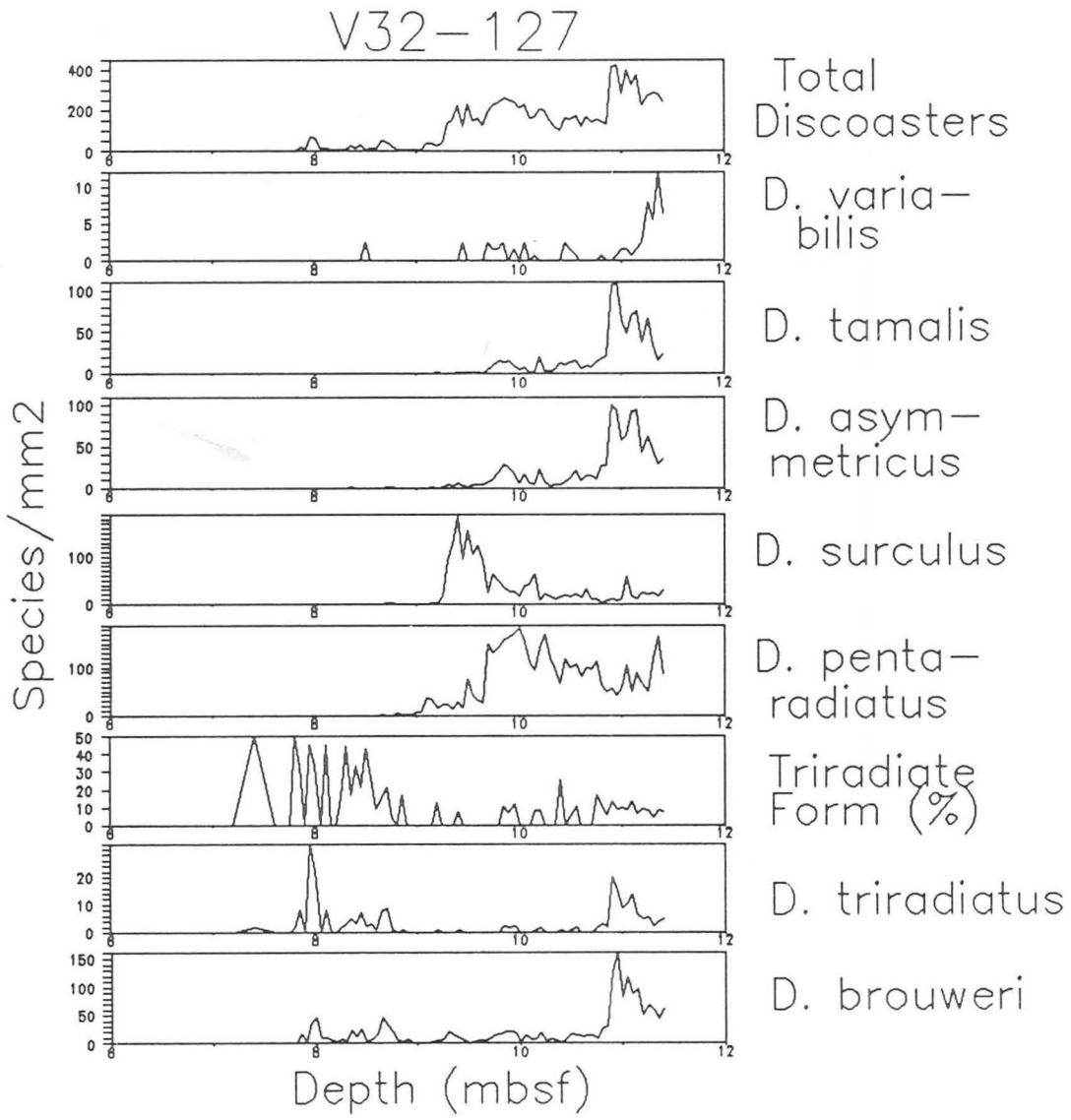

B5: Abundance of Discoaster species/mm2 versus depth at Core V32-127

APPENDIX C

The relationship between Total Discoaster abundance, C. pelagicus, Diatoms and C. macintyrei versus depth and age in Indo-Pacific Sites:

ODP 709C
ODP 716B
ODP 677A

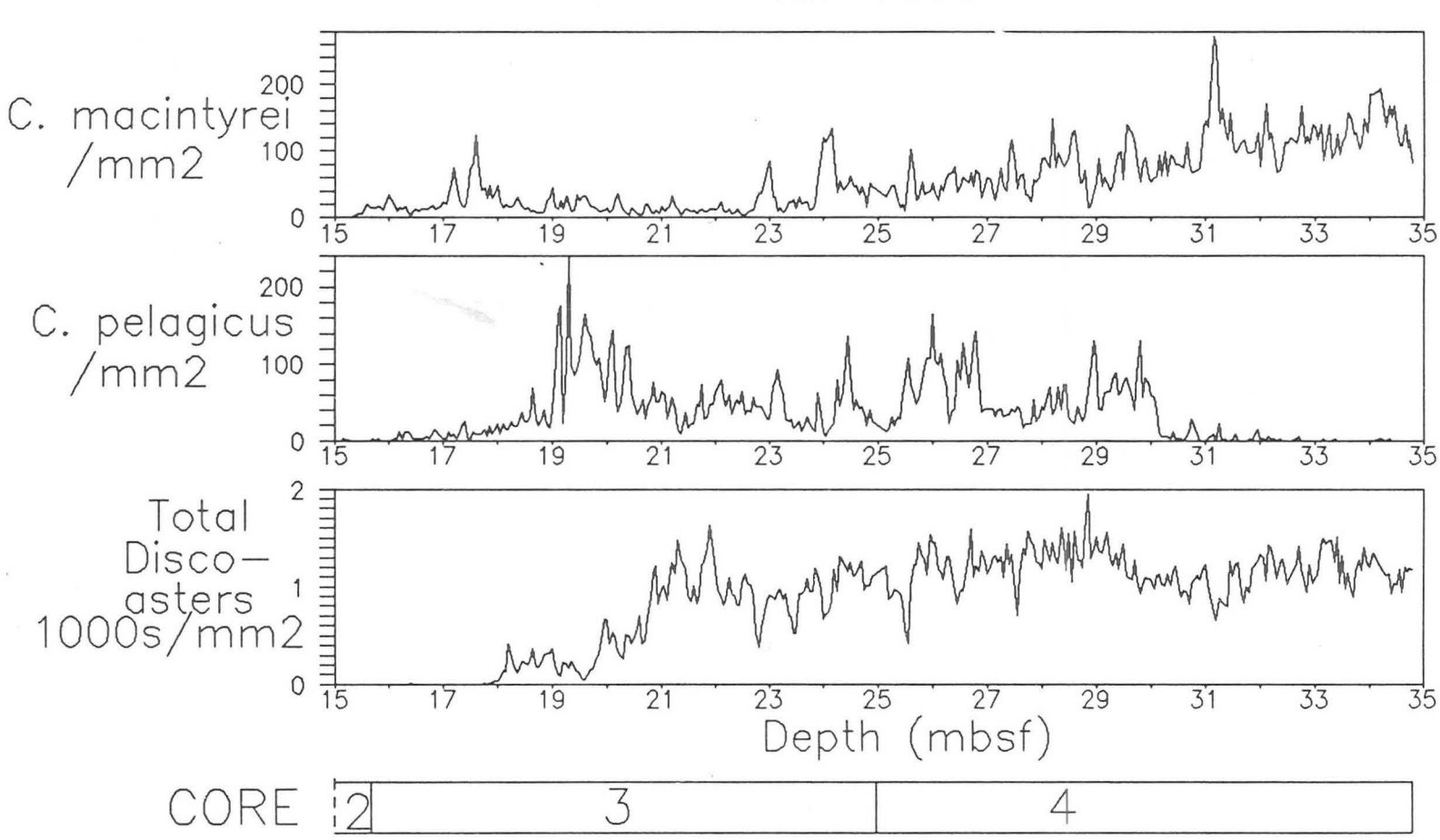

C1: Abundance of Total Discoasters, C. pelagicus, and C. macintyrei/mm2 at ODP 709C.

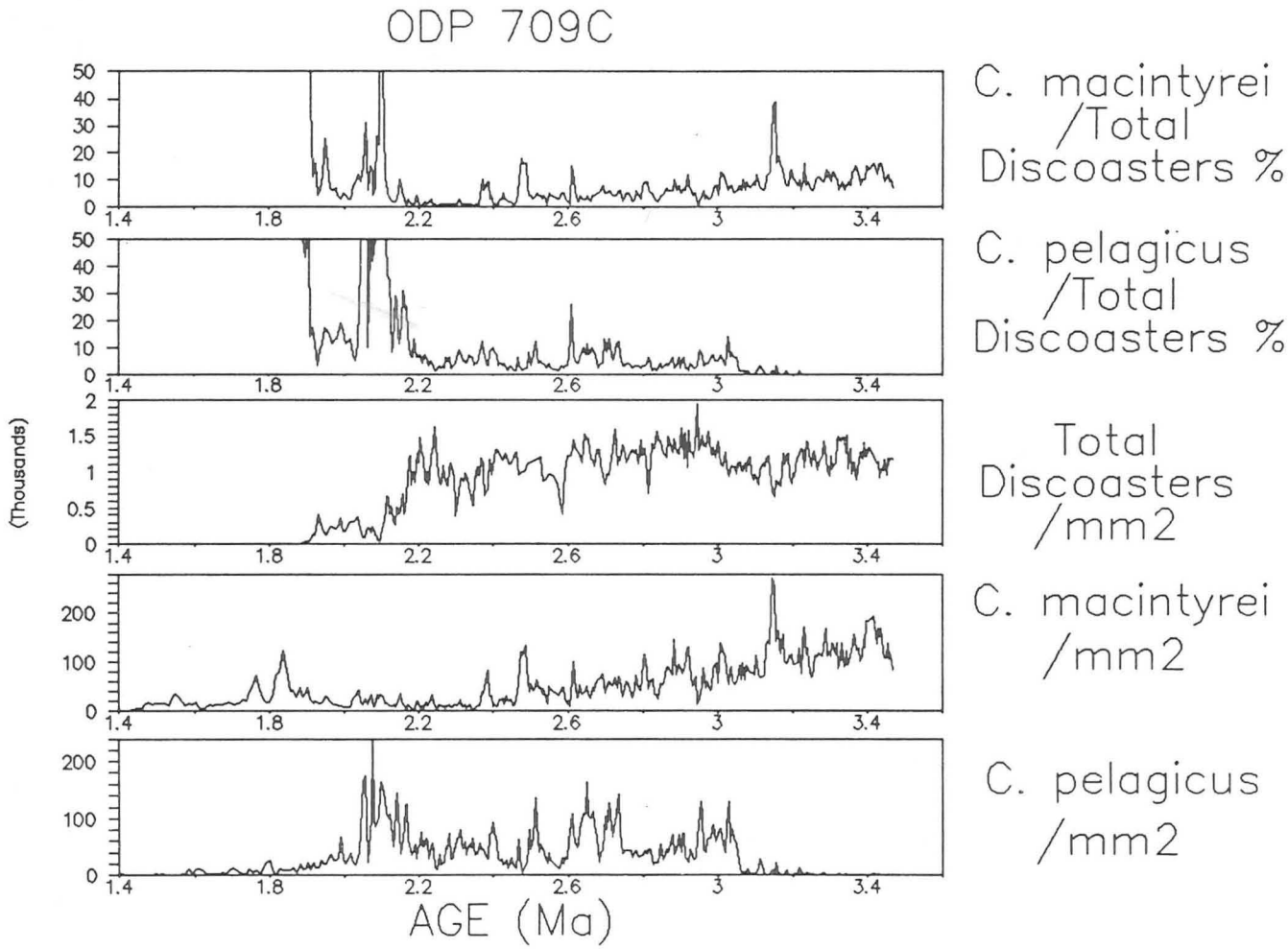

C2: Relative abundance relationship of C. pelagicus and C. macintyrei with Total Discoasters/mm2 at ODP 709C between 1.89–3.50 Ma.

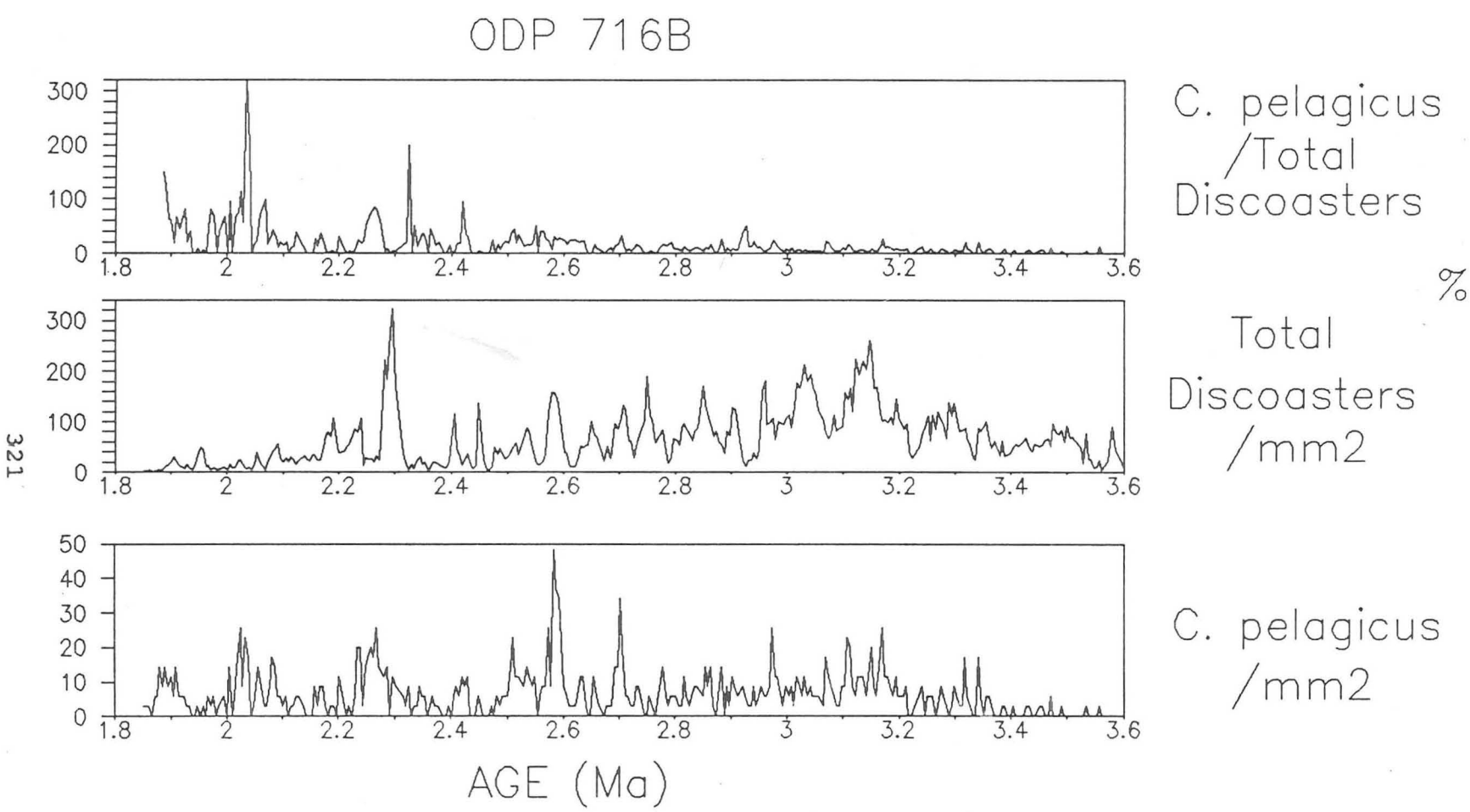

C3: Relative abundance relationship of C. pelagicus with Total Discoasters/mm2 at ODP 716B between 1.89–3.6 Ma.

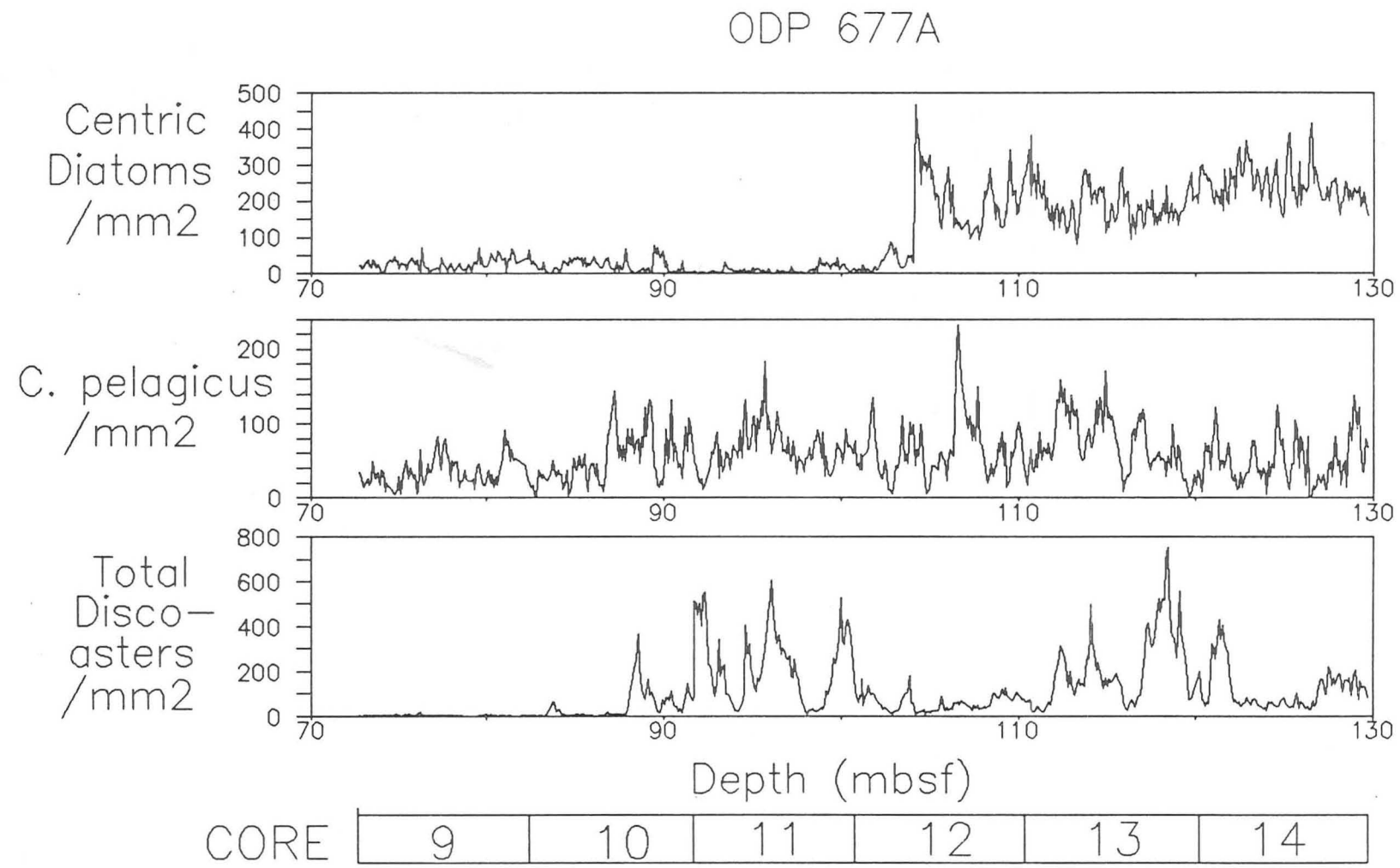

C4: Abundance of Total Discoasters, C. pelagicus and Centric Diatoms/mm2 at ODP 677A.

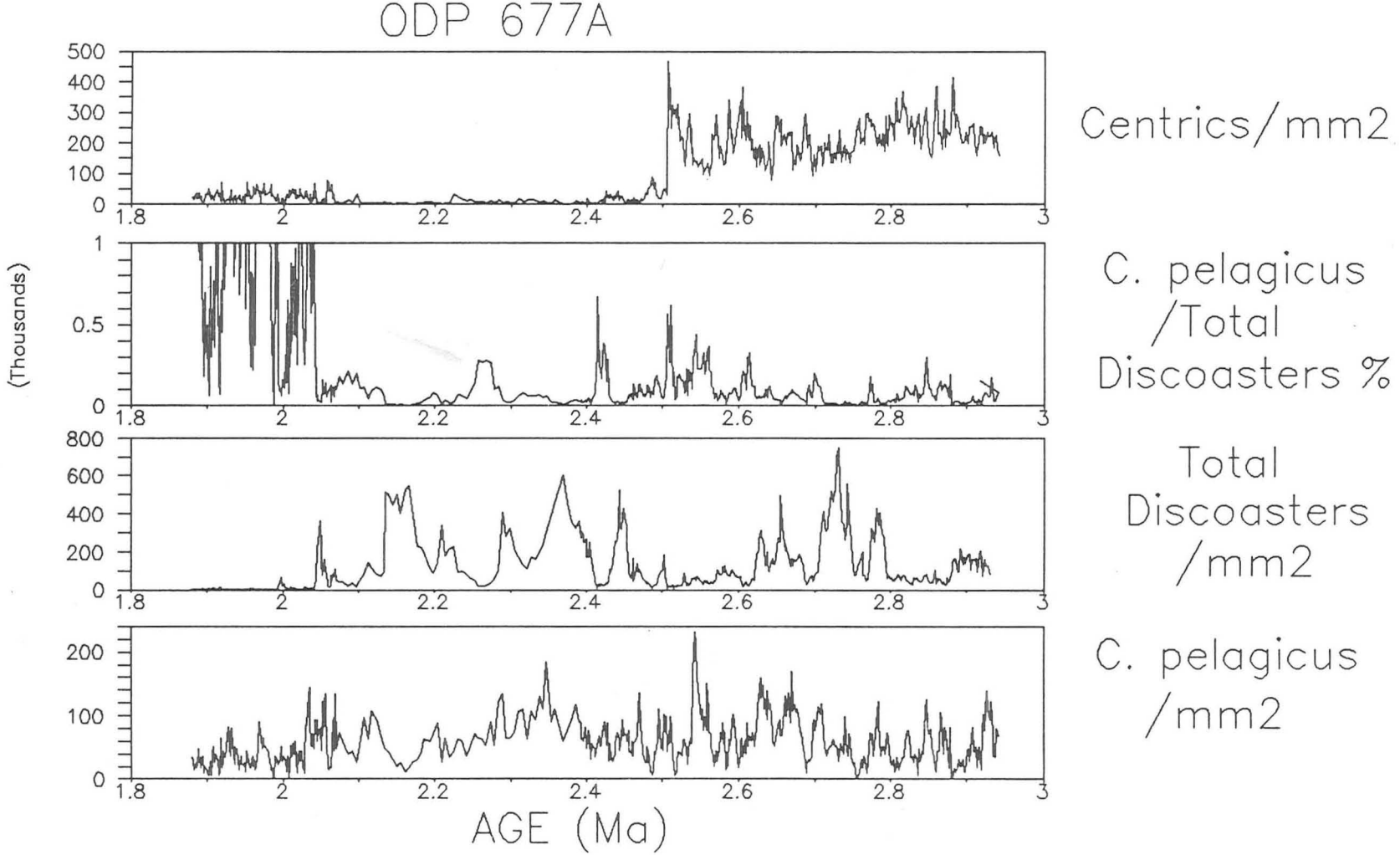

C5: Relative abundance relationship of C. pelagicus with Total Discoasters/mm2 and abundance of centric diatoms/mm2 at ODP 677A between 1.89–2.90 Ma.

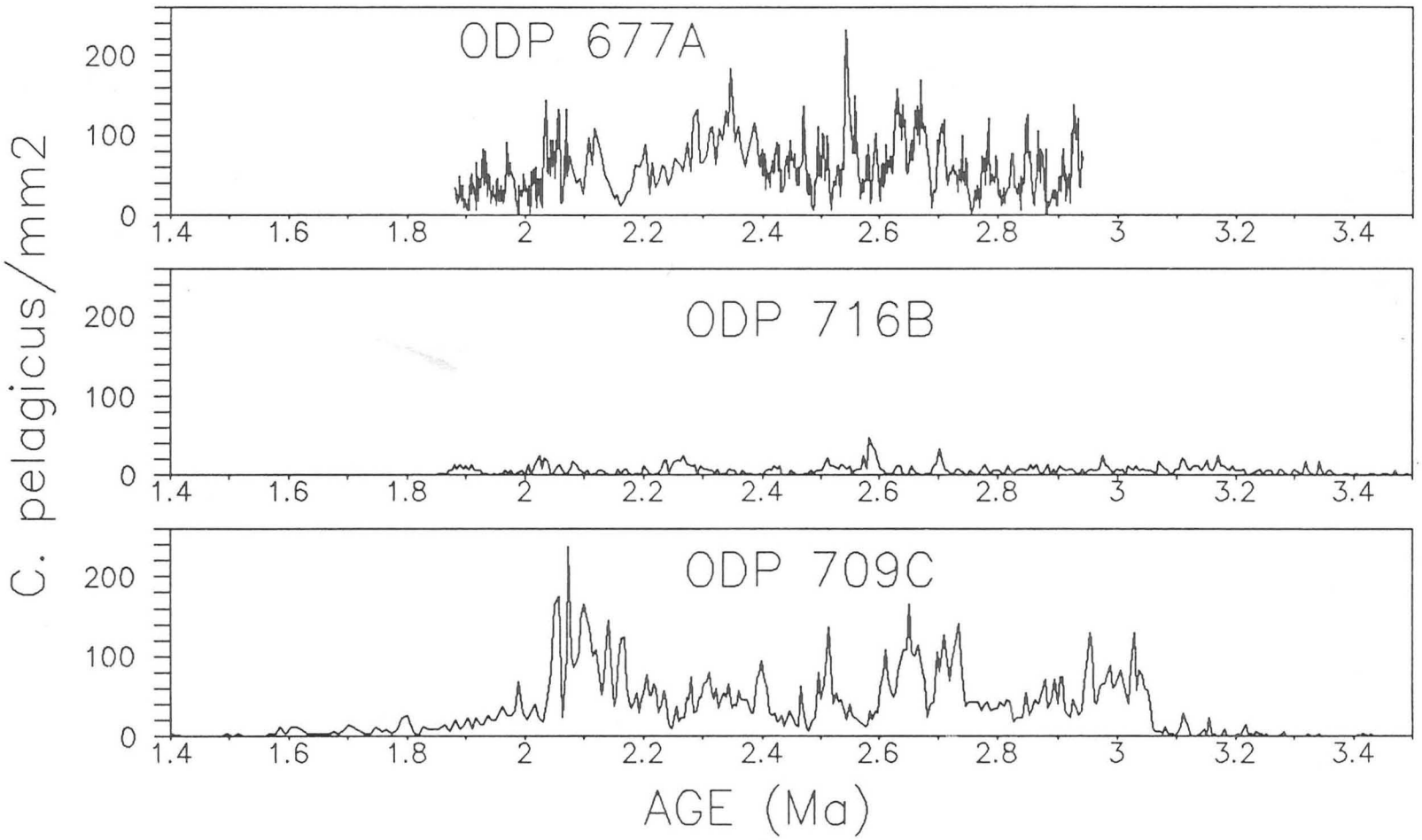

C6: Abundance of C. pelagicus/mm2 at ODP Sites 709C, 716B AND 677A

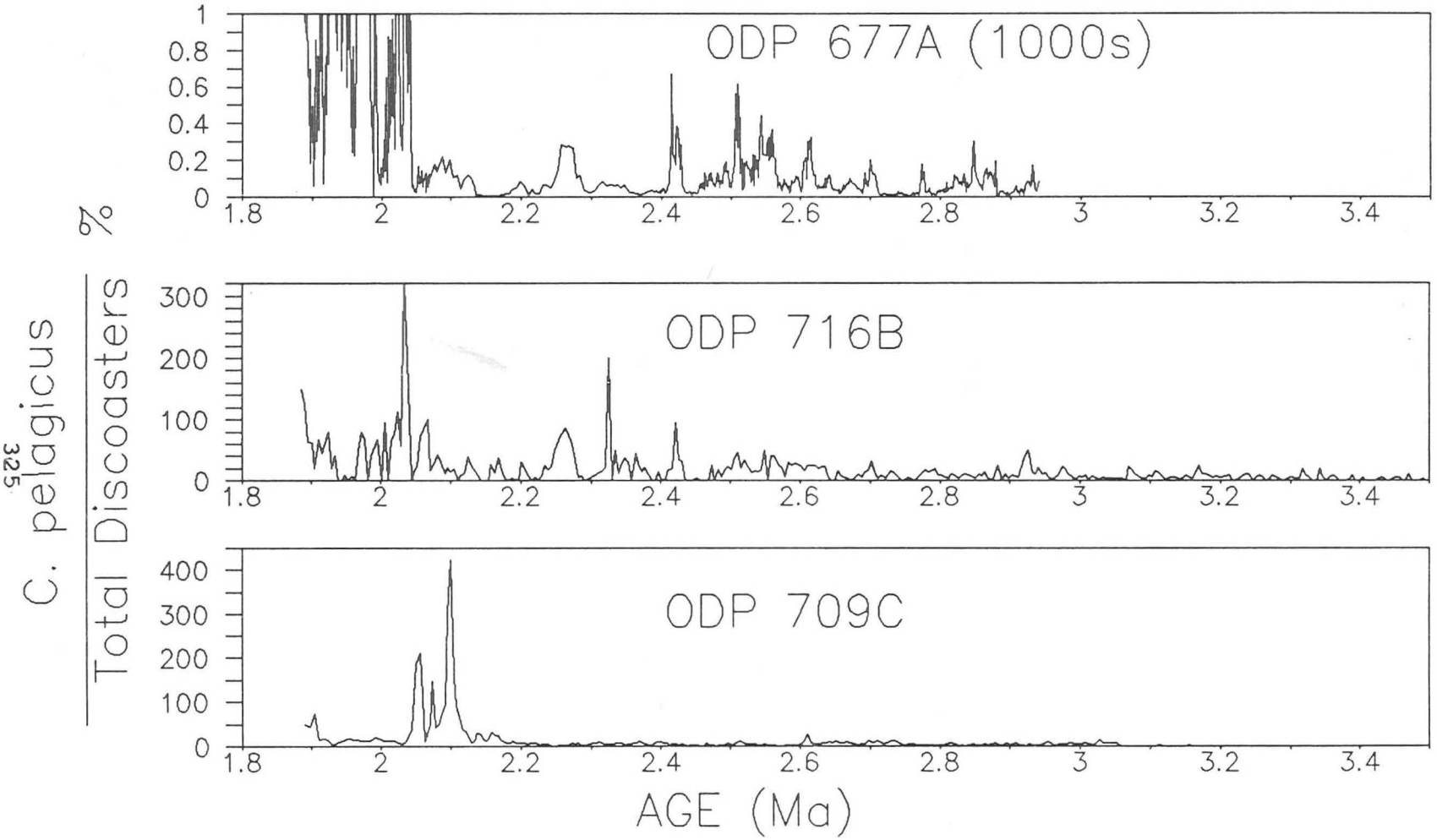

C7: Relative abundance relationship of C. pelagicus with Total Discoasters /mm2 at ODP Sites 709C, 716B and 677A